Investigating the origins of Pancreatic Ductal Adenocarcinoma

Rute Machado de Morais Ferreira

University College London
Cancer Research UK London Research Institute
and
The Francis Crick Institute

PhD Supervisor: Axel Behrens

A thesis submitted for the degree of
Doctor of Philosophy
University College London
September 2015

Declaration

I Rute Machado de Morais Ferreira confirm that the work presented in this thesis is my own. Where information has been derived from other sources, I confirm that this has been indicated in the thesis.

Abstract

Pancreatic ductal adenocarcinoma (PDAC) comprises 85% of all pancreatic cancers and is characterized by an extremely poor prognosis. It is becoming increasingly obvious that attention has to be focused on early tumour development, when the disease is still manageable. Thus, in this study, I aimed to assess the contribution of adult acinar and duct cells to PDAC development and to identify PDAC tumour-initiating cells (TICs).

Our laboratory had previously identified Fbw7 as a potent tumour suppressor in PDAC (unpublished data). *Fbw7*$^{F/F}$*; KRas*$^{LSL\text{-}G12D/wt}$*; Pdx1-Cre* mice exhibited accelerated PDAC onset compared with *KRas*$^{LSL\text{-}G12D/wt}$*; Pdx1-Cre* mice. I confirmed this observation and demonstrated that Fbw7 loss in the pancreatic epithelium had a greater proliferative effect in ductal cells, in the presence and absence of *KRas*^{G12D}, leading to increased numbers of duct cells positive for phosphorylated histone 3. The selective loss of Fbw7 in adult ductal cells with concomitant *KRas*^{G12D} expression (*Fbw7*$^{F/F}$; *KRas*$^{LSL\text{-}G12D/wt}$*; Ck19-CreER* mice) led to PDAC development, which was not preceded by mucinous lesions. These results were confirmed with the loss of p53 with simultaneous *KRas*^{G12D} expression in adults duct cells (*p53*$^{F/F}$; *KRas*$^{LSL\text{-}G12D/wt}$*; Ck19-CreER* mice). The absence of mucinous PDAC precursors was not dependent on the genotype, as loss of Fbw7 in *KRas*^{G12D}-expressing acinar cells allowed the development of mucinous murine pancreatic intraepithelial neoplasia (PanIN). Additionally, I induced bystander PanINs using orthotopic transplantation of PDAC cells. These results provide evidence that ductal cells can originate PDAC and that different pancreatic cells types might adopt different routes to PDAC development. Additionally, the observation of bystander PanINs questioned the sole pre-neoplastic nature of these lesions highlighting the need for a deeper understanding of PDAC biology.

In the present work, I have also described CD9 as a marker of TICs within PDAC derived from pancreatic progenitors and adult ductal cells. CD9^{High} PDAC cells exhibited higher *in vitro* organoid-forming capacity, compared with CD9^{Low} cells, isolated from the primary tumour and after long-term cultures. Contrasting with CD9^{Low} tumour cells, CD9^{High} cells were capable of forming secondary tumours at low numbers, demonstrating efficient tumour-initiating capacity and recapitulating the histology of the primary tumour source. These results could provide useful information for the development of PDAC targeted therapies.

Acknowledgement

During the course of these four years many people had great impact on my life both in a professional and in a personal way.

First of all, I would like to thank my supervisor Dr Axel Behrens for the guidance and stimulation of critical thinking. I would also like to thank all the current and past members of the Mammalian Genetics Laboratory for the scientific discussion in the lab, and the not so scientific discussions at the pub. Namely, I would like to thank Dr. Rocio Sancho for all the scientific help during the beginning and development of my studies, as well as for allowing me to collaborate in her work, which led to the development of my projects. I would like to thank Dr. Rocio Sancho, Dr Catherine Cremona and Dr. Ralph Gruber for critically reading the thesis and Hendrik Messal (fellow PhD student) for, not only reading the thesis, but also for all those valuable discussions about anything and everything. While not naming remaining members of the group, every single person had a great impact in my life and I am thankful for their input and friendship.

I would like to thank my thesis committee members Dr Erik Sahai and Dr Ilaria Malanchi for the valuable advise during the course of my studies.

I am extremely grateful for having the opportunity to work in such a well-resourced institute and; thus, several members of various research facilities have to be acknowledged. I am especially grateful to Emma Nye, Dr Bradley Spencer and Richard Stone from the Experimental Histopathology facility for all their friendship and help with the immunohistochemistry, Professor Gordon Stamp, head of the Experimental Histopathology facility, for all the help with the tumour histology and classification and the knowledge on the human PDAC from a clinical perspective. I would also like to thank the LRI FACS facility for the help with the cell sorting, Dr Richard Mitter from the Bioinformatics unit for the microarray analysis, all the members of the Biological Resources Unit at LRI and CH for their continuous care of the experimental animals, Dr Sally Leevers and her team for their support and Cancer Research UK for funding.

Finally, a big thank you to everyone outside the laboratory (family and friends) for the never-ending understanding of my working hours, the intense one-way discussions about my work and the love that only great people are able to give. I am honestly grateful.

Table of Contents

Table of figures

List of tables

Abbreviations

AB	Alcian blue
a.b.	Arbitrary units
ABC	Avidin-Biotin Complex
ACC	Acinar cell carcinomas
ADAM10	A desintegrin and metalloprotease 10
ADC	Antibody-drug conjugates
ADM	Acinar-to-Duct metaplasia
Agr2	Anterior Gradient 2
ALDH	Aldehyde dehydrogenase
AMH	Anti-müllerian hormone
APC	Allophycocyanin
ATP	Adenosine triphosphate
BMP	Bone morphogenetic protein
bp	base pairs
CAE	Carcinoembryonic antigen
CAII	Carbonic anhydrase II
CCK	Cholecystokinin
CD	Cluster of differentiation
cDNA	Complementary DNA
CDKs	Cyclin-dependent kinase
CDKN2A	Cyclin-dependent kinase Inhibitor 2A
cJun	Cellular Jun
CK	Cytokeratin
Cpa	Carboxypeptidase A
Cre	Cre recombinase
CSC	Cancer stem cell
CT	Computed tomography
CTSE	Cathepsin E

Cul1	Cullin-1
CXCR4	C-X-C chemokine receptor type 4
D	Aspartic acid
DBA	Dolichos biflorus agglutinin
ddH_2O	Double distilled water
DEPC	Diethyl pyrocarbinate
Dll1	Delta-like gene 1
DMEM	Dulbecco's modified eagles's medium
DNA	Deoxyribonucleic acid
dNTPs	Deoxynucleotide triphosphates
DPC4	Deleted in pancreatic carcinoma locus 4
DSL	Delta Serrated Lag2
DT	Diphtheria toxin
DTR	Diphtheria toxin receptor
EDTA	Ethylenediaminetetraacetic acid
EGF-LR	Epidermal growth factor -like repeats
EGFR	Epidermal growth factor receptor
Ela1	Elastase I
EMT	Epithelial to mesenchymal transition
EpCam	Epithelial cell adhesion molecule
ER	Oestrogen receptor
ESA	Epithelial-specific antigen
FACS	Fluorescent activated cell sorting
FBP	F-box protein
FBW7	F-box and WD repeat domain containing-7
FCS	Foetal calf serum
FGF	Fibroblast growth factor
Foxn1	Forkhead box protein N1
F7KCk19-CreER	*$Fbw7^{F/F}$; $KRas^{LSL\text{-}G12D/WT}$; Ck19-CreER*
F7KEla1-CreER	*$Fbw7^{F/F}$; $KRas^{LSL\text{-}G12D/WT}$; Ela1-CreER*

F7Pdx1-Cre	*Fbw7$^{F/F}$; Pdx1-Cre*
F7KPdx1-Cre	*Fbw7$^{F/F}$; KRas$^{LSL\text{-}G12D/WT}$; Pdx1-Cre*
G	Glycine
g	Gram
GAP	GTPase-activating protein
GDF	Growth and differentiation factor
GDP	Guanosine diphosphate
GEF	Guanine nucleotide exchange factor
GEM	Genetically engineered mouse
GF	Growth factor
GFP	Green fluorescent protein
GRB2	Growth factor receptor binding
GSI	ɣ-secretase inhibitor
GTP	Guanosine triphosphate
Her-2/Neu	Human epidermal growth factor receptor 2
Hes1	Hairy/Enhancer of Split-1
Hnf1β	Hepatocyte nuclear factor-1-beta
H&E	Hematoxylin and eosin
IF	Immunofluorescence
IHC	Immunohistochemistry
IgG	Immunoglobulin G
IMS	Industrial methylated spirit
IP	Intraperitoneal
IPMN	Intraductal papillary mucinous neoplasm
ITPN	Intraductal tubular papillary neoplasm
Kb	Kilo base pairs
KC	LSL-KRAS^{G12D}; Pdx1-Cre
KPdx1-Cre	KRas$^{LSL\text{-}G12D/WT}$; Pdx1-Cre

KPC	LSL-KRAS^{G12D}; P53$^{lox/ox\ or\ lox/+}$ (specified); Pdx1-Cre
LKB1	Liver kinase B1
LNR	LIN-NOTCH repeats
LOH	Loss of heterozygosity
LRI	London Research Institute
LSL	loxP-Stop-loxP
m	Murine
M	Molar
MAML	Mastermind-like
MCN	Pancreatic mucinous cystic neoplasm
MDM2	Mouse double minute 2 homolog
MEN1	Multiple endocrine neoplasia type 1
mg	Miligram
mL	Mililitre
mM	Milimolar
Mmp7	Matrix metalloproteinase-7
MO	Morpholino antisense oligonucleotide
MRI	Magnetic resonance imaging
MRP1	Motility related protein 1
Muc	Mucin
n.a.	Not applicable
NBF	Neutral buffered formalin
Ngn3	Neurogenin 3
ng	Nanogram
NICD	Notch intracellular domain
Nkx	NK homeobox
NLS	Nuclear localization signal
NOD/SCID	Non obese diabetic/ severe combined immunodeficiency
n.s.	not significant

p	phosphorylated
P	Postnatal day
PanIN	Pancreatic intraepithelial neoplasia
PAS	Periodic acid-Schiff
PBS	Phosphate buffered saline
PCR	Polymerase chain reaction
PDAC	Pancreatic ductal adenocarcinoma
PDL	Pancreatic duct ligation
PDK1	Phosphoinositide-dependent kinase 1
PDX 1	Pancreatic and duodenal homeobox 1
Pen	Penicillin
PET	Pancreatic endocrine tumors
pH3	Phosphorylated Histone 3
PIP_2	Phosphatidylinositol 4,5-bisphosphate
PIP_3	Phosphatidylinositol 3,4,5-triphosphate
PI3K	Phosphatidylinositol 3-kinase
Ptf1a	Pancreas transcription factor 1a
Px	Partial pancreatectomy
p53KEla1-CreER	$p53^{F/F}$; $KRas^{LSL-G12D/WT}$; Ela1 -CreER
p53KHnf1β-CreER	$p53^{F/F}$; $KRas^{LSL-G12D/WT}$; Hnf1β –CreER
p53KPdx1-Cre	$p53^{F/F}$; $KRas^{LSL-G12D/WT}$; Pdx1-Cre
Q-PCR	Quantitative real-time PCR
RAF	Rapidly accelerated fibrosarcoma
RAM	RBPJ-associated molecule
Rb	Retinoblastoma
RBP-J J	Recombination signal binding protein for immunoglobulin kappa
RIP	Rat insulin promoter
RNA	Ribonucleic acid

RTK	Receptor tyrosine kinase
SC	Cystadenomas
SCF	Skip1-Cul1-Fbox
SD	Standard deviation
Shh	Sonic hedgehog
SH2	Src homology 2
SH3	Src homology 3
SKP1	S-phase-kinase-associated protein-1
SMA	Smooth muscle alpha-actin
SMAD4	Mothers against decapentaplegic homolog 4
SPT	Solid pseudopapillary tumors
STK11	Serine/threonine kinase 11
Strep	Streptomycin
TACE	Tumour necrosis factor-α converting enzyme
TAE	Tris acetate EDTA buffer
TE	Tris-EDTA
TEMs	Tetraspanin-enriched microdomains
TFF2	Trefoil Factor 2
TIC	Tumour initiating cell
TGFβ	Transforming growth factor-β
U	units
Ub	Ubiquitin protein
UPS	Ubiquitin-proteasome system
V	Valine
v/v	Volume per volume
WHO	World Health Organization
w/v	Weight per volume

YFP	Yellow fluorescent protein
α	Alpha
β	Beta
β gal	Beta galactosidase
δ	Delta
µg	Microgram
µL	Microlitre
µm	Micrometre
µM	Micromolar
5-FU	Fluorouracil

Chapter 1. Introduction

1.1 The mammalian pancreas

Mammalian life is sustained by the complex coordination of internal organs, which, as systems, work together to perform crucial body functions. However, this intricacy is not only observed in organ systems, and sometimes, a single organ can serve as an equivalent representation of such complexity. The pancreas is probably one of the best examples of multifunctioning organs, where an exocrine and an endocrine compartment work in harmony to participate in different functions, but it might be one of the least understood.

Residing in the abdominal cavity, the pancreas is a component of both digestive and endocrine systems. Topologically, the human pancreas is divided into three regions: head, body and tail. The head of the pancreas is located in the concavity of the duodenum, where it establishes a direct connection with the duodenum and bile duct (ampulla of Vater). The body is located below the stomach and the tail borders the spleen. In the mouse, the pancreatic organ is not as well defined, consisting of a soft and diffuse tissue mass divided into three lobes: the splenic lobe (corresponding to the human pancreatic tail), the gastric lobe (corresponding to the human pancreatic body) and the duodenal lobe (corresponding to the human pancreatic head and body) (Figure 1a). Although pancreatic size and shape might differ between mammals, pancreatic composition remains conserved (Figure 1b). An exocrine and an endocrine compartment, each consisting of different cells, constitute the pancreas. The exocrine portion comprises 95% of the entire pancreatic gland and is represented by two main cell types: acinar and duct cells. Embedded in the exocrine pancreas, surrounded by acinar tissue, we find the endocrine pancreatic compartment organised in spheroidal structures entitled Islets of Langerhans.

Acinar cells are arranged in aggregates named acini and are thought to be the main functional cell type within the exocrine gland, producing over 20 proenzymes and enzymes which are then secreted to aid digestion. These acini rest at the tips of an intricate network of channels lined by the second exocrine cell type, the ductal cells, which conduct the acinar-derived enzymes to the duodenum through the main pancreatic duct. The endocrine islets of Langerhans are crucial in blood sugar regulation,

as their main cellular components are beta (β)-cells, alpha (α)-cells, delta (δ)-cells and PP-cells, which produce and secrete insulin, glucagon, somatostatin and pancreatic polypeptide, respectively, hormones that are mainly involved in glucose homeostasis (Slack, 1995, Benitez et al., 2012, Puri and Hebrok, 2010).

Given the distinct function and composition of each compartment, they are usually studied separately, impairing the comprehensive understanding of the organ as a whole.

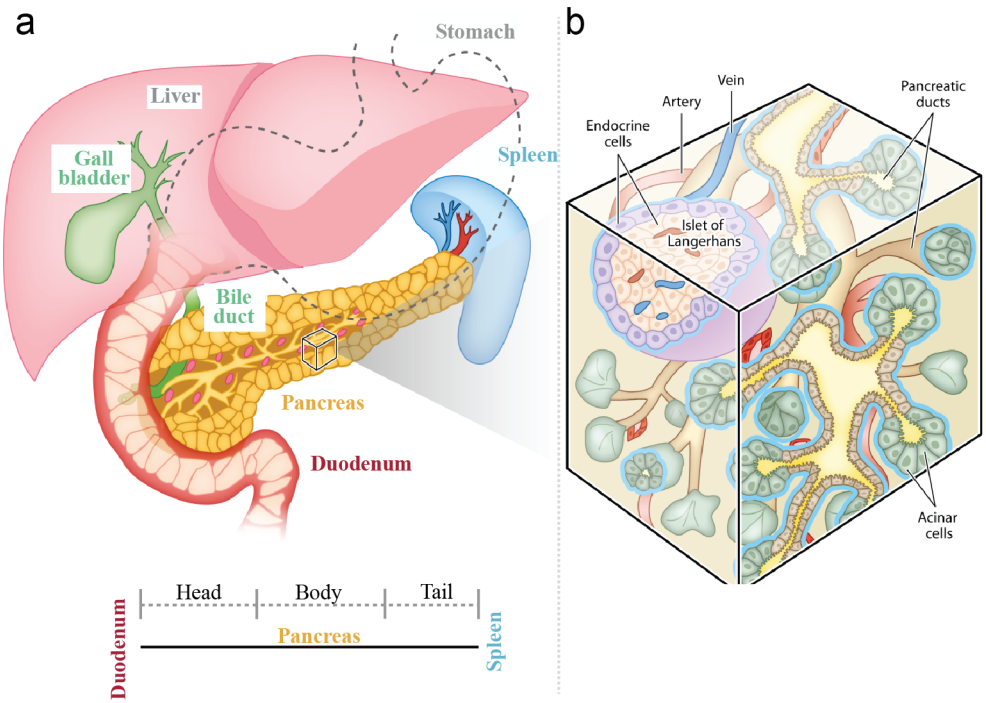

Figure 1 – Illustration of the human pancreas and its cellular components

a) Schematic representation of the human pancreas. The pancreas (in yellow) is located in the peritoneal cavity surrounded by stomach (above), spleen (right) and intestine (left). The main pancreatic duct is connected to the liver by the common bile duct. The figure also illustrates the virtual subdivision of the human pancreas into 3 main regions: head; body; tail. **b)** Schematic illustration of the two pancreatic compartments and their cellular composition. The exocrine pancreas consists of a mass of acinar cells located at the tips of a network of ducts. The endocrine compartment is organized in islets of Langerhans embedded in the exocrine compartment. Figure adapted from Shih et al., 2013

1.1.1 Pancreatic developmental biology

Driven by the alarming outcomes of pancreatic diseases, considerable attention has been devoted to the understanding of pancreatic development,.

The complex process of mouse pancreatic organogenesis can be subdivided into three distinct stages: primary transition (from embryonic day E9.5 to E12.5); secondary transition (from E12.5 to birth); and the postnatal period (from birth to onset of adolescence) (Pictet et al., 1972).

Initial determination steps dictated by a notochord-induced repression of endodermal Sonic Hedgehog (*Shh*) allows the specification, at E8.5, of the position of the pancreatic buds in the foregut endoderm (Hebrok et al., 1998) (Figure 2a). The patterning of the endoderm and commitment to a pancreatic fate is dictated by extrinsic signals originating from surrounding tissues such as the cardiac mesoderm and endothelial cells. These molecular signals induce the formation of dorsal and ventral pancreatic buds that become morphologically evident at E9.5 (Spagnoli, 2007). Subsequent elongation, with concomitant stomach and duodenum rotation, leads to their fusion and consequent formation of the primordial unified pancreas. Concurrently, cellular proliferation leads to an increase in size and to a transient state of epithelial stratification, promoting microlumens to coalesce, giving rise to a primitive network of ducts composed of multipotent progenitors (Villasenor et al., 2010, Puri and Hebrok, 2010).

On a molecular level, pancreatic specification signals induce the expression of transcription factors important for pancreatic induction and identity maintenance. Some of the transcription factors present in the primordial pancreas are restricted to the pancreatic domain, such as Pancreatic and duodenal homeobox (Pdx) 1, Pancreas transcription factor 1a (Ptf1a, also known as p48) and Sox9, while the expression of others (Gata4/6, Foxa1/2, Onecut1, Hes1, Tcf2, Prox1 and Mnx1) extends to the foregut endoderm (Figure 2a). It is not yet well known which transcription factors regulate pancreatic fate; however, amongst the above, Pdx1 and Ptf1a appear to be key for pancreatic identity. Ectopic pan-endodermal expression of Pdx1 and Ptf1a, during *Xenopus* embryogenesis, converted duodenal domains into pancreatic endoderm. In the same study, morpholino antisense oligonucleotide (MO) injection against both transcription factors, in combination or individually assessed, led to the loss of exocrine pancreas (Solomon Afelik, 2006). Additionally, homozygous deletion of Pdx1 during

mouse embryonic development prevents pancreatic tissue formation, leading to lethality soon after birth with no additional abnormalities (Jonsson et al., 1995).

During secondary transition, tightly controlled signals derived from the epithelium and mesenchyme regulate cell lineage determination of the pancreatic progenitors. *In vivo* analysis of fixed tissue, together with lineage tracing experiments, have demonstrated that, during the secondary transition, expansion and branching generates a topological organization of the pancreas that largely resembles that of the adult animal. In the beginning of the secondary transition, multipotent progenitors lose their potency and become committed to the acinar cell lineage at the tips while the stalk becomes composed of bipotent progenitors that develop towards endocrine and ductal cell fates (Shih et al., 2013) (Figure 2b).

Knowledge of the specific regulatory cues is scarce, however, genetic studies have implicated Notch signalling as one of the main epithelium-induced regulators of early pancreatic growth and differentiation. Impairment of Notch signalling by deletion of Notch ligand delta-like gene 1 (Dll1) or its intracellular mediator, Recombination Signal Binding Protein for Immunoglobulin kappa J (RBP-J), in the murine embryonic pancreatic domain, accelerates the onset of endocrine over exocrine differentiation and promotes pancreatic growth arrest (Edlund et al., 1999). Similar observations were made by deletion of the Notch downstream effector Hairy/Enhancer of Split-1 (Hes1). *Hes1*$^{-/-}$ mice displayed pancreatic hypoplasia due to premature endocrine differentiation (Madsen et al., 2000).

The influence of the microenvironment adds a layer of complexity to pancreatic organogenesis. Explant cultures of pancreatic primordium have demonstrated that the mesenchyme plays a crucial role in providing the environmental cues necessary for epithelium growth and differentiation. Cultured pancreatic buds devoided of mesenchyme failed to differentiate into the pancreatic cell lineages and displayed architectural abnormalities (Golosow and Grobstein, 1962). Although the effect of the mesenchyme on pancreatic development has long been observed, light is only recently being shed on the pathways involved. Critical pathways include FGF, Wnt and BMP (Shih et al., 2013).

In response to the environmental signals, gene expression profiles change. Multipotent progenitors give rise to two main pancreatic precursors: acinar precursors located at the

tips of the pancreatic primordium, where they lose Pdx1 expression and acquire acinar determined signatures with expression of Ptf1a, carboxypeptidase A (Cpa) and c-myc (Zhou et al., 2007) and duct/endocrine precursors, identified by the expression of Pdx1, NK homeobox (Nkx) 6.1, Nkx6.2 and Sox9 (Figure 2b). The molecular mechanism underlying the dual fate determination has been suggested to rely on a cross-repressive interaction between Ptf1a and Nkx6.1/6.2. Immunofluorescence analyses have shown a temporal window where both transcription factors are expressed in the multipotent domains. Nkx6.1- and Nkx6.2-deficient mouse embryos exhibit ectopic Ptf1a expression in the trunk of the pancreatic primordium with a simultaneous reduction in the number of endocrine progenitors and an increase in acinar cell markers. Moreover, Nkx6.1 or 6.2 ectopic expression driven by the Pdx1 promoter (Pdx1-Nkx6.1/2) repressed Ptf1a expression and impaired acinar cell differentiation. Conversely, Pdx1-Ptf1a ectopic expression blocked endocrine differentiation and devoided the pancreatic trunk of Nkx6.1 expression (Zhou et al., 2010). Once cells are committed to an acinar fate, these cells polarize, form aggregates at the tip of the primordial trunk and continue to mature and proliferate until adolescence (Desai et al., 2007).

Still during secondary transition, pancreatic trunk bipotent progenitors undergo the last step of cell fate determination and become committed to endocrine progenitors or ductal exocrine lineages (Figure 2c). The key transcription factor that marks the onset of endocrine differentiation is Neurogenin 3 (Ngn3). It has been observed that, prior to endocrine cell delamination from the primordial ductal network, a subset of bipotent progenitors upregulate Ngn3, becoming committed to the endocrine lineage, while the remaining progenitors retain Sox9, Tcf2 and onecut1, determining duct cell fate. The importance of Ngn3 has been extensively demonstrated and highly studied, mainly due to the fact that a better understanding of endocrine specification could aid in the development of therapeutic tools for diabetes. Ngn3-deficient mouse pancreata exhibit a complete lack of endocrine lineages with concomitant aberrant ductal morphology (Magenheim et al., 2011). The ductal enlargement observed during that study was most apparent in areas where Ngn3-positive progenitors usually reside, emphasizing the preferential ductal lineage fate determination over endocrine fate when Ngn3 is lost, rather than loss of endocrine progenitors alone. Additionally, the authors demonstrated that the increased number of Ngn3-expressing cells during development, by gamma

secretase inhibitor treatment (previously shown to promote *in vitro* endocrine differentiation of embryonic pancreatic progenitors (Mason and Mahoney, 2010)), was accompanied by a thinning of the ductal network (Magenheim et al., 2011).

Following Ngn3 expression, endocrine progenitors, expressing Pdx1, Ngn3 and Mafa (amongst other genes), exit the cell cycle, delaminate from the primitive ducts, further differentiate into the different pancreatic hormone-producing cells (β-, α-, δ- and PP-cells) (Figure 2c) and aggregate in clusters designated Islet of Langerhans (Desgraz and Herrera, 2009).

The knowledge of the mechanisms involved in pancreatic development constitutes a powerful tool in the understanding of the organ in the context of disease. However, thorough comprehension of disease mechanisms requires a deeper assessment of the adult scenario.

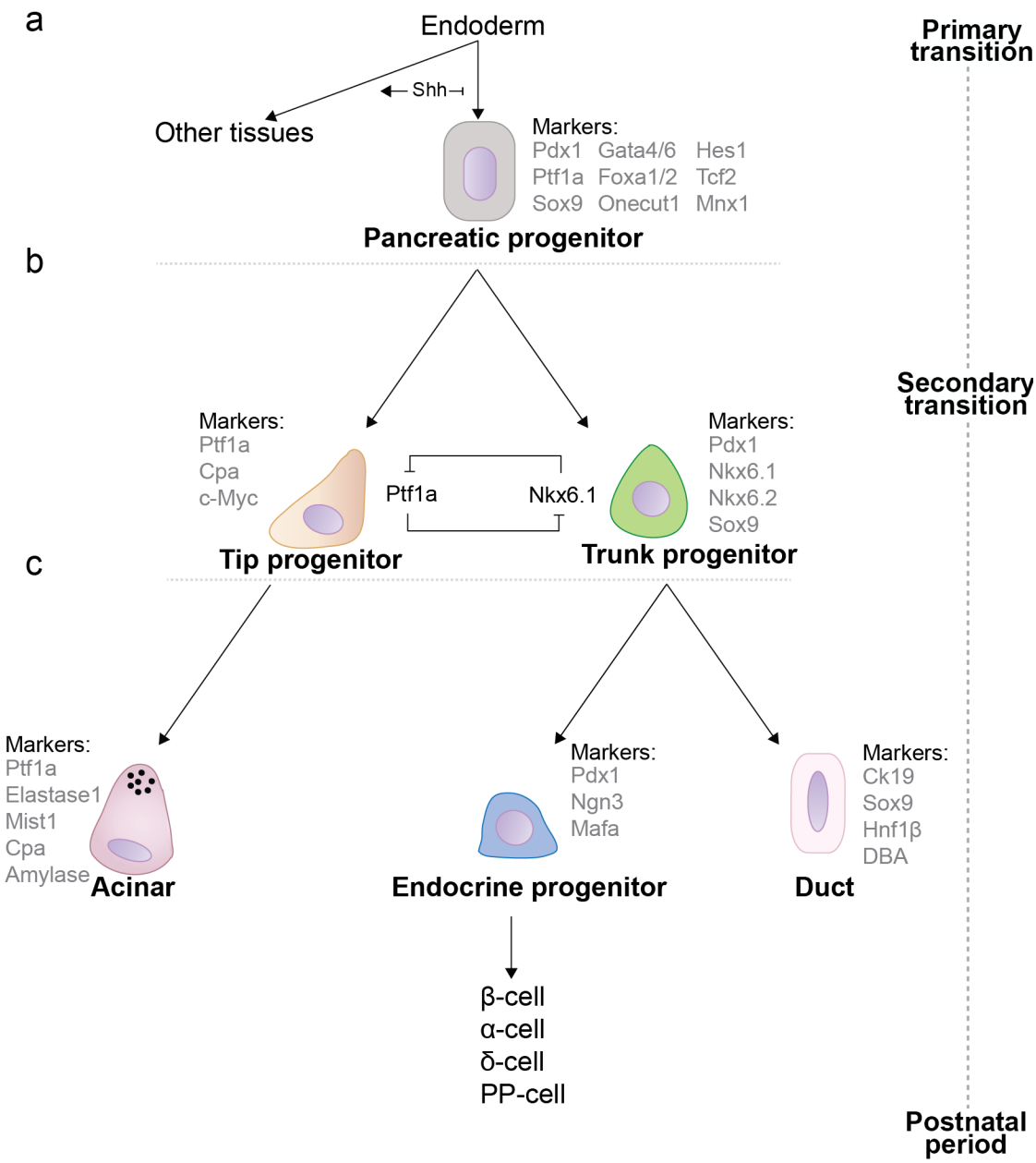

Figure 2 – Schematic representation of the main events in pancreatic embryogenesis

a) Primary transition - Repression by Shh dictates the pancreatic bud position. The pancreatic bud is constituted of progenitors expressing transcription factors restricted to the pancreatic bud (Pdx1, Ptf1a, Sox9) and transcription factors whose expression is extended to the remaining endoderm (Gata4/6, Foxa1/2, Onecut1, Hes1, Tcf2, Mnx1). Primary transition terminates with the formation of a primordial trunk with multipotent progenitors. **b)** Secondary transition – The expression of Nkx6.1 suppresses Ptf1a and vice versa. Multipotent progenitors commit to acinar cells or bipotent trunk progenitors. Tip progenitors express Ptf1a, Cpa and c-Myc while trunk progenitors express markers of both endocrine and ductal cells (Pdx1, Nkx6.1, Nkx6.2, Sox9). **c)** Bipotent trunk progenitors differentiate between endocrine or exocrine lineages. Ngn3 expression specifies the endocrine fate.

1.1.2 The adult pancreas and organ plasticity

Throughout pancreatic development, the primordial pancreas is exposed to a wide range of genetic, epigenetic and environmental factors, which modulate cellular responses that regulate organogenesis. During this period, epithelial sheets are composed of progenitors provided with delicate machinery capable of detecting and responding, with a high level of plasticity, to a complex signalling network. In most tissues, it is thought that the differentiated progeny matures and loses flexibility of cellular identity in response to environmental cues. However, genetic, and epigenetic, manipulations of developmental pathways in differentiated tissues have uncovered a latent ability of cells to de-differentiate or directly convert into a different lineage. Moreover, during disease development, it is observed that differentiated cells become more plastic and up-regulate embryonic pathways (Graf, 2011).
Regarding the murine pancreas, at the onset of puberty (weaning), the pancreatic topological organization and cellular differentiation are complete. While knowledge gained from the homeostatic organ suggests that the pancreas is generally quiescent, increasing evidence reveals that a large number of differentiated pancreatic cells have the capacity to change cellular fate and rapidly proliferate upon stimulation.

In order to identify and understand pancreatic plasticity, injury models and gene expression modulation approaches have been developed to challenge the pancreas into unveiling its latent capabilities. The most commonly used injury models are: (1) pancreatic duct ligation (PDL), (2) partial pancreatectomy (Px), (3) β-cell depletion by drug treatment or genetically engineered mouse (GEM) models, and (4) induction of a pancreatic inflammatory response, i.e., pancreatitis by caerulein treatment.
PDL consists of the ligation of the main duct near the tail. Ductal obstruction leads to accumulation of the pancreatic secretion, composed of the acinar-derived digestive enzymes, with consequent onset of cell death-triggered pancreatitis (Watanabe et al., 1995). This method leads to a quick, and drastic, ablation of the acinar cell compartment, with consequent slower duct and islet cell destruction, and it has been extensively used to uncover certain plasticity in pancreatic cell fate. Partial pancreatectomy, as the name indicates, is the surgical removal of a portion of the pancreas. Removal of up to 90% of the rat pancreas has been demonstrated to promote a

drastic remodelling of the organ leading to tissue regeneration. β-cell depletion has also been shown to induce β-cell neogenesis from different pancreatic cell sources. Treatment with the cytotoxic agents streptozotocin or alloxan leads to selective β-cell death due to the drug's glucose resemblance and subsequent uptake via Glut2 transporters. Alternatively, GEM models can be used to specifically deplete this population by expression of diphtheria toxin (DT), or its receptor (DTR), driven by β-cell specific promoters (Ferrer et al., 2007). Lastly, the induction of pancreatitis by the use of caerulein has also been used as a pancreatic injury. Caerulein is a cholecystokinin analogue, a peptide hormone involved in digestion, which induces the premature activation and release of acinar cell-produced digestive enzymes, leading to vast acinar cell death. Examples of the use of such strategies and their outcomes are discussed below.

1.1.2.1 Endocrine cells

As previously mentioned, the endocrine pancreas harbours a group of hormone-producing cells, clustered into islet of Langerhans. During pancreatic organogenesis, through an intricate web of signalling events, a common post mitotic Ngn3-expressing progenitor is able to give rise to insulin producing β-cells, glucagon-producing α-cells, somatostatin-producing δ-cells and pancreatic polypeptide-producing PP-cells (Slack, 1995, Benitez et al., 2012, Puri and Hebrok, 2010). Amongst all endocrine cells, the greatest efforts have been dedicated to the study of β-cell biology. β-cells constitute a key component in the control of glucose homeostasis due to their ability to sense variations in blood sugar levels and respond accordingly, by producing and secreting insulin. Insulin is a crucial hormone for survival as it is responsible for the cellular uptake of glucose from the blood, regulating the metabolism of carbohydrates and fat, and prevents glucose release from the liver. The lack of glucose regulation can cause hyper- or hypoglycaemia, leading to cardiovascular diseases, neuropathy, nephropathy, kidney failure, retinopathy and cataracts or brain related complications. In the absence of stimuli, β-cell mass remains unaltered. However, in the presence of a higher insulin requirement, such as pregnancy, autoimmune loss of β-cells (Type 1 diabetes), genetic insulin resistance or insufficient β-cell mass (type 2 diabetes) and obesity, the elevated

systemic glucose stimulates β-cells to initiate a proliferative program increasing cell mass by self-replication (Teta et al., 2007, Rieck and Kaestner, 2010). Notwithstanding the fact that β-cells re-enter the cell cycle to cope with insulin depletion-induced stress, in the case of diabetes, an alternative β-cell source is required for the continuous insulin demand. The search for new methods to obtain β-cells has demonstrated that non insulin-producing endocrine cells have the ability to alter their identity towards a β-cell fate. Such is the case for α-cell, a combinatory treatment of alloxan and PDL led to a dramatic β-cell neogenesis by α-cells in the mouse pancreas (Chung et al., 2010). Additional evidence was generated by specific β-cell deletion using GEM models. In the lab of Pedro L. Herrera, β-cell depletion was achieved by expression of DTR under the control of the rat insulin promoter (RIP) followed by DT treatment. β-cell neogenesis was observed and lineage tracing analysis, where α-cells were labelled before DT exposure, allowed the identification of glucagon-expressing cells as the source of newly formed insulin-producing cells (Thorel et al., 2010). Recent evidence also implicates δ-cells as a source for β-cells following β-cell ablation during puberty (Chera et al., 2014).

The ability of other endocrine cells to repopulate the endocrine gland after β-cell loss is interesting, and per se, demonstrates that pancreatic differentiated cells are capable of altering their identity upon stimulation.

1.1.2.2 Acinar cells

Acinar cells are the most abundant cell type in the exocrine pancreas. Constituting 95% of the exocrine gland, the acinar cells are roughly triangular in shape and cluster in globular structures, named acini, at the terminal ducts. Their role in digestion is achieved by continuous production and secretion of over 20 proenzymes and enzymes into the ductal network, which conducts them into the duodenum. Besides their functional and morphological differences compared with other pancreatic cells, acinar cells present a specific transcriptional profile that allows their identification by immunostaining. The most commonly used markers include: Ptf1a, Mist1, Elastase I (Ela1), Cpa1 and amylase. As the major constituent of the pancreas, unparalleled efforts have been undertaken to thoroughly assess their regenerative potential and possible use

in current diabetic-related medicine. In the adult animal, acinar cells have been shown to be characterized by a low proliferative potential during homeostasis (Desai et al., 2007) and thus, similarly to the assumption made for the whole organ, were thought to have low regenerative potential. The first hint that these cells could be a valuable and abundant source for β-cell regeneration emerged from *in vitro* studies, where the rat pancreatic acinar cell line AR42J initiated insulin and GLUT2 protein expression, with concomitant c-peptide detection (a by-product of insulin hormone processing), when exposed to the signalling molecules betacellulin and activin A (Mashima et al., 1996). However, the conclusions taken from this study were still questionable, as the cell line used was derived from a chemical-induced exocrine pancreatic tumour and exhibits major physiological differences from true acinar cells (Christophe, 1994).

In vivo models have since been used to address acinar cell plasticity. Initial studies ruled out acinar cells as a plastic pancreatic population. Desai and co-workers generated an acinar cell-specific transgenic mouse model where a tamoxifen-inducible mutated form of Cre recombinase (CreER) was expressed under the control of the Elastase1 promoter (Ela1 - acinar cell specific enzyme). In this model, the Cre recombinase is fused to a mutated ligand-binding domain of the human oestrogen receptor (ER) and, only in the presence of tamoxifen, it can translocate to the nucleus. Tamoxifen treatment, in mice harbouring a Rosa26-loxP-STOP-loxP (LSL) –LacZ, allowed the removal of the stop cassette, by recombination of the loxP sites, and linage tracing of acinar cells by LacZ expression. Px, PDL and pancreatitis induced by caerulein, failed to demonstrate LacZ-labelled newly formed β-cells, indicating that mature acinar cells lose their ability to alter cellular fate during adulthood (Desai et al., 2007). As with most lineage tracing and surgical approaches, the efficiency of labelling, and/or the extent of the injury induced may compromise the outcome. Nonetheless, efforts to demonstrate acinar cell plasticity persisted and, in 2008, Zhou and co-workers were able to reprogram acinar into insulin-producing cells *in vivo*. For this study, a mixture of adenovirus co-expressing one of the three key pro-endocrine developmental transcription factors (Pdx1, Ngn3 and Mafa), with nuclear GFP, was injected into the pancreas of acinar-specific lineage traced mice (*Cpa1CreERT2; R26LSL- β galactosidase* (βgal)). Soon after transduction, lineage traced cells up-regulated an endocrine program and exhibited

insulin content and secretion with co-expression of additional β-cell markers (Zhou et al., 2008).

Additional evidence has been obtained for acinar cell plasticity without the need for genetic manipulation. It has been observed that, although inefficiently, long term assault via prolonged PDL, can induce pre-labelled acinar cells to convert into β-cells (Pan et al., 2013). Moreover, the *in vivo* treatment of adult alloxan-treated mice with ciliary neurotrophic factor and epidermal growth factor demonstrated that acinar cells could convert into β-cells, restoring normal glycaemia (Baeyens et al., 2013). These results support the assumption that Desai and co-workers might have missed the labelling of acinar cells capable of conversion, possibly due to the use of different Cre mouse lines, or that the extent of injury was not enough to induce an acinar-dependent endocrine cell regeneration.

If acinar cells are capable of restoring endocrine tissue, although with limited capacity, it is reasonable to investigate their ability to regenerate the exocrine pancreas. In vitro strategies have highlighted the capacity of acinar cell explants to convert into ductal cells when cultured on nitrocellulose filters with stimulating factors (Githens et al., 1994). Nowadays, there is far-reaching knowledge of their ability to acquire a ductal molecular profile and morphology upon injury *in vivo*. It has been extensively observed that PDL, Px and caerulein treatments stimulate intense ductal cell expansion upon acinar cell death (Slack, 1995). By the use of lineage tracers, it was possible to identify that the observed ductal expansion was, in fact, a transdifferentiation of acinar cells into ductal cells, denominated acinar-to-duct metaplasia (ADM) (Means et al., 2005). ADM will be extensively addressed in this thesis (see 1.6.2, page 74).

1.1.2.3 Ductal cells

Despite their proportionally small tissue representation, the ducts play a crucial role in pancreatic physiology. Ductal cells are responsible for the production of bicarbonate-rich fluid which, combined with the acinar-derived enzymes, forms the pancreatic juice. Moreover, ductal cells are also responsible for the delivery of the pancreatic juice into the duodenum, to help digestion. The pancreatic ductal compartment consists of a convoluted network of ducts that can be subdivided according to their calibre and

histological features. Proximal to the bile duct, with the biggest calibre and initiating the network, is the main duct, composed of a columnar epithelium. Branching out of the main duct are the interlobular ducts constituted of cuboidal epithelia, which divide into intralobular and intercalated ducts containing flat cells. At the terminal end of the ductal network, a poorly characterized ductal cell, named centroacinar cells, is located (Reichert and Rustgi, 2011) (Figure 3). While ductal cells seem to differ morphologically between different segments, so far, their identification relies on common marker expression: cytokeratin 19 (CK19), Sox9, hepatocyte nuclear factor-1-beta (Hnf1β) and the surface affinity for the dolichos biflorus agglutinin (DBA).

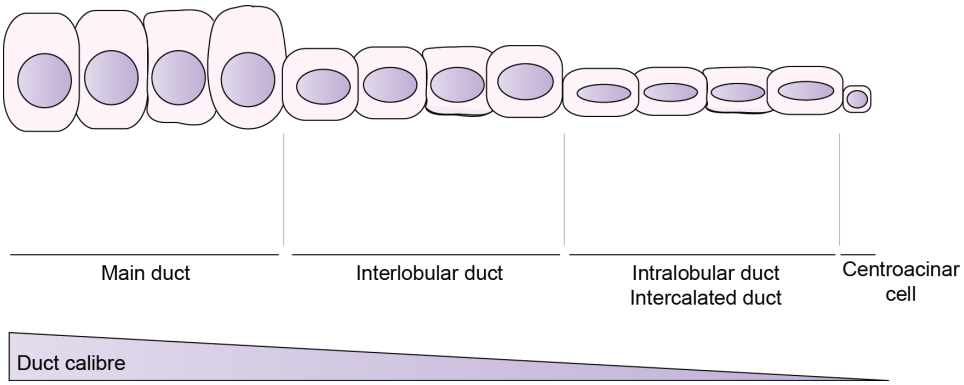

Figure 3 – Schematic representation of the ductal network and cellular composition

The ductal network is composed of ducts of different calibres and different histological features. The main duct has the largest calibre and is composed of columnar cells. Interlobular ducts have a reduced calibre, compared with the main duct, and are composed of cuboidal cells. Branching out of intelobular ducts are the intralobular ducts that give rise to the intercalated ducts. Both present flat cells. At the tips of the ductal network, centroacinar cells connect with the acinus.

Despite their low proliferative index, similar to acinar and endocrine cells (Githens, 1988), lessons from development have exposed the possibility of a higher plasticity for ductal cells compared with other pancreatic cell types. During pancreatic organogenesis, the population of progenitors sits in a primordial network, which culminates in the development of the ductal system. Therefore, the presence of a facultative stem cell population in the adult ductal compartment is hypothesised. Initial *in vitro* cultures of human ductal tissue demonstrated that cultured ductal cells reactivate an embryonic program, up-regulating Pdx1 and subsequently converting into insulin-producing cells able to respond to the presence of glucose (Bonner-Weir et al., 2000). *In vivo* evidence

of ductal plasticity was obtained after Px of rat pancreata. Bonner-Weir and co-workers observed, in 1993, that after 90% Px, part of the ductal compartment drastically increased proliferation with concomitant Pdx1 expression. Furthermore, during regeneration of the damaged organ, it was observed that 6% of the ductal cells in the main duct expressed insulin with 1% exhibiting insulin granules (Bonner-Weir et al., 1993, Bonner-Weir et al., 2004). In a different study, the pancreatic tail of Balb/c mice was ligated, with, as observed for other models, a measurable regeneration of the β-cell population. The phenomenon was shown to be dependent on the expression of the endocrine fate determinant Ngn3. By tracing Ngn3 expression using Ngn3-nLacZ mice, the authors demonstrated that β-cell neogenesis was derived from the ductal cells given its co-expression with CK19 (Xu et al., 2008). Despite the numerous studies demonstrating the occurrence of insulin-expressing clusters near/within ducts upon injury, lineage-tracing analysis was still needed to unquestionably demonstrate the potential of ductal cells for β-cell neogenesis.

Conflicting results have been presented regarding ductal cell plasticity. The use of duct cell specific, tamoxifen inducible, Cre-expressing mice, where *Hnf1β* (Hnf1β-CreER) and *Sox9* (Sox9-CreER^{T2}) promoter expression drive βgal labelling, pointed towards an absence of ductal cell-derived endocrine neogenesis. PDL and β-cell ablation were used as models of injury to promote β-cell regeneration. Notwithstanding observation of β-cell mass expansion, no contribution from the pre-labelled ducts was detected (Solar et al., 2009, Kopp et al., 2011). On the other hand, the use of carbonic anhydrase II (*CAII*) or *Ck19* genes driving a tamoxifen inducible Cre (CreER) have shown otherwise. In the first study, *CAII-CreER; Rosa26-LSL-LacZ* mice showed a marked increase in the number of labeled endocrine cells, after PDL, in the ligated pancreatic tail compared with controls (Inada et al., 2008). Genetic modulation of Fbw7 protein, a recognition component (F-box) of a Skp1-Cul1-Fbox (SCF)-type ubiquitin ligase, has also unveiled the ability of ductal cells to convert into insulin-expressing cells. Deletion of Fbw7 in ductal Ck19-expressing cells led to the conversion of a small number of labeled cells into functional β-cells. The authors demonstrated that Ngn3 protein is a direct target of Fbw7-dependent proteasomal degradation and thus, deletion of the ligase component led to Ngn3 accumulation and consequent ductal cell transdifferentiation (Sancho et al., 2014). These contradictory results can be explained by the selective labelling of ductal

cells with the different Cre lines. Hnf1β-CreER and Sox9-CreER^{T2}, although efficient, only labelled 65% of the ductal population. It is still an open question if the same ductal populations were labelled with the different Cre drivers or if progenitor-like ductal cells could have been selectively unlabelled. Moreover, Sox9 labelled cells showed Ngn3 upregulation upon injury.

As demonstrated by Sancho and co-workers, it is possible that the stability of the Ngn3 protein was not enough for completion of the endocrine differentiation program (Sancho et al., 2014). Since the extent of the injury dictates the signals to which the cells are exposed, different levels of injury could culminate in different outcomes.

Lastly, ductal cells were also shown to be able to generate acinar cells. By the use of a duct specific Cre mouse model (Sox9-CreER) with a Cre-dependent lineage tracer, the authors were able to identify traced acinar cells when tamoxifen treatment was performed in the adult mouse. In this study, it was not clear if this was a plasticity of the ductal cells converting into acinar cells or if a pool of progenitors residing within the ductal tree expresses Sox9 (Furuyama et al., 2011). This finding is still under debate (Carpentier et al., 2011).

Nonetheless, the observations obtained so far for acinar, endocrine and ductal cells unveil a cellular plasticity within the pancreas that might compensate for cellular loss after sustained injury (Figure 4).

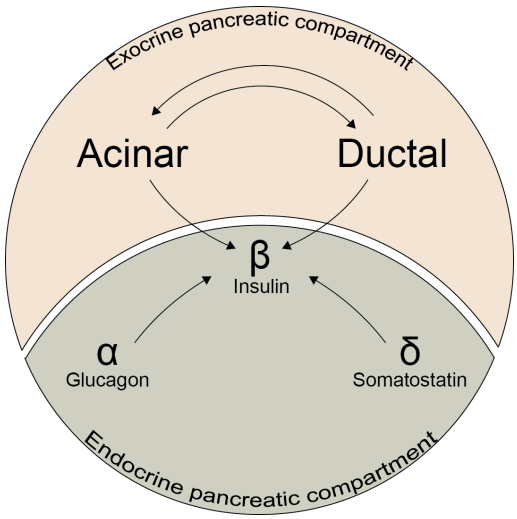

Figure 4 – Pancreatic cellular plasticity

Summary of the cellular plasticity observed for the different pancreatic compartments. Glucagon (α) and somatostatin (δ)-producing cells can transdifferentiate into insulin-producing β-cells. Acinar cells can give rise to ductal cells and β-cells and ductal cells can give rise to acinar cells and β-cells.

1.2 Pancreatic cancer

Cellular plasticity is an important feature of tissues exposed to damage and provides a unique tool for organ/tissue regeneration. However, the same mechanism used to repopulate different lineages after injury uncovers a cellular vulnerability to neoplastic hits. As mentioned before, all pancreatic cell types are provided with a cellular and genetic flexibility, which enables their tumourigenic transformation. Therefore, mimicking the pancreatic complexity, a whole spectrum of pancreatic tumours has been identified. The three most common pancreatic neoplasias will be described here. With defined histological features, resembling their normal counterparts, and characterized molecular alterations, pancreatic tumours can be presented as endocrine tumours (harbouring multiple endocrine neoplasia type 1-MEN1 mutations, amongst others) (Mingyi Chen, 2012), acinar cell carcinomas (harbouring APC/β-catenin mutations) and ductal adenocarcinomas (harbouring mutations in a wider range of genes, see 1.3.2, page 37 (Hezel, 2006) (Table 1).

Pancreatic cancer type	% of pancreatic cancers	Histological presentation	Genetic alterations	References
Endocrine tumours (Gastrinomas, Insulinomas, Glucagonomas, Somatostatinomas)	1-2%	Round to oval nuclei; Granules; Hormone production	MEN1; VHL, NF-1; TSC; Loss of 1 and 11q; Gain of 9q	(Mingyi Chen, 2012)
Acinar cell carcinoma	< 2%	Polygonal shape; Zymogen granules	APC/β-catenin	(Stelow et al., 2006b, Hezel, 2006)
Ductal Adenocarcinoma	> 85%	Ductal morphology; Desmoplasia	KRAS; TP53, SMAD4, p16INK4A	(Hezel, 2006)

Table 1 - Summary of the histological features and genetic alterations of pancreatic tumours

For the purposes of this thesis, only pancreatic ductal adenocarcinomas, from now on referred to as PDAC, will be addressed.

1.3 Pancreatic Ductal Adenocarcinoma (PDAC)

Comprising more than 85% of all pancreatic cancers, PDAC, whose name stems from its histological resemblance to ductal cells, is a devastating disease representing the fourth most common cancer-related death across the world (Hariharan et al., 2008). Contrasting with other tumour types, the increase in PDAC biology knowledge is not reflected in a improved patient outcome, where mortality mimics incidence rates (Jemal et al., 2008). Thus, although an overwhelming number of detailed and well-crafted studies have been conducted so far, much remains to be understood about the disease.

1.3.1 Clinical data and disease management

The absence of specific symptoms (abdominal pain and rare jaundice) and the aggressive nature of the disease, with early lymphatic and haematogenic dissemination to the lungs and liver (Schneider et al., 2008, Rhim et al., 2012), are the main contributors to the low prognosis of PDAC. Less than 4% of patients survive 5 years after diagnosis, due to presentation of unresectable cancerous tissue and presence of metastatic disease. Nonetheless, even in the manifestation of a localized tumour, a combination of surgery and chemotherapy only increases the 5-year survival to 20%, (Hezel, 2006).

Increased susceptibility to PDAC has been documented for some environmental and genetic factors such as advanced age, chronic pancreatitis, smoking, obesity, long-standing diabetes and familial history (Everhart, 1995, Fuchs, 1996, de Gonzalez et al., 2003, Schenk et al., 2001), with some risk factors showing a stronger evidence over others. Hereditary PDAC has been reported, which accounts for approximately 10% of all PDAC cases. If little is known about the genetic alterations that confer increased PDAC risk in a hereditary context, less is known about the initial causative mutations. Nevertheless, germline mutations in the tumour suppressors *INK4A*, *LKB1*, *MLH1*, the hereditary pancreatitis-causing gene *PRSS1* and the cystic fibrosis gene *CFTR*, have been reported (Whitcomb et al., 1996, Jaffee et al., 2002). Given the accentuated paracrine effect that exocrine dysfunctions, such as pancreatitis, might exert on normal tissue (by induction of reactive oxygen species and growth factor and cytokine-induced

responses), it is not surprising that familial pancreatitis, induced by mutations in the cationic trypsinogen gene *PRSS1*, appears to be the major risk factor, increasing PDAC risk by 50-fold in older patients (Lowenfels et al., 1997). The role of pancreatitis in PDAC onset will be discussed in detail in the thesis (see 1.5.2, page 71).

Initial detection methods rely on imaging by computed tomography (CT) coupled with intravenous administration of contrasting agents. Additional imaging approaches might be required if negative results are obtained (Hidalgo, 2010). Serological marker detection usually represents the least invasive approach for tumour diagnosis/monitoring. However, the search for PDAC specific biomarkers has constituted a challenge. The haematogenic presence of the tumour-associated antigen CA19-9 has been described as a biomarker for PDAC presence (Forsmark et al., 1994). However, non-specificity reports and the high percentage of false negatives compromises its value (Chan et al., 2014).

When PDAC is detected, staging is performed so that the therapeutic strategy can be outlined. Given the usually advanced stage of the disease at the time of diagnosis, and the complications of surgical procedures performed in aged patients, less than 15% of patients are candidates for surgical resection. Consequently, adjuvant and neoadjuvant therapies have been developed to improve prognosis. Response to chemotherapy has not been uniform for PDAC patients (Bittoni et al., 2014). Nonetheless, encouraging results have been obtained with pre-surgical FOLFIRINOX treatments, a combinatory treatment using fluorouracil (5-FU, pyrimidine analogue), irinotecan (topoisomerase I inhibitor), oxaliplatin (platinum-based antineoplastic agent, alkylating agent) and leucovorin (folinic acid) (Ferrone et al., 2015), or, more efficiently, Gemcitabine (nucleoside analogue) alone (Burris et al., 1997), or in a dual combination with either Erlotinib (HER1/EGFR tyrosine kinase inhibitor) (Moore et al., 2007) or cisplatin (platinum-based antineoplastic agent, alkylating-like agent) (Palmer et al., 2007).

Despite all efforts to improve treatment, the drastic PDAC stromal reaction, which, notwithstanding its possible role in slowing down tumour progression (Wang et al., 2014) forms a barrier impairing chemotherapy perfusion (Erkan et al., 2012), the low tumour vascularization (Olive et al., 2009) and the inherent cellular resistance to the drugs (Miranda-Lorenzo et al., 2014) compromise chemotherapy response. In order for

better neoadjuvant treatments to be generated, a deep understanding of PDAC molecular biology is crucial.

1.3.2 PDAC molecular genetics

Molecular analyses of patient derived PDAC have unravelled a comprehensive range of genetic alterations within these tumours. Advanced stage tumours are characterized by a marked aneuploidy, which might be the result of mutations in genomic stability regulator genes. Recent genetic analyses have identified at least 63 different gene alterations to be present and relevant in PDAC development/maintenance. Despite the fact that this overwhelming genetic variability culminates in the development of high inter- /intra-tumour heterogeneity, there is a consistency in the signalling pathways affected: apoptosis, DNA damage repair, cell-cell adhesion, invasion and cell cycle regulation (Jones et al., 2008). Some of the most common molecular abnormalities found in PDAC will be discussed below and include: mutations in the tumour suppressors *TP53*, *SMAD4* and *CDKN2A*, mutations in the *KRAS* proto-oncogene and de-regulations of pancreatic embryonic signalling pathways.

1.3.2.1 KRAS proto-oncogene and effector pathways

KRAS, named after Kirsten rat sarcoma viral oncogene homolog, where it was first described (E H Chang, 1982), is a small GTPase protein, consisting of 188 amino acids (approximately 21kDa), and it is involved in the intracellular transduction of extracellular signals. KRAS activity is tightly regulated by a switch between an active and inactive state, depending on the type of guanoside N phosphate it is bound to. Activation occurs upon binding to guanosine triphosphate (GTP) promoted by guanine nucleotide exchange factors (GEFs). The active, GTP-bound, KRAS undergoes conformational changes allowing it to interact with downstream effectors. At the same time, KRAS also interacts with GTPase-activating proteins (GAPs), which induce the removal of GTP by enhancing KRAS intrinsic ability to hydrolyse GTP into guanosine diphosphate (GDP) (Figure 5).

Upon stimulation of receptor tyrosine kinases (RTKs), and their consequent activation, the growth factor receptor binding (GRB2) adaptor protein, which under basal conditions is bound to the SOS domain of the GEF protein by the Src homology 3

(SH3) domain, is recruited to the plasma membrane and interacts with the RTK, via its SH2 domain. This leads to the proximity of the GEF with RAS and consequent formation of the RAS-GTP active complex (Rajalingam et al., 2007). When active, KRAS promotes transduction of cell surface-derived signals and activates a convoluted signalling cascade involving numerous pathways that culminate with a gene expression response that affects growth, differentiation and apoptosis (Figure 6).

KRAS point mutations, leading to KRAS activation, are found in almost all PDAC (over 90%) (Waddell et al., 2015) and mainly occur (98%) in codon 12 (exon 1), resulting in a amino acid change from Glycine (G) to either Aspartic acid (D) or Valine (V), referred to as G12D and G12V, respectively. These mutations impair the intrinsic hydrolytic activity, by blocking KRAS interaction with the GAP, which results in a constitutively active form of RAS with persistent signal transmission. Besides its overwhelming presence in late-stage PDAC, *KRAS* mutations are the first genetic alteration found in the early stages of tumour development, suggesting a key role in PDAC biology. Several mouse models have addressed PDAC requirement for *KRas* mutations showing that not only is it crucial for murine PDAC (mPDAC) initiation, it is also required for tumour maintenance. By means of a tetracycline inducible oncogenic KRas, it was possible to remove the oncogenic insult at different points. It was observed that silencing mutant KRas, at either early or late stages of tumour growth, halts mPDAC development with noticeable tumour regression (Collins et al., 2012a). Although the RAS protein is involved in the activation of numerous downstream signalling pathways, the canonical RAF/MEK/ERK and PI3K/PDK1/AKT pathways are the main ones involved in PDAC tumourigenesis (Eser et al., 2014).

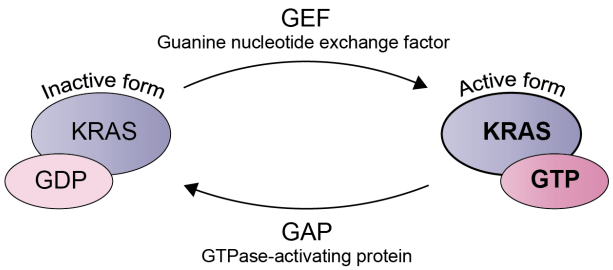

Figure 5 – The KRAS switch

Illustration of the switch between the inactive and the active form of KRAS. Inactive KRAS is bound to GDP. Guanine nucleaotide exchange factors catalyse the dissociation of GDP and the binding of GTP molecules. GTP-bound KRAS is active and promotes downstream signal transduction. Inactivation of KRAS occurs by GTPase-activating proteins that increase the rate of GTP hydrolysis.

1.3.2.1.1 RAF/MEK/ERK pathway

In a very simplified description, oncogenic KRAS activates the rapidly accelerated fibrosarcoma (RAF) serine/threonine-specific kinase, leading to consequent downstream phosphorylation and activation of the tyrosine/threonine kinase MEK (1/2). MEK activates, by phosphorylation, the extracellular signal-regulated kinase (ERK) protein (Seger and Krebs, 1995), and ERK phosphorylates downstream effectors modulating proliferation and other cellular functions (Figure 6). Members of this pathway are rarely mutated in PDAC. However, BRAF, a member of the RAF family, has been reported to be mutated in 7 to 15% of human PDAC. Interestingly, BRAF and KRAS point mutations are mutually exclusive, emphasizing the importance of this pathway for PDAC development. In the absence of KRAS mutations, BRAF mutations might be selected to activate the pathways (Calhoun et al., 2003). Additionally, activation of the pathway downstream of RAS by the constitutive expression of mutant BRAF ($BRAF^{V600E}$) in the embryonic pancreas, has demonstrated that this pathway alone is capable of PDAC formation, similarly to KRAS mutant mice (Collisson et al., 2012).

1.3.2.1.2 PI3K/PDK1/AKT pathway

In a very brief overview, phosphatidylinositol 3-kinase (PI3K) is composed of a catalytic p110 and regulatory p85 subunits. Activation of PI3K leads to the conversion of phosphatidylinositol 4,5-bisphosphate (PIP_2) into phosphatidylinositol 3,4,5-triphosphate (PIP_3), allowing PIP_3 to subsequently bind and activate the complex phosphoinositide-dependent kinase 1 (PDK1)/AKT. This activation can be inhibited by the phosphatase and tensin homolog (PTEN) protein that dephosphorylates PIP_3 to PIP_2. Activated serine/threonine-specific protein kinase AKT promotes cell survival and proliferation through modulation of the activity of several downstream effectors. Activation of the PI3K/PDK1/AKT pathway can be accomplished in three different ways: (1) activated RTKs promote the binding of the PI3K-p85 domain to their phospho-YxxM motif triggering p110 activation; (2) GRB2 proteins bind to scaffolding proteins and the complex binds to p85; (3) interestingly, activation of the RAS pathway

also activates PI3K-p110 domain independently of p85 (Castellano and Downward, 2011) (Figure 6).

Despite the absence of point mutations in components of this pathway in human PDAC, strong evidence supports its crucial role in PDAC development and maintenance. It has been observed that PDAC cell lines and tumour tissue samples exhibit low expression of the tumour suppressor PTEN. Methylation-specific PCR analyses have suggested promoter methylation to be the main cause of PTEN downregulation. The consequent AKT activation was shown to lead to increased cell proliferation that could be counteracted by the PI3K inhibitor, LY294002 (Asano et al., 2004). Moreover, constitutive *in vivo* pancreatic expression of an active form of PI3K ($PIK3CA^{H1047R/+}$), which presents a mutation in the catalytic domain of p110α, was demonstrated to generate PDACs, phenocopying the observations obtained with mouse models with *KRas* oncogenic pancreatic expression (Eser et al., 2013). These results were further strengthened by inhibition of this pathway in mutant KRas-derived murine PDAC. Genetic deletion of PDK1 (AKT activatior upon PIP_2 to PIP_3 conversion) abrogated $KRas^{G12D}$-induced PDAC formation, while the loss of Craf, component of the RAF/MEK/ERK pathway, in $KRas^{G12D}$ mouse model of PDAC had no inhibitory effect in PDAC formation (Eser et al., 2013).

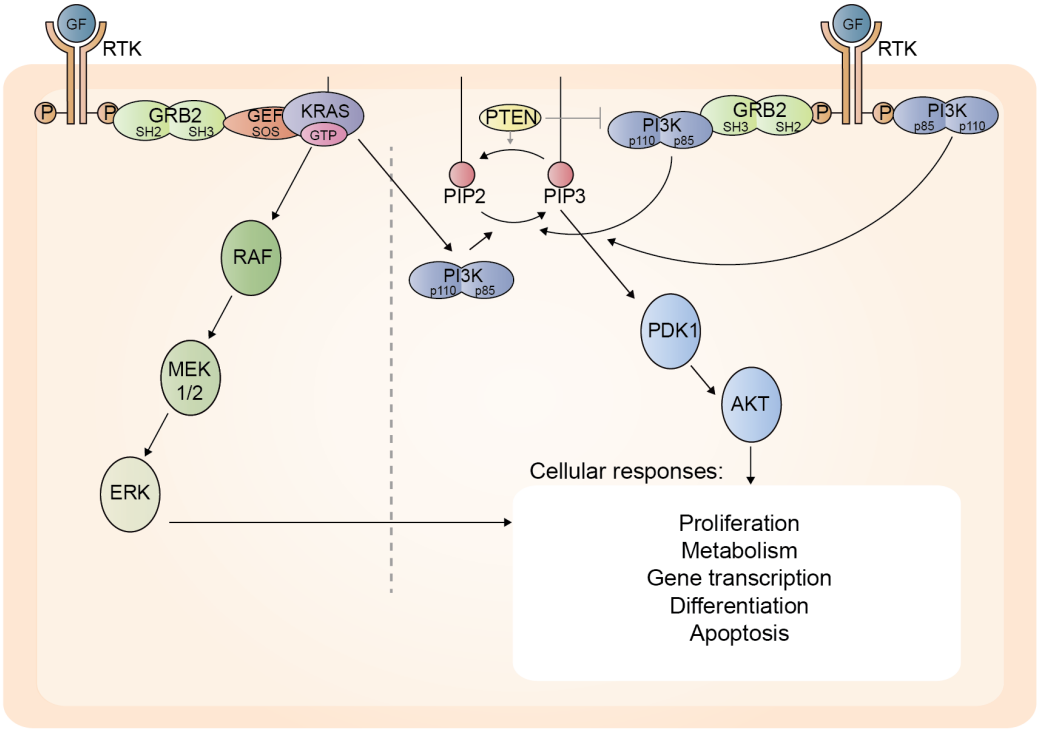

Figure 6 – RAS signalling via RAF/MEK/ERK and the PI3K pathway

The figure provides a simplified overview of RAS canonical signalling and its interaction with the PI3K pathway. Activation of KRAS occurs by growth factor (GF) binding to receptor tyrosine kinases (RTK). Active KRAS (GTP) signals downstream to RAF/MEK/ERK. The PI3K signalling pathway can be activated by RAS or independent of RAS. Active PI3K promotes PIP3 formation from PIP2 and initiates downstream activation of PDK/AKT. PTEN can inhibit PI3K-dependent signalling.

1.3.2.2 The *CDKN2A tumour suppressor*

The ability to escape checkpoints during the cell cycle is a very important feature of tumour cells. For this reason, cell cycle regulators are commonly altered in human cancers. Cell cycle initiation, and progression, roughly depends on the formation and activation of complexes containing the following proteins: cyclins and cyclin-dependent kinases (CDKs). These proteins are the main regulators of the cell cycle. Nonetheless, they are also a target for regulation by CDK inhibitors. Two inhibitor families have been described based on their structure and CDK specificity: the CIP/KIP family and, the focus of this sub-chapter, the INK4/ARF family (Lim and Kaldis, 2013).

One of the most studied CDK inhibitors is the cyclin-dependent kinase inhibitor 2A (CDKN2A), which is involved in the inhibition of the G1/S phase transition of the cell cycle. This gene encodes 2 proteins: $p16^{INK4a}$ and $p14^{ARF}$ (or $p19^{ARF}$ in mice) derived from alternative splicing. The different proteins generated by the *CDKN2A* gene have independent functions in regulating cell cycle progression. While $p16^{INK4a}$ inhibits the phosphorylation of the Retinoblastoma (Rb) protein by the complex cyclin1-CDK4/6, which is required for G1-S progression in the cell cycle, $p14^{ARF}$ inhibits mouse double minute 2 homologue (MDM2)-dependent proteasomal degradation of p53, stabilizing it (Kim and Sharpless, 2006) (Figure 7).

Preliminary indication of the involvement of *CDKN2A* in pancreatic cancer arose from the higher familial predisposition to PDAC development in *CDKN2A* germline mutation-harbouring siblings (Whelan et al., 1995). In depth analysis of sporadic PDAC revealed an overwhelming representation (over 80% of PDAC) of *CDKN2A* inactivation (Rozenblum et al., 1997). These mutations have been documented, in PDAC, to affect $p16^{INK4a}$ alone or both $p16^{INK4a}$ and $p14^{ARF}$, while mutations affecting only $p14^{ARF}$ have never been observed. The occurrence of these mutations has only been described for advanced PDAC, positioning them as a later requisite for PDAC development. In line with the observation, the genetic ablation of both $p16^{INK4a}$ and $p19^{ARF}$, in the mouse pancreas, had a drastic synergistic effect on PDAC progression when combined with KRAS embryonic oncogenic activation. However, deletion of the tumour suppressors alone failed to promote tumourigenesis excluding them as PDAC drivers (Aguirre, 2003).

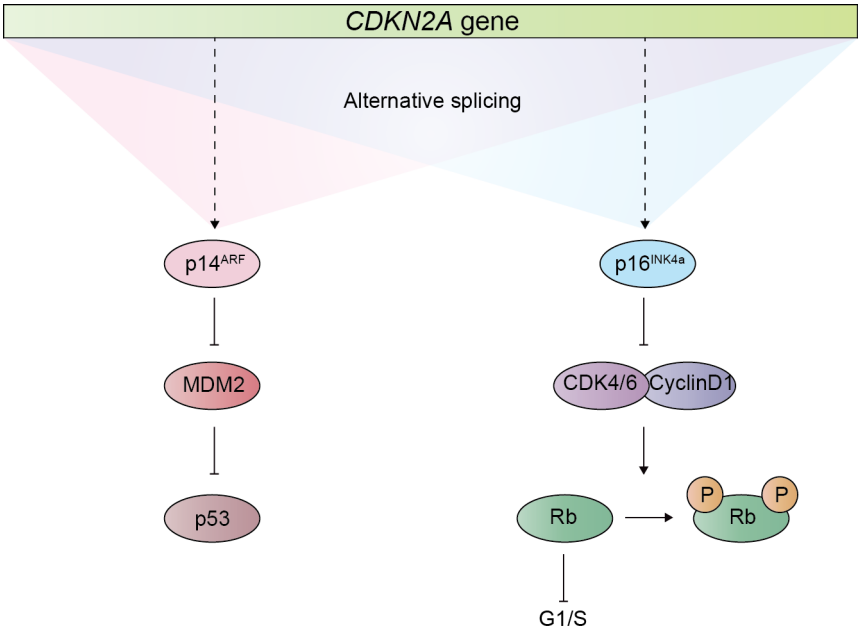

Figure 7 – The *CDKN2A* tumour suppressor gene and encoded proteins

The figure provides a simplified view of the two main protein encoded by the *CDKN2A* gene, products of alternative splicing. *CDKN2A* encodes $p14^{ARF}$ and $p16^{INK4a}$. Protein $p14^{ARF}$ inhibits MDM2-dependent p53 proteasomal degradation. Protein $p16^{INK4a}$ inhibits CDK4/6-dependent Rb phosphorylation. This step is required to release inhibitory Rb function over E2F and promote consequent G1/S progression of the cell cycle.

1.3.2.3 The *TP53 tumour suppressor*

The p53 protein, also referred to as the gardian of the genome, is a potent tumour suppressor involved in the regulation of a vast number of key cellular features. Activation of this protein can be initiated by different stimuli that induce cellular stress, leading to induction of numerous cellular responses including differentiation, DNA damage repair, cell cycle arrest, apoptosis and senescence, among others. Given the protein's broad impact on cellular biology, extensive and thorough studies have been performed to understand how this protein is regulated and to shed light on the mechanisms by which it exerts its effect. However, a comprehensive knowledge is still yet to be achieved. p53 functions, mainly, as a transcriptional regulator, inducing or repressing gene expression upon activation. Stimuli lead to p53 binding to DNA with consequent promotion/repression of expression of downstream effectors involved in the above-mentioned cellular responses. Nevertheless, p53 has also been shown to harbor some transcriptionally-independent functions, mainly for apoptotic responses (Vogelstein et al., 2000).

Regulation of p53 is a critical step for maintenance of cell viability. Levels of this protein are tightly controlled by transcriptional and post-translational mechanisms. The key p53 post-translational regulator is MDM2. The *MDM2* gene encodes an E3 ubiquitin-ligase protein. By promoting the addition of ubiquitin chains to the target protein, E3 ligases generate the critical signal for proteasome-dependent protein degradation. Hence, MDM2 facilitates p53 ubiquitination, inducing its degradation by nuclear and cytoplasmic proteasomal degradation (Figure 8). A further regulatory mechanism has been observed for MDM2, as it is able to physically bind to the NH2-terminal domain of p53, directly inhibiting its transcriptional activity (Moll and Petrenko, 2003, Oliner et al., 1993). A third layer of complexity is achieved with p53's ability to transcriptionally regulate MDM2. This creates an autoregulatory negative feedback loop with p53 regulating MDM2 expression and MDM2 regulating p53 protein stability and function (Figure 8). Thus activation of a p53-dependent response can be achieved by the induction of post-translational modifications that promote conformational changes allowing the protein to evade MDM2-dependent degradation. Conversely, activation can also be promoted by induction of changes on the MDM2 protein impairing its ability to recognise p53 (Moll and Petrenko, 2003).

The protein p53 was initially implicated in tumour progression due to the observation that a familial condition caused by p53 mutations, Li-Fraumeni syndrome, led to increased susceptibility to tumour development. It was later described that this disease is a rare autosomal-dominant disorder that relies on germline inactivating mutations of the *p53* and *CHEK2* genes, the latter being able to stabilize p53 (Marielle WG Ruijs, 2009, Srivastava et al., 1990). Additional evidence from mouse models indicated that the absence of p53 protein, by generation of a mouse harbouring a homozygous p53 null allele, greatly increases spontaneous tumour susceptibility (Donehower et al., 1992). Nowadays, it is known that aberrant expression of *p53* is one of the most common features of human cancers, with point mutations being observed in 50% of these tumours (Freed-Pastor and Prives, 2012).

Mutations in *p53* are also extremely common in PDAC patients. While no *p53* mutation has been observed in early phases of disease development, more than 80% of the later stage tumours harbour p53 aberrant expression (Rozenblum et al., 1997). The late presentation of *p53* mutations, together with their high incidence in PDAC and the fact that Li-Fraumeni syndrome patients do not present pancreatic cancer, led to the suggestion that this gene could be more important for PDAC progression rather than initiation. Confirming the hypothesis, whole body genetic ablation of p53, both heterozygous and homozygous, using mouse models, failed to give rise to pancreatic tumours. However, it drastically promoted the formation of malignant lymphomas and sarcomas (Donehower et al., 1992). Moreover, the expression of a gain of function mutant form of p53 ($Trp53^{R172H}$), present in human PDAC, failed to induce PDAC formation by itself. Nonetheless, it demonstrated a drastic synergistic effect when concomitantly expressed with oncogenic $KRas^{G12D}$ (Hingorani et al., 2005).

PDAC is characterized by an intricate landscape of abnormalities. Detailed analyses of human samples have documented a step-wise acquisition of chromosomal aberrations that would initiate the activation of cell cycle checkpoints and, consequently, hinder cell survival and proliferation. Thus, it is likely that p53 inactivation confers a clear growth advantage on tumour cells.

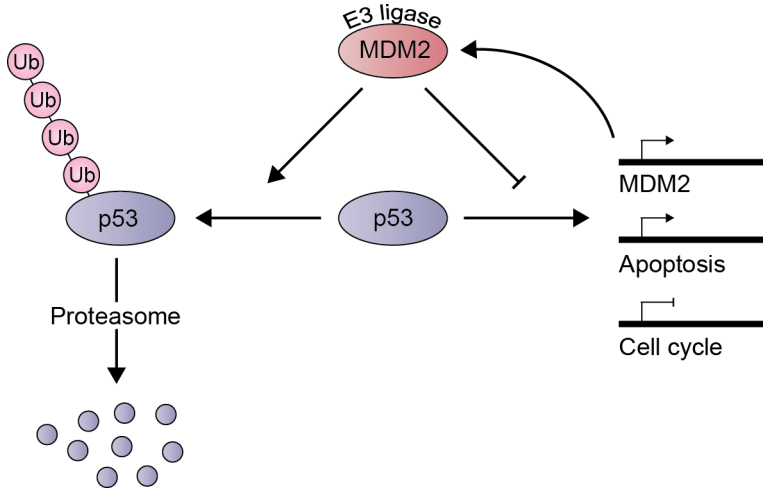

Figure 8 – MDM2-p53 regulation (feedback loop)

Simplified illustration of p53 regulation and the feedback loop. The E3 ligase MDM2 targets p53 for proteasomal degradation. MDM2 is also able to directly bind to p53, inhibiting its transcriptional activity. The protein p53 functions mainly as a transcriptional regulator, repressing cell cycle progression genes and promoting the expression of apoptotic genes and of its own regulator MDM2.

1.3.2.4 SMAD4 and TGFβ signalling

SMAD4 (mothers against decapentaplegic homolog 4), also known as "deleted in pancreatic carcinoma locus 4" (DPC4), is a fundamental component of the transforming growth factor-β (TGFβ) family. The TGFβ signalling pathway plays a crucial role in modulating key cellular responses including tissue morphogenesis, apoptosis, proliferation and differentiation. The TGFβ pathway can be activated by various different ligands, including bone morphogenetic proteins (BMPs), growth and differentiation factors (GDFs), anti-müllerian hormone (AMH), activin, nodal and TGFβ (Weiss and Attisano, 2013). However, for the purpose of understanding the pathway and its involvement in pancreatic cancer, a simplified view will be provided.

Two types of cell surface serine/threonine kinase receptors detect TGFβ signals, type I and type II. Upon external signal stimulation, and consequent formation of a heterotetrameric complex, the receptor II, which is constitutively phosphorylated, phosphorylates receptor I, activating it for signal transduction. Signal transduction is carried out by type I receptor substrates called SMAD proteins, referred to as SMADs from hereafter. There are different types of SMADs responsible for signal transduction of specific signals and with different modes of action: receptor-regulated SMADs, coSMADs and antagonistic SMADs. SMAD1, 2, 3, 5 and 8 are designated receptor-regulated SMADs, as they are direct substrates of the TGFβ-family receptor. Regarding their function, while SMAD2 and SMAD3 are involved in signalling stimulated by TGFβ's, activins, and nodals, SMAD1, SMAD5 and SMAD8 transduce BMP-derived stimuli. On the other side of the spectrum, antagonistic SMAD6 and SMAD7 inhibit the activating function of receptor-regulated SMADs. Despite the distinctive roles of receptor-regulated SMADs, all of them associate with a coSMAD to be able to translocate to the nucleus and regulate transcription. The only known coSMAD is SMAD4, making it a key component of the TGFβ signalling pathways (Figure 9) (Massagué, 1998).

Another important feature to be mentioned is the ability of this pathway to stimulate activation of other equally important signalling pathways, such as the RAS signalling pathway. RAS pathway activation occurs independently of SMADs. Despite being a serine-threonine kinase, TGFβ receptor II can also autophosphorylate tyrosine residues, although inefficiently. Moreover, it can also be tyrosine-phosphorylated by Src proteins.

This tyrosine phosphorylation constitutes a docking site for the SH2 domain of the GRB2 adaptor protein, initiating the RAS signalling cascade (Figure 9) (Zhang, 2009).

As the name indicates, *DPC4* (*SMAD4*) is frequently lost in pancreatic cancers. It was initially observed that 90% of PDAC harbours allelic loss at chromosome 18q. Detailed genetic mapping of a wide range of pancreatic tumours enabled the identification of a consensus lost region at 18q21.1, where *SMAD4* is located (Hahn et al., 1996). Following the identification of the tumour suppressor, it has been observed that *SMAD4* is lost in about 30% of PDAC, although its expression is reduced in about 55% of PDACs due to additional inactivating mutations (Iacobuzio-Donahue et al., 2000b). Loss of *SMAD4* expression is a late event in PDAC tumourigenesis (Wilentz et al., 2000), thus attributing a tumour progression-related role to the protein. Supporting the hypothesis is the observation that blocking the TGFβ signalling pathway, by genetic deletion of either TGFβ receptor type II or SMAD4 in mouse pancreas, has no effect in tumour formation, unless in combination with oncogenic KRAS, where it accelerates tumour onset (Ijichi et al., 2006, Bardeesy et al., 2006b).

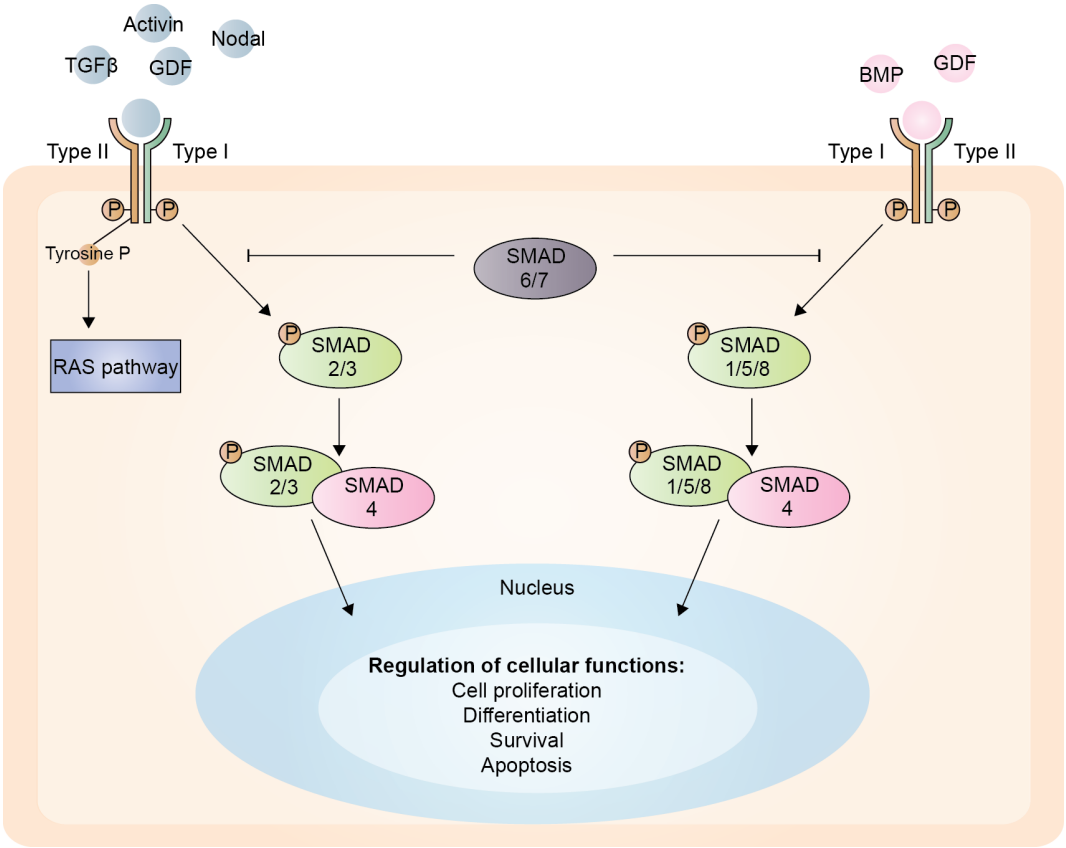

Figure 9 – TGFβ and BMP signalling

Simplified illustration of TGFβ and BMP signalling. Upon receptor activation receptor-regulated SMADs (green) get phosphorylated and associate with the coSMAD4 (pink). This complex is translocated to the nucleus where it transcriptionally regulates several cellular functions. The signal can be blocked by the inhibitory activity of antagonistic SMADs 6 and 7. Type II receptors can also, inefficiently, activate the RAS pathway.

1.3.2.5 NOTCH pathway and FBW7 regulation

During tumourigenesis, cells acquire the ability to re-enter cell cycle and modulate their own growth, as well as the microenvironment. It is thought that tumourigenesis roughly recapitulates embryonic development. Hence, it is not surprising to find de-regulated embryonic pathways in cancer cells. One important pathway activated in PDAC is the Notch signalling pathway (Jones et al., 2008).

The NOTCH pathway is a highly conserved pathway responsible for the mediation of short-range signals, whose function is crucial during embryonic development and adulthood. Although it is mainly known to participate in cell fate decisions, NOTCH is also involved in survival and cell cycle regulation, under specific signals. It is functional in different cell types, promoting different cellular responses. Therefore, and highlighting its importance, genetic alterations in this pathway lead to a long list of human disorders and cancers (Andersson et al., 2011).

There are 4 Notch receptors, NOTCH1, NOTCH2, NOTCH3 and NOTCH4. These receptors are located at the cell surface and are composed of: (1) extracellular EGF-like repeats (EGF-LR) enabling receptor/ligand interactions; (2) LIN-NOTCH repeats (LNR) adjacent to the membrane which modulate the interaction between the receptor's extracellular and intracellular domains; (3) a RBPJ-associated molecule (RAM) domain (4) six intracellular ankyrin repeats (which enable protein-protein interaction) flanked by nuclear localisation signals (NLS); (5) a PEST domain responsible for rapid protein degradation, preventing the signal peptide from long lasting signal transmission; and (6) a transactivation domain (Figure 10a). NOTCH receptors respond to two types of ligands: Delta-like and Jagged/Serrate. NOTCH ligands are transmembrane proteins and thus, in order for Notch signal activation, cell-cell contact is required. There are 3 Delta-like ligands, Delta1, Delta3 and Delta4, and 2 Jagged ligands, Jagged1 and Jagged2. Although structurally different, both ligand types share a Delta Serrated and Lag2 (DSL) domain that mediate the interaction between the ligand and the EGF-like repeats of the receptors. Upon ligand/receptor interaction, the receptor exposes an extracellular cleavage site susceptible to the protease activity of the transmembrane proteases ADAM10 (A desintegrin and metalloprotease 10) and ADAM17, also known as TACE (tumour necrosis factor-α converting enzyme). This step is followed by another cleavage mediated by a membrane protein, designated ɣ-secretase, leading to the release

of the NOTCH receptor intracellular domain (NICD) to the cytoplasm. NICD contains nuclear localisation signals allowing it to be translocated to the nucleus, where it binds to RBP-J (Fiúza and Arias, 2007). In the absence of activated Notch, RBP-J is bound to DNA exerting a repressive effect on gene transcription. However, upon Notch activation, NICD binds to RBP-J, inducing the recruitment of transcription co-activator mastermind-like (MAML). The formation of the complete complex ultimately leads to transcription of NOTCH targets; the best studied so far being the transcriptional repressors HES (1 and 5) and HEY1 (Figure 10b). Following transcription, HES and HEY lead to repression of differentiation and promotion of proliferation (Borggrefe and Oswald, 2009).

As mentioned before, the NOTCH pathway is implicated in tumourigenesis. Similarly, the role of NOTCH in PDAC biology has been described. By comparing normal tissue expression with pancreatic precursors, Miyamoto and co-workers have detected that several members of the pathway were upregulated in early stages of PDAC, both at the RNA and protein level, with consequent upregulation of the transcriptional target HES1. Moreover, ectopic NOTCH activation in normal pancreas explant cultures led to the *in vitro* generation of PDAC precursors – ADM (see 1.6.2, page 74) (Miyamoto et al., 2003). Additionally, it has been documented that a panel of PDAC cell lines treated with ɣ-secretase inhibitor (GSI) have reduced proliferation indexes and reduced colony formation ability in soft agar compared with untreated cultures. When GEM models harboring a heterozygous deletion of the tumour suppressor p53 with concomitant KRas oncogenic activation in the embryonic pancreas were treated with GSI after precursor lesions were observed, they exhibited a reduction in the progression from precursors to PDAC (Plentz et al., 2009).

Given the broad cellular responses that NOTCH modulates, its regulation has to be extremely tight. Different responses might be achieved depending on the level of activation. This hypothesis was originated due to the observation that, unlike most signalling pathways, the NOTCH pathway does not exhibit an intracellular signal amplification. Instead, a stoichiometric relationship is observed, where one ligand binds to the receptor, releasing one downstream effector. Additionally, post-translation regulation ensures a proper signal transduction by enhancing activation or inducing

repression of the pathway. For the purposes of this thesis, only proteasome-mediated regulation by the protein FBW7 will be discussed.

The FBW7 protein is an F-box component of the S-phase-kinase-associated protein-1 (SKP1)-cullin-1 (Cul1)-Fbox protein (FBP) (SCF)-type E3 ubiquitin ligases, members of the ubiquitin-proteasome system (UPS). The UPS is an important pathway that allows quick and regulated protein degradation. Due to its ability to alter protein levels, it is crucial for cellular homeostasis and signal response. The initiation of the pathway is dependent on the activation of ubiquitin protein (Ub) by an E1 Ub-activating enzyme, in an adenosine triphosphate (ATP)-dependent manner. The activated Ub is then transferred to an E2 Ub-conjugating enzyme. Lastly, an E3 ligase promotes the transfer of the activated Ub to a specific substrate, establishing the protein degradation signal (Ravid and Hochstrasser, 2008).

Protein degradation is a highly selective event, relying on the identification of specific substrates. In the case of SCF-type E3 ligases, the F-box protein provides such specificity. Although different classes of F-box proteins have been described, only FBWs will be discussed. As the name indicates FBWs are WD-40 repeat containing-F-box proteins. These repeats form a circularized β-propeller that recognizes serine and threonine phosphorylation signals at specific consensus sequences (phosphodegrons) (Cardozo and Pagano, 2004).

The list of substrates of the FBW7-containing E3 ligase is ever-growing. Some of the substrates identified include c-Myc, cyclin E, NOTCH, c-Jun, and Mcl-1 (Figure 10b). Given its main targets, FBW7 has been described as a potent tumour suppressor and plays a major role in cell differentiation, proliferation and maintenance of genomic stability. *FBW7* deletion and the consequent increase in downstream targets has been implicated in several human cancers (Cheng and Li, 2011, Sancho et al., 2010). However, its relevance in PDAC biology has been poorly addressed. The first report of FBW7 deregulation in PDAC was submitted by Calhoun and co-workers, who have identified that 6% of PDAC present cyclin E overexpression partially due to inactivating mutations in the *FBW7* gene (Calhoun et al., 2003). Additional studies also described a link between the RAS pathway and FBW7 by demonstrating that Ha-RAS activation inhibits FBW7-dependent cyclin E degradation (Minella et al., 2005).

Nonetheless, FBW7 involvement in PDAC biology, as well as its role in mediating NOTCH de-regulation in PDAC, is still an open question.

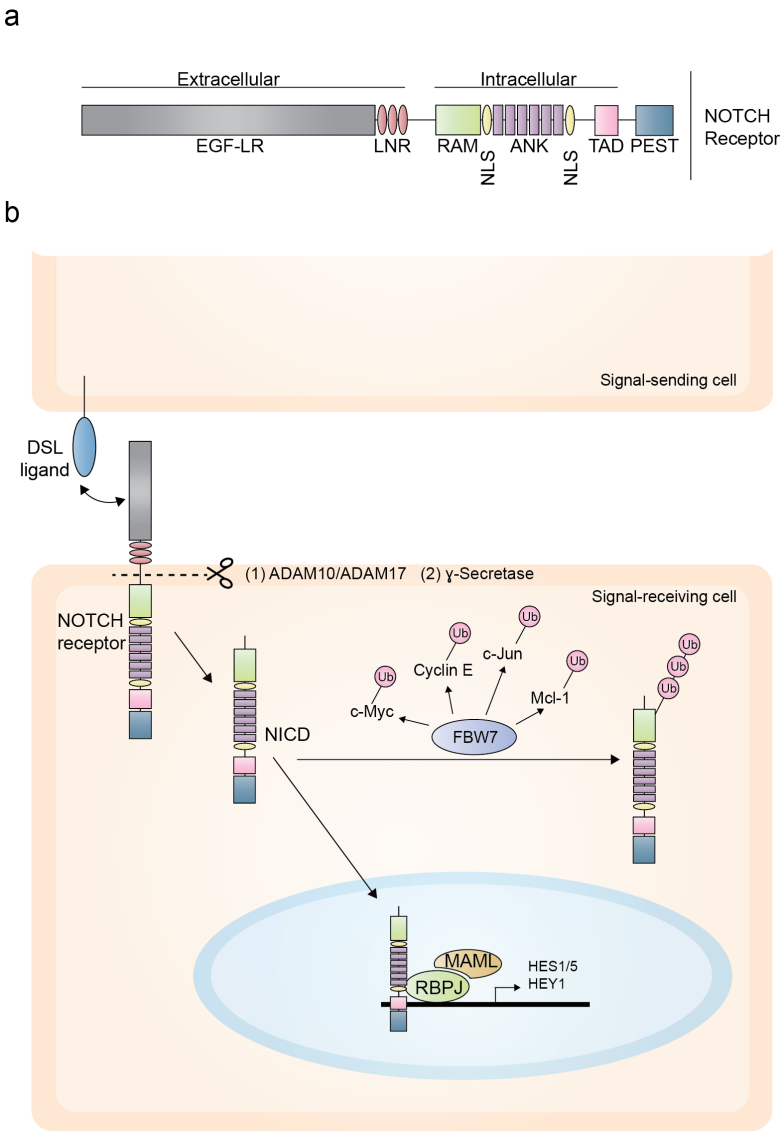

Figure 10 – The NOTCH signalling pathway and FBW7

a) Schematic representation of the domains present in the NOTCH receptor. EGF-LR – EGF-like repeats. LNR – LIN-NOTCH repeats. RAM - RBPJ-associated molecule domain. NLS – Nuclear localisation signal. ANK – ankyrin repeats. TAD – transactivation domain. PEST – protein degradation domain **b)** Simplified illustration of the NOTCH signalling pathway and FBW7-dependent degradation of substrates. NOTCH ligands are present at the surface of neighbouring cells, thus, cell to cell contact is crucial. Upon binding of the NOTCH receptor (via EGF-LR) to the DSL region on the ligand, the transmembrane domain gets cleaved by ADAM10/ADAM17 and γ-secretase. The intracellular domain (NICD) is released to the cytoplasm, translocated to the nucleus and forms a complex with RBPJ and MAML. This transcription-activating complex leads to expression of transcriptional repressors (HES1/5 and HEY). FBW7 provides a post-translational regulation of NOTCH and additional proteins by proteasome-dependent degradation.

1.4 Morphological clinical presentation of PDAC and precursor lesions

At the time of diagnosis, PDAC patients already exhibit an advanced stage of the disease. Low response to chemotherapy and high aggressiveness impair any chance of patient survival. Great knowledge has been gained on the molecular requirements for PDAC development and maintenance. However, despite the use of this information in the improvement of chemotherapy, little success has been obtained (Bittoni et al., 2014). Therefore, better understanding of the initial events leading to PDAC onset and the comprehension of its precursor lesions are crucial to improve early detection and change current survival figures.

Following the development achieved for other tumour types, a progression model has been proposed for pancreatic cancer (Hruban et al., 2000a). Based on morphological and histological analysis, lesions with increased cellular atypia have been described. These lesions were postulated as precursors of PDAC based on their genetic alteration landscape (Cubilla and Fitzgerald, 1976). Observations made so far have identified 4 types of neoplastic precursors which can present a convergent evolution towards PDAC: intraductal papillary mucinous neoplasia (IPMN); pancreatic mucinous cystic neoplasm (MCN), intraductal tubular papillary neoplasm (ITPN) and pancreatic intraepithelial neoplasia (PanIN) (Hruban et al., 2007).

These lesions have been detected and documented before nomenclature was established. Hence, it is very common to find different references to these morphological entities, such as “lesions”, “metaplasias”, “hyperplasias” and “dysplasias”. The absence of a universal classification hampered the identification and consequent distinction of these independent precursors. To address this issue, the “Pancreas Cancer Think Tank” meeting, involving several experts, was held in 1999 to generate a standard categorization (Kern et al., 2001). A consensus nomenclature, and mode of operation for diagnosis, was generated. Nevertheless, there is still great controversy and difficulty in the distinction between lesions.

1.4.1 Intraductal Papillary Mucinous Neoplasm (IPMN) precursor

IPMNs were initially described as rare mucin-secreting pancreatic cancers. Nowadays, they are classified as infrequent cystic pancreatic lesions. On a morphological and histological level, IPMNs, as the name indicate, are characterized by a columnar epithelium with a papillary architecture and detectable mucin (Muc) production, identified by either immunohistochemistry or alcian blue/periodic acid-Schiff stain (AB/PAS). They consist of large legions (≧1cm), usually detectable by medical imaging techniques, such as computed tomography (CT) and magnetic resonance imaging (MRI), and are thought to generated from the increased proliferation of the main pancreatic duct epithelium or major branches. Concerning their clinical significance, it has been observed that one third of patients harbouring IPMNs progress to invasive carcinoma. As mentioned before for precursor lesions in general, there is an on-going discussion for the classification of these lesions (Cooper et al., 2013). Several subtypes of IPMNs have been described based on histological features and mucin expression. However, the diversity reported might be overestimated as some of the identified lesions have similar features but appear to be classified under different names. According to World Health Organization (WHO) Classification of Tumours of the Digestive System, there are four types of IPMNs with different grades of dysplasia: Gastric, Intestinal, Pancreatobiliary and Oncocytic (Hamilton and Aaltonen, 2000) (Table 2). Given the variable classification, several attempt were made to fully characterize IPMN subtypes (Yonezawa et al., 2008, Cooper et al., 2013, Distler et al., 2014), which will be summarised below:

Gastric IPMN, the most common subtype and presenting low-grade dysplasia, is characterized by a papillary columnar epithelium with mild atypical nuclei located basally and supranuclear mucin production. While other IPMN are thought to be mainly formed from the main duct, the gastric type is found on branching ducts. It is very similar to another low-grade precursor, PanIN-1 (see 1.4.4, page 59), being separated from this lesion on the basis of size and location within the ductal network. Gastric IPMN are larger lesions than PanINs. Regarding mucin production, these lesions express Muc5ac (a secreted mucin) and Muc6 (membrane mucin) but do not express

Muc1 and Muc2 (membrane-associated mucins). From a clinical point of view, the gastric subtype rarely progresses to invasive carcinoma (Figure 11a).

Intestinal IPMN, originating in the main duct and with low to intermediate dysplasia, resembles colorectal villous adenoma for its morphological appearance and mucin expression. These lesions are characterized by long papillae composed of columnar epithelium with oval and elongated nuclei. The level of dysplasia is higher compared to the gastric type, thus, it is not surprising that their association with invasive carcinoma, mainly to colloid (mucinous noncystic) pancreatic carcinoma, is greater (20 to 40%). Regarding mucin expression for immunologic diagnosis, intestinal IPMNs express the intestinal marker CDX-2, Muc2 and Muc5ac, being negative for Muc1 and Muc6 (Figure 11b).

Pancreatobiliary IPMNs present high-grade dysplasia, being commonly associated with invasive carcinoma, and are characterized by the presence of complex branching papillae, lined by a cuboidal epithelium containing round nuclei. Similarly to the intestinal type, pancreatobiliary IPMNs have their origin in the main duct. These lesions exhibit Muc1 and Muc5ac expression, being negative for Muc2 (Figure 11c).

Oncocytic IPMNs, the rarest type of IPMNs, are very similar to the pancreatobiliary type regarding histo- and morphologic features, with a complex branching of the epithelium. However, they exhibit a large number of goblet cells and cells with denser cytoplasm. Inconsistent data has been gathered regarding their mucin production. However, they appear to express Muc5ac and Muc6 (Figure 11d).

IPMN subtype	Origin (duct)	Immunologic diagnosis	Level of dysplasia
Gastric	Branching	$Muc5ac^+$ $Muc6^+$	low/mild
Intestinal	Main	$Muc5ac^+$ $Muc2^+$ $CDX\text{-}2^+$	high
Pancreatobiliary	Main	$Muc5ac^+$ $Muc1^+$	high
Oncocytic	Main	$Muc5ac^+$ $Muc6^+$	high

Table 2 - Summary of IPMN subtypes and main features

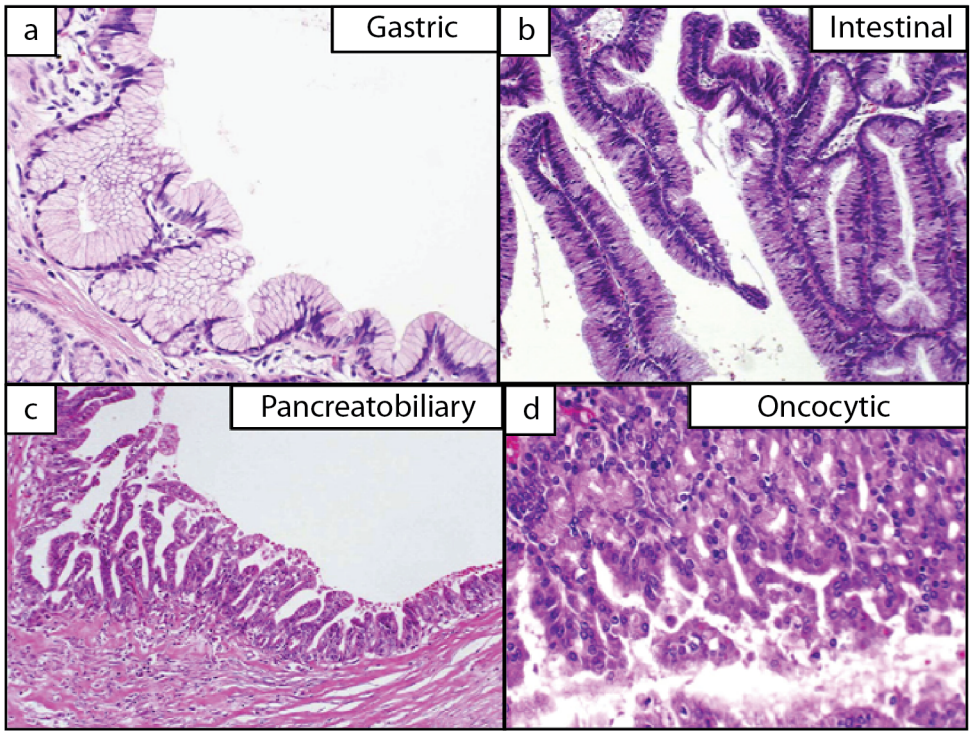

Figure 11 – Histological features of IPMN subtypes

a) H&E of gastric IPMN showing papillary columnar epithelium with basally oriented nuclei and abundant supranuclear cytoplasm. b) H&E of intestinal IPMN showing long papillae composed of columnar epithelium and pseudostratified nuclei. c) H&E of pancreatobiliary IPMN showing branching papillae lined by cuboidal cells. d) H&E of oncocytic IPMN showing complex arborizing papillae composed of cuboidal and columnar cells. Adapted from Tanaka et al., 2012 with permission from Elsevier (see Chapter 6, Appendix)

1.4.2 Pancreatic Mucinous Cystic Neoplasm (MCN) precursor

MCN lesions are the least common neoplastic precursors found in pancreatic cancer patients, although they are the largest (median size between 60 and 100 mm). Similar to IPMNs, MCNs are cystic lesions with high mucin production presenting Muc5ac and Muc2 expression. However, they have no detectable connection to the ductal network and occur in the body or tail of the pancreas. Detection of these lesions is usually accidental and presents a favourable prognosis. Nevertheless, reports have suggested a worse prognosis in comparison to IPMNs (Hamilton and Aaltonen, 2000). Histologically, MCNs present a flat columnar epithelium with occasional papillae and a fibrous pseudocapsule (Figure 12). Cells have expanded cytoplasm with nuclei located basally and supranuclear mucin production. The level of dysplasia can vary from low to high and progression culminates in PDAC. They can be readily distinguished by the presence of an ovarian-like stroma, which is their main diagnostic feature (Distler et al., 2014, Cooper et al., 2013, Yonezawa et al., 2008).

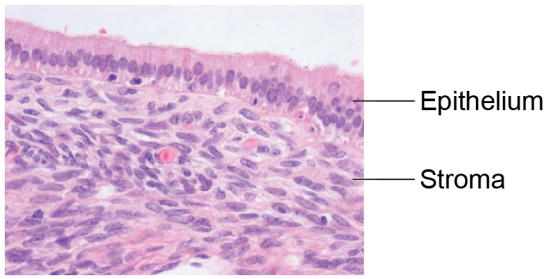

Figure 12 – Histological features of MCN lesions

H&E of MCN showing flat columnar epithelium and underlying ovarian type stroma. Adapted from Distler et al., 2014. For permission of use see Chapter 6, Appendix.

1.4.3 Intraductal Tubular Papillary Neoplasm (ITPN) precursor

Recently, as a consequence of sub fragmenting the IPMN category, a new precursor lesion has been included to the list by the WHO, entitled intraductal tubular papillary neoplasm. Abundant, and localized tubular nodules, with little mucin production, characterize this neoplasm. These lesions are highly dysplastic and somewhat resemble the pancreatobiliary IPMNs. However, the prognosis is relatively favourable. The recent established nomenclature, and its underrepresentation within exocrine neoplasias (0.9%), impairs the proper definition of this lesion. Nonetheless, reports so far indicate that it is located in the main duct or major branches and can be found throughout the pancreas (head, body and tail). Cells can be cuboidal or columnar, arranged in a cribriform epithelium, with round nuclei. Although mucin production is low, as assessed by the almost absent AB/PAS stain, membrane-associated mucins present in PDAC are also present in the pre-neoplastic precursor, such as Muc1 and, less frequently, Muc6 (Cooper et al., 2013).

1.4.4 Pancreatic Intraepithelial Neoplasia (PanIN) precursor

By far the most common pre neoplastic PDAC precursor, and the most thoroughly studied, is the pancreatic intraepithelial neoplasia. Being the first documented pre-neoplastic lesion, the variability in its classification is not unexpected. Similarly to the approach undertaken for other precursors, a consensus was generated for diagnosis and classification of PanINs (Hruban et al., 2001). According to several reports, PanINs are microscopic lesions (<5mm) that occur mainly in intralobular ducts.
A sub classification for PanINs has also been proposed and, despite the fact that, in broad terms, all PanINs express the same mucins (Muc1, Muc6 and Muc5ac), they can be distinguished by their increased degrees of architectural and cytological atypia (Table 3) (Yonezawa et al., 2008, Hamilton and Aaltonen, 2000).

PanIN1 is the earliest stage of PanIN development with low-grade dysplasia. In the human it can be subdivided into two different types (1A and 1B) according to its architecture. However, such distinction is not made in the mouse where only PanIN1 is

reported. As mentioned before, PanIN1 resembles the gastric IPMN, but can be distinguished from these lesions based on their smaller size.

PanIN1-A is characterized by a flat epithelium composed of cells with a prominent enlargement of the cytoplasm (columnar) towards the lumen and nuclei located basally (Figure 13). Abundant mucin is produced and, thus, it can be clearly identified at early stages of development by AB/PAS stain. It is a fairly common lesion being observed in 40% of the pancreata not presenting invasive carcinoma (Figure 13).

PanIN1-B presents a papillary or pseudostratified architecture with the same histological and molecular features observed in PanIN1-A (Figure 13).

PanIN2 lesions are characterized by a columnar epithelium with papillary architecture. Dysplasia is greater than in the previous PanINs, with increased nuclear abnormalities, such as loss of polarity and nuclear enlargement (Figure 13). Similarly to the lower-grade PanINs, PanIN2 is highly mucinous and readily detected by AB/PAS stain. Moreover, proliferation is not evident, although some rare mitoses are reported.

PanIN3 is characterized by the presence of a papillary, micropapillary or true cribriform epithelium. Fragmentation and budding of epithelial clusters towards the lumen is occasionally detected in combination with necrosis. Loss of polarity concomitant with nuclear positioning near the lumen is frequently observed (Figure 13). It is a highly proliferative lesion but mitoses are abnormal. These lesions present a lower mucin production compared to other lesions. If not absent, they exhibit low AB/PAS stain and Muc5ac. PanIN3 is present in nearly all PDAC specimens reported so far. However, their observation in the absence of invasive carcinoma has not been reported. Due to their high frequency and prominent dysplasia, a distinction between pre-neoplastic and neoplastic is close to impossible. It has been suggested that these lesions actually constitute a PDAC extension. Hence, they are also referred to as “carcinoma in situ” (Hruban et al., 2007, Cooper et al., 2013).

PanIN grade	Histo/Cytological features	Markers
1A	Flat columnar epithelium Supranuclear mucin, Round to oval nuclei	Muc5ac AB/PAS
1B	(micro) Papillary columnar epithelium Supranuclear mucin Round to oval nuclei	Muc5ac AB/PAS
2	Papillary columnar epithelium Nuclear abnormalities Pseudo-stratification	Muc5ac AB/PAS
3/"carcinoma in situ"	Papillary to cribriform cuboidal epithelium Severe nuclear abnormalities Budding of clusters Frequent mitosis Loss of polarity	-

Table 3 - Summary of histological and cytological features of human PanINs

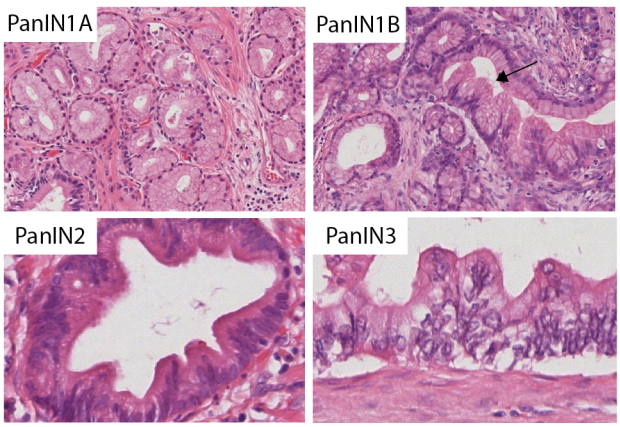

Figure 13 – Histological features of PanIN lesions

H&E showing histological features of human PanIN lesions. PanIN1A presents a flat epithelium with columnar cells and nuclei located basally. PanIN1B (black arrow) constitutes a papillary variant of PanINA. PanIN2 present papillary architecture with moderate cytological atypia. PanIN3 presents loss of nuclear polarity and papillary architecture with cuboidal and columnar cells. Images are not in the same scale. Adapted from Distler et al., 2014.For permission of use see Chapter 6, Appendix.

Despite the efforts made for a unanimous classification of PanINs, some inconsistencies have been pointed out. Importantly, PanINs are found in almost all pancreata analysed for other pancreatic diseases besides PDAC (Cooper et al., 2013), which questions the true prognostic power of these lesions to predict PDAC development.

1.4.5 PDAC progression model

Regardless of the type of tumour and the field of expertise, cancer progression models constitute a valuable tool for the understanding of the tumourigenic process by dissecting and simplifying complex events. Vogelstein has provided a crucial contribution to the elaboration of such a approaches, using colorectal cancer as his model of choice (Vogelstein and Kinzler, 1993).

Epidemiological data, together with *in vitro* and *in vivo* approaches, have been used to understand how a normal cell undergoes transformation. Initial evidence indicated that cancer incidence increases with age. Furthermore, exposure to carcinogenic cues, such as radiation, were shown not to have an immediate effect on tumour formation. Tumour manifestation occurs with long latency, indicating that one damaging hit (mutation) is not sufficient for cancer development. Instead, a prolonged survival of the mutation-containing clone, with further acquisition of genetic alterations, would explain this observation (Miller, 1980). *In vitro* and *in vivo* experiments with genetic transfer and ectopic expression, respectively, of oncogenes have also demonstrated the increased tumorigenic power of cooperation. It has been observed that some oncogenes have little to no effect on tumour formation when present on their own. However, the concomitant expression of one additional hit promotes a synergetic response, thus highlighting that additional hits promote the acquisition of greater tumourigenic features (Land et al., 1983). Interestingly, the gradual acquirement of genetic alterations can be correlated with morphological and histopathological features. It has been observed for human cancers that higher-grade tumours present a wider panel of genetic alterations when compared with lower-grade neoplasms. Moreover, human cancer data has demonstrated the presence of more than one genetic alteration in more aggressive tumours when compared with less aggressive/progressed ones (Alexandrov et al., 2013).

The beauty of these models is the ability to infer cause/consequence relationships and make predictions based on current stages. Thus the proposal of a human tumour progression model, and consequent verification by mouse model strategies, constituted a pillar in colorectal cancer patients' prognosis, as it provided critical information for the development of better genetic screening and chemoprevention approaches (Vogelstein and Kinzler, 1993).

The establishment of a model requires an unequivocal identification of lesions preceding the neoplasm. The identification of early lesions for cancers of accessible regions, such as the cervix and colon, is relatively non-invasive and thus possible to easily screen. However, other types of tumours, such as PDAC, require invasive approaches impairing access. Consequently, screening is not performed in the absence of symptoms. Therefore, the PDAC progression model has been inferred based on exhaustive assessments of PDAC resection specimens, pancreata of non-cancerous patients and mutational analysis (Hruban et al., 2000b, Hruban et al., 2000a).

The triggering forces for the proposal of the PDAC progression model were: (1) the identification, in non-cancerous patients, of hyper proliferative ducts, commonly found in cancer; (2) the consequent observation that these proliferative ductal regions exhibited a higher level of atypia when present in cancer patients (Cubilla and Fitzgerald, 1976); and (3) the documentation that highly dysplastic lesions commonly occurred within regions presenting mild atypia (Furukawa et al., 1994). The model was re-enforced by the identification of a similar phenomenon in conditions with increased risk of pancreatic cancer development. Such was the case for pancreatitis and the presence of hyper-proliferative ducts (Yanagisawa et al., 1993). Although powerful and informative, the cases reported until then were only based on morphological features and thus, sensitive to misinterpretation. It was also possible that these abnormal ducts were just hyperplastic and reactive to environmental cues. A correlation with tumour development was only implied.

Genetic tools provided the missing link between these structures and PDAC development. Assessment of the mutational landscape of these putative precursor lesions led to the observation that they harbour a simpler, although, similar genetic profile as their tumour counterpart (Kanda et al., 2012, Yanagisawa et al., 1993, Caldas et al., 1994). Microdissection of the different precursor lesions, of different grades, with follow up genetic analysis have allowed the elaboration of a progression model that correlates the sequential acquisition of genetic alterations with the increase in morphological and cytological dysplasia (Hruban et al., 2000a, Hruban et al., 2000b, Kanda et al., 2012).

In summary: *KRAS* mutations are the most common genetic alterations found in human PDAC. Not only are *KRAS* mutations the most common, they are also the earliest mutation, detected in 30% of PanIN1 lesions increasing to approximately 75% representation in PanIN3 (Feldmann et al., 2007). This is also the case for the remaining precursor lesions where it was observed that one third of the early IPMNs present *KRAS* mutations, culminating in 50% of invasive IPMN. Additionally, MCNs also harbour *KRAS* mutations in 20% of early lesions to 89% in malignant lesions (Delpu et al., 2011).

Another equally prevalent abnormality in PDAC is epidermal growth factor receptor (EGFR) and human epidermal growth factor receptor 2 (Her-2/neu) overexpression. From the immunohistochemical analyses of PDAC and adjacent duct hyperplastic lesions, it was observed that, in contrast to the absence of expression in normal ducts, 82% of the flat hyperplastic ducts exhibit high levels of Her-2/neu expression which increases in proportion with the increase in atypia (Day et al., 1996).

Other mutational events present in PDAC have also been identified in pre-neoplastic lesions. However, their absence in low-grade precursors suggests a role in the progression of dysplasia and excludes their involvement in tumour initiation. Such is the case for *SMAD4*, *CDKN2A* and *p53*, amongst other less represented molecular alterations.

As a surrogate for *CDKN2A* mutations, the expression of $p16^{INK4a}$ has been analyzed. It has been observed that, although in cancer-associated PanINs $p16^{INK4a}$ expression is low, PanINs in the context of pancreatitis present normal expression until later stages (low expression observed in 0% of PanIN1-A, 11% of PanIN1-B, 16% of PanIN2 and 40% for PanIN3) (Rosty et al., 2003). *P53* mutations are also detected at later stages of tumour development. Mutations in this gene are barely seen in early precursors, such as PanIN1 (0%), but are evident in a subset (12%) of PanIN3 (Delpu et al., 2011). Lastly, *SMAD4* mutations have also been observed in precursor lesions. Despite their absence in PanIN1 and 2, *SMAD4* mutations, and consequent reduced expression, is observed in 30% of high-grade PanIN3 (Hong et al., 2011).

Given that PanINs are the most abundant precursor lesion, the pancreatic progression model (Figure 14), proposed by Hruban and co-workers (Hruban et al., 2000a) is now

accepted worldwide and used as a starting point for further in-depth analyses. Nonetheless, the fact that the data obtained for the generation of the model was based on fixed resected tissue, and the lack of screening methods, hinders the complete understanding of these lesions and their immediate role in tumour formation. In fact, the results obtained with the analysis of *KRAS* mutations have been controversial. While some have reported a high percentage of ductal lesions harbouring *KRAS* mutations, others show that this event only occurs in a small proportion of low-grade precursors (Lüttges et al., 1999, Löhr et al., 2005). This suggests that, either oncogenic *KRAS* might not be the only driving force for PDAC development, or that low-grade lesions do not necessarily progress to PDAC. Instead, they might be indicative of increased risk of development. Furthermore, the predictive power of PanIN presence is also being investigated. It has been observed, in a short-term study (10 years follow up), that the presence of PanIN lesions in the surgical margins upon PDAC resection does not correlate with increased risk of relapse (Konstantinidis et al., 2013). Additionally, PanINs have also been observed in the presence of other pancreatic neoplasms, such as acinar cell carcinomas (ACCs), MCNs, pancreatic endocrine tumours (PETs), cystadenomas (SCs), and solid pseudopapillary tumours (SPTs) (Stelow et al., 2006a). The ubiquitous presence of PanINs challenges their status as PDAC precursors, suggesting a broader relevance and origin in pancreatic insults. Thus, the successive evolution from low-grade lesion to PDAC is still under debate.

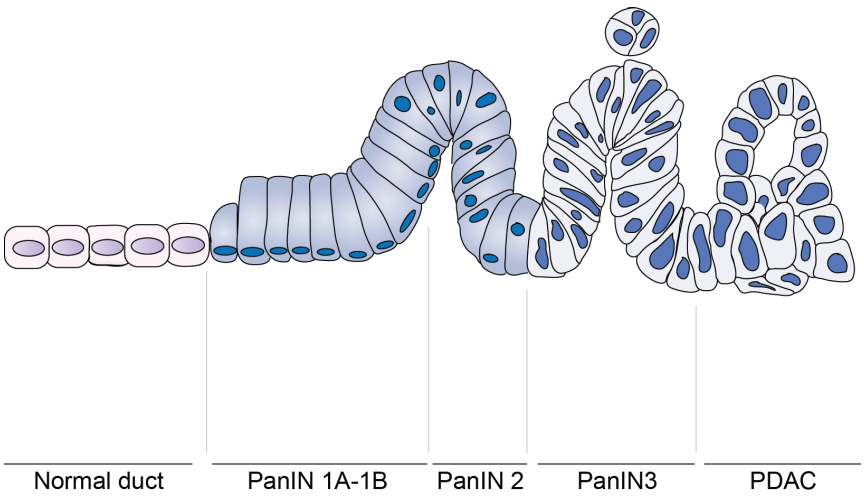

Figure 14 - PDAC progression model based on human data

Illustration of the histological and architectural features of PDAC and its precursor lesions. Normal ducts are thought to acquire mutations leading to the generation of PanIN1A-1B, which progress to PanIN2, PanIN3 and PDAC.

1.4.6 PDAC cell of origin hypothesis (clinical data-based assumption)

The identification of a cancer's cellular origin has immeasurable benefits for the clinic as it provides unique information about tumour molecular origins/dependencies.
PDAC is usually a moderately differentiated tumour with glandular, duct-like structures surrounded by abundant stroma. On a histological level, it presents large/medium tubular structures that can be papillary or cribriform. While its precursors are usually mucinous with a columnar epithelium, PDAC is less mucinous, presenting cuboidal cells with variable-sized nuclei. If well differentiated, neoplastic duct structures can be difficult to distinguish from normal ducts. These tumours retain some of the markers present in ductal cells, such as CK7, 8, 18 and 19, Muc1 and HNF1β, but also upregulate others, such as the embryonic transcription factor Pdx1 and carcinoembryonic antigen (CAE) (Hamilton and Aaltonen, 2000). Moreover, early studies detected hyperplastic ducts before and during PDAC onset. Given the morphological resemblance of PDAC and PanIN cells with pancreatic ductal cells, and the observation of hyperproliferative ducts before, and upon tumour formation, it was proposed that PDAC would have its origin in a ductal cell. Recent findings have challenged this hypothesis, as it will be discussed in this thesis (see 1.6.2, page 74).

1.5 Genetically engineered mouse models (GEMs) of PDAC

Great discoveries and deep understanding of PDAC biology and genetics can be achieved based on analyses of tumour resected fixed tissue. Clinical observations have provided the driving force for the understanding of the genetic and environmental components leading to PDAC. However, correlation analyses have to be challenged and put to the test so that stronger statements can be made. While in vitro studies are useful for isolated questions, the big picture can only be obtained by modulating cellular responses in their own environment. Animal models are powerful tools to shed light into the mechanisms of pathogenesis.
Initial pancreatic cancer models used to understand PDAC biology were based on xenografts, where human tumour cells are transplanted in the mouse (subcutaneous or orthotopic tumours). Considering the injected cells are already coming from an

established tumour, issues such as the cell of origin and mechanisms of tumour initiation are difficult to address. Additional approaches took advantage of carcinogens to induce tumourigenesis. The results obtained with these approaches, although histologically mimicking the human disease, failed to clarify the events under a precise molecular alteration (Bardeesy et al., 2001). The generation of GEMs completely revolutionized cancer research. Deletion or ectopic expression of specific genes can, nowadays, be easily achieved. A great contribution was the generation of a Cre recombinase-dependent genetic manipulation. The Cre-based system provides an incomparable genetic tool that allows the irreversible induction of a genetic alteration by the recombination, and consequent excision, of DNA sequences flanked by loxP recognition sites (Sauer, 1998). Cre is expressed under the control of a tissue-specific promoter allowing tissue-specific genetic modulation. Similar to the specificity provided by Cre models, other approaches have been developed that serve a similar purpose. Lastly, the possibility to regulate Cre function provided another layer of control. This was achieved by fusing Cre to a mutated ligand-binding domain of the human oestrogen receptor (ER). Only in the presence of tamoxifen (an oestrogen agonist/antagonist), Cre is translocated to the nucleus and mediates loxP recombination and DNA excision (Feil et al., 1996).

In the pancreatic cancer field, mouse models have been crucial to the understanding of: (1) the role of oncogenes and tumour suppressors in PDAC; (2) progression from normal tissue to neoplasia; (3) the cellular origin of pancreatic tumours; (4) the impact of the environment, such as inflammation, in PDAC development; and (5) the interplay between genetic and environmental insults. These finding are explored below and will be subdivided into embryonic or postnatal models.

1.5.1 Lessons from embryonic GEMs of PDAC

In this chapter, a summary of the most common GEM models used (Table 4) and the main findings obtained will be discussed.

The role of oncogenes and tumour suppressors in PDAC - **Progression Model**

Studies have identified several genetic and epigenetic alterations to be present in both PDAC and its pre-neoplastic precursors. While these changes are observed, a cause/consequence relationship was not solid. GEM models have helped to clarify the role of these molecular aberrations and, thus, to better understand the step-wise progression of the disease.

Initial attempts to create a GEM model for PDAC were made by ectopically expressing oncogenic $KRas^{G12D}$ under the control of the *Ck19* (duct marker in adult pancreas; progenitor population during development) or *Elastase 1* (*Ela1* - acinar cell marker in embryonic development and adulthood) promoters (Grippo et al., 2003, Brembeck et al., 2003). However, in both cases, *KRas* oncogenic expression was dependent on the regulation of the respective promoters used, and thus, the levels of expression did not mimic the human scenario.

In 2003, Hingorani and co-workers generated a more physiologically relevant mouse model where *KRas* oncogenic expression was regulated by its own promoter (Hingorani et al., 2003). In this model, an oncogenic $KRas^{G12D}$ sequence, preceded by a loxP-STOP-loxP (LSL) cassette, was knocked-in after the promoter region of the *KRas* locus and upstream of the coding sequence. This mouse model was then crossed to a Pdx1-Cre deleter strain. In this model, the expression of the transcription factor Pdx1 at E8.5, in embryonic pancreatic progenitors, drives Cre expression, promoting the excision of the STOP cassette and transcription of the oncogenic $KRas^{G12D}$. For the first time, a multi-step carcinogenesis of PDAC was documented, closely recapitulating the human disease. These animals developed murine PanINs (mPanINs) as early as 2 weeks of age. As proposed for the human disease, these mPanIN lesions progressed from grade 1 to 3 and culminated with focal murine PDAC (mPDAC) development close to one year of age (Hingorani et al., 2003). Similar results were obtained using the Ela1-tTA/tetO-Cre model (Cre expression is promoted by tTa regulated by the Elastase promoter, in the absence of doxycycline) in combination with another endogenously regulated

oncogenic *KRas* (*KRas*$^{+/LSLG12Vgeo}$) (Guerra et al., 2007). Since Elastase expression starts in the embryo, at E16.5, tumourigenesis begins before birth, in embryonic acinar cells. Doxycycline untreated *KRAS*$^{+/LSLG12Vgeo}$*; Ela1-tTA/tetO-Cre* mice developed focal low-grade mPanINs at 3 months, meeting the consensus classification described by Hruban and co-workers in the 2006 pancreatic GEM model report (Hruban, 2006). Over time, these lesions increased in grade and, at one year of age, half of the mice presented PDAC, supporting the progression model. These studies confirmed the common *KRAS* mutation found in humans (G12D) as being sufficient for PDAC initiation and progression. Nonetheless, the long latency of tumour onset also confirmed the observed need for additional molecular abnormalities for tumour development.

It is known from the clinic that PDAC harbours more than just *KRAS* mutations. Given their absence in low-grade lesions and presence in the established tumour, these additional molecular alterations were suggested to be involved in the progression from pre-neoplastic to neoplastic disease. Such is the case for alterations in the genes *CDKN2A*, *p53* and *SMAD4*. Similarly, GEM models were created that either deregulated these genes alone, or in combination with KRas constitutive activation. In summary, deletion of either p16^{INK4A}/p19^{ARF} (*Ink4a/Arf*$^{lox/lox}$), p16 ^{INK4A} or p53, in *KRas*^{G12D}*; Pdx1-Cre* or *KRas*$^{+/LSLG12Vgeo}$; *Ela1-tTA/tetO-Cre* mice, led to a drastic acceleration of tumour formation with no observable effect in the absence of oncogenic KRas (Bardeesy et al., 2006a, Aguirre, 2003, Guerra et al., 2011). Similarly, deletion of Tgfβ receptor 2 (Tgfbr2$^{lox/lox}$), with concomitant expression of oncogenic KRas^{G12D} in the embryonic pancreas (Ptf1a-Cre), significantly accelerated PDAC onset while having no effect in tumour formation when deleted alone (Ijichi et al., 2006). These mouse models have shed light on the importance and role of the tested oncogenes and tumour suppressors. Moreover, they have strengthened the proposed progression model by demonstrating the time-wise requirement for genetic alteration. An increasing number of genes and pathways are being put to the test using similar approaches, providing an extremely detailed understanding of the key players involved in PDAC tumourigenesis (Hanlon et al., 2010, Eser et al., 2013, Pérez-Mancera et al., 2012).

Molecular alterations	Driver	Target cell	PanIN onset	PDAC onset	Reference
***KRas*$^{+/LSL-G12D}$**	*Pdx1-Cre*	Progenitor (E8.5)	2w	1y	(Hingorani et al., 2003)
***KRas*$^{+/LSL-G12D}$**	*p48/Ptf1a-Cre*	Progenitor (E9.5)	2w	1y	(Hingorani et al., 2003)
***KRas*$^{+/LSLG12Vgeo}$**	*Ela1-tTA/tetO-Cre No Dox*	Acinar progenitor (E16.5)	3m	50% 1y	(Guerra et al., 2007)
***KRas*$^{+/LSL-G12D}$ *Ink4a/Arf*$^{lox/lox}$**	*Pdx1-Cre*	Progenitor (E8.5)	No info	7/11w	(Aguirre, 2003)
***KRas*$^{+/LSL-G12D}$ *Ink4a/Arf*$^{lox/lox\ lox/+}$**	*Pdx1-Cre*	Progenitor (E8.5)	No info	2/8m	(Bardeesy et al., 2006a)
***KRas*$^{+/LSL-G12D}$ *p53*$^{lox/lox\ or\ lox/+}$**	*Pdx1-Cre*	Progenitor (E8.5)	No info	1.5/5m	(Bardeesy et al., 2006a)
***KRas*$^{+/LSL-G12D}$ *p16*$^{lox/lox}$**	*Pdx1-Cre*	Progenitor (E8.5)	No info	4.5m	(Bardeesy et al., 2006a)
***KRas*$^{+/LSL-G12D}$ *p53*$^{lox/lox}$ *p16*$^{lox/lox\ or\ lox/+}$**	*Pdx1-Cre*	Progenitor (E8.5)	No info	6/7w	(Bardeesy et al., 2006a)
***KRas*$^{+/LSLG12Vgeo}$ *p53*$^{lox/+}$**	*Ela-tTA/tetO-Cre No Dox*	Acinar progenitor (E16.5)	No info	6m	(Guerra et al., 2007)
***KRas*$^{+/LSL-G12D}$ *Tgfbr2*$^{lox/lox\ or\ lox/+}$**	*p48/Ptf1a-Cre*	Pancreatic progenitor (E9.5)	3w	2/6m	(Ijichi et al., 2006)

Table 4 - Summary of the most commonly used prenatal PDAC GEM models and their respective phenotypes

Table summarising the most commonly used mouse models of PDAC targeting the pancreas of pre-natal mice. w – weeks. m – months. y – years

1.5.2 Lessons from postnatal GEMs of PDAC

PDAC is more prevalent in the aged population, thus it is very improbable that the driving mutations occur during human embryogenesis. The likeliest scenario is the acquisition of somatic mutations during adulthood. Hence, embryonic GEMs are limited in their capacity to fully mimic the human disease. Moreover, embryonic models do not answer the longstanding question of the cell of origin of PDAC (see 1.6.2, page 74). Thus, conditional modulation of gene expression constitutes an invaluable tool for investigating PDAC in the adult (Table 5).

Tumourigenic resistance of the adult pancreas (possible stem cell-like pool?)

A plethora of studies have demonstrated that $KRas^{G12D}$ activation in pancreatic progenitors is sufficient to drive tumourigenesis by induction of mPanIN lesions. Nonetheless, progenitor cells are thought to harbour the required activated mechanisms to rapidly respond to oncogenic hits. Thus, it does not answer the question of whether *KRas* oncogenic mutations would be able to transform an adult population. In order to address this issue, the activation of the oncogenic hit has been induced in the adult pancreas. Studies have addressed the ability of both adult acinar and ductal cells to give rise to PDAC. However, ductal-specific targeting has been unsuccessful (see 1.6.2, page 74). Thus, the main findings obtained so far targeted adult acinar cells. Guerra and co-workers have activated $KRas^{G12V}$ in acinar cells of an adult mouse. $KRas^{+/LSLG12Vgeo}$; *Ela1-tTA/tetO-Cre* mice (tet-off system) were treated with doxycycline until 2 months of age (P60) to prevent Cre-dependent recombination. After doxycycline removal, mice were followed up to one year with no detectable histological aberration (Guerra et al., 2007). In a follow up study, the concomitant homozygous deletion of *p53* or $p16^{INK4A}/p19^{ARF}$, with $KRAS^{G12V}$ expression, in adult acinar cells, also failed to induce any neoplastic growth (Guerra et al., 2011). These results suggest a high refractory nature of the adult organ to tumourigenesis. It is known that inflammation constitutes a high PDAC susceptibility state. Thus, the authors repeated the approaches with parallel induction of pancreatic inflammation (pancreatitis). Pancreatitis was induced with caerulein, a cholecystokinin analogue, treatment that promotes the premature activation and uncontrolled release of the acinar digestive enzymes, with consequent damage to the pancreas, mainly to acinar cells. The inflammatory environment acted

synergistically with *KRas* mutations to promote the formation of pre-neoplastic precursors and rare focal murine PDAC at 8 months post-Cre expression (Guerra et al., 2007). Human PDAC aetiology had already established pancreatitis as a main risk factor. Nonetheless, theses studies have re-classified pancreatic inflammation as a crucial component of PDAC development.

In contrast to the above-mentioned studies, it has been observed that adult acinar cells are, in fact, able to give rise to $KRAS^{G12D}$-dependent murine PanIN initiated mPDAC development (Habbe et al., 2008). This observation can be explained by: either the non-comparable tumourigenic capacity of different *KRas* mutations (G12D vs G12V); the use of different Cre lines and consequently the different population targeted, or due to the different age of induction (6 weeks versus 8 weeks of age).

	Molecular alterations	Cre Driver	Target cell	Observation	Reference
Acinar	*$KRas^{+/LSLG12Vgeo}$*	*Ela1-tTA/tetO-Cre* Dox up to P60	Adult **acinar** P60	ADM, PanIN and PDAC development require pancreatitis	(Guerra et al., 2007)
	$KRas^{+/LSLG12Vgeo}$ $p53^{lox/lox}$ or $Ink4A/Arf^{lox/lox}$	*Ela1-tTA/tetO-Cre* Dox up to P60	Adult **acinar** P60	ADM, PanIN and PDAC development require pancreatitis	(Guerra et al., 2011)
	$KRas^{+/LSL-G12D}$	*$Ela\text{-}Cre^{ERT2Tg/+}$* Tamox at 6w	Adult **acinar** 6w	PanIN without requirement of pancreatitis	(Habbe et al., 2008)
	$KRas^{+/LSL-G12D}$	*$Mist1Cre^{ERT2/+}$* Tamox at 6w	Adult **acinar** 6w	PanIN without requirement of pancreatitis	(Habbe et al., 2008)
	$KRas^{+/LSL-G12D}$ $p53^{lox/lox}$	*CPA1-CreER*	Adult **acinar** P60	PanIN and PDAC development in the presence of pancreatitis	(Friedlander et al., 2009)
Endocrine	*$KRas^{+/LSL-G12D}$ alone or in combination w/ $p53^{lox/lox}$*	*RIP-CreER*	Adult **β-cells** P30/P60	No transformation without caerulein. Chronic pancreatitis induced PDAC only in double mutants.	(Friedlander et al., 2009)
Duct	*$KRas^{+/LSL-G12D}$*	*Ck19-CreER* Tamox at 6w	Adult **duct** 6w	No transformation. Rare PanIN Unspecific Cre diver.	(Ray et al., 2011)
	$KRas^{+/LSL-G12D}$	*Sox9-CreER* Tamox at P10	Postnatal **duct** P10	No transformation Rare PanIN Possible unspecific Cre line.	(Kopp et al., 2012)

Table 5 - Summary of the most commonly used postnatal PDAC GEM models and their respective phenotypes

Table summarising the most commonly used mouse models of PDAC targeting the pancreas of postnatal mice. P – postnatal day. w – weeks. Dox – Doxycycline. Tamox - tamoxifen

1.6 PDAC cell of origin

A great part of understanding the nature of any tumour is the knowledge of the cells from which it originates. The awareness of the cell of origin has already been shown to provide crucial information regarding the initial stages of tumour development in different organs, as well as the molecular mechanisms involved in early tumourigenesis (Gangopadhyay et al., 2013, Jordan, 2007, Barker, 2014). Additionally, the identification of a more tumourigenic population can provide valuable insight into the biology of the organ homeostasis and regeneration. The search for pancreatic adult progenitor cells and PDAC cell of origin has been restless. An increasing amount of evidence points to the existence of cells with different tumourigenic potential, urging for a different handling in the clinic.

1.6.1 PDAC heterogeneity and tumour molecular subtypes

PDAC, as described before, is a disease that exhibits an extremely poor prognosis. This unfortunate phenomenon can be partially attributed to its extremely aggressive nature coupled with the lack of distinctive symptoms. Nonetheless, effective therapies should be capable of tumour remission, which is not the case. An important factor for evasion of chemotherapy is the heterogeneity of the tumour (Dexter and Leith, 1986). In fact, detailed genetic analyses have broadened the panel of molecular alterations detected in PDAC. In 2008, a comprehensive analysis of deletions, amplifications, mutations and gene expression of 24 PDAC patient samples identified an average of 63 genetic alterations whose functions spread over 12 signalling pathways (Jones et al., 2008). Furthermore, whole genome sequencing and copy number variation studies on 100 tumour samples from PDAC have reinforced the great genetic variation present in these tumours. Chromosomal rearrangements were frequent and led to the deregulation of genes known to be important for PDAC development, as well as the identification of new potential drivers. Genetic instability was found to be extremely important to the chemotherapy outcome and thus, PDAC was sub-classified into 4 different categories according to their chromosomal structure: stable; locally rearranged, scattered and unstable (Waddell et al., 2015). In a different study, a distinctive classification was

made where a combined analysis of publicly available transcriptional datasets of resected PDAC with the laboratory's own microdissected PDAC gene expression microarray data, was performed. In this study, a 62-gene molecular PDAC signature (PDAssigner) was obtained, that assigned particular expression profiles to different tumour subtypes with distinct clinical outcomes and responses to therapy. The subtypes were named "classical" (with a better prognosis), "exocrine-like" (with an intermediate prognosis) and "quasi-mesenchymal" (with the worst registered prognosis) due to the main functions of the genes expressed in each signature. Hence, the "classical" type expressed epithelial genes and genes commonly involved in adhesion, the "exocrine-like" type exhibited high expression of genes involved in production and secretion of acinar cell digestive enzymes and the "quasi-mesenchymal" was shown to express high levels of genes associated with the mesenchyme (Collisson et al., 2011). At this point a complete understanding of the underlying reason for the different subtypes is not obvious. A correlation with *KRAS* dependency was proposed, but it does not segregate the samples into 3 different groups. One possible explanation for the different expression is that the expression is reminiscent profile of the cell of origin. It has been hypothesised that PDAC could arise from different pancreatic cellular compartments and thus the consequent tumours would be expected to fall into different profiles.

1.6.2 Pancreatic cellular compartment of origin

As mentioned above, the human data obtained for PDAC and its pre-neoplastic lesions has suggested that PDAC arises from ductal cells. Nevertheless, the cellular compartment of origin of PDAC is still a subject of pronounced debate. Using the knowledge of the detailed marker expression of the different pancreatic compartments, it was possible to generate GEM models that are specific for distinctive cell lineages (Table 5).

Up to the initiation of the currently presented study, attempts to provide solid proof of a duct cellular origin had failed to demonstrate the tumourigenic capacity of these cells. Encouraging data on the ductal origin was originally provided by the deletion of *Pten*, an antagonist of the PI3K/PDK1/AKT pathway, in the embryonic pancreas. $Pten^{lox/lox}$*; Pdx1-Cre* mice exhibit an acceleration of the previously observed $KRas^{LSL\text{-}G12D/wt}$*; Pdx1-*

Cre model. This acceleration was suggested to be due to centroacinar cell expansion, a specialized type of ductal cells, and consequent transformation (Stanger et al., 2005). Nevertheless, Pdx1-Cre targeting is not specific to the ducts and thus the finding was later put to the test.

Specific ductal cell targeting was achieved with the use of *Ck19-CreER* or *Sox9-CreER* mice. Both Ck19 and Sox9 have been proposed to be exclusively expressed in the ductal network. Crossing $KRas^{LSL\text{-}G12D/wt}$ with *Ck19-CreER* or *Sox9-CreER* failed to generate PDAC. The only observation, in both studies, was the presence of extremely rare PanINs, detected long after tamoxifen-induced recombination (Ray et al., 2011, Kopp et al., 2012). Thus, the current results discouraged PDAC as having its origin in the ductal compartment and triggered an extensive search for the cell of origin.

It has been extensively demonstrated that plasticity is a characteristic of all pancreatic cells (see 1.1.2, page 26). Since the ductal cell of origin hypothesis was not confirmed, attention has been focused on the remaining cellular compartment. In order to narrow down the responsible compartment, Friedlander and co-workers used cell-specific Cre drivers that restricted the *KRAS* oncogenic activation to endocrine β-cells (*RIP-CreER*) and acinar cells (*CPA1-CreER*) (Friedlander et al., 2009). Two observations were made from this study. Firstly, it was reinforced that inflammation is important for promotion of tumour development, as the absence of a caerulein treatment failed to give rise to tumours in both compartments. Secondly, while β-cells required the concomitant homozygous deletion of p53 and caerulein treatment to induce rare mPDAC, acinar cells responded strongly with $KRas^{G12D}$ alone and inflammation. Furthermore, the use of the *RIP-CreER* model showed some labelled exocrine cells. Thus, it seemed that acinar cells constituted the main cellular source for PDAC.

Although it seems counterintuitive, several studies had previously focused on the PDAC tumourigenic capacity of acinar cells. It had been previously reported that c-myc ectopic expression in acinar cells, by means of a Ela1-myc transgene, culminated in the formation of acinar cell carcinomas in half of the mice, while the other half presented a mass of duct-like cells which progressed to ductal adenocarcinomas (Sandgren et al., 1991). In a following study, a similar approach expressing TGFα (Ela1-TGFα) was undertaken. It was observed that acinar cells from transgenic mice would progressively gain a ductal morphology with parallel upregulation of ductal markers (Wagner et al.,

1998). This observation was then named acinar-to-duct metaplasia (ADM, conversion of an acinar cell into a ductal cell) and was thought to precede PanIN formation leading to PDAC. In accordance with these observations, it was demonstrated that soon after $KRas^{G12D}$ activation in the embryonic pancreas, ADM was the predominant morphological change. Interestingly, normal acinar cells near the ADM ductal clusters also presented ductal cell markers. Moreover, in the same study, a time course analysis demonstrated that early mPanIN lesions retain some acinar markers suggestive of an acinar cell origin or a partial acinar contribution to the pre-neoplastic lesion (Zhu et al., 2007).

Nowadays, it is known that *KRas* mutations induce ADM *in vivo* and *in vitro* (Shi et al., 2012). Furthermore, caerulein-induced pancreatitis promotes extensive ADM, which might at least partially be the cause of the acceleration of acinar-derived PDAC observed in caerulein-treated $KRas^{+/LSLG12Vgeo}$*; Ela1-tTA/tetO-Cre* mice (Guerra et al., 2007).

In summary, despite the ductal morphology, the greatest amount of evidence supports an acinar cell origin for PDAC via ADM-PanIN-PDAC progression (Figure 15). Nonetheless, a ductal cell origin cannot be excluded solely based on the studies performed so far.

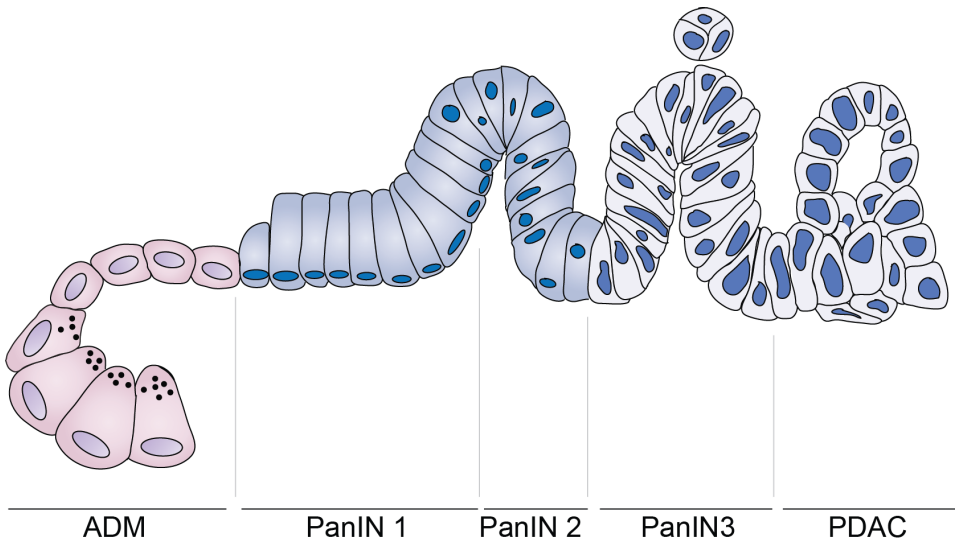

Figure 15 – PDAC progression model based on GEM data

Illustration of the histological and architectural features of PDAC and its precursor lesions. Acinar cells undergo a transdifferentiation step, named Acinar to ductal metaplasia – ADM, and acquire a ductal morphology. These duct-like structures progress towards PDAC via the intermediate development of murine PanIN1, PanIN2 and PanIN3.

1.6.3 Tumour-initiating cells

Tumour-initiating cells (TICs), commonly referred to as cancer stem cells (CSCs), are an interesting, yet, still controversial concept. Tumours can be roughly seen as a hierarchical organization, where, over time, mutations in a cell or in a small group of cells confer a growth advantage over the neighbouring population.

Xenograft-based studies have demonstrated that a high number of tumour cells is required to establish the new tumour, upon transplantation (Polyak and Hahn, 2006). While cell death is expected due to implantation procedures and crosstalk with the host, it would be estimated that, if all tumour cells have the same tumourigenic potential, that a smaller number of cells would be required for tumour formation. Hence, the theory of cancer stem cells emerged, as the subpopulation of cells within tumours with a unique capacity to initiate and maintain tumour development, and it has been a subject of discussion ever since (Jordan et al., 2006).

A plethora of studies have been conducted in order to identify a cancer population responsible for tumour generation and maintenance. As a result, the establishment of subpopulations with high tumourigenic capacity, self-renewal ability and increased proliferative index have been detected for tumours of different organs, such as the brain, intestine, breast and the haematopoietic system (Barker, 2014, Gangopadhyay et al., 2013, Wang and Dick, 2005).

1.6.4 Clinical relevance of cancer stem cells

CSCs are of extreme importance given their unique role in tumour initiation. However, many other features enhance their importance and relevance in therapeutic outcome. Chemotherapy drugs are developed based on the molecular information provided by cancer cell lines and patient biopsy samples. This means that the average molecular aberrations are detected while lowly represented changes are diluted out. CSCs constitute a minority in the tumour. Thus, while chemotherapies are designed for the molecular dependencies of the bulk tumour, they usually fail to target the CSC subpopulation. Tumour recurrence, despite evident remission after chemotherapy, has been a common finding, reported extensively (Vidal et al., 2013). Resistance to

chemotherapy can be attributed to several factors such as selection of resistant clones and microenvironment protection, amongst others. Nevertheless, CSCs have been shown to efficiently evade chemotherapy, *in vitro* and *in vivo*, by numerous mechanisms, such as dormancy, efflux pump-mediated drug exclusion or adapted molecular regulation (Rich and Bao, 2007).

An additional layer of importance is given concerning the metastatic process. A parallel connection between CSCs and epithelial to mesenchymal transition (EMT) has been suggested. EMT is a biological process by which epithelial cells acquire a more mesenchymal phenotype, as a consequence of changes in the transcriptional profile. This enhances the migratory and invasive nature of these cells, allowing them to leave the primary tumour and colonize distant sites. It has been observed in different cancers that the CSC population harbours an increased metastatic potential, with a more pronounced EMT phenotype. Specific pharmacological targeting of these cells greatly reduces their invasive and colonization capacity (Sampieri and Fodde, 2012).

Great knowledge has strengthened the relevance of CSCs in pathogenesis. Thus, the identification of such cells, and the understanding of their biology, might have immeasurable benefits for the development of better chemotherapeutic strategies.

1.6.5 Pancreatic cancer stem cells

PDAC is an extremely heterogeneous disease with poor response to chemotherapy. As discussed above, both heterogeneity and drug resistance can be attributed to the comprehensive molecular alterations and chromosome instability observed in these tumours, coupled with the intense desmoplastic reaction and low vascularity that accompanies tumour formation (Olive et al., 2009, Samuel and Hudson, 2011). However, evidence for a pool of cells with distinct and enhanced tumour-initiating potential has been documented (Hermann et al., 2007).

The embryonic progenitor cells of the developing pancreas are equipped with extremely efficient molecular machineries capable of great plasticity. However, the regenerative capacity is greatly reduced after birth (Solar et al., 2009, Pan et al., 2013). Analogously, the ability to generate PDAC in mouse models decreases with age. When *KRas* mutations are targeted to the pancreatic embryonic progenitors, by the use of Pdx1-Cre

or Ptf1a-Cre mice, pre-neoplastic mPanIN lesions can be observed as soon as two weeks after birth, with PDAC onset at one year of age (Hingorani et al., 2003). Oncogenic insults in young mice, soon after birth, greatly delayed tumour onset as seen by Guerra and co-workers. Activation of oncogenic $KRas^{G12D}$ 10 days after birth initiated the tumourigenic program in acinar cells (*KRas*$^{+/LSLG12Vgeo}$*;Elas-tTA/tetO-Cre*, doxycycline up to P10) with detectable early-grade mPanINs only at 6 months and rare focal PDAC one year post Cre-mediated recombination. The effect of age on tumourigenesis is even more obvious in adult mice. In the same study, the *KRas*^{G12V} mutation was induced in adult acinar cells (P60) where no pathogenesis was observed up to one year, even with concomitant homozygous deletion of p53 (Guerra et al., 2007). These results nicely point to an exhaustion or reduction in the tumour-initiating population with age.

Tumour formation can be induced in the adult pancreas, however it requires the concomitant presence of an inflammatory environment (Guerra et al., 2011). It has been described before that pancreatitis-induced regeneration relies on the repression of exocrine programs and the re-activation of embryonic pathways with simultaneous re-expression of embryonic markers, such as Pdx1 (Jensen et al., 2005). Thus, it is reasonable to conjecture that adult PDAC tumourigenesis is dependent on the presence of stem cells/committed progenitors or the reactivation of stem cell programs.

The search for tumour-initiating cells led to the development of technical strategies that could test, both *in vivo* and *in vitro,* the phenotypic tumourigenic differences between these cell populations. Currently accepted cancer stem cell assays rely on the identification of surface markers that enable the physical separation of this population versus the remaining tumour cells. This allows the comparison of the two populations regarding their ability to self-renew and give rise to differentiated progeny. Most commonly used *in vitro* assays compare the cellular capacity to grow as spheroids in non-adherent conditions where tumour-initiating cells overcome anoikis. Additionally, recent strategies have been developed, which rely on the ability of tumour-initiating cell to form organoids in soft matrices (Clarke et al., 2006). While *in vitro* approaches allow the high-throughput study of this specialized subpopulation, as the name indicates, the ultimate test for a tumour-initiating property is their unique ability to generate tumours in recipient mice, when isolated from the bulk, non-tumour-initiating population. Thus,

for a cell to be proposed as a tumour-initiating cell, it has to generate *in vivo* tumours in recipient mice, following injection of a small number of cells, and to recapitulate the cellular heterogeneity present in the primary tumour (Clarke et al., 2006).

The increasing evidence for cellular heterogeneity within PDAC tumours triggered the search to define the tumour-initiating population. Cell surface marker screening of human PDAC samples demonstrated heterogeneity in expression of CD44, CD24, and Epithelial-specific antigen (ESA), previously described cancer stem cell markers. Transplantation into Non-obese diabetic/ Severe combined immunodeficient (NOD/SCID) mice indicated that $CD44^+CD24^+ESA^+$ cells had the highest tumour initiating potential, where as few as 100 cells were capable of PDAC initiation, phenocopying the primary human tumour (Lee et al., 2008). In a different study, Hermann and co-workers identified a subpopulation expressing prominin1 (also known as CD133). The orthotopic transplantation of these isolated cells was able to generate tumours with as little as 500 cells, while their negative counterpart failed to do so even when 10^6 cells were transplanted. Tumours generated after serial transplantation of $CD133^+$ cells maintained the histological features observed in the first generation tumours, indicating a stem cell-like capacity to give rise to differentiated progeny. Moreover, as suggested for most cancer stem cells, the $CD133^+$ population was shown to be more resistant to common PDAC chemotherapy (Gemcitabine). Interestingly a double positive population for CD133 and C-X-C chemokine receptor type 4 (CXCR4) was present at the migratory front of the tumour. Orthotopic transplantation of $CD133^+CXCR4^+$ versus $CD133^+$ cells demonstrated that both populations presented the same tumourigenic capacity, but tumour cells circulating in the blood were only detected when xenografts were performed with the double positive population. These results indicate that the tumour-initiating population described in this study contained a metastatic group of cells. This suggests that the tumour-initiating population is the one responsible for metastasis from PDAC tumours, highlighting the need for specific targeting of PDAC TICs (Hermann et al., 2007).

Despite the encouraging results, immunohistochemical analysis of these CD133, CD44 markers in human neoplastic pancreas indicates that cells positive for either CD133, CD44 or both might be more represented than what was initially reported (Matsuda et al., 2012, Immervoll et al., 2011). Moreover, some caveats in the studies mentioned

above, such as the possible inclusion of stromal cells in the cellular fraction that was negative for the selected tumour-initiating marker, might compromise the findings proposed. Thus, it is still not clear if CD133 or CD44 can identify a tumour-initiating population in the pancreas, or even if one exists.

1.7 Aim of this Thesis

Pancreatic ductal adenocarcinoma has been extensively studied. However, regardless of the great amount of molecular and histological knowledge gained so far, prognosis has remained poor with only 4% of the patients surviving more than 5 years (Hezel, 2006). It is becoming increasingly obvious that attention has to be focused on the initial stages of tumour development, when the disease is still manageable. In the study presented here, I aimed to investigate the origins of PDAC in the different pancreatic exocrine compartments at early stages of tumour development to better understand the contributions of each compartment to PDAC development. Additionally, I aimed to specifically identify the PDAC tumour-initiating cell for the future development of targeted chemotherapeutic strategies.

Chapter 2. Materials & Methods

2.1 Materials

2.1.1 Reagents and Consumables

The consumables and reagents used for the development of this study were acquired from the companies listed or the Cancer Research-UK London Research Institute (LRI) Central Services:

0.5 ml, 1.5 ml, 2 ml tubes	Eppendorf (Cambridge, UK)
100bp DNA ladder	Life Technologies (NY, USA)
1 kb DNA ladder	Life Technologies (NY, USA)
1 ml, 5 ml, 50 ml syringes	BD Plastipak (Oxford, UK)
5 ml, 10 ml, 25 ml serological pipettes	Corning (Corning, USA)
15 ml, 50 ml tubes	Corning (Corning, USA)
18G, 19G needles	BD Microlance (Oxford, UK)
6 cm diameter dishes (adherent cells)	Corning (Corning, USA)
10 cm diameter dishes (adherent cells)	Corning (Corning, USA)
25 cm2 flasks (adherent cells)	Corning (Corning, USA)
75 cm2 flasks (adherent cells)	Corning (Corning, USA)
150 cm2 flasks (adherent cells)	Corning (Corning, USA)
25 cm2 flasks (suspension culture)	Sarstedt (Leicester, UK)
75 cm2 flasks (suspension culture)	Greiner bio-one (Stonehouse, UK)
6-well plate (flat bottom)	BD Falcon (Oxford, UK)
24-well plate (flat bottom)	BD Falcon (Oxford, UK)
96-well plate (flat bottom)	BD Falcon (Oxford, UK)
96-well plate (non-sterile)	Nunc (Rochester, USA)
LS MACS columns	Miltenyi Biotec (Sussex, UK)
QuandroMACS separator	Miltenyi Biotec (Sussex, UK)
3,3,5-Triiodo-L-trhyronine	Sigma-Aldrich (Poole, UK)
4-hydroxytamoxifen	Sigma-Aldrich (Poole, UK)
ABC Kit Vector Laboratories	Vector Laboratories (Peterborough, UK)

Adenovirus	Gene Transfer Vector Core (Iowa USA)
Advanced DMEM/F12	Life Technologies (NY, USA)
Agarose	Bioline (London, UK)
Alcian Blue	Sigma-Aldrich (Poole, UK)
Ammonium chloride	LRI/CR-UK (London, UK)
Ammonium persulfate	Sigma-Aldrich (Poole, UK)
Ampicillin	Sigma-Aldrich (Poole, UK)
B27 Supplement	Life Technologies (NY, USA)
Bovine Pituitary Extract	BD Biosciences (Oxford, UK)
Bovine serum albumin	Sigma-Aldrich (Poole, UK)
Bromophenol blue	Sigma-Aldrich (Poole, UK)
Caerulein	Sigma-Aldrich (Poole, UK)
Calcium Chloride	Sigma-Aldrich (Poole, UK)
Cell strainer (45 μm Nylon)	BD Falcon (Oxford, UK)
Cell strainer (70 μm Nylon)	BD Falcon (Oxford, UK)
Cholera Toxin	Sigma-Aldrich (Poole, UK)
Collagenase type V	Sigma-Aldrich (Poole, UK)
Collagenase P	Roche (Welwyn Garden City, UK)
Collagen Rat Tail type I	BD Biosciences (Oxford, UK)
Coverslips	Menzel-Glaeser (Braunschweig, Germany)
DAB solution	BioGenex (Burlingame, UK)
DAPI	Sigma-Aldrich (Poole, UK)
ddH2O	LRI/CR-UK (London, UK)
Dexamethasone	Sigma-Aldrich (Poole, UK)
DirectPCR Lysis Reagent	Viagen Biotech (Los Angeles, USA)
Disodium tetraborate	AppliChem (Darmstadt, Germany)
DMEM	Life Technologies (NY, USA)
DyeEx® 2.0 Spin Kit	QIAGEN (Crawley, UK)
EDTA	Sigma-Aldrich (Poole, UK)
EGF (human)	PeproTech (London, UK)
Embedding cassetes	Tissue Tek (Basingstoke, UK)
Eosin Y	Sigma-Aldrich (Poole, UK)

Ethanol	Fisher Scientific (Loughborough, UK)
Ethidium Bromide	Sigma-Aldrich (Poole, UK)
FACS tubes	Becton Dickinson (Oxford, UK)
FGF-basic (human)	PeproTech (London, UK)
FGF10 (human)	PeproTech (London, UK)
Fluorescent Mounting Medium	DAKO (Ely, UK)
Foetal calf serum (FCS)	PAA (Yeovil, UK)
Gastrin	Sigma-Aldrich (Poole, UK)
GoTaq PCR DNA Polymerase	Promega (Southampton, UK)
Glucose	Sigma-Aldrich (Poole, UK)
Glycerol	Sigma-Aldrich (Poole, UK)
Glycine	Sigma-Aldrich (Poole, UK)
Goat serum	Sigma-Aldrich (Poole, UK)
Harris Hematoxylin (Shandon)	Fisher Scientific (Loughborough, UK)
HBSS Ca2-/Mg2-	Invitrogen (Paisley, UK)
Histo-Clear	Fisher Scientific (Loughborough, UK)
Hydrochloric acid	Fisher Scientific (Loughborough, UK)
Hydrogen peroxide	Sigma-Aldrich (Poole, UK)
Illustra™ GFX DNA Purification Kit	GE Healthcare (Little Chalfont, UK)
Industrial methylated spirit (IMS)	LRI/CR-UK (London, UK)
Isopropanol	Fisher Scientific (Loughborough, UK)
ITS+ premix	BD Biosciences (Oxford, UK)
MACs separation columns, 25 MS	Miltenyi Biotec (Surrey, UK)
Marvel skimmed milk powder	A1 Laboratory Supplies Ltd (Enfield, UK)
Matrigel, Growth Factor Reduced	BD Biosciences via VWR
Mayer`s hematoxylin	LRI/CR-UK (London, UK)
Magnesium Chloride	LRI/CR-UK (London, UK)
N-2 supplement	Life Technologies (NY, USA)
N-Acetylcysteine	Sigma-Aldrich (Poole, UK)
Neutral buffered formalin (NBF)	LRI/CR-UK (London, UK)
Nicotinamide	Sigma-Aldrich (Poole, UK)
Nu-Serum IV	BD Biociences (Oxford, UK)

Paraffin wax	Tissue Tek (Basingstoke, UK)
Paraformaldehyde	Sigma-Aldrich (Poole, UK)
PBS	Life Technologies (NY, USA)
Peanut oil	Sigma-Aldrich (Poole, UK)9
Penicillin/Streptomycin	Life Technologies (NY, USA)
Periodic Acid-Schiff	Sigma-Aldrich (Poole, UK)
Phenol Chloroform Isoamyl Alcohol 24:24:1	Sigma-Aldrich (Poole, UK)
Proteinase K	Melford Laboratories (Ipswich, UK)
Rainbow markers	GE Healthcare (Little Chalfont, UK)
Rat tail Collagen type I	BD Biosciences (Oxford, UK)
Ribonuclease	Sigma-Aldrich (Poole, UK)
RNase-Free DNase Set	QIAGEN (Crawley, UK
RNeasy Mini-kit	QIAGEN (Crawley, UK)
Sodium Acetate	Sigma-Aldrich (Poole, UK)
Sodium Chloride	LRI/CR-UK (London, UK)
Sodium Fluoride	Sigma-Aldrich (Poole, UK)
Soybean trypsin inhibitor	Sigma-Aldrich (Poole, UK)
Superfrost Ultra Plus charged slides	Menzel-Glaeser (Braunschweig, Germany)
Superscript III cDNA synthesis kit	Life Technologies (NY, USA)
SYBR Green	Life Technologies (NY, USA)
Taq PCR Core Kit	Qiagen (Crawley, UK)
Tamoxifen	Sigma-Aldrich (Poole, UK)
Tris	Sigma-Aldrich (Poole, UK)
Trisodium Citrate	Sigma-Aldrich (Poole, UK)
Trypan Blue	Sigma-Aldrich (Poole, UK)
Trypsin	Life Technologies (NY, USA)
Vi-Cell™ sample vial	Beckman Coulter (High Wycombe, UK)
Waymouth's MB725/1 Medium	BD Biosciences (Oxford, UK)
Xylene	LRI/CR-UK (London, UK)

2.1.2 Media and Buffers

Blocking Buffer (IF/IHC)	final concentration:
Bovine serum albumin	1%
Goat/Donkey Serum	10%
Triton X-100	0.4%
PBS	89.6%

Citrate Buffer	
Sodium citrate	2.94 g
HCl (0.2 M)	18 ml
ddH2O	up to 1 l

DMEM (complete Media)	
DMEM	445 ml
(+ 4.5 g/l glucose, + l-glutamine, + pyruvate)	
FCS	50 ml
1% (v/v) Penicillin/Streptomycin (10000 U/ml)	5 ml

DNA Extraction Buffer	
DirectPCR Lysis Reagent (mouse tail)	95 µl
Proteinase K (10 mg/ml)	5 µl

Harri's hematoxylin	
Hematoxylin	2.5 g
Absolute alcohol	25 mL
Potassium alum	50 g
ddH20	500 mL
Sodium iodate	0.5g
Glacial acetic acid	20 mL

G solution – 1 L (stock)	volume (final concentration):
HBSS	1L
CaCl2 (0.119 M)	0.4 mL (47.6 µM)
Glucose	0.9 g

MACS sorting buffer – 50 mL	volume (final concentration):
PBS endotoxin free	49.8 mL
BSA	0.25g (0.5% w/v)
EDTA (0.5M)	200 µL (2 mM)
FACS Buffer – 500 mL	volume (final concentration):
PBS endotoxin free	490 mL
FCS	10 mL (2% v/v)

Pancreatic ducts 2D media - 50mL (stock)	volume (final concentration):
Advanced DMEM/F12	45.72 mL
Nu-Serum (100x stock)	2.5 mL (1x)
Bovine Pituitary Extract (3 mg/ml stock)	420 µL (25 µg/mL)
ITS+ premix (100x stock)	250 µL (1x)
EGF (100 µg/mL stock)	10 µL (20 ng/mL)
Cholera Toxin (1 mg/mL stock)	5 µL (100 ng/mL)
3,3,5-Triiodo-L-thyronine (50 µM stock)	5 µL (5 nM)
Dexmethasone (20 µg/mL stock)	1 mL (1 µM)
Glucose	0.25g (5 mg/mL)
Nicotinamide	66mg (1.22 mg/mL)
Penicillin/Streptomycin (100x stock)	500 µL (1x)

Pancreatic organoid media - 50mL (stock)	volume (final concentration):
Advanced DMEM/F12	37.275 mL
B27 (100x stock)	1mL (1x)
N-Acetylcysteine (625 mM stock)	100 µL (1.25 mM)
Gastrin (10 µM stock)	50 µl (10 nM)
EGF (100 µg/mL stock)	25 µL (50 ng/mL)

RSPO1-conditioned media (100% stock)	5 mL (10%)
NOGGIN-conditioned media (100% stock)	5 mL (10%)
FGF10 (100 µg/mL stock)	50 µL (100 ng/mL)
Nicotinamide (500 mM stock)	1 mL (100 mM)
Penicillin/Streptomycin (100x stock)	500 µL (1x)

Phosphate buffered saline (PBS)	final concentration:
KCl	3 mM
NaCl	136 mM
$Na_2HPO_4 \bullet 2\ H_2O$	8 mM
KH_2PO_4	15 mM

Protein loading buffer (Laemmli buffer) final concentration

Tris-HCl (pH 6.8)	63 mM
SDS (w/v)	2% (w/v)
Glycerol (v/v)	10% (v/v)
bromophenol blue (w/v)	0.0025% (v/v)
β-mercaptoethanol (v/v)	2.5% (v/v)

Sodium acetate buffer

1 M sodium acetate	99 ml
1 M acetic acid	960 µl
ddH_2O	up to 1 l

Tris-EDTA buffer (10mM Tris Base, 1mMEDTA, 0.05% Tween, pH9.0)

Tri base	1.21g
EDTA	0.37g
ddH_2O	1000mL

10X Waymouth's (100mL)	volume (final concentration)
10X Waymouth's powder	14g (1X)
7.5% (w/v) Sodium Bicarbonate	30mL (2.25% (w/v))
Adjust the pH to 7.3	

1X Waymouth's complete media (100mL)	volume (final concentration)
1X Waymouth's	98.725 mL
Trypsin Inhibitor (40mg/mL)	250 µL (0.1mg/mL)
Dexamethasone (4mg/mL)	25 µL (0.001mg/mL)
FCS	1 mL (1%)

2.1.3 Oligonucleotides

The primers indicated in the tables below were used in the present study for mouse genotyping PCR (table 1), mouse Q-PCR (table 2) and generating the southern blotting probes (table 3)

Table 6 - Mouse genotyping primers

Gene/alelle	Primer Sequence	PCR product
Fbxw7 Wild type allele (wt) Floxed allele (F) Deleted allele (*Δ*)	Forward: 5'– CAGTGGAGTGAAGTACAACTCTGG – 3' Reverse: 5'– GCATATTCTAGAGGAGGGTATCGG – 3' Deleted reverse: 5' – GGCCAGCCTGGTCTGTATAGAG – 3'	wt: 288 bp F: 388 bp *Δ*: 744 bp
Cre	Forward: 5' – CGGTCGATGCAACGAGTGATGAGG – 3' Reverse: 5' – CCAGAGACGGAAATCCATCGCTCG – 3'	Cre: 600 bp
p53 Wild type allele (wt) Floxed allele (F) Deleted allele (*Δ*)	Forward: 5' – CACAAAAACAGGTTAAACCCAG – 3' Reverse: 5' – GAAGACAGAAAAGGGGAGGG – 3' Delta: 5'– AGCACATAGGAGGCAGAGAC – 3'	wt: 288 bp F: 370 bp *Δ*: 612 bp
KRas$^{LSL-G12D}$ Wild type allele (wt) Floxed allele (LSL) Recombined allele (Lox)	1: 5' – GTCTTTCCCCAGCACAGTGC – 3' 2: 5' – CTCTTGCCTACGCCACCAGCTC – 3' 3: 5' –AGCTAGCCACCATGGCTTGAGTAAGTCTGCA - 3'	wt: 622 bp LSL: 500 bp Lox: 650 bp
Rosa26-LSL-YFP Wild type (wt) Floxed (mut) Recombined (Lox)	1: 5'– GCGAAGAGTTTGTCCTCAACC – 3' 2: 5'– AAAGTCGCTCTGAGTTGTTAT – 3' 3: 5'– GGAGCGGGAGAAATGGATATG – 3'	wt: 600 bp mut: 300 bp Lox: 650 bp
Pten Wild type allele (wt) Floxed allele (F) Deleted allele (*Δ*)	Forward: 5' – CCATCACACTAAGGTCTGTGG – 3' Reverse1: 5' – ACTCCCACCAATGAACAAAC – 3' Reverse2: 5'– CCAGTAGTGATAGAACGGAAGTC – 3'	wt: 135 bp F: 346 bp *Δ*: 410 bp

Table 7 - Mouse Q-PCR primers

Gene	Primer Sequence
Cd9	Forward: 5' – ATATTCGCCATTGAGATAGCC – 3' Reverse: 5' – TGGTAGGTGTCCTTGTAAAACTCC – 3'
Cd44	Forward: 5' – GGCTCATCATCTTGGCATCT – 3' Reverse:5' – GCTTTTTCTTCTGCCCACAC – 3'
Ck19	Forward: 5' – TGACCTGGAGATGCAGATTG – 3' Reverse: 5' – CCTCAGGGCAGTAATTTCCTC – 3'
EpCam	Forward: 5' – AGAATACTGTCATTTGCTCCAAACT – 3' Reverse: 5' – GTTCTGGATCGCCCCTTC – 3'
Pdx1	Forward: 5' – GAAATCCACCAAAGCTCACG – 3' Reverse: 5' – CGGGTTCCGCTGTGTAAG – 3'
Ptf1a	Forward: 5' – GGGACGAGCAAGCAGAAGTA – 3' Reverse: 5' – CGCGGTAGCAGTATTCGTG – 3'
Pol II	Forward: 5' – AATCCGCATCATGAACAGTG – 3' Reverse: 5' – TCATCCATTTATCCACCACCT – 3'
Sox 9	Forward: 5' – GTACCCGCATCTGCACAAC – 3' Reverse: 5' – CTCCTCCACGAAGGGTCTCT – 3'
Fbw7 (exon 5)	Forward: 5' – TTCATTCCTGGAACCCAAAGA – 3' Reverse: 5' – TCCTCAGCCAAAATTCTCCAGTA – 3'

2.1.4 Antibodies

Table 8 - Primary Antibodies

Primary Antibody (reactivity)	Species (details)	Application, (Dilution, antigen retrieval)	Supplier, Cat Number
APC Rat isotype control	Rat monoclonal (IgG2b, κ)	FACS (1:500,na)	BD (Oxford, UK), 553991
CD9 (mouse)	Rat monoclonal (KMC8.8 IgG2a)	IHC-p (1:100, TE), IHC-IF (1:100, TE), FACS (1:500,na)	Santa Cruz (CA, USA), sc-18869
CD44-APC (mouse)	Rat monoclonal (IM7, IgG2b, κ)	FACS (1:500,na)	BD (Oxford, UK), 559250
CD44S (mouse)	Rat monoclonal (A020, IgG2b)	IHC-p (1:100, SC), IHC-IF (1:100, SC), FACS (1:1000,na)	Chemicon/Millipore (Watford, UK), MAB2137
CD45-PE (mouse)	Rat monoclonal (30-F11, IgG2b, κ)	FACS (1:500,na)	BD (Oxford, UK), 9012-9459
CK19 (mouse)	Rat monoclonal (IgG2a, κ)	IHC-p (1:100, SC) IHC-IF (1:100, SC)	DSHB (Iowa, USA), Troma-III
DBA-Biotin (mouse)	-	MACS (1:100,na)	Vector Laboratories (Peterborough, UK), B-1035
DBA-Fluorescein (mouse)	-	IHC (1:100,SC)	Vector Laboratories (Peterborough, UK), FL-1031
DBA-Rhodamine (mouse)	-	IHC-IF (1:100,SC)	Vector Laboratories (Peterborough, UK), RL-1032
E-Cadherin (mouse)	Rabbit monoclonal (IgG)	IHC-p (1:400, SC)	Cell Signalling, (Hitchin, UK), 3195
GFP	Goat polyclonal (IgG)	IHC-p (1:300, SC) IHC-IF (1:100, SC)	Abcam (Cambridge, UK), ab6673

HNF1beta (human/mouse)	Rabbit polyclonal	IHC-p (1:200, SC) IHC-IF (1:200, SC)	Sigma-Aldrich (Poole, UK), HPA002083
Hes1 (mouse)	Rabbit polyclonal	IHC-p	Chemicon/Millipore (Watford, UK), AB5702
Phosphorylated histone 3 (mouse)	Rabbit polyclonal IgG	IHC-p (1:100, SC) IF-p (1:100, SC)	Santa Cruz (CA, USA), sc-8656-R
Ptf1alpha (human/mouse)	Rabbit polyclonal	IHC-p (1:1000)	Beta Cell Consortium (Tennessee, USA), AB2153
pERK (p44/42 MAPK)	Rabbit, polyclonal	IHC 1:100	Cell Signalling, (Hitchin, UK), 4370
Rat IgG2a isotype control	Rat monoclonal (IgG2a)	IHC-p (1:100, TE), IHC-IF (1:100, TE), FACS (1:500,na	Santa Cruz (CA, USA), sc-3883
B-catenin	Rabbit polyclonal	IHC-p (1:200, SC)	Sigma-Aldrich (Poole, UK), C2206

Table 9 - Secondary Antibodies

Secondary Antibody	Species	Application, Dilution	Supplier, Cat Number
Alexa Fluoro 488, anti Mouse	Donkey anti-Mouse IgG	IHC-IF (1:200) FACS (1:2000)	Life Technologies (NY, USA) A21245
Alexa Fluoro 488, anti Mouse	Goat anti-Mouse IgG	IHC-IF (1:200) FACS (1:2000)	Life Technologies (NY, USA) A11029
Alexa Fluoro 488, anti Rabbit	Donkey anti-Rabbit IgG	IHC-IF (1:200) FACS (1:2000)	Life Technologies (NY, USA) A21206
Alexa Fluoro 488, anti Rabbit	Goat anti-Rabbit IgG	IHC-IF (1:200) FACS (1:2000)	Life Technologies (NY, USA) A11008
Alexa Fluoro 546, anti Mouse	Goat anti-Mouse IgG	IHC-IF (1:200) FACS (1:2000)	Life Technologies (NY, USA) A10036
Alexa Fluoro 546, anti Rabbit	Donkey anti-Rabbit IgG	IHC-IF (1:200) FACS (1:2000)	Life Technologies (NY, USA) A10040
Alexa Fluoro 568 anti Mouse	Donkey anti-Mouse IgG	IHC-IF (1:200) FACS (1:2000)	Life Technologies (NY, USA) A10037
Alexa Fluoro 568 anti Rabbit	Donkey anti-Rabbit IgG	IHC-IF (1:200) FACS (1:2000)	Life Technologies (NY, USA) A11011
Alexa Fluoro 555 anti Rat	Goat anti Rat IgG	IHC-IF (1:200) FACS (1:2000)	Life Technologies (NY, USA) A21434
Alexa Fluoro 647 anti Rat	Goat anti Rat IgG	IHC-IF (1:200) FACS (1:2000)	Life Technologies (NY, USA) A21247
Biotin-conjugated anti-Goat	Rabbit, anti-Goat IgG	IHC-p 1:250	Vector Laboratories (CA, USA) BA-5000
Biotin-conjugated anti-Mouse	Horse anti-Mouse IgG	IHC-p 1:400	Vector Laboratories (CA, USA) BA-2000
Biotin-conjugated anti-Rabbit	Goat anti-Rabbit IgG	IHC-p 1:250	Vector Laboratories (CA, USA) BA-1000
Biotin-conjugated anti-Rat	Rabbit, anti-Rat IgG	IHC-p 1:250	Vector Laboratories (CA, USA) BA-4000

2.2 Methods

2.2.1 Animal work

2.2.1.1 Housing and animal care

All mice used during the course of this study were housed in the Biological Resource Unit, at either Lincoln's Inn Fields or Clare Hall sites, of the London Research Institute. Mice were culled by Schedule 1 Methods, in accordance with the Animal Scientific Procedures Act 1986 (revised in 1997), via cervical dislocation followed by exsanguination through the severing of a major blood vessel. New-borns were culled by decapitation and death confirmed by verification of onset of rigor mortis. All scientific procedures performed during the course of this study were approved by the London Research Institute Animal Ethics, following UK home Office guidelines.

2.2.1.2 Mouse lines

Mouse Line	Reference
Ck19-CreER	(Means et al., 2008)
Ela1-CreER	(Desai et al., 2007)
$Fbw7^{F/F}$	(Hoeck et al., 2010)
Hnf1β-CreER	(Solar et al., 2009)
$KRas^{LSL-G12D/wt}$	(Jackson, 2001)
Nu/Nu	(Flanagan, 1966)
$p53^{F/F}$	(Marino et al., 2000)
Pdx1-Cre	(Hingorani et al., 2003)
$Pten^{F/F}$	(Lesche et al., 2002)
Rag2KO	(Hao and Rajewsky, 2001)
Rosa26-LSL-YFP	(Srinivas et al., 2001)

2.2.1.3 Tamoxifen preparation and injections

For an inducible regulation of Cre recombinase expression, CreER mouse models were used. In these mice, Cre recombinase is fused to a mutated ligand-binding domain of the human oestrogen receptor. Thus, Cre is expressed but unable to translocate to the nucleus. Cre function is dependent on hydroxytamoxifen (metabolic product of tamoxifen) administration. A 20 mg/mL of tamoxifen solution was prepared by dissolving the tamoxifen powder in peanut oil. To promote dissolution, the mixture was subjected to 3 cycles of 15-minute incubations at 50C°C followed by 15 minutes on a rotating wheel. To induce Cre-dependent recombination of the floxed alleles present in the various genotypes used, mice were intraperitoneally injected once a day (for two consecutive days) with 5 µL/g bodyweight of the 20 mg/mL stock solution.

2.2.1.4 Hydroxytamoxifen preparation

When local pancreatic induction of Cre recombinase fucntion was required, the intraperitoneal injection of tamoxifen was substituted by the intrapancreatic injection of 4-hydroxytamoxifen (see surgery section). A 10 mg/mL solution of 4-hydroxytamoxifen was prepared by dissolving 10 mg of 4-hydroxytamoxifen in 1 mL of peanut oil. Dissolution was promoted by cooled sonication of the mixture for 2 cycles of 30 minutes (30 s on/off cycle) using a BioRuptor water bath. Mice were subjected to surgery (see 2.2.1.7, page 97) and 100 µL of the 10 mg/mL 4-hydroxytamoxifen solution was injected directly into the tail of the pancreas.

2.2.1.5 Acute pancreatitis – caerulein treatment

To induce acute pancreatitis, mice were subjected to a short caerulein treatment. A stock solution of caerulein was prepared to a final concentration of 100 µg/mL by dissolving 1 mg of caerulein in 10 mL of PBS. Working solutions were obtained by dissolving the stock solution to a concentration of 10 µg/mL in PBS. Mice were intraperitoneally injected 6 times a day, at hourly intervals, for 2 days. Per injection the caerulein dose was as follows: 5 µl per gram of body weight of caerulein (50 µg/kg of body weight).

2.2.1.6 Chronic pancreatitis – caerulein treatment

To induce chronic pancreatitis, mice were subjected to a long caerulein treatment. A stock solution of caerulein was prepared to a final concentration of 100 µg/mL by dissolving 1 mg of caerulein in 10 mL of PBS. Working solutions were obtained by dissolving the stock solution to a concentration of 10 µg/mL in PBS. Mice were intraperitoneally injected 3 times a day, at hourly intervals, for 3 consecutive days, for 4 weeks. Per injection the caerulein dose was as follows: 5 µl per gram of body weight of caerulein (50 µg/kg of body weight).

2.2.1.7 Surgery – Intrapancreatic/ductal injection of cells/ substances

Twenty-four hours before the surgery Rimadyl (Carprofen-based anagesis) was added to the water. Two mL of 50 mg/ml Rimadyl solution were added to 1 L of water. On the day of the surgery, mice 8 to 12 weeks of age (genotype depending on the experimental goal, specified in result section) were subcutaneously injected with Rimadyl 1 hour before surgery. For the subcutaneous injection of Rimadyl, a 1:10 dilution was prepared with a stock solution of 50 mg/mL. Mice were injected with 1µ of the solution per gram of body weight. Following anaesthesia by Isoflurane inhalation, the abdominal and splenic areas were shaved and their eyes protected with Lacri-lube. The shaved area was thoroughly cleaned with Medihex-4 (surgical scrub) and a sterile incise drape was used to cover the non-shaved parts. With sterile surgical scissors, a small incision was performed in the skin and the peritoneal wall exposed. After opening the peritoneum, the pancreas was located and either a tumour cells suspension in growth factor reduced matrigel (50 µL) or (2) 4-hydroxytamoxifen (100 µL) were injected in the pancreatic tail. Having concluded the procedure, the peritoneal was sutured with absorbable sutures and the skin closed with clips. A dose of 0.05 mg/Kg of Vetergesic was subcuteneosly injected immediately after surgery and the mice placed in a clean cage on a heating pad until recover. The next day, mice were subcutaneously injected with Rimadyl as before and the drinking water was supplemented Rimadyl for three days.

2.2.1.8 Limiting-dilution transplantation assay of cells in mouse flanks

To assess the tumour initiating capacity of $CD9^{High}$-expressing cells, epithelial tumour cells were obtained either from primary tumours of GEM models or from GEM tumour-derived organoids. In both cases, tumour cells were identified by GFP expression, enabled by the presence of the lineage tracer R26-LSL-YFP. Following fluorescence activated cell sorting for CD9 expression and CD45 exclusion (pan-immune cell marker), serial dilutions of single $GFP^{+}CD9^{High}CD45^{-}$ cells were prepared (200, 2000, 20.000 and 200.000 cells) in 50 µL of growth factor-reduced matrigel and injected in the flank of age and gender matched NuNu immunodeficient mice. To control for tumour development and tumor-initiating potential of the selected population, the negative counterpart (GFP^{+}, $CD9^{Low}CD45^{-}$ cells) were injected in the opposite flank. Tumour measurements were performed twice a week and volume was calculated using the following equation: volume = (1/2)*length*width*height (Tomayko and Reynolds, 1989). Tumours were collected when one of the flanks exhibited a tumour of $1cm^3$ in volume or when location of the tumour presented a health hazard.

2.2.2 Primary cell manipulation

2.2.2.1 Primary pancreatic wild type and tumour cell isolation

To isolate primary pancreatic wild type and tumour cells, a modified version the protocol described before (Reichert et al., 2013) was applied. The mouse was culled by cervical dislocation followed by exsanguination, according to the Home Office guidelines. The pancreas was dissected out carefully, including the tail, body and head of the pancreas, as well as the connection with the bile duct. The dissected pancreas was immediately put in 5 mL of cold G solution (see 2.1.2, page 86) and kept on ice. Under the primary tissue culture hood, the pancreas was placed on paraffin and mechanically dissociated with curved scissors. The minced pancreas was then transferred to a 50 mL falcon with 15 mL of collagenase V (1 mg/mL in DMEM plus 1% (v/v) Penicillin/Streptomycin (10,000U/mL with no FCS). Following a 20 minute incubation in a water bath at 37°C with gentle shaking, 15 mL of ice-cold G solution were added to stop the reaction. The digested pancreas was centrifuged at 300g for 5 minutes with no break, the supernatant discarded and then incubated in Trypsin-EDTA for 5 minutes at room temperature. To stop the reaction, 2 mL of Soybean Trypsin Inhibitor were added, followed by 15 mL of ice-cold G solution and centrifugation for 5 minutes at 300g. The supernatant was ressuspended in 10mL of PBS with 2% (v/v) FCS and passed through a 70 μm filter. At this point, the isolated single cells could be used for different applications such as, direct culture, Dolichos biflorus agglutinin magnetic bead cell sort (DBA-MACS), xenograft experiments, fluorescent activated cell sorting/analysis or biochemical experiments (see respective sections).

2.2.2.2 Dolichos biflorus agglutinin magnetic bead cell sort (DBA-MACS)

Pancreatic ductal cells present DBA lectin in their cell surface allowing the isolation of these cells by magnetic bead cell sorting. In order to isolate pancreatic ductal cells, a modified version of the protocol described before (Reichert et al., 2013) was applied. Following pancreatic cell isolation, as described above, single cells were ressuspended in 3ml of MACS sorting buffer (0.5% BSA and 2mM EDTA in endotoxin free PBS) with 1:200 DBA-FITC conjugated antibody. The suspension was incubated for 10

minutes, at 4 °C in the dark, with mild shaking and then 2.8 mL of MACS sorting buffer were gently mixed. Following centrifugation at 300 g for 5 minutes with no break, the cell pellet was ressuspended in 360 µL of Sorting buffer plus 40 µL of anti-FITC-Microbeads and incubated for 15 minutes at 4 °C with gentle shaking. Cells were washed by adding 4 mL of MACS sorting buffer and centrifuging the suspension at 300 g for 5 minutes with no break. After discarding the supernantant, cells were ressuspended in 2 mL of MACS orting buffer and kept on ice until the separation columns were ready for use. For primary pancreatic wild type and tumor cells DBA-MACS, LS MACS columns were used. The preparation of columns consisted on placing them on a QuadroMACS separator and adding 3 mL of MACS sorting buffer. After the buffer had flowed through the columns by gravity, the cells suspension was then applied to the buffered columns. At this point the labelled cells are retained in the columns by magnetic forces. The columns were washed three times by adding 2 mL of MACS sorting buffer and allow flow by gravity. After the lst washing, the columns were removed from the stand and placed in collection tubes. To allow separation of the cells from the columns, 3 mL of MACS sorting buffer were added to the columns and with the plunger, flushed to the tube. At this point the isolated ductal cells were used for different purposes.

2.2.2.3 Flow cytometry and Fluorescent activated cell sorting (FACS)

Following primary pancreatic cell isolation as described above, cells could then be used for flow cytometry analysis or cell sorting. Single cells were ressuspended in endotoxin free PBS with 2% (v/v) FCS (FACS buffer) and then split into the different control and test samples (unstained, secondary antibodies alone, primary plus secondary antibodies, and/or conjugated primary antibody, and FMOs (fluorophore minus one, where all combinations of the fluorophores used, minus one, are included for specific signal detection purposes). Cells were pelleted into a 96-well plate (round bottom) for 3 minutes at 300 g, the supernatant was discarded by rapidly inverting the plate, and the cells ressuspended in 100 µL FACS buffer with the appropriate primary antibody (specific dilutions were used for different antibodies, see 2.1.4, page 92). All primary antibodies were incubated for 30 minutes on ice. Following incubation, cells were

pelleted at 300 g for 3 minutes, at room temperature, and washed 3 with 100 µL of FACS buffer. Secondary antibody was diluted in FACS buffer and 100 µL were added to the cells. Incubation was performed in the dark for 30 minutes at 4°C. Cells were washed 3 times in FACS buffer and ressuspended in FACS buffer containing DAPI 0.003 mM (1 µL per mL of buffer from 3mM stock). A sortings were performed in one of the three flowing machines: FACS ARIA fusion, FACS Aria or Influx, using the diva software and adjusting the flow pressure to 20psi. Flow cytometry was performed using Fortessa Diva and analysis was carried out using FlowJo 9 software.

2.2.2.4 2D primary pancreatic ductal cell culture

Pancreatic ductal cells were grown in 2D, on top of a rat tail type I collagen matrix, on a 6-well plate. The matrix had to be prepared the day before, as to allow the collagen to set. For each well of the 6-well plate, a 1.5 mL of collagen solution were prepared by mixing 2.31 mg/mL of cold rat tail collagen solution with 0.0165 mL of 1M NaOH (1.65% (vol/vol)) and 100 µL of 10X sterile PBS (10% (vol/vol)), and toping up with sterile ice-cold deionized water. The solution was poured into a well of a 6-well plate and allowed to set O.N. in the incubator (37 °C). The next day, and after primary pancreatic cell isolation and DBA-MACS (see 2.2.2.2, page 99), the isolated ductal cells were ressuspended in PDAC media composed of Advanced DMEM/F12 supplemented with 1X Nu-serum, 25 µg/mL of bovine pituitary extract, 1x ITS+ premix, 20 ng/mL of EGF, 100 ng/mL of cholera toxin, 5 nM of 3,3,5-Triiodo-L-thyronine, 1 µM of Dexmethasone, 5 mg/mL of glucose, 1.22 mg/mL of Nicotinamide and 1x P/S. The media was changed every other day to maintain the culture. Both wild type and tumour primary pancreatic ductal cells grow very slowly in these conditions and thus, this methods was only used to maintain the cells for long periods of time.

2.2.2.5 2D primary pancreatic ductal cell passaging

To remove the pancreatic ductal cells from the collagen matrix, the collagen sheet was transferred into a 50 mL falcon tube with 10 mL of collagenase type V in DMEM (1 mg/mL). Following 15 minutes incubation at 37°C in a water bath, the cells were

pelleted at 300 g for 5 minutes at 4 °C. The supernantant was discarded, 1 mL of 1X trypsin was added and a 5-minute incubation at room temperature took place. To stop the reaction, 2 mL of soybean trypsin inhibitor were added, followed by 25 mL of ice-cold G solution. Cells were pelleted as before and either re-plated (see 2.2.2.4, page 101) or used for various purposes.

2.2.2.6 3D primary pancreatic ductal cell culture - organoid

Following primary pancreatic cell isolation and, in some specified cases, DBA-MACS, the isolated cells were ressuspended in 100% Growth factor reduced matrigel and placed in a 24-well plate as 50 to 100 µL drop. The matrigel solidifies at warm temperatures so, to allow the formation of a matrix, the 24-well plates were then incubated for 15 minutes at 37 °C. After the matrigel was set, organoid media composed of Advanced DMEM/F12 supplemented with 1x B27, 1.25 mM N-Acetylcysteine, 10 nM Gastrin, 50 ng/mL EGF, 10% RSPO1-conditioned media, 10% NOGGIN-conditioned media, 100 ng/mL FGF10, 100 mM Nicotinamide and 1X P/S, was added. Cells were passaged once a week.

2.2.2.7 3D primary pancreatic ductal cell passaging

To obtain a single cell suspension of the organoid cultures, the matrigel-embedded organoids were ressuspended in 15 mL of endotoxin free PBS. Organoids were pelleted for 5 minutes at 1500 rpm, to assure the matrigel goes to the bottom of the tube, and the PBS discarded. Dissociation was carried out for 10 minutes with 500 µL of 1mg/ml trypsin at 37 °C, and immediately inactivated with 1 mL of 1X soybean trypsin inhibitor. A washing step was performed with an additional 15ml of endotoxin free PBS and single cells were either ressuspended in matrigel for further expansion or passed by a 40 µm cell strainer and used for downstream experiments.

2.2.2.8 Explant culture of mouse primary acinar cells

It has been demonstrated that acinar cells have the ability to *in vivo* transdifferentiate into duct-like cells upon injury and in the context of pancreatitis and tumour formation. Recently, this phenomena was mimicked in vitro, allowing the culture of explants of acinar tissue which undergo ADM (Means et al., 2005). Before starting the procedure the cell culture plates were coated with an ice-cold rat tail collagen I solution composed of 5.5mL of 4.5g/mL Rat tail Collagen I solution, 550 µL of 10X Waymouth's medium and 336.7 µL of 0.34N NaOH. Each well of a 6-well plate was covered with 800 µL of the aforementioned collagen solution and placed in the incubator until needed (approximately 3h).

In order to obtain the acinar explants, the mouse of interest was culled by cervical dislocation followed by exsanguination, as mentioned above. With the help of sterile tweezers, the pancreas was dissected out, including the tail, body and head of the pancreas. The dissected pancreas was immediately put in 20 mL of ice-cold HBSS with 1x P/S and kept on ice. Under the primary tissue culture hood, the pancreas was placed on a 1.5 mL eppendorf, minced with sharp scissors and transferred to a 50mL falcon tube containing 30 mL of ice-cold HBSS 1x P/S. Centrifugation at 2000rpm at 4 °C for 2 minutes was carried to remove any floating fat or mesenteric tissue that could have been extracted during the pancreas dissection. After discarding the supernatant, the remaining pancreatic tissue was enzymatically digested in 5mL of 2 mg/mL collagenase P, dissolved in HBSS, in a 37°C water bath for 15 minutes with occasional shaking. The digestion was stopped by adding 5 mL of ice-cold HBSS supplemented with 5% FCS and the digestion was centrifuged for 2 min at 4 °C at 2000 rpm. Following 2 washing steps with 10m L ice-cold HBSS supplemented with 5% FCS, the pellet was ressuspended in 5mL of the same solution and filtered twice. Initially it was passed through a 500 µm sterile cone-mesh followed by a 105µm mesh. These filtering steps allow the purification of small acinar cell aggregates by removal of big cell clumps. The acinar cell aggregate suspension was then added, in a drop-wise manner, on top of a HBSS solution supplemented with 30% FBS and centrifuged at 1000rpm at 4°C for 2 minutes. This density-based separation step allows the elimination of any acinar or duct single cells that could contaminate and compromise the explant culture. The pellet was ressuspended in Waymouths complete medium and either used immediately for culture

or Ad-CMV-Cre infected and then embedded. Acinar aggregates were embedded in collagen by mixing equal volumes of the cell suspension and collagen solution (700 µL 10x Waymouth's medium supplemented). The mixture was added to the pre-coated plates (2 mL of embedding suspension per well of a 6-well plate), the plates were carefully placed at 37°C in the incubator for the collagen to set for 1 hour and 3 mL of Waymouth's media were added. Cultures were followed under the microscope, the media was changed every two days and duct structures harvested after 7 days of culture.

2.2.2.9 Harvest of acinar explant-derived duct structures

As mentioned above, culturing *KRasG12D* mutation-harbouring acinar explants under the above conditions induces the formation of ring structures composed of pancreatic duct-like cells. The structures take an average of 7 days to form and, once formed, they can be harvested for further culture or downstream biochemical applications. To harvest the cells, the media was aspirated and the collagen sheet was placed in a 15mL tube with 5mL of 1mg/mL collagenase P solution in HBSS. Following a 15 minute incubation at 37°C in a water bath, the digestion solution was centrifuged at 2000rpm for 5 minutes at 4°C. The cell pellet was washed once with ice-cold PBS and cells ressuspended in appropriate buffer or media, depending on the downstream application.

2.2.2.10 Adeno virus transduction

To induce in vitro Cre recombinase-mediated excision of loxP site, cells harbouring alleles flanked by loxP sequences (e.g. LSL-KRasG12D) were transduced with Adeno-CMV-Cre-GFP virus. This procedure was performed in duct-derived organoids and acinar cells aggregates harbouring the following alleles: $p53^{F/F}$; $KRas^{LSL\text{-}G12D/wt}$; *R26-LSL-YFP*. For ductal cell infection, duct-derived organoids were dissociated into single cells (see 2.2.2.7, page 102), the single cell suspension was incubated with 0.375 µl of either Adeno-Cre-GFP or Adeno-GFP (Gene Transfer Vector Core) in 1.5ml of organoid media for 1hour at 37°C. Following transduction, cells were pelleted, ressuspended in matrigel and a drop of 25 µl was placed in the center of each well of a 24-well plate. A 15 minute incubation at 37°C was carried out to set the matrigel and

500 µl of organoid media were added with the same amount of fresh Ad-CMV-Cre-GFP virus. Acinar cell aggregates were infected immediately after their isolation from primary tissue, as described for ductal cells. Following transduction, the cell suspension was mixed in a 1:1 ratio with collagen solution (as described for expant culture), placed on top of rat tail collagen I pre-coated plates and allowed to set for 1h at 37°C before adding Waymouth's media. In both cases, media was changed 24h later. Infection efficiency was estimated by quantifying the percentage of GFP expressing cells, and the efficiency of recombination assessed by DNA isolation and genotyping for the floxed and delta alleles. All infection steps were carried out in a Category II Containment Suite

2.2.2.11 In vitro self-renewal assessment – organoid formation

Assessment of in vitro self renewal ability was performed as described in (Huch et al., 2013). Pancreatic duct cells were either isolated from primary tumours by DBA MACS. Isolated cells were incubated with CD9 primary antibody (1:500) for 30 minutes on ice. Following 3 washes with ice-cold PBS with 2% FCS, a 30 minute incubation with a secondary antibody (1:2000) was performed on ice and in the dark. Cells were washed three times with PBS with 2% FCS, passed through a 40 µm cell strainer and DAPI was added (1:1000) from a stock solution of 3 mM. Fluorescence activated cell sorting allowed the separation between the $CD9^{High}$ and $CD9^{Low}$ populations. One hundred cells of each population was sorted directly into wells of a pre-cooled 96-well plate (100cells/well) containing 20 µL of ice-cold matrigel. Or 1000 cells were plated into single wells of a 24-well plate. Following sorting, the matrigel was allowed to set at 37°C for 15 minutes and organoid media was added. Organoids were counted and measured using ImageJ 10 days later.

2.2.3 Cellular and molecular biology

2.2.3.1 Histology - Tissue processing

For histological studies, tissues were collected from recently sacrificed mice and placed in 10% neutral buffered formalin (NBF) solution overnight (approximately 16h) for protein cross-linking and consequent tissue fixation. The next day, the NBF solution was replaced by 70% ethanol. The fixed and dehydrated tissue was paraffin embedded sectioned in 3 or 4 μm paraffin sections, for pancreas or tumour analysis, respectively, using a manual microtome (RM2235 Leica) and placed in a 37°C water bath to unfurl. Sections were mounted on Superfrost Ultra Plus charged slides (Menzel-Glaeser) and incubated in the oven for 15 minutes to increase adherence.

2.2.3.2 Hematoxylin and eosin (H&E) stain

Histological enquiry based on tissue morphological features was carried out by analysis of hematoxylin and eosin stains. This procedure takes advantage of the affinity of certain compounds for particular cellular structures. Hematoxylin is a dark blue coloured basic compound that binds acidic or basophilic structures, namely nucleic acids, giving the nucleus a blue colour. Eosin is a pink compound that binds basic or eosinophilic structures, namely proteins, staining the cytoplasm and membranes pink. To perform the stain, 3 or 4 μm paraffin section sections, for pancreas and tumours, respectively, were obtained and de-waxed in xylene two times for 10 minutes. Re-hydration was carried out by incubations in water solutions with decreasing ethanol concentration: 2x in 100% ethanol for 3 minutes, 1x in 95% (v/v) ethanol for 3 minutes, 1x in 80% (v/v) ethanol for 3 minutes, 1x in 50% (v/v) ethanol for 3 minutes and 1x in running water for 5 minutes. Nuclear staining was performed by incubating the hydrated sections in Harri's hematoxylin solution for 5 minutes and washed in running tap water for 5 minutes. Differentiation was performed for 5 seconds in 1% (v/v) acid alcohol (1% HCL in 70% alcohol) and sections were washed in running tap water for 5 minutes. Cytoplasm staining was accomplished by incubation of the section in 1% (w/v) eosin Y and final washing in running tap water for 5 minutes. Before mounting, the section were dehydrated through graded alcohols: 2x in 70% (v/v) ethanol for 3 minutes,

and 2x in 00% ethanol for another 3 minutes. At the final step sections were cleared twice in xylene for 3 minutes and mounted with DPX mounting medium (Raymond A. Lamb). All H&E stains were performed by the experimental histopathology facility.

2.2.3.3 Histological analysis

Histological analysis, the identification of tumour progression and the classification of mPDAC from different GEM models was performed with the help of London Research Institute's experienced consultant histopathologist Professor Gordon Stamp.

2.2.3.4 Immunohistochemistry

For protein detection in the embedded tissues, thin sections were obtained and re-hydrated as performed for H&E stains. Antigen retrieval was performed to expose the masked epitopes and different antibodies required different antigen retrievals (see 2.1.4, page 92). The most common antigen retrieval performed was a heat-based treatment with 10 mM Sodium citrate buffer pH 6.2. In sum, dissolving 2.94 g of sodium citrate in water and adjusting the pH with HCl to 6.2 performed a 1L 10 mM of sodium citrate solution. Sections were submerged in this solution and microwaved for 10 minutes at full power, avoiding boiling. Following the heat treatment, section were placed in a sink, under a barely running tap for 5 minutes to both cool and dilute the buffer solution to prevent salt crystallisation. Slides were washed with PBS and the endogenous peroxidase was blocked by a 10-minute treatment in 1.6% (v/v) solution of hydrogen peroxide in PBS (13.3mL of 30% (v/v) H_2O_2 in 250 mL final volume of PBS) terminated by a 5-minute incubation in dH2O. To stain the slides, the excess fluid was carefully wiped from the slide and a barrier around the tissue section was drawn using a hydrophobic pen. Section were first blocked for 45 minutes with a blocking solution composed of PBS supplemented with 10% (v/v) donkey serum, 1% BSA (w/v), 0.4% (v/v) Triton X-100 and then incubated either overnight at 4°C or 1h at room temperature with the primary antibody diluted in the blocking solution. Slides were kept in a humid chamber until the end of the incubation. Following primary antibody incubation, the appropriate secondary antibody conjugated with biotin was used. The secondary

antibody dilution depended on the antibody used (see 2.1.4, page 92), antibodies were diluted in the blocking solution and incubated, at room temperature for 45 minutes. Before the end of the secondary antibody incubation, the Avidin-Biotin Complex (ABC) solution was prepared by adding 9 µL of reagent A and B from the VECTASTAIN ABC kit to 1mL of PBS. The sections were incubated with ABC solution for 30 minutes in a humid chamber, at room temperature, and then washed 3 times for 3 minutes in PBS. For developing the staining, the Peroxidase substrate kit DAB from Vector was used. This last step was performed under a microscope to closely monitor the signal strength. The DAB solution was performed as instructed by the kit. Two drops of Buffer solution were added to 5mL of distilled water. The solution was mixed and 4 drops of DAB substrate solution were added. After mixing, 2 drops of provided hydrogen peroxide solution were added and the DAB solution was mixed again. DAB solution was applied to the washed slides, the signal monitored and the reaction stopped my immersing the slides in distilled water. To counterstain the nuclei a light hematoxylin protocol was followed. Slides were immersed in hematoxylin (120mL Mayer's Hematoxylin and 80mL of dH_2O) for 1 minute and then washed with tap water for 5 minutes. Lastly, the slides were dehydrated through incubations in 70% and 100% IMs, cleared in xylene and mounted with DPX.

2.2.3.5 Immunofluorescence

For immunofluorescence analysis, thin sections were obtained and re-hydrated as performed for H&E stains. Antigen retrieval was performed to expose the masked epitopes and different antibodies required different antigen retrievals (see 2.1.4, page 92). Following antigen retrieval (as described for immunohistochemistry), the sections were washed with PBS a barrier was drawn around the tissue section using a hydrophobic pen. Section were first blocked for 45 minutes with a blocking solution composed of PBS supplemented with 10% (v/v) serum of the species of the secondary antibody to use, 1% BSA (w/v), 0.4% (v/v) Triton X-100 and then incubated either overnight at 4°C with the primary antibody diluted in the blocking solution. Slides were kept in a humid chamber until the end of the incubation. Following primary antibody incubation, the appropriate secondary antibody conjugated with the fluorophore of

interest was used. The secondary antibody dilution depended on the antibody used (see 2.1.4, page 92), antibodies were diluted in the blocking solution together with DAPI (0.003 mM) for DNA stain, and incubated, at room temperature for 2 hours. Following incubation with the secondary slides were washed 3 times for 5 minutes in PBS and incubated in 0.1 % (w/v) Sudan Black B in 70% (v/v) ethanol to reduce autofluorescence. Slides were washed 3 times in PBS for 5 minutes, mounted with DAKO mounting media and kept in the dark until imaging.

2.2.3.6 Alcian Blue and Periodic acid-Schiff stain

To detect mucinous structures in pre-neoplastic lesion of PDAC the alcian blue and periodic acid-schiff stain was performed for being extensively used to detect these lesions. Alcian blue (AB) is a polyvalent basic dye that stains acidic polysaccharides and mucopolysaccharides. Tissues that stain positive for this dye are called alcianophilic and acquire a dark blue colour. The Periodic acid-Schiff (PAS) stain detects polysaccharides and mucosubstances. Tissues that stain positive for this method acquire a purple/magenta colour. The AB/PAS stain is a combination of both methods where AB is performed first. It is important to bear in mind that acid mucin that are also PAS-positive will not stain for PAS after the AB stain is performed.

To perform the stain in paraffin section, the paraffin was first removed by xylene treatment twice for 5 minutes. The tissue was incubated in 100% IMS for 3 minutes twice and incubated once in 70% IMS for 3 minutes. After washing in tap water, the slides were incubated for 5 minutes in alcian blue solution (1% (w/v) Alcian blue – 1 g in 100 ml of 3%(v/v) acetic acid). Slides were then washed intensively in tap water and then distilled water before the performing the PAS satin. Following washes, slides were incubated in 1% (w/v) periodic acid in distilled water for 5 minutes and washed again in distilled water. The Schiff reagents was obtained from Fisher and the tissue was incubated in the solution for 15 minutes with a follow up washing step of 10 minutes in running tap water. The nuclei were counterstained with Mayers hematoxylin for 1 minute. The stain was differentiated in 1% acid alcohol for a few second (arbitrary time, dependent on monitoring) and washed in tap water for 5 minutes. For mounting, the

tissue was dehydrated in ethanol and cleared in xylene as mentioned before (see 2.2.3.2, page 106), and slides were mounted with coverslips using DPX mounting medium.

2.2.3.7 DNA isolation from tissue for genotyping

For genotyping, murine tissue fragments (ear or tail snips) were incubated in 100 µL of DirectPCR Lysis Reagent (Viagen) supplemented with 3 µL of Proteinase K (10mg/mL, Melford) overnight at 56 °C in a shaking platform. The next day, the enzyme was inactivated by a 45-minute incubation at 85 °C. Samples were vortexed and centrifuged at full speed for 15 minutes (eppendorf Centrifuge 5415 D). For genotyping purposes, 2 µL of extracted DNA solution were used for PCR. DNA solution was kept at -20 °C.

2.2.3.8 DNA isolation from tissue embedded in paraffin blocks for genotyping

To extract DNA from tissue embedded in paraffin block, sections 10-20 10 µm section were obtained in one eppendorf tube. Paraffin was removed by adding 1 mL xylene and incubating the tube at 55°C for 15 minutes. Following incubation the samples were centrifuged and the supernatant discarded. A second xylene incubation was performed to ensure complete removal. Before the next step, tubes were opened to release pressure. Following xylene incubations and, 1 mL of 100% ethanol was added to the pellet and the samples were incubated for 15 minutes. Tubes were centrifuged, the supernatant discarded and an additional ethanol washing step was performed. Following centrifugation, the supernatant was carefully discarded and the tubes were left opened to allow the pellet to air dry. One mL of Proteinase K (final concentration of 0.5 mg/mL) in digestion buffer (100nM NaCl, 10mN Tris-HCl pH8, 25mM EDTA pH8 and 0.5% SDS) was added to the dry pellet and the samples were incubated overnight at 55°C.
The next morning DNA precipitation was performed. An equal volume of phenol/chloroform/isoamyl alcohol (Ameresco) was added to the digestion solution. The tubes were centrifuged for 2 minutes and the upper aqueous phase was collected to a new tube. The previous step was repeated. Following removal of the aqueous phase, 330 µL were removed to a new tube and ammonium acetate (7.5M) was added (1/2 of the original volume). Additionally, 2.5 times the volume were added of 100% ethanol.

The solution was incubated at -20°C overnight. The next morning, the solution was centrifuged for 20 minutes at 4 °C at maximum speed (eppendorf Centrifuge 5415 D), the ethanol was decanted and the pellet was allowed to air dry. The dry pelleted was eluted in 20 µL of TE buffer overnight at 4°C. For genotyping, 200 to 500 µg/mL of DNA were used.

2.2.3.9 Polymerase Chain Reaction (PCR)

After DNA isolation, genotyping PCR was performed using approximately 2 µL of the isolated DNA.

A mixture of 20 µL of final volume was prepared containing the following components:

1x Coral Load PCR Buffer	2 µL (10X stock)
1x Solution Q (DMSO based)	4 µL (5X stock)
dNTPs (0.25 mM)	0.2 µL (25mM stock)
Forward primer (1 µM)	0.2 µL (100 µM stock)
Reverse primer (1 µM)	0.2 µL (100 µM stock)
Taq-polymerase (0.2 U)	0.2 µL (5 U/µL stock)
ddH_2O	11.2 µL
DNA	2 µL

The list of primers can be found in Table 6 (page 90). PCR program below:

(1) Initial denaturation:	94 °C for 3 minutes
(2) Denaturation within cycle:	94 °C for 30 seconds
(3) Annealing:	55 °C for 45 seconds
(4) Extension within cycle:	72 °C for 45 seconds
(5) Repeat 2, 3 and 4 34 times (35 cycles total)	
(6) Final extension:	72 °C for 10 minutes

2.2.3.10 Agarose gel electrophoresis

PCR products for *Fbw7*, *Rosa26-LSL-YFP*, *Cre*, *p53*, *Rosa-CAG-Tomato* and *Pten* were separated on a 1.5% (w/v) agarose (Bioline) gel. The $KRas^{LSL\text{-}G12D}$ PCR product was separated using a 3% (w/v) agarose gel. The gel was prepared diluting the appropriate amount of agarose in 1X TAE and dissolving by heat treatment. Following cooling down of the solution, ethidium bromide (10 mg/mL, Sigma-Aldrich) was added (1 µL per 100 mL of gel solution). The PCR producr was loaded in totality and the gel was subjected to 120 V until a clear separation was observed. To determine band size, 10 µL of 1 Kb DNA Ladder (Invitrogen) was loaded in parallel.

2.2.3.11 RNA isolation

For large amounts of material RNA extraction was performed using the RNeasy Mini- or RNeasy Midi-kit (QIAGEN) according to the manufacturer's instructions. Cells were obtained from cultured condition or from primary tissue and lysed by physical rupture using an 18-gauge needle (BD) and passing the material through it several times. On-Column DNase digestion was performed using the RNase-Free DNase Set (QIAGEN). RNA concentrations and quality were measured using the NanoDrop spectrophotometer (Thermo Scientific. The ratio of OD_{260}/OD_{280} between 1.8 and 2.0 were considered as indicative of a non-contaminated RNA sample. RNA was immediately used for cDNA synthesis or stored at -80 °C.

For small amounts of tissue, such as RNA extraction after cell sorting of primary tumours for microarray purposes (1-50x10^3 cells), the MagMAX^{TM}-96 Total RNA Isolation Kit (Ambion) was used. This protocol is a bead based isolation where nucleotide-binding beads bind to both DNA and RNA, thus, DNase treatment is essential. RNA extraction was performed according to the manufacturer's instructions. All solutions are provided. Final RNa elution was performed with 20 µL of Elution buffer and the quality and concentrations were analysed using a Bioanalyser using Nano or Pico chips (Agillent Technologies).

2.2.3.12 cDNA synthesis

RNA amounts were standardised using RNase-free water and cDNA suntehsis was performed using the Superscript III First-Strand cDNA synthesis kit (Invitrogen). Random hexamer primers were used (Invitrogen). For each sample, 500 ng of RNA were used as a template for cDNA synthesis.

The cDNa synthesis mix was composed of (Kit components):

Hexamer primers:	4 µL
5X RT Buffer	8 µL
Protector RNase inhibitor	1 µL
dNTPs	4 µL
Reverse transcriptase enzyme	1 µL
RNA	500 ng
DEPC water	(up to 40µ)

Tubes were placed in 25°C for 10 minutes, followed by one hour at 50°C and 5 minutes at 85°C. The synthesised cDNA was diluted 1:10 with DEPC water and stored at -20°C for downstream applications.

2.2.3.13 Quantitative real-time PCR

For quantitative real-time (Q-PCR) analysis, cDNa was diluted 1:10 in DEPC-treated ddH_2O. 4 µL of diluted cDNA were used per Q-PCR reaction, which was conducted in triplicates. Q-PCR was performed measuring Express SYBER®GreenER on an ABI7500 (Applied Biosystems). Data were analysed using the SDS software (Applied Biosystems). Primers were designed using the Universal ProbeLibrary Assay Design Center from Roche, avoiding intronic regions. Normalization was performed against values of Polimerase II, Actin and Tubulin.

List of Q-PCR primers can be found in Table 7 (page 91).

To exclude primer dimer and unspecific amplification, a “no template control was included” and dissociation and standing curves were performed. To retrieve Ct values, the threshold was set within the exponential phase of the amplification plots.

Components of each reaction:

Express Syber®GreenER	10 µL
Primer mix (Forward and reverse 5 µM each)	2 µL
cDNA	4 µL
DEPC water	5 µL

2.2.3.14 Statistical analysis

Statistical analysis dependen on the experiment performed. Since, in most experiments, the number of biological and technical replicates did not exceed 20, the Student's *t*-test (which assumes normal distribution of samples) could not be used. Thus, un-parametric tests (does not assume normal distribution, distribution is unknown) were used. For paired samples (normalized to each other) the Wilcoxon paired test was used. For unpaired samples (most of the experiments performed), the Mann Whitney U-test was used. Data was presented as mean +/- standard deviation (S.D.). $P \leqq 0.05$ was considered statistically significant. The exact value of significance are represent for each experiment.

Chapter 3. Results

3.1 Pancreatic ductal adenocarcinoma can originate from either acinar or duct cells. Acinar and duct-derived PDAC have different progression models.

3.1.1 Introduction to the aim

Pancreatic ductal adenocarcinoma (PDAC) constitutes the most common type of pancreatic neoplasias and carries an alarmingly low prognosis (Ryan et al., 2014). Due to the non-specific nature of its symptoms, PDAC is detected at late stages of tumour development when the presence of metastases and the tumour burden reduce the possibility of resection (Ryan et al., 2014). Therefore, improvement of current therapeutic strategies relies on a better understanding of both the molecular and cellular biology of the initial tumourigenic events, when disease is still manageable.

Knowledge gained from clinical observations, and genetically engineered mouse (GEM) models, have greatly contributed to the proposal of a step-wise progression model, where sequential genetic alterations correlate with morphologic abnormalities (Hruban et al., 2000a). However, there is still much to be discovered regarding molecular players and cellular origins.

FBW7, the substrate recognition component of an SCF-type E3 ubiquitin ligase, has been described as a potent tumour suppressor in several organs (Welcker and Clurman, 2008). Its importance in the gastrointestinal tract was highlighted by Rocio Sancho, a postdoctoral fellow in our group, who described Fbw7 as a haploinsufficient tumour suppressor that regulates intestinal tumourigenesis (Sancho et al., 2010). Additional work unveiled the potential role of Fbw7 in pancreatic tumourigenesis as its deletion in the mouse embryonic pancreas induced pancreatic hyperplasia (Sancho et al., 2014). While Fbw7 mutations had been identified in some human pancreatic tumours (Calhoun et al., 2003), no in depth studies had been conducted on the role of this protein in PDAC development and progression. Therefore, the obvious need for further assessment led Rocio Sancho to address the tumour suppressive role of Fbw7 in the pancreas using genetically engineered mouse models.

The most commonly used GEM to study PDAC biology has been developed by Dr David Tuveson's laboratory, which promotes the induction of an activating mutation (G12D) in the endogenous PDAC driver gene - *KRas* ($KRas^{LSL\text{-}G12D/wt}$). In the model described by Hingorani and co-workers, the $KRas^{LSL\text{-}G12D/wt}$ mutation was induced in pancreatic progenitor cells, by means of a Pdx1-Cre (see 1.5.1, page 68), leading to the recapitulation of the human disease. The $KRas^{LSL\text{-}G12D/wt}$*; Pdx1-Cre* animals initially developed low-grade murine pancreatic intraepithelial neoplastic lesions (mPanIN1-2), which later progressed to high-grade mPanIN3 lesions and PDAC (Hingorani et al., 2003).

By crossing $Fbw7^{F/F}$ mice (where exon 5 is flanked by loxP sites, allowing its removal after Cre expression and consequent formation of a truncated and non functional protein (Jandke et al., 2011)), with the previously described $KRas^{LSL\text{-}G12D/wt}$*; Pdx1-Cre* mouse model, Rocio Sancho observed a drastic acceleration of PDAC development, confirming *Fbw7* as a tumour suppressor in the embryonic pancreas. Moreover, before the start of my project, to study the role of Fbw7 in the adult pancreas, Rocio Sancho took advantage of an inducible Cre model that targets the exocrine pancreas, mainly ductal cells (Ck19-CreER) and could verify that, also in the adult organ, Fbw7 deletion with concomitant oncogenic $KRas^{G12D}$ activation led to PDAC onset (all mouse models will be explained in detail in the sections below).

Thus, I aimed to follow up on Rocio Sancho's observations and assess and characterize the effect of Fbw7 deletion in $KRas^{G12D}$-induced mPDAC derived from embryonic and adult pancreas.

3.1.2 Fbw7 embryonic deletion drastically accelerates KRas^{G12D}-induced murine PDAC development

To interrogate the effect of Fbw7 deletion in the KRas^{G12D}-induced embryonic murine PDAC model, I obtained, from Rocio Sancho, *KRas$^{LSL\text{-}G12D/wt}$; Pdx1-Cre mice*, hereinafter referred to as KPdx1-Cre, and the Fbw7$^{F/F}$; *KRas$^{LSL\text{-}G12D/wt}$; Pdx1-Cre*, hereinafter F7KPdx1-Cre mice.

As mentioned above, and as it has been described (Hingorani et al., 2003), the KPdx1-Cre mice present an activating mutation in the *KRas* locus, leading to the constitutive activation of the Ras pathway. This mutation is inactive in the absence of Cre due to the presence of a lox-STOP-lox (LSL) cassette before the inserted mutated sequence. Upon Cre expression, the loxP sites recombine and the STOP cassette is excised, allowing *KRas^{G12D}* expression. In this model, Cre expression is driven by the Pdx1 promoter. Pdx1 is a transcription factor expressed during pancreatic embryonic development (from embryonic day 8.5) and thus, recombination of the STOP cassette occurs in pancreatic progenitors, being present in all pancreatic differentiated cells of the adult mouse (Figure 16a)

The F7KPdx1-Cre model also induces *KRas^{G12D}* expression in pancreatic progenitors. However, this model presents and additional genetic alteration in the *Fbw7* gene. Exon 5 on both copies of Fbw7 harbours loxP sites, flanking the region. Upon Cre expression, exon 5 is excised resulting in a non-functional truncated protein (Jandke et al., 2011) (Figure 16a). The deletion of the protein Fbw7 in the F7Pdx1-Cre model has been assessed before and demonstrated to be efficient (Sancho et al., 2014).

Simultaneous Fbw7 deletion and constitutive oncogenic KRas activation markedly decreased the survival of F7KPdx1-Cre mice compared to KPdx1-Cre, with a median survival of approximately 30 days (Figure 16b). F7KPdx1-cre mice were euthanized due to weight loss and growth retardation (data not shown), with visible swelling of the abdomen. Autopsies and histological analysis of 4-week-old F7KPdx1-Cre mice revealed the presence of a hyperplastic ductal epithelium with papillary architecture, sometimes cribriform, resembling the KPdx1-Cre model at 20 weeks of age. A strong stromal expansion (desmoplasia), characteristic of pancreatic tumours, was also observed (Figure 16c).

Human PDAC, marked by accentuated expression of the duct cell marker CK19, is known to be deregulated in several key signalling pathways, such as the RAS and NOTCH pathways (Hingorani et al., 2003, Hezel, 2006). In order to address the molecular profile of the generated murine tumours, I performed immunohistochemical analysis on murine PDAC (mPDAC) from KPdx1-Cre and F7KPdx1-Cre for Notch downstream effector, Hes1, for phosphorylated Erk (pERK, downstream effector of Ras) and for CK19. Analyses revealed that mPDAC from both KPdx1-Cre and F7KPdx1-Cre mice expressed CK19 (Figure 16d, first row). I additionally observed high levels of nuclear Hes1, indicating an increase in Notch signalling, and phosphorylated Erk (pERK), indicative of active KRas signalling (Figure 16d, second and third rows) in both models when compared with wild type controls (Pdx1-Cre). Interestingly, the increase in Hes1 protein levels seemed to be more pronounced in F7KPdx1-Cre mPDAC mice when compared to KPdx1-Cre-derived PDAC (Figure 16d).

Results obtained with the KPdx1-Cre model confirmed previously published data (Hingorani et al., 2003). Additionally, these results demonstrate that mPDAC generated by the F7KPdx1-Cre model resembles, on a morphological and molecular level the mPDAC in the KPdx1-Cre model. Therefore, Fbw7 deletion with concomitant KRas oncogenic activation does not change the tumour type but accelerates mPDAC formation of the commonly used KPdx1-Cre model.

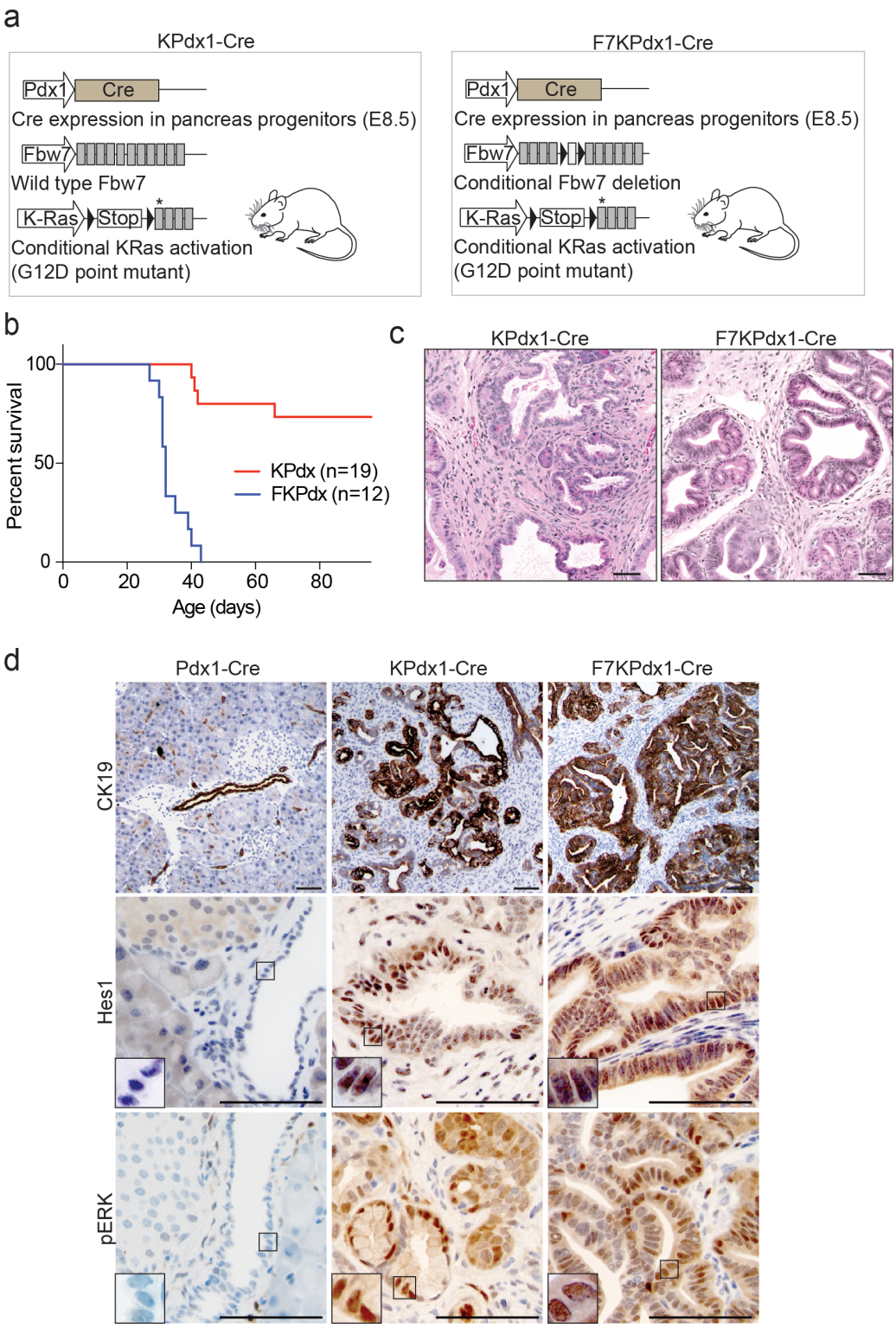

Figure 16 - Fbw7 embryonic deletion drastically accelerates KRas^{G12D}-induced mPDAC development

a) Schematic representation of the KPdx1-Cre (*KRas$^{LSL\text{-}G12D/wt}$; Pdx1-Cre*) and the F7KPdx1-Cre (*Fbw7$^{F/F}$; KRas$^{LSL\text{-}G12D/wt}$; Pdx1-Cre*) mouse models. Scheme shows Cre expression driven by the Pdx1 promoter. *Fbw7* wild type gene or with loxP sites (black

triangles) flanking exon 5, and *KRas* gene with a STOP cassette, flanked by loxP sites, preceding the mutation (asterisk) in exon 1. **b)** Survival analysis. Kaplan-Meier curve, generated by Rocio Sancho, with 19 KPdx1-Cre mice (red) and 12 F7KPdx1-Cre mice (blue). Mice were euthanized upon observation of deteriorating health conditions within the project license limits. **c)** Hematoxylin (nuclear) and eosin (cytoplasmic) (H&E) stain of mPDAC of a 20-week-old KPdx1-Cre mouse and a 4-week-old F7KPdx1-Cre mouse. **d)** Immuno-histological analysis of Cytokeratin 19 (CK19), Hes1 and phosphorylated ERK (pERK) of Pdx1-Cre (wild type control) pancreas and KPdx1-Cre and FKPdx1-Cre derived mPDAC.
All scale bars represent 100µm.

3.1.3 The F7KPdx1-Cre model encompasses an initial ductal transformation step, preceding classic signs of mPDAC oncogenesis

While human PDAC clinical observations have suggested a ductal origin for this disease, mouse model approaches have described acinar cells to be the origin of mPDAC. It has been proposed that, upon oncogenic hits, acinar cells transdifferentiate into ductal cells (Acinar to ductal metaplasia - ADM) expressing the marker CK19, which progress to PanIN (low-grade to high-grade) and PDAC (Zhu et al., 2007, Shi et al., 2012, Guerra et al., 2007). Since the Pdx1-Cre mouse line induces Cre-dependent recombination in both acinar and ducal compartments, I wanted to further characterize our model by analysing early time points of tumour development and describe the initial alterations of both compartments (Figure 17). Since, during the first weeks after birth, the mouse pancreas sill undergoes considerable morphologic alterations (Shih et al., 2013) (1.1.1, page 21), I included a time point analysis of the Pdx1-Cre wild type control mice, to better distinguish the oncogene-related morphological alterations from the ones derived from normal pancreatic development. Therefore, Pdx1-Cre and F7KPdx1-Cre mice were euthanized at postnatal days 0 (P0), 3 (P3) and 7 (P7) (Figure 17a,b).

Time point analysis of control mice (Pdx1-Cre) demonstrated that at P0, the pancreas already contained all differentiated cells, acinar cells, ductal cells and clusters of endocrine cells, however lobule organization was still not obvious (Figure 17a1). Ductal cells in newborn pancreas did not show frequent mitotic figures (not quantified) (Figure 17a4) and expressed CK19 (Figure 17a7), while acinar cells were negative for this cytokeratin marker (Figure 17a10). Three days after birth (P3), lobules became evident, ductal cells exhibited a clear cuboidal morphology in a flat epithelium and expressed CK19, however, acini still presented an immature morphology with no clear CK19 expression (Figure 17a2,5,8,11). One week (7 days) after birth the topological organization of the pancreas resembled that of the adult organ (Figure 17a3,6,9,12).

It is described that the KRas oncogenic activation, in the embryonic pancreas, allows a normal pancreatic development and initial transformation events are only, and rarely, detected 2 weeks after birth (Hingorani et al., 2003). I confirmed that Fbw7 deletion greatly accelerates $KRas^{G12D}$-initiated tumour development, as 7 days after birth CK19-expressing PDAC is already evident, presenting multifocal ductal structures with

papillary architecture, pseudo-stratified epithelium, loss of cell polarity, and desmoplasia (Figure 17b3,6,9).

Interestingly, Fbw7 deletion on top of KRas oncogenic activation appeared to have little impact on pancreatic organo- and morphogenesis, as pancreata of new-born (P0) F7KPdx1-Cre mice (Figure 17b1) were shown to possess a roughly similar cellular composition and topological architecture to that observed in Pdx1-Cre control mice (Figure 17a1), with the main difference being observed in the ductal compartment (described below). Careful analyses of different time points revealed an increase in the number and type of atypical ductal structures in the F7KPdx1-Cre compared with Pdx1-Cre. At P0, ducts of F7KPdx1-Cre mice were already crowded, with obvious and frequent mitotic figures (Figure 17b4). At P3, ductal cells did not resemble the ones observed in the control. F7KPdx1-Cre ductal cells, at P3, became enlarged with expansion of the cytoplasm towards the duct lumen and increased nuclear size (not measured) (Figure 17b25). Surprisingly, similar to control mice (Figure 17a10,11) acinar cells from F7KPdx1-Cre mice, at P0 and P3, did not show any obvious CK19 expression (Figure 17b10,11) suggesting that transformation of the ducts preceded acinar to ductal metaplasia (ADM).

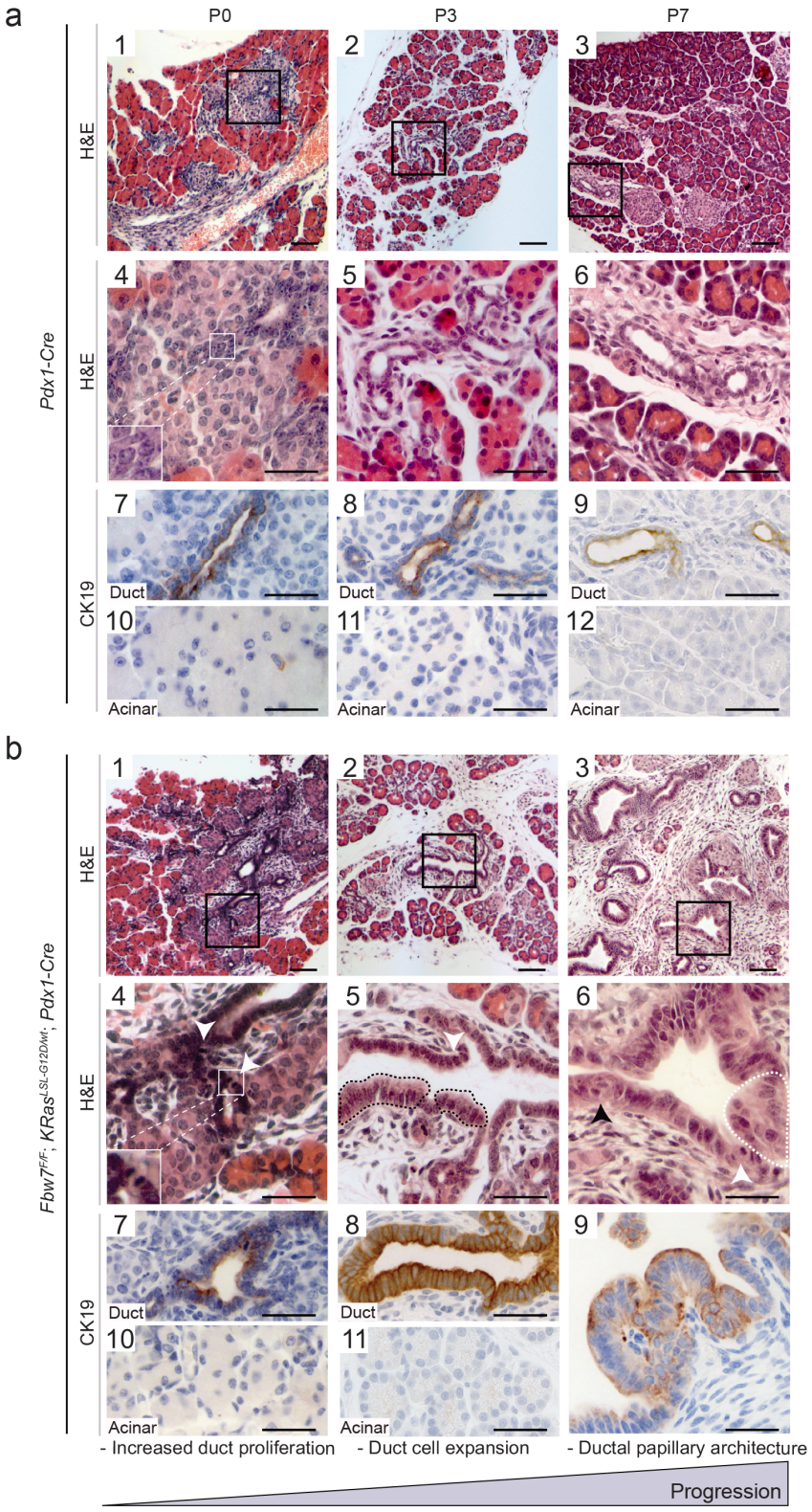

Figure 17 - The F7KPdx1-cre model encompasses an initial ductal transformation step that precedes ADM

Time-course analysis of normal pancreatic and PDAC development in the Pdx1-Cre and F7KPdx1-Cre mouse models. Animals were culled at postnatal day (P) 0, 3 and 7.

(Figure 17, legend continued)

a 1-11 show the respective wild type controls (Pdx1-Cre) for **b 1-11** (F7KPdx1-Cre).
a) Time point histological analysis of pancreas of the Pdx1-Cre mouse model at P0, P3 and P7. **1-3)** H&E low magnification of pancreas of **1** - P0, **2** - P3 and **3** - P7. **4-6)** H&E high magnification of pancreas of **4** - P0, **5** - P3 and **6** - P7. High magnification of nuclei in P0 demonstrates absence of mitotic figures in ductal cells. **7-9)** Ck19 immunohistochemical analysis of ductal cells of 7 - P0, 8 - P3 and 9 - P7. 10-12) CK19 immunohistochemical analysis of acinar cells of **10** - P0, **11** - P3 and **12** - P7.
b) Time point histological analysis of pancreas of the F7KPdx1-Cre mouse model at P0, P3 and P7. **1-3)** H&E low magnification of pancreas of **1** - P0, **2** - P3 and **3** - P7. **4-6)** H&E high magnification of pancreas of 4 - P0, 5 - P3 and 6 - P7. High magnification of nuclei in P0 demonstrates presence of mitotic figures in ductal cells. White arrows show mitotic figure. Black arrow shows loss of polarity (nuclear orientation) **7-9)** Ck19 immunohistochemical analysis of ductal cells of **7** - P0, **8** - P3 and **9** - P7. **10-11)** Ck19 immunohistochemical analysis of acinar cells of **10** - P0 and **11** - P3.
For each time point two litters, each comprising of more than 3 Pdx1-Cre animals and at least two F7KPdx1-Cre, were used for histological analysis.
Scale bars in **a1-3** and **b1-3** represent 100 μm. Scale bars in **a4-12** and **b4-11** represent 50 μm.

ADM is described as the initial step towards tumour formation from mutated acinar cells. However, ADM is also observed in wild type acinar cells, in response to inflammatory cues, with no progression to PDAC (Liou et al., 2013). Hence, ADM can be both a pre-neoplastic entity and a response to injury. Thus, it is still not clear if ADM is a compulsory lesion for PDAC formation. For this reason, I wondered if the observed ductal transformation also preceded the classical pre-neoplastic mPDAC lesions, mPanINs, described to be the progeny of the PDAC-initiating ADM. It has been described that mPanINs are classified from low (PanIN1) to high-grade (PanIN3) according to their cellular dysplasia and marker signature (see 1.4.4, page 59) (Hruban et al., 2000a, Hruban et al., 2001). Human PanINs are mucinous structures and have been shown to be identified by alcian blue (AB) or periodic acid-schiff (PAS) stain, which detect polysaccharides present in mucins (see 2.2.3.6, page 109) (Yonezawa et al., 2008).

I performed AB/PAS stain in P0, P3, P7 (one week) and P14 (2 weeks) pancreatic samples from F7KPdx1-Cre mice to detect when mPanINs first appear in the F7KPdx1-Cre model (Figure 18a).

As a positive control for the AB/PAS stain, I used pancreatic samples from a 20-week-old KPdx1-Cre mice. These mice are known to develop rare low-grade mPanINs as early as 2 weeks after birth (Hingorani et al., 2003). Thus, 20-weeks after birth, several mPanINs were expected. mPanIN quantification was performed by counting the number of AB/PAS positive lesions per mm^2 of pancreatic tissue (Figure 18b).

At P0 and P3, no lesions histologically similar to mPanINs were observed (Figure 18a P0, P3). Moreover, AB/PAS stains failed to identify AB/PAS positive structures at these early time points (Figure 18b, P0, P3). AB/PAS positive structures were only detected in the F7KPdx1-Cre mouse 7 days after birth (P7) and increased in number one week later (P14) (Figure 18a,b P7, P14).

These results suggest that the F7KPdx1-Cre model follows a similar mPDAC progression as described for the KPdx1-Cre mice and that evident ductal atypia precedes early grade mPanINs.

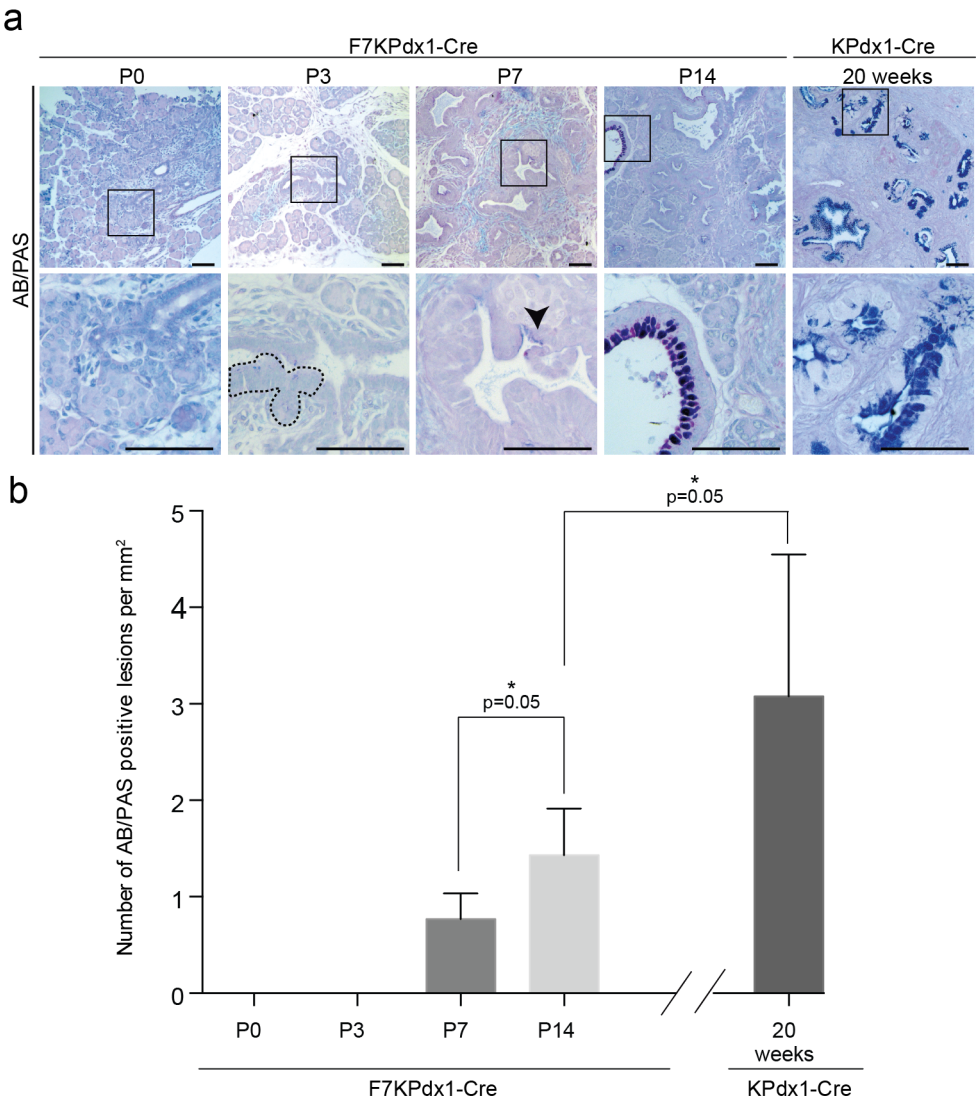

Figure 18 - The F7KPdx1-Cre model encompasses an initial ductal transformation step that precedes mPanIN

Time-course analysis of AB/PAS positive lesions development in the F7KPdx1-Cre model.
a) AB/PAS stain of F7KPdx1-Cre pancreas at P0, P3, P7 and P14. KPdx1-Cre mice pancreas was also collected 20 weeks after birth to be used as a positive control for the AB/PAS stain of mPanIN lesions. **b)** Number of AB/PAS positive lesions per mm^2 of pancreatic tissue. For quantification, 2 mice per time point were used and 3 levels of tissue were stained for quantification (n mice = 2). Bar chart shows the mean values. Error bars indicate standard deviation (SD). Statistical significance was tested with the Mann-Whitney test. P values are indicated
All scale bars represent 100 µm.

3.1.4 Fbw7 embryonic deletion mainly affects duct cells

It has been reported that ductal cells demonstrate the highest levels of *Fbw7* expression amongst all pancreatic compartments (Sancho et al., 2014). Given the previous observation that ductal cells seem to undergo oncogenic transformation before acinar cells show signs of disturbance (ADM and PanIN) in the F7KPdx1-Cre model, I hypothesized that the ductal cellular compartment might respond more significantly to Fbw7 deletion when compared to acinar cells. The effect of Fbw7 deletion was assessed by the change in number of proliferative cells.

Proliferation was assessed by counting the number of cells positive for the mitotic marker phosphorylated histone 3 (pH3). I performed immunofluorescence stain on pancreas from *Fbw7$^{F/F}$; Pdx1-Cre* (F7Pdx1-Cre) and Pdx1-Cre control mice for pH3 (Figure 19a) and observed a statistically significant increase in the percentage of pH3-positive cells in the ducts upon embryonic Fbw7 deletion (F7Pdx1-Cre mice), compared with ducts from Pdx1-Cre control mice. No change in the number of pH3-positve cells was observed for the acinar compartment after Fbw7 deletion (Figure 19b). These results indicate that, in terms of proliferation, Fbw7 deletion mainly affects the ductal compartment.

I next tested if the concomitant expression of the activated *KRas^{G12D}* would also preferentially affect one compartment over the other, in the absence of Fbw7. To avoid detecting increased proliferation due to secondary effects of tumourigenesis, such as inflammation, I focused on early stages of tumour development (P0). I performed pH3 immunofluorescence stains on pancreas of P0 F7KPdx1-Cre mice and compared them with P0 Pdx1-Cre mice (Figure 19c). While no increase in proliferation was detected in acinar cells, the ductal compartment of F7KPdx1-Cre mice showed a marked increase in the number of pH3 positive cells compared with ducts of a Pdx1-Cre P0 pancreas (Figure 19d). These observations support the idea that Fbw7 deletion, with or without KRas oncogenic activation, mainly affects ductal cells. Contrasting with commonly accepted proposals of the non-involvement of ductal cells in tumour development (Ray et al., 2011, Kopp et al., 2012), these results highlight a possible contribution of the ductal compartment to PDAC.

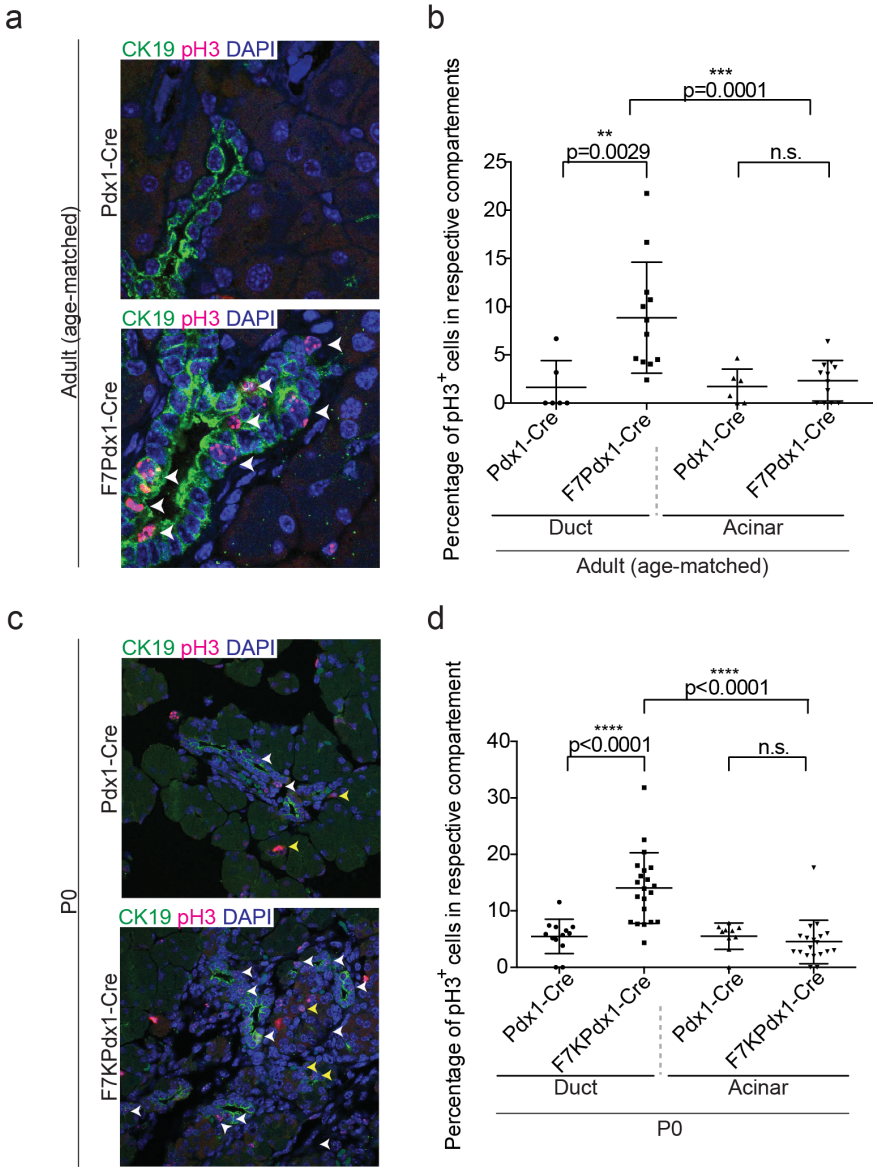

Figure 19 - Fbw7 embryonic deletion mainly affects duct cells

a) Immunofluorescence staining of Ck19 and pH3 in age-matched pancreas of Pdx1-Cre control and F7Pdx1-Cre mice. 8 and 15 weeks old mice were used. For each age, the control Pdx1-Cre and F7Pdx1-Cre were siblings collected at the same time **b)** Percentage of pH3 cells in acinar or ductal compartments of age-matched Pdx1-Cre and F7Pdx1-Cre mice (calculated as number of pH3 cells$^{\text{duct or acinar}}$/total cells$^{\text{duct or acinar}}$)*100) **c)** Immunofluorescence staining of Ck19 and pH3 in pancreas of P0 Pdx1-Cre control and F7KPdx1-Cre mice. **d)** Percentage of pH3 cells in acinar or ductal compartments of P0 Pdx1-Cre and F7KPdx1-Cre mice (calculated as number of pH3 cells$^{\text{duct or acinar}}$/total cells$^{\text{duct or acinar}}$)*100).

The number of pH3-positive cells was counted per genotype, per cellular compartment (acinar vs duct). pH3-positive cells are indicated in white for ducts and yellow for acinar cells. Each dot represents one pancreatic region used for quantification. For the quantification, 2 mice per time point were used and 3 levels of tissue were stained (n mice=2). Graph shows mean values +/- SD. Statistical significance was tested with the Mann-Whitney test. P values are indicated.

3.1.5 Fbw7 loss in KRas^{G12D}-expressing adult ductal cells induces mPDAC without low-grade mPanIN (1-2) formation

To better assess the role of ductal cells in PDAC development, I generated mice where Fbw7 protein deletion and simultaneous KRas^{G12D} activation could be induced, mainly, in ductal cells by means of a Ck19-CreER inducible mouse line (*Fbw7$^{F/F}$; KRas$^{LSL-G12D/wt}$; Ck19-CreER*, hereinafter referred to as F7KCk19-CreER). For full characterization of the F7KCk19-CreER mouse model, such as lineage tracing analysis and recombination efficiency see 4.1.2, page 162.

Similar to the models explained above, upon Cre expression, and its subsequent translocation to the nucleus following tamoxifen treatment, the exon 5 of *Fbw7* is excised, deleting the protein, and the *KRas^{G12D}* mutation is expressed. However, this model differs from the previous F7KPdx1-Cre in two key aspects: (1) the Ck19, and not the Pdx1, promoter drives Cre expression, which is active in ductal cells, allowing ductal cell targeting, (2) this models harbours a mutant version of Cre that only translocates to the nucleus in the presence of metabolized tamoxifen. Therefore, the silencing of Fbw7 and expression of the oncogenic KRas can be induced by tamoxifen treatment. Since PDAC mainly affects adults, Cre-mediated recombination was stimulated in adult animals by treating 8-week-old mice with intraperitoneal (IP) tamoxifen injections (Figure 20a).

One month following tamoxifen treatment, mice became symptomatic and were euthanized due to swollen abdomen and rapid breathing (the rapid breathing will be explained in 3.1.6). Post mortem analysis revealed the presence of pancreatic tumours, which were immediately fixed, embedded in paraffin and tissue sections were obtained for histological analysis. Histologically, F7KCk19-CreER generated tumours resembled mPDAC, exhibiting dysplastic ductal structures with papillary architecture and accentuated desmoplasia (Figure 20b H&E), as previously observed by Rocio Sancho.

Similarly to the human disease, I also observed strong Ck19 protein levels together with high Hes1 and pERK protein levels (Figure 20b). These results support the role of ductal cells in PDAC development and add ductal cells to the group of currently known PDAC cells of origin.

PDAC can originate from different types of precursor lesions such as IPMN, MCN, ITPN and PanIN (see 1.4, page 54) (Distler et al., 2014, Yonezawa et al., 2008, Hruban et al., 2007). GEM models have been used to better understand the causative events for the different lesions. It is hypothesized that different pre-neoplastic lesions might be determined by the cell of origin, or, alternatively, by the genetic alteration induced (von Figura et al., 2014, Bardeesy et al., 2006b, Hingorani et al., 2003, Guerra et al., 2007).

It is currently accepted that murine PanIN lesion are derived from acinar cells which, upon oncogenic hits and pancreatitis, undergo ADM and progress toward PDAC (Tuveson et al., 2006, Grippo and Sandgren, 2012, Guerra et al., 2007). Since the F7KCk19-CreER model mainly targets ductal cells, with some, acinar cells targeting being reported (Ray et al., 2011), I decided to, first confirm that transformation was occurring in ductal cells and, secondly, to closely analyse how PDAC is formed in this context.

To investigate tumour progression, I tamoxifen-treated 8-week-old F7KCk19-CreER mice and collected the pancreas at different time points (0, 14, 21 and 28 days post tamoxifen treatment). To control for, and detect, morphological alterations soon after tamoxifen treatment (Day 0), I also collected the pancreas of wild type non-tamoxifen treated 8-week-old mice.

To most accurately identify the sequence of morphological alterations, I looked for morphological deviations from wild type pancreas. Given the fact that tamoxifen-induced, Cre-dependent, recombination is not a synchronous event, i.e. some cells receive the metabolized tamoxifen before others, transformation is not expected to be synchronous. Therefore, I searched for lesions that were frequent at initial stages and persisted at later time points with simultaneous appearance of structures with higher cellular atypia. Thus, as performed for the human disease, a linear progression was identified, where ductal cells progressively acquire higher levels of dysplasia (Figure 20c).

At day 0, no alteration was detected in the pancreas when compared with pancreata of 8-week-old wild type mice, except a possible crowding of the ducts. Two weeks after tamoxifen treatment, while the acinar compartment remained morphologically unchanged, ducts became obviously crowded and a ductal cell expansion towards the lumen was discernible, similar to that detected in the F7KPdx1-Cre model at P3 (Figure

17b2 and 5). This result confirmed a duct-specific transformation from the Ck19-CreER-dependent cell targeting. Three weeks (Day 21) after tamoxifen treatment, I detected an increase in ductal dysplasia in F7KCk19-CreER mice. Ducts became papillary and shedding of clusters toward the lumen was observed. At this time point, ductal structures closely resembled *carcinoma in situ* (also known as mPanIN3), which is characterized by papillary or cribriform epithelium, occasional fragmentation of epithelial clusters and low or negative for AB/PAS (low-grade PanIN markers) (Cooper et al., 2013, Hruban et al., 2007). Onset of focal mPDAC was detected one month after tamoxifen treatment with loss of duct cell polarity in the papillary structures and pronounced desmoplasia (Figure 20c H&E, CK19 day 28).

During mPDAC development, I did not detect lesions morphologically similar to mPanIN1 or mPanIN2 (low-grade). Interestingly, consistent with the previous finding, in all of the tested time points before tumour onset, I did not observe AB/PAS positive structures, the commonly used marker for low-grade mPanINs (Figure 20c AB/PAS).

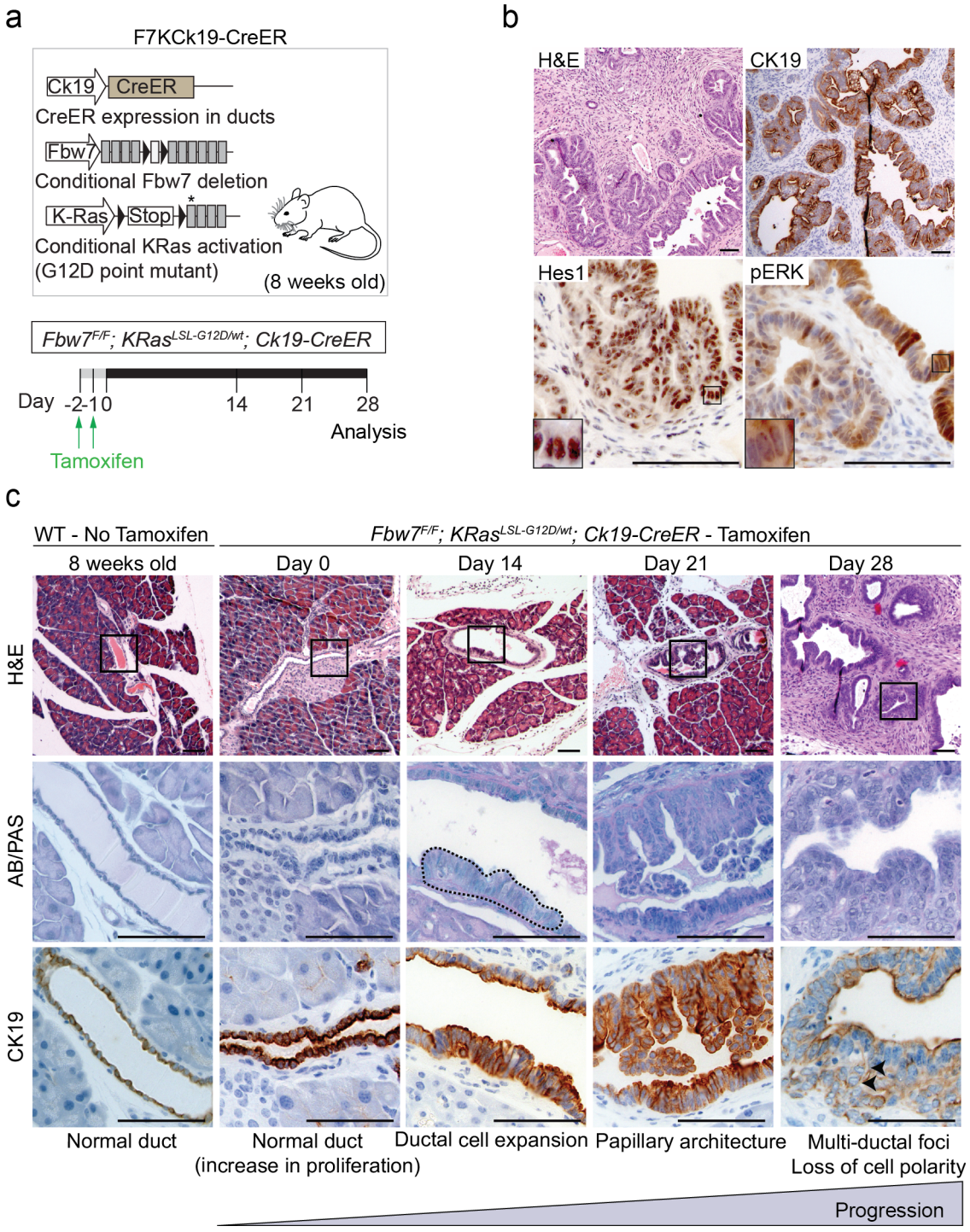

Figure 20 - Fbw7 loss in KRas^{G12D}-expressing ductal cells induces mPDAC without low-grade mPanIN formation

a) Schematic representation of the F7KCk19-CreER mouse (*Fbw7$^{F/F}$; KRas$^{LSL-G12D/wt}$, Ck19-CreER* and experimental approach). Black triangles indicate loxP sites and asterisk indicates the exon with the G12D mutation. 8-week-old mice were intraperitoneally injected with tamoxifen (100 mg/kg of body weight) once a day for two days. Pancreatic tissue was collected for analysis at day 0, 14, 21 and 28 after last tamoxifen dose. **b)** Histological analysis of F7KCk19-CreER-derived mPDAC. One

(Figure 20, legend continued)

month after tamoxifen treatment, H&E (upper left), CK19 (upper right), Hes1 (lower left) and pERK (lower right) stain. **c)** Immunohistological analysis of wild type (WT) 8-week-old pancreas and time-course analysis of mPDAC development in the F7KCk19-CreER model. Animals were culled at P0, P14, P21 and P28 after last tamoxifen injection. The figure displays low magnification H&E stain (first row) of different time points. Regions of interest are marked. Second row shows AB/PAS for the respective regions of interest. Third row shows CK19 immunological staining for the respective regions of interest. Black dashed line illustrates the ductal cell expansion. Black arrowheads indicate loss of cell polarity.
For histological analysis, more than 6 animals per time point were used. Four levels of tissue were obtained for H&E and immunostaining to thoroughly assess the morphological changes.
All scale bars represent 100 μm.

3.1.6 Uncoupling cell of origin from genetic alteration effect during PDAC oncogenesis

Results obtained so far suggest that either duct cell-derived murine PDAC does not evolve from low-grade mPanINs, or that Fbw7 deletion promotes mPDAC in a low-grade mPanIN independent manner.

While the observation of low-grade mPanINs in the F7KPdx1-Cre model (Figure 18a) argues against the latter, the observed AB/PAS positive lesions were in fact rare in F7KPdx1-Cre mice when compared to the number detected in the KPdx1-Cre model (Figure 18b). Therefore, I aimed to more elegantly dissociate the effect of cell of origin versus genetic alteration on tumour development.

The experimental approach is schematically summarized in Figure 21. To understand if loss of Fbw7 protein was the cause of early mPanIN absence, I interrogated Fbw7 loss effect with simultaneous $KRas^{G12D}$ genetic activation in the acinar compartment (by using a tamoxifen inducible, acinar cell specific, Cre line, Elastase1-CreER or Ela1-CreER). If the absence of mPanIN1 and mPanIN2 in the F7KCk19-CreER was due to ductal cell targeting, then the acinar cell-derived PDAC progression from F7KEla1-CreER should allow the easy detection of low-grade mPanINs (Figure 21a). I obtained additional confirmation by using the duct cell specific induction of alternative genetic alterations that have been shown to accelerate PDAC development through mPanIN1-mPanIN2-mPanIN3 progression in the developing pancreas. It has been described that p53 or PTEN deletion, on top of KRas oncogenic activation, in the embryonic pancreas accelerates mPDAC oncogenesis with initial development of mPanIN1 (Hill et al., 2010, Guerra et al., 2007). Thus, I decided to induce the same genetic alterations using the duct-specific Cre mouse model (Ck19-CreER). The detection of low-grade mPanIN lesions formed from duct-targeted cells would suggest that the absence of low-grade mPanIN in the F7KCk19-CreER was a genotype specific event. On the other hand, if no mPanIN1 and 2 lesions would be observed, it would indicate that their absence in the F7KCk19-CreER was a cell of origin specific phenotype (Figure 21b).

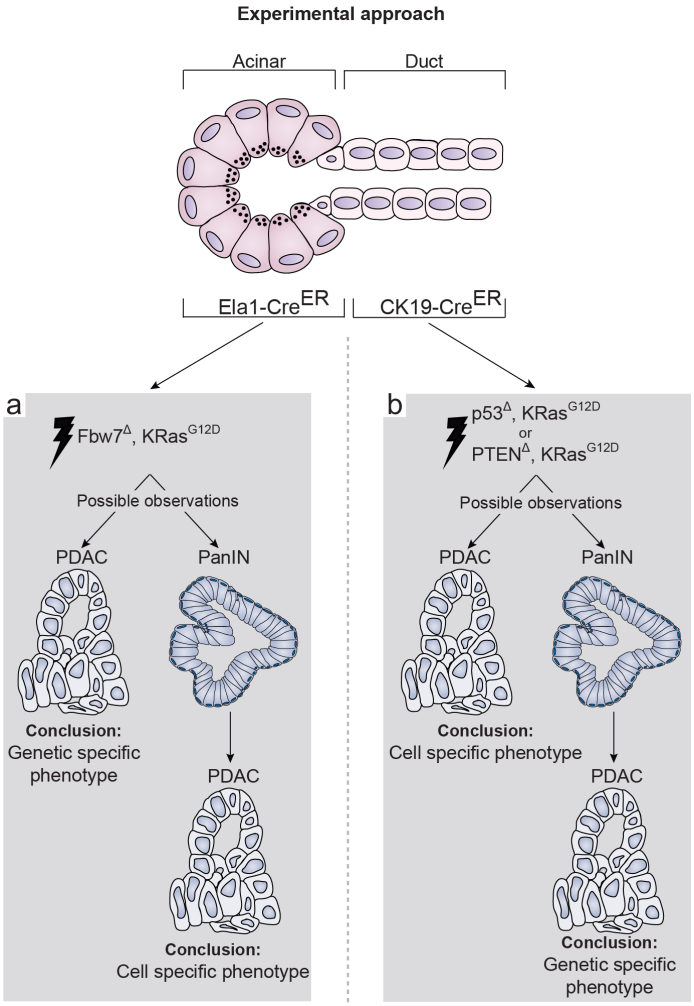

Figure 21 - Uncoupling cell of origin from genetic alteration effect during PDAC oncogenesis

Experimental approach undertaken to uncouple the effect of cell of origin from genetic alteration in PDAC initiation and progression. The mouse Cre lines used identify the pancreatic compartment that they target in the figure. Ela1-CreER induces tamoxifen-dependent recombination in acinar cells while Ck19-CreER targets duct cells. **a)** Fbw7 deletion will be induced in $KRas^{G12D}$-expressing acinar cells (F7KEla1-CreER). If tumour formation occurs without low-grade mPanIN formation, it indicates that Fbw7 deletion is the decisive factor for the lack of formation of these pre-neoplastic lesions. Therefore, the absence of mPanIN1 and mPanIN2 in the F7KCk19-CreER model was a genetic specific event. However, if low-grade mPanINs are detected, then Fbw7 deletion has no role in pre-neoplastic lesion determination. **b)** p53 or PTEN deletion (two genetic alterations described to induce mPDAC via mPanIN1-mPanIN2-mPanIN3 progression) will be induced in $KRas^{G12D}$-expressing duct cells (p53KCk19-CreER or PTEN-KCk19-CreER). PDAC formation in the absence of low-grade mPanIN suggests that ductal cells, regardless of the oncogenic hit, do not evolve into PanIN1 and PanIN2 during PDAC development, i.e. cell specific phenotype. However, if low-grade mPanIN lesions are detected, we can conclude that ductal cells, like acinar cells, can generate low-grade PanINs and their absence in the F7KCk19-CreER model was an Fbw7 deletion-specific phenotype.

In order to test this hypothesis, I generated a panel of mouse models where the same genetic alteration was induced in the embryonic pancreas (Pdx1-Cre), or in adult acinar (Ela1-CreER) or adult ductal (Ck19-CreER) compartments (Table 10)

Analyses started by assessing if and how mPDAC is formed in PTEN-KCk19-CreER mice. PTEN, an antagonist of the PI3K/PDK1/AKT pathway (a pathway involved in PDAC formation (Eser et al., 2013)), has been shown to be a potent tumour suppressor in the developing pancreas (Stanger et al., 2005, Hill et al., 2010). To test its role during adult pancreatic tumourigenesis, from duct cells, I deleted the tumour suppressor PTEN in $KRas^{G12D}$, CK19-expressing cells. CK19 is a cytokeratin expressed in pancreatic ducts. However, other murine tissues are known to express it, such as epithelial cells in the oral cavity, lung, liver, kidney, stomach and intestine (Ray et al., 2011). PTEN is also a potent tumour suppressor in the lung, which has been shown to cooperate with oncogenic KRas during lung tumourigenesis (Iwanaga et al., 2008, Cui et al., 2014). Therefore, it is not surprising that intraperitoneal injections of tamoxifen in PTEN-KCk19-CreER mice led to the rapid development of lung hyperplasia and respiratory distress. Unfortunately, mice had to be euthanized only two weeks after tamoxifen-induced recombination with only minor alteration to the pancreas (data not shown). As a side observation, F7KCk19-CreER also developed lung tumours. However, the pancreatic tumours appeared before mice had to be culled from respiratory distress.

To avoid whole body dissemination of tamoxifen, and consequent recombination outside the pancreas, I decided to inject 4-hydroxytamoxifen (the active metabolite of tamoxifen) intrapancreatically by non-invasive ultrasound-guided injection. A drawback of this approach is the trail of injectable substance that is dragged with the needle upon removal after injection. As a consequence, and due to PTEN's role as tumour suppressor in the skin (Ming and He, 2009), mice promptly developed papillomas on the injection site (data not shown), impeding long term analysis of pancreatic tumourigenesis. Hence, I decided to stop the assessment of PTEN deletion and focus on the remaining models.

Full genotype	Abbreviation	Activation	Target cell	Usage in study
P53$^{F/F}$; KRas$^{LSL-G12D/wt}$; Ck19-CreER	p53KCk19-CreER	Adult 8 weeks (conditional)	Duct	Used
Fbw7$^{F/F}$; KRas$^{LSL-G12D/wt}$; CK19-CreER	F7KCk19-CreER	Adult 8 weeks (conditional)	Duct	Used
PTEN$^{F/F}$; KRas$^{LSL-G12D/wt}$; CK19-CreER	PTEN-KCk19-CreER	Adult 8 weeks (conditional)	Duct	Used
P53$^{F/F}$; KRas$^{LSL-G12D/wt}$; Ela1-CreER	p53KEla1-CreER	Adult 8 weeks (conditional)	Acinar	Not used
Fbw7$^{F/F}$; KRas$^{LSL-G12D/wt}$; Ela1-CreER	F7KEla1-CreER	Adult 8 weeks (conditional)	Acinar	Used
PTEN$^{F/F}$; KRas$^{LSL-G12D/wt}$; Ela1-CreER	PTEN-KEla1-CreER	Adult 8 weeks (conditional)	Acinar	Not used
P53$^{F/F}$; KRas$^{LSL-G12D/wt}$; Pdx1-Cre	p53KPdx1-Cre	Embryonic (E8.5)	Whole pancreas	Used
Fbw7$^{F/F}$; KRas$^{LSL-G12D/wt}$; Pdx1-Cre	F7KPdx1-Cre	Embryonic (E8.5)	Whole pancreas	Used

Table 10 - Mouse models generated for the study

p53, Fbw7 or PTEN homozygous deletion was induced together with KRas^{G12D} oncogenic activation in different pancreatic cell types, at different stages of development. The mouse line Pdx1-Cre was used to induce recombination in the developing pancreas by Pdx1-driven Cre expression at E8.5. Ck19-CreER was used to induce recombination in adult (8-week-old) duct cells by Ck19-driven CreER expression. Ela1-CreER was used to induce recombination in adult (8-week-old) acinar cells by means of Elastase1-driven CreER expression. CreER-dependent genetic recombination was induced by tamoxifen treatment.

3.1.7 Fbw7 loss in *KRas^{G12D}*-expressing adult acinar cells leads to low-grade mPanIN formation

Acinar cells have been shown to generate PDAC upon oncogenic hits. These fully committed exocrine cells regain plasticity in the oncogenic context and transdifferentiate into ductal cells by a process named acinar to ductal metaplasia (ADM). ADM can further progress to PDAC with the intermediate development of PanIN1, 2 and 3 lesions (Guerra et al., 2007, Tuveson et al., 2006, Grippo and Sandgren, 2012, Habbe et al., 2008). Formation of mPanIN lesions, from acinar cells upon oncogenic transformation, appears to be a robust phenotype, as different genetic alterations, such as the simultaneous deletion of p16^{INK4A}/P19^{ARF} in KRas^{G12D}-expressing adult acinar cells, with induced pancreatitis, also leads to mPDAC development with initial mPanIN1 formation, as observed for *KRas^{G12D}* genetic alteration alone (Guerra et al., 2011).

In order to assess if, and how, Fbw7 deletion, with KRas^{G12D} oncogenic activation, leads to PDAC from acinar cells, I generated *Fbw7$^{F/F}$; KRas$^{LSL-G12D/wt}$; Ela1-CreER* mice, hereinafter F7KEla1-CreER, where Fbw7 deletion and KRas^{G12D} simultaneous activation occurs in acinar cells and is dependent on tamoxifen treatment (Figure 22a).

Adult acinar cells are extremely resistant to multiple oncogenic hits. While it is described that, induction of oncogenic genetic alterations in embryonic or young acinar cells (up to 6-week-old mice) leads to tumour formation, the same does not happen if recombination is induced in the adult compartment (8-week-old mice) without additional injuri, even when potent tumour suppressors are deleted in a *KRas^{G12D}*-expressing background (Guerra et al., 2011, Habbe et al., 2008). In line with published data, I observed no pancreatic phenotype in F7KEla1-CreER mice 3 months after tamoxifen treatment in 8-week-old mice (data not shown). Since pancreatitis is a known promoter of PDAC, and it has been shown to accelerate KRas^{G12D}-dependent PDAC, a combinatory caerulein treatment, to induce acute pancreatitis, was used to promote mPDAC formation in the adult animal as described before (Carrière et al., 2009, Carrière et al., 2011).

Caerulein is a cholecystokinin analogue that promotes the premature activation and uncontrolled release of acinar-produced digestive enzymes. This release induces extensive acinar cell death and promotes the generation of an inflammatory

environment stimulating remaining acinar cells to transdifferentiate into ductal cells (ADM). If the treatment is performed in a wild type scenario, regeneration of the organ occurs within 7 days, metaplastic ductal lesions regress and the pancreas adopts a normal morphology. However, in the presence of oncogenic $KRas^{G12D}$, metaplastic structures persist and tumourigenesis is promoted (Morris et al., 2010).

As shown in Figure 22a, I induced genetic recombination by intraperitoneal tamoxifen injection over a 5-day period (one injection per day – 100 mg/kg of body weight/day). One week after recombination, mice were subjected to an acute pancreatitis protocol by caerulein intrapancreatic injections (6 IP injections per day, given at hourly intervals, over 2 days (50 µg/kg of body weight/injection) (see 2.2.1.5, page 96)). In order to compare the results obtained with those observed for the F7KCk19-CreER model, I collected the pancreas from F7KEla1-CreER tamoxifen- and caerulein-treated mice 1 month after pancreatitis (same time point as before) (Figure 22a). Surprisingly, while F7KCk19-CreER mice already presented mPDAC at this particular time point in the absence of caerulein (Figure 20b), the F7KEla1-CreER mice only showed low-grade atypia with extensive ADM and stromal expansion, even after caerulein treatment (Figure 22b, low magnification H&E). Interestingly, I observed ductal dysplastic lesions with flat epithelium, expanded cytoplasm toward the lumen and nuclei located basally exhibiting low-grade atypia (Figure 22b high magnification H&E), characteristic of mPanIN1. Supporting their ductal appearance and low-grade PanIN biology, these structures were highly positive for Ck19 and presented supranuclear mucin production identified by AB/PAS stain (Figure 22b).

The number of AB/PAS positive lesions was quantified for F7KEla1-CreER and F7KCk19-CreER pancreas, one month after tamoxifen induced, Cre-dependent, recombination. Quantification was performed counting the number of positive lesions per transformed area. Transformed area was used, instead of total area, for normalization purposes, given the difference in extent of pancreatic transformation in both models. Comparison of AB/PAS positive lesions in both models, demonstrated that Fbw7 deletion with simultaneous $KRas^{G12D}$ expression, in acinar cells, leads to extensive appearance of mPanIN1, AB/PAS positive lesions (Figure 22c,d).

The results demonstrate that deletion of Fbw7 in $KRas^{G12D}$-expressing adult acinar or ductal cells has different effects. While ductal cell-targeting led to mPDAC oncogenesis

without the development of low-grade mucinous mPanINs, acinar cell-targeting promoted the formation of mPanIN1 lesions. This suggests that Fbw7 deletion has no role in determination of the pre-neoplastic lesion and mode of progression, proposing the cell of origin to be an important factor in this decision. Nonetheless, I could not observe PDAC in the F7KEla1-CreER model, and thus, while longer time points are still to be analysed, further confirmation of the observed phenotype was necessary.

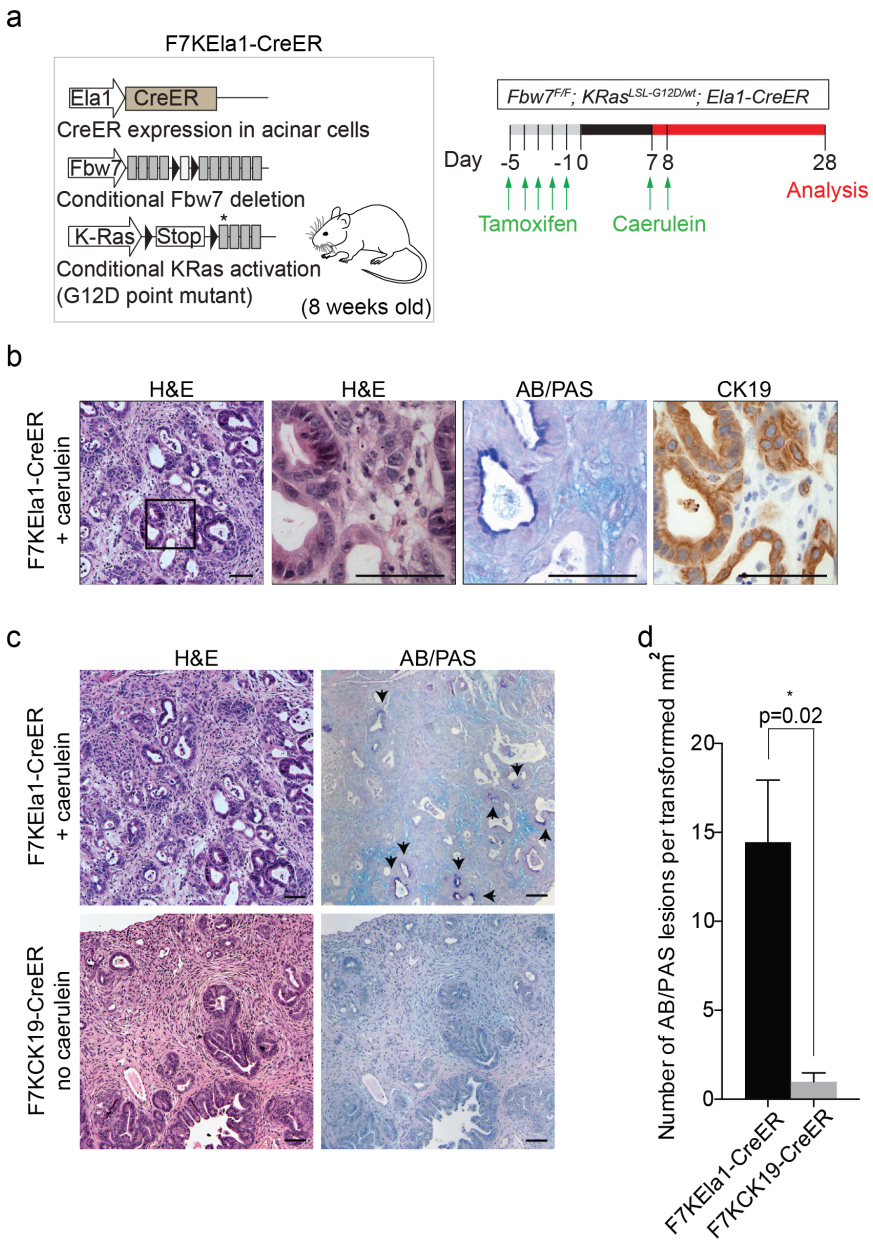

Figure 22 - Fbw7 loss in *KRas*^{G12D}-expressing adult acinar cells leads to low-grade PanIN formation

a) Schematic representation of the F7KEla1-CreER mice (*Fbw7*$^{F/F}$*; KRas*$^{LSL\text{-}G12D/wt}$*, Ela1-CreER*) and experimental approach. Black triangles indicate loxP sites and

(Figure 22, legend continued)

asterisk indicates the exon with the G12D mutation. 8-week-old mice were intraperitoneally injected with tamoxifen for a 5-day period (one injection per day – 100 mg/kg of body weight/day). One week after tamoxifen treatment, mice were subjected to an acute caerulein protocol with 6 IP injections per day, given at hourly intervals, over 2 days (50 μg/kg of body weight/injection). Mice were culled 1 month after the last tamoxifen injection and the pancreas was removed and used for histological analysis. Eight mice were used and 4 levels of tissue of each pancreas were analysed. **b)** Histological analysis of F7KEla1-CreER pancreas one month after tamoxifen treatment. From left to right: H&E low magnification (region of interest illustrated by black square); H&E, AB/PAS and Ck19 stain of region of interest. **c)** H&E and AB/PAS representative images of acinar (F7KEla1-CreER) and duct (F7KCk19-CreER) Fbw7 deleted, oncogenic $KRas^{G12D}$ pancreas, one month after tamoxifen treatment. Black arrows show AB/PAS positive lesions. **d)** Number of AB/PAS positive lesions per transformed area (mm^2) in F7KEla1-CreER and F7KCK19-CreER mice, one month after tamoxifen treatment. For quantification, 2 mice were used and 3 levels of tissue were stained (n mice=2). Bar chart shows the mean values plus SD. Statistical significance was tested with the Mann-Whitney test. P values are indicated.
All scale bars represent 100 μm.

3.1.8 p53 loss in *KRas^{G12D}*-expressing adult ductal cells mimics the F7KCK19-CreER phenotype

Since F7KEla1-CreER mice did not form murine PDAC, up to one month following recombination, it was difficult to uncouple the genetic alteration from the cell of origin in determination of tumour progression. Hence, I decided to confirm if other genetic profiles would also lead to duct-derived PDAC development without low-grade mPanIN formation.

P53 is commonly deleted or mutated in PDAC patient samples (Rozenblum et al., 1997). The role of p53 in pancreatic tumourigenesis has been extensively demonstrated by its simultaneous deletion with KRas oncogenic activation in the developing pancreas. While the loss of p53 alone has no effect in the pancreas, it drastically accelerates *KRas^{G12D}*-driven PDAC oncogenesis via mPanIN1-2 and 3 formation (Bardeesy et al., 2006a, Hingorani et al., 2005). The role of p53 in adult mPDAC tumourigenesis was also assessed where the concomitant expression of *KRas^{G12V}* and pancreatitis greatly accelerated acinar cell-derived PDAC development. However, no comment was made regarding the mode of progression (Guerra et al., 2011). If it is in fact true that tumours derived from duct cells do not evolve from low-grade PanIN lesions, I hypothesized that p53 deletion in *KRas^{G12D}*-expressing adult duct cells should reproduce the F7KCk19-CreER phenotype.

To address this question, I treated 8-week-old *p53$^{F/F}$; KRas$^{LSL\text{-}G12D/wt}$; Ck19-CreER* mice, hereinafter p53KCk19-CreER, with tamoxifen (intraperitoneal injection) to induce duct specific recombination (Figure 23a). These mice exhibited swollen abdomen and respiratory distress (due to recombination in the lungs, as well as in the pancreas) close to one month after tamoxifen injections, at which time they were euthanized. Post mortem analysis revealed extensive pancreatic damage with the presence of a solid mass replacing the pancreatic organ and expansion of this mass to the intestine. Histological evaluation at endpoint demonstrated the presence of mPDAC represented by multiple foci of ductal transformation, loss of basement membrane from the epithelial structures and extensive desmoplasia (Figure 23b). It has been described that mPanIN lesions, although precursors to mPDAC, are also observed at the end stage of murine tumour development, as progression is not synchronous (Collins et al., 2012b, Hingorani et al., 2005). My analysis of late stage mPDAC did not identify low-grade

mPanIN lesions providing the first indication that duct derived PDAC does not encompass mPanIN1 or 2 generation. To confirm that low-grade mPanINs were not missed during tumour development, I collected the pancreas of p53KCk19-CreER mice at day 0, 21, 28 and 35 after tamoxifen treatment and assessed the morphological alterations. Pancreata of, 8-week-old, wild type mice were also collected to serve as a control for morphological changes (Figure 23c).

Similar to the approach taken for the F7KCk19-CreER, I searched for lesions with low-grade dysplasia at initial time points that increase in frequency over time, with concomitant appearance of higher-grade dysplasia at later time points. Initial morphological deviations from wild type and control time point (Day 0) ducts were detected 21 days post recombination, I could observe the crowding of the ductal epithelium with cellular enlargement of some ductal regions towards the lumen. Unlike mPanIN lesions, which also exhibit cytoplasmic expansion, the nuclei of these morphologic alterations were not organized basally. Instead, they expanded with the cytoplasm and occupied different positions within the cells (Figure 23c Day 21, H&E). 28 days post recombination, while most pancreatic regions remained unaltered, with only the ductal expansion being detected, I could observe the initial appearance of papillary structures. However, I still could not detect any evidence of columnar epithelium characteristic of low-grade mPanINs (Figure 23c Day 28, H&E). Consistent with the failure to identify lesions morphologically similar to previously described mPanIN1 and mPanIN2, I could not detect any AB/PAS positivity at any of the time points (Figure 23c AB/PAS panel), indicating that, also in the p53KCk19-CreER model, duct-derived mPDAC is not preceded by mPanIN formation.

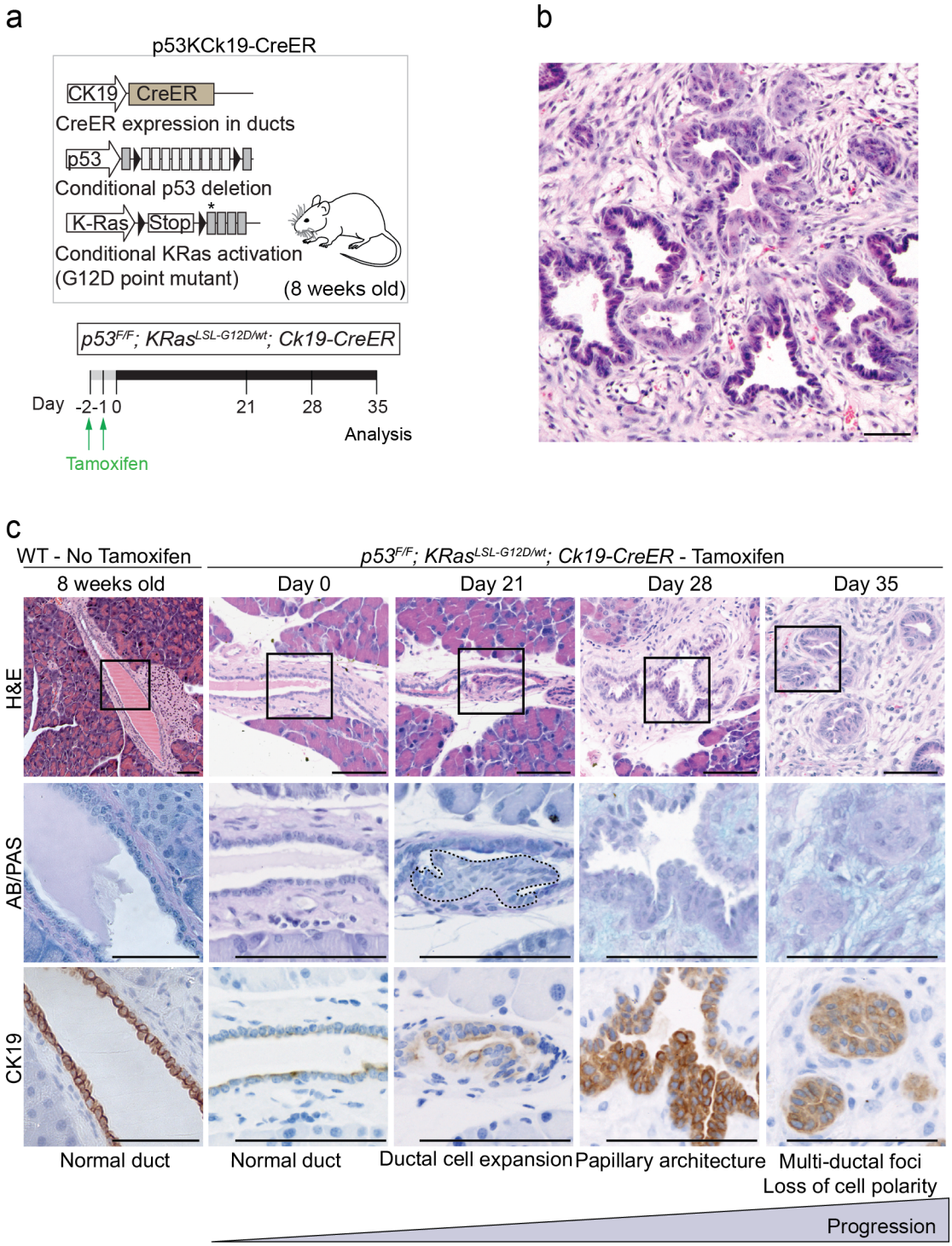

Figure 23 - P53 loss in KRas^{G12D}-expressing adult ductal cells mimics the F7KCk19-CreER phenotype

a) Schematic representation of the p53KCk19-CreER mouse (*p53$^{F/F}$; KRas$^{LSL-G12D/wt}$, CK19-CreER)* and experimental approach. Black triangles indicate loxP sites and asterisk indicates the exon with the G12D mutation 8-week-old mice were intraperitoneally injected with tamoxifen (100 mg/kg of body weight) once a day for two days. Pancreatic tissue was collected for analysis at day 0, 21, 28 and 35 after last

(Figure 23, legend continued)

tamoxifen dose. **b)** H&E of p53KCk19-CreER-derived mPDAC, 35 days after tamoxifen treatment. **c)** Immunohistological analysis of wild type (WT) 8-week-old pancreas and time-course analysis of mPDAC development in the p53KCk19-CreER model. Animals were culled at P0, P21, P28 and P35 after last tamoxifen injection. The figure displays low magnification H&E stains (first row) of different time points. Regions of interest are marked. Second row shows AB/PAS stain for the respective regions of interest. Third row shows CK19 immunological staining for the respective regions of interest. Pancreas of four p53KCk19-CreER mice were used for the histological analysis of the time points day0, 21 and 28. Three mice were used for time point day 35. Black squares in the H&E identify regions of interest magnified in AB/PAS and CK19 panels. Black dashed line illustrates the ductal expansion.
All scale bars represent 100 μm.

Interestingly, simultaneous with mPDAC formation, I detected pancreatic regions containing a different type of tumour. Histologically, the additionally found tumours exhibited a mesenchymal differentiation, composed of a homogeneous mass of spindle shaped cells (Figure 24a and b H&E).

To better understand the biology and origin of these tumours, I performed immunohistological analysis for the ductal epithelial marker Ck19 and the mesenchymal marker smooth muscle alpha-actin (SMA). These tumours were SMA positive and Ck19 negative, corroborating a mesenchymal differentiation (Figure 24b). With the help provided by our on-site consultant histopathologist, Professor Gordon Stamp, the origin of these tumours was identified as being external to the pancreas and possibly derived from the mesenteric tissue surrounding the organ.

In fact, by analysing *R26-LSL-YFP; Ck19-CreER* mice, where the expression of the yellow fluorescent protein is under the control of the Rosa26 promoter and preceded by a loxP flanked STOP cassette (Figure 24c), I have observed that the Ck19-CreER mouse line, upon tamoxifen treatment, promotes recombination in the pancreatic mesothelium as well, demonstrated by the YFP immunological staining (Figure 24d), confirming the previously published detection of Ck19-expressing cells in this tissue (Terada, 2011).

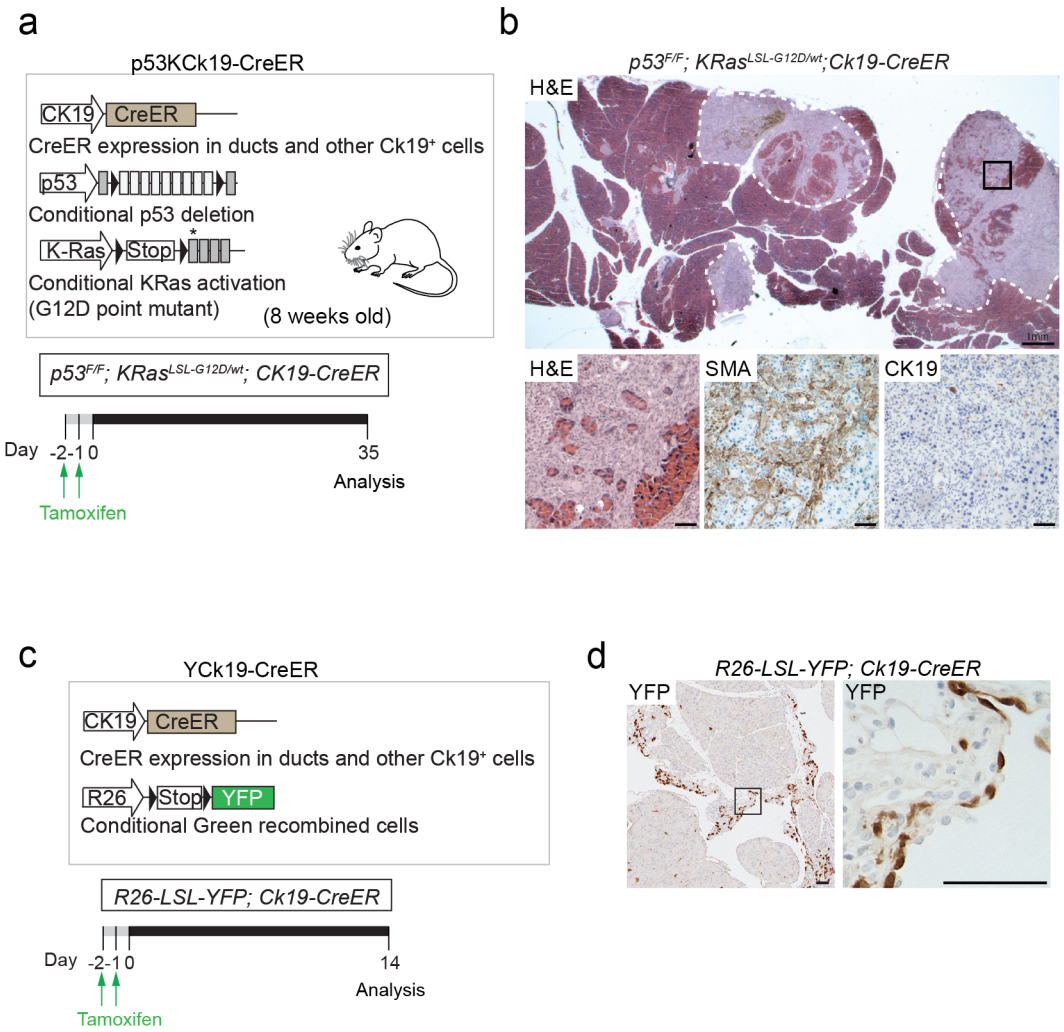

Figure 24 - p53KCk19-CreER mice also develop mesenteric tumours

a) Schematic representation of the p53KCk19-CreER mouse (*p53$^{F/F}$; KRas$^{LSL-G12D/wt}$, Ck19-CreER*) and experimental approach. Black triangles indicate loxP sites and asterisk indicates the exon with the G12D mutation. 8-week-old mice were intraperitoneally injected with tamoxifen (100 mg/kg of body weight) once a day for two days. Pancreatic tissue was collected for analysis 35 days after last tamoxifen dose. **b)** Immunohistological analysis of mesenteric tumours detected in the p53KCk19-CreER model. Upper image: H&E of a p53KCk19-CreER mouse pancreas, 5 weeks after tamoxifen-induced recombination. White dashed lines surround the mesenteric tumours and black square marks region of interest. Lower panels: magnifications of region of interest. From left to right: H&E, immunohistochemical stain for Smooth muscle alpha-actin (SMA) and Ck19. **c)** Schematic representation of the YCk19-CreER (*R26-LSL-YFP, Ck19-CreER*) to lineage trace recombined cells with the Ck19-Cre model. YFP can be recognised by the GFP antibody, hence its description as green cells. **d)** Immunohistochemical stain for the lineage tracer YFP in pancreatic samples from an YCk19-Cre mouse, 14 days after tamoxifen-induced recombination. High magnification demonstrates recombination in the pancreatic mesothelium.
All scale bars represent 100 µm except when indicated otherwise in the figure.

3.1.9 PDAC oncogenesis promotes low-grade mPanIN formation in wild type adjacent tissues

In this study, I have detected a different route of PDAC progression from those described so far. While it is commonly accepted that PDAC progresses from low-grade PanIN (Hruban et al., 2000a), PanINs are also observed in the context of other pancreatic diseases, such as acinar cell carcinomas, mucinous cystic neoplasms, pancreatic endocrine tumours, serous cystadenomas, solid pseudopapillary tumours and ampullary tumours. Therefore, it is still debatable if these ductal structures solely constitute PDAC pre-neoplastic lesions (Recavarren et al., 2011, Stelow et al., 2006a). While studying tumour progression in the F7KCk19-CreER, I did not identify low-grade mPanINs (1-2) before tumour onset (Figure 20c). However, when carefully analysing the end-stage sample, rare mucinous structures were identified by AB/PAS stain (Figure 22d). Moreover, lineage-tracing analysis (Rosa26-LSL-YFP) of the F7KEla1-CreER (F7KYEla1-CreER - Figure 25a) revealed the presence of rare, yet identifiable, AB/PAS positive low-grade mucinous mPanINs that were negative for YFP, suggesting the absence of genetic modification by Cre-mediated recombination, (Figure 25b).

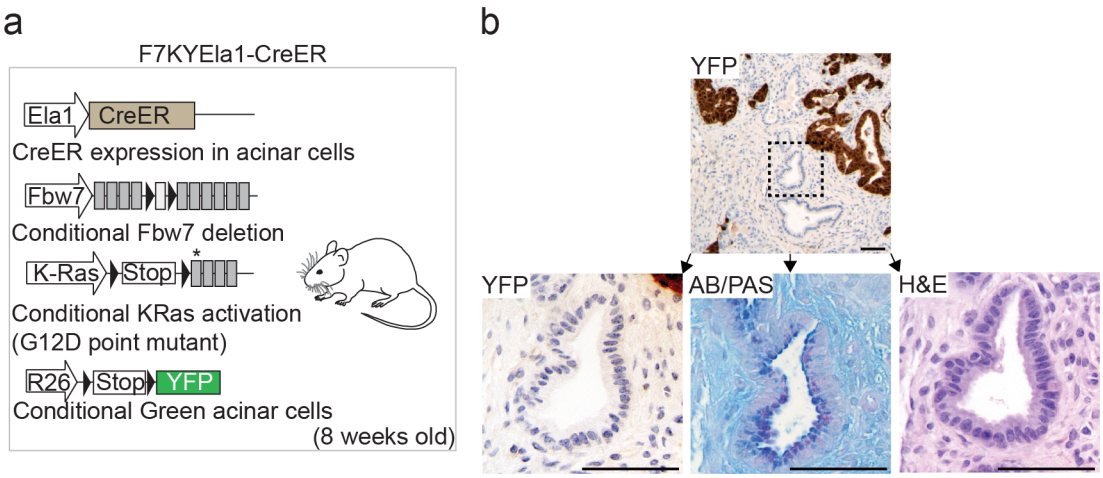

Figure 25 - Occurrence of lineage tracing negative mPanINs in the F7KYEla1-CreER model

a) Schematic representation of the F7KYEla1-CreER (*Fbw7$^{F/F}$; KRas$^{LSL-G12D/wt}$, Rosa26-LSL-YFP; Ela1-CreER)* model. Black triangles indicate loxP sites and asterisk indicates the exon with the G12D mutation. YFP can be recognised by the GFP antibody, hence its description as green cells. **b)** Eight 8-week-old mice were intraperitoneally injected with tamoxifen for a 5-day period (one injection per day - 100mg/kg of body weight/day). One week after tamoxifen treatment, mice were

(Figure 25, legend continued)

subjected to an acute pancreatitis protocol with 6 caerulein IP injections per day, given at hourly intervals, over 2 days (50 µg/kg of body weight/injection). Mice were culled 1 month after last caerulein injection and the pancreas was removed and used for histological analysis. Upper panel demonstrates low magnification of YFP stain. YFP negative mPanIN highlighted by dashed black square. Lower panels present magnification of region of interest. From left to right: YFP, AB/PAS and H&E. AB/PAS positive, GFP negative lesions were observed in at least 2 of the 8 mice used. All scale bars represent 100 µm.

Given the conspicuous presence of mPanIN in non-PDAC scenarios, their increased incidence with age, the low risk of progression to PDAC (Hruban et al., 2001) and my observation of their unlabelled occurrence upon mPDAC onset, I hypothesized that low-grade PanIN could represent a reactive response from acinar cells to damage. This would imply that wild type tissues could generate low-grade mPanINs as bystander entities, in the absence of $KRas^{G12D}$ mutations, in response to PDAC formation in adjacent areas. Thus, I attempted to induce bystander mPanINs in unlabelled wilt type pancreas in a homograft model with YFP-labelled tumour cells.

To readily, and abundantly, obtain mPDAC tumour cells, I took advantage of the *$p53^{F/F}$; $KRas^{LSL\text{-}G12D/wt}$; R26-LSL-YFP; Pdx1-Cre* mouse model, hereinafter p53KYPdx1-Cre. In this model, p53 homozygous deletion is induced simultaneously with $KRas^{G12D}$ oncogenic activation in embryonic pancreatic progenitors. Additionally, the Cre-dependent recombined cells express the lineage tracer YFP, allowing easy detection of tumour cells. It has been described that p53KYPdx1-Cre mice develop murine PDAC (Bardeesy et al., 2006a), therefore, I obtained primary mPDAC tumour cells by enzymatic dissociation of p53KYPdx1-Cre derived tumours and expanded them *in vitro*.

It has been recently shown that murine PDAC tumour cells can be grown *in vitro* as organoids, retaining their molecular signature and recapitulating PDAC development upon homograft transplantation (Boj et al., 2014). Therefore, after enzymatic dissociation, I plated the isolated cells in matrigel with organoid media (see 2.2.2.6, page 102). After two passages in culture it was possible to observe that all organoids were YFP lineage-traced. Nonetheless, to avoid the presence of rare genetically unrecombined cells in the culture (YFP-negative cells) that could compromise the interpretation of the results, I FAC sorted the isolated tumour cells for YFP (similar excitation and emission wavelength as GFP) (Figure 26a). This YFP pure PDAC tumour cell culture was then dissociated into single cells and used for orthotopic transplantations into the pancreas 10-week-old immunodeficient *Nu/Nu* mice. Nu/Nu mice were subjected to surgery for opening of the peritoneum and YFP-labelled tumour cells, mixed in matrigel, were injected into the tail of the pancreas (see 2.2.1.7, page 97). The pancreas of these mice was removed 14 and 21 days after surgery (Figure 26a). 14 days post surgery, histological analysis (H&E) and immunohistochemical analysis

allowed the detection of a focal Ck19 positive, YFP-labelled mPDAC (Figure 26b). According to published reports (Boj et al., 2014), the orthotopic transplantation of isolated PDAC cells from p53KYPdx1-Cre tumour-derived organoids recapitulated PDAC development, whereby AB/PAS-positive mPanINs are formed as well as AB/PAS-negative PDAC. As expected, and demonstrating the ability of the tumour cells to recapitulate early stages of tumour development, I observed YFP-labelled low and high-grade mPanINs positive for AB/PAS, as well as AB/PAS-negative advanced YFP-mPDAC (Figure 26b1). Surprisingly, as early as 14 days after orthotopic transplantation, I could observe, within the host tissue, regions of ADM with the initial development of small ductal mucinous structures. These duct-like lesions were Ck19-positive with expanded cytoplasm. Their mucinous nature was identified by AB/PAS positivity and, importantly, they were YFP-negative, specifying their wild type background (Figure 26b2). Longer time points confirmed the hypothesis. 21 days following orthotopic transplantation, I could detect, near the YFP-positive tumour, YFP-negative flat ductal structures containing columnar epithelium typical of mPanIN1. These structures were immunohistochemically positive for early mPanIN markers, such as AB/PAS and Muc5AC, while labelled tumour cells were negative for both markers (Figure 26c). The fate of these mucinous ductal structures was not followed. Nevertheless, the results suggest that low-grade PanINs can be formed as a response to tumour formation in a wild type scenario and not necessarily only as a pre-neoplasm.

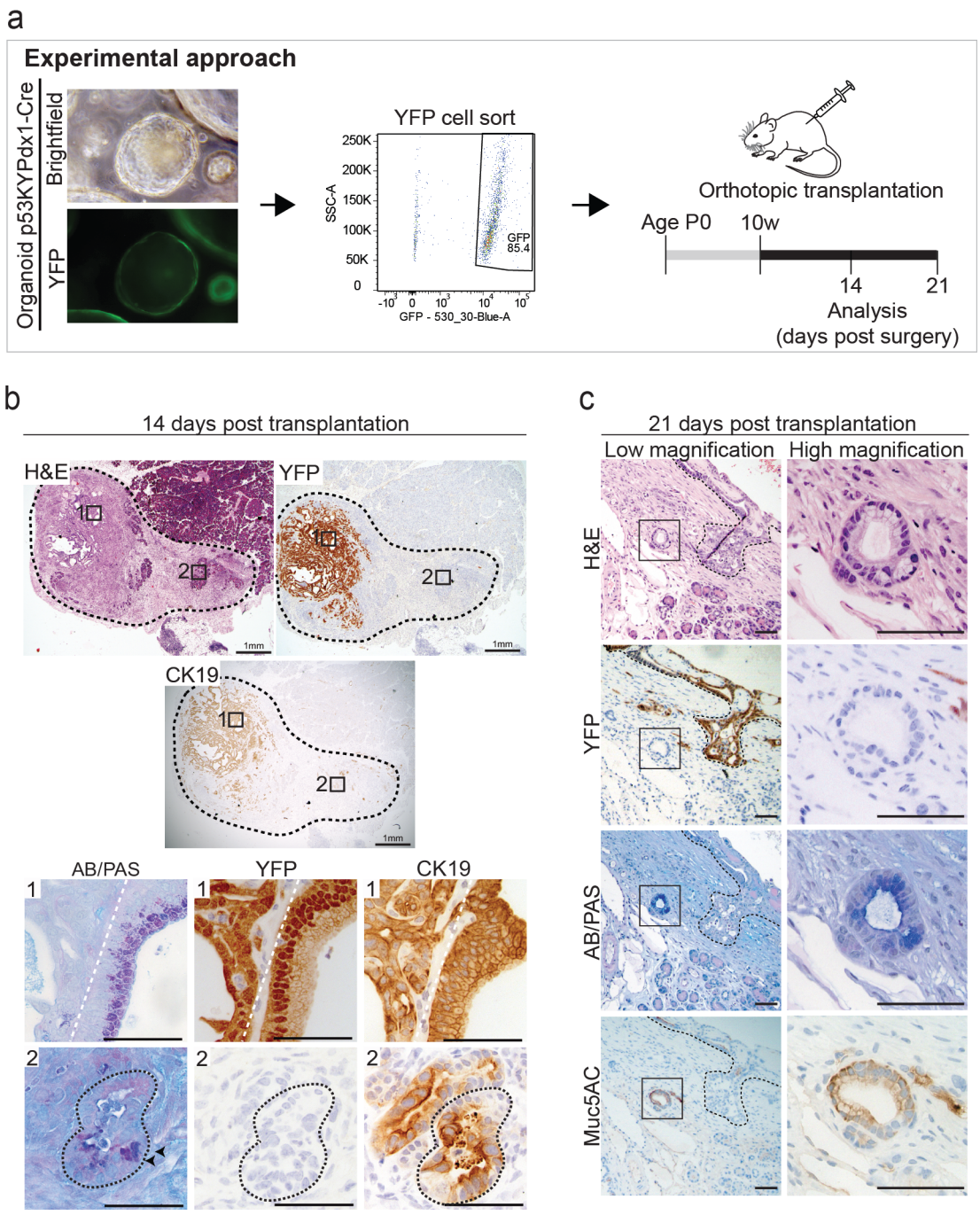

Figure 26 - PDAC oncogenesis promotes low-grade mPanIN formation in adjacent wild type tissues

a) Schematic representation of the experimental approach to induce bystander mPanIN formation. p53KYPdx1-Cre mice were euthanized at 5 weeks. Tumour cells were isolated and expanded *in vitro* as organoids. YFP fluorescence activated cell sorting was performed to exclude any YFP-negative cells. $500x10^3$ cells were mixed with 50 µl of growth factor reduced matrigel and orthotopically transplanted into the pancreas of *Nu/Nu* mice. **b)** Histological analysis of orthotopic tumours 14 days post transplantation. Four mice were injected with PDAC tumour cells. First row with low magnification H&E and YFP and CK19. Black dashed line representing the extent of

(Figure 26, legend continued)

damage caused by PDAC formation. Black squares highlight regions of interest. **1** and **2** - YFP-tumour regions and mucinous YFP-negative region, respectively. **1** – AB/PAS, YFP and Ck19 staining of tumour-derived mPDAC (left) and mPanIN lesion (right) separated by white dashed line. **2** - AB/PAS, YFP and Ck19 staining of bystander lesion with mucinous structure. Black arrowheads show mucinous cells. **c)** Histological analysis of orthotopic tumours 21 days post transplantation. Four mice were injected with PDAC tumour cells. H&E, YFP, AB/PAS and Muc5AC staining were performed. Pictures on the right are magnifications of region of interest on the left. Black dashed line delineates YFP-PDAC. All scale bars represent 100 μm, except if stated otherwise in the figure.

3.2 Discussion: The impact of the compartment of origin on PDAC development and the role of Fbw7 in pancreatic tumourigenesis

3.2.1 Fbw7 as a tumour suppressor in PDAC

As for most diseases, PDAC has a strong genetic component, which can be exploited for improvement of current therapies. The understanding of the molecular key players during PDAC oncogenesis is, therefore, of great importance and extensively investigated (Schneider et al., 2008, Hezel, 2006).

FBW7 mutations have been identified in human pancreatic tumours (Calhoun et al., 2003). However, no in depth studies had been performed before the start of this thesis. Rocio Sancho had identified Fbw7 as a strong tumour suppressor in mPDAC development, where the homozygous deletion of Fbw7 in the embryonic pancreas, with concomitant $KRas^{G12D}$ activation (the main PDAC driver mutation), led to strong acceleration of mPDAC initiation and progression compared to KPdx1-Cre mice. I could confirm that F7KPdx1-Cre mice developed murine PDAC with close recapitulation of the human disease on a molecular and morphological level.

Results obtained during the assessment of the role of Fbw7 in PDAC biology deviated the scientific interrogation. The mechanism by which Fbw7 accelerates mPDAC tumourigenesis and how Fbw7 is regulated in this context are still open questions (In depth discussion in Chapter 5, page 202).

3.2.2 A new mPanIN-independent mPDAC progression model for duct-derived tumours

Great effort has been employed towards a better understanding of PDAC biology and progression. The knowledge gained on the lesions that precede PDAC offers incomparable opportunities to detect and tackle PDAC at its earliest stages of development. Data obtained from the clinic, together with molecular studies and dynamic mouse model approaches, have allowed the identification of pre-neoplastic lesions that, in a step-wise manner, evolve to PDAC (Hruban et al., 2007).

The most common lesions found in PDAC patients are PanIN lesions and, based on mouse model findings, are now thought to originate from acinar cells through an intermediate process known as acinar to ductal metaplasia (Guerra et al., 2007, Zhu et al., 2007, Grippo et al., 2003, Tuveson et al., 2006).

Interestingly, results obtained in this thesis have highlighted the possibility of a different mode of progression. I have observed that F7KPdx1-Cre mice develop murine PDAC with morphological alterations to the ductal compartment preceding both ADM and mPanIN lesions. Moreover, Fbw7 loss had a higher proliferative impact in the ductal compartment. Analysis of F7Pdx1-Cre mice revealed an increase in phosphorylated histone 3 (pH3) in the ductal compartment compared with acinar cells. It is possible that acinar and ductal cells have different recombination efficiencies in the Pdx1-Cre model, which could compromise the interpretation of the results. While confirmation of equal recombination should be performed, there is no evidence in the literature that suggests a difference.

Additionally, the concomitant expression of oncogenic $KRas^{G12D}$ did not change the outcome, as analysis of pH3 in pancreas of P0 F7KPdx1-Cre mice revealed an increase in proliferation in ductal cells, while no change was detected in acinar cells at early stages. This suggests that the acceleration of PDAC in the developing pancreas might be partially due to the contribution of the ductal compartment to tumourigenesis.

In fact, I confirmed that Fbw7 homozygous deletion with simultaneous oncogenic $KRas^{G12D}$ activation in adult ductal cells was sufficient to develop murine PDAC, re-adding ductal cells to the group of potential PDAC cells of origin.

PDAC has been proposed to arise from IPMN, MCN, ITPN or PanIN lesions (Hamilton and Aaltonen, 2000). Interestingly, based on histology and mucinous staining, I did not find any of the previously described mucinous pre-neoplastic lesions during duct-derived mPDAC development. Fbw7-deleted, $KRas^{G12D}$-expressing, duct-derived tumours developed through an increased acquisition of cellular dysplasia and nuclear atypia. I observed initial crowding of the ducts, possibly due to an increase in proliferation (not assessed in the Ck19-CreER model), with focal cytoplasmic and nuclear expansion towards the lumen. The increase in dysplasia over time led to a papillary architecture of the epithelium, which culminated in structures resembling murine *carcinoma in situ* (mPanIN3) and mPDAC.

It is still not clear if determination of the type of pre-neoplastic lesion is dependent on the cell of origin or the genetic alteration induced (von Figura et al., 2014, Hingorani et al., 2003, Guerra et al., 2007, Bardeesy et al., 2006b). I observed that the same tumourigenic genetic alteration in different pancreatic compartments of origin promoted different phenotypes. While acinar cells, in the F7KEla1-CreER mouse model, developed mucinous positive low-grade mPanIN lesions, as expected for acinar-derived transformation, ductal cells from F7KCk19-CreER mice (same oncogenic background) failed to do so, evolving to PDAC in the absence of described mucinous pre-neoplastic lesions. Confirming my results was the observation that different genetic alterations, such as p53 homozygous deletion with $KRas^{G12D}$ oncogenic activation, led to a similar phenotype when induced in the ductal network (Figure 27). Therefore, results strongly suggest that the mode of PDAC progression is highly dependent on the cellular compartment of origin and not so much the oncogenic hit driving tumourigenesis (In depth discussion in Chapter 5, page 205)

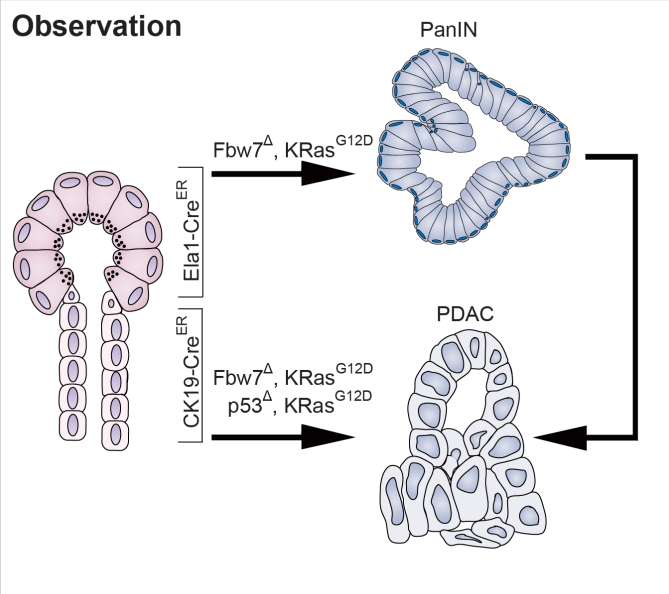

Figure 27 - Uncoupling cell of origin from genetic activation on PDAC development and progression

Schematic representation of the results obtained with F7KCk19-CreER, p53KCk19-CreER and F7KEla1-CreER mice.
I have observed that, the homozygous deletion of either Fbw7 or p53 in $KRas^{G12D}$-expressing duct cells forms mPDAC without the intermediate formation of low-grade mPanIN lesions, while the deletion of Fbw7 in $KRas^{G12D}$-expressing acinar cells leads to the development of mPanIN1 lesions.

While extremely encouraging, these results still leave some questions unanswered due to technical issues. While Fbw7 deletion in *KRas*^{G12D}-expressing ductal cells led to mPDAC, the same was not observed for acinar cells following the same time after induction. Hence, it is still not clear if F7KEla1-CreER mice can develop mPDAC, which raises the question, if Fbw7 loss was capable of inducing KRas^{G12D}-driven mPDAC in acinar cells, would they progress via mPanIN? In order to address this question, F7KEla1-CreER mice should be analysed at longer time points after tamoxifen treatment. Simultaneously, it has been shown that chronic pancreatitis is more efficient in inducing acinar cell-derived mPDAC than the acute treatments (Guerra et al., 2007). Thus, the caerulein protocol should be changed and the acute treatment, after tamoxifen, should be substituted for a prolonged exposure to caerulein.

Mouse models are powerful tools to study biology in the context of a whole organism. However, biological systems are not straightforward and some caveats arose during this study. It is known that CK19 is expressed in several epithelial tissues, besides pancreatic ductal cells, such as the oral cavity, lung, liver, kidney, stomach and intestine (Ray et al., 2011). Its expression has also been reported in the mesothelium (Terada, 2011). Therefore, regarding the p53KCk19-CreER model, I cannot exclude the effect of the mesenteric tumour in promoting a hostile environment that suppresses mPanIN formation.

Moreover, during the course of my studies, I, and other member of our research group, have realized that Ck19-CreER also promotes some limited recombination in acinar cells, as reported previously (Means et al., 2008). The reason for this acinar cell recombination is not immediately clear. Immunohistochemical analysis of the Ck19 protein shows no Ck19 protein in the acinar compartment. Given their plasticity and ability to quickly convert into ductal cells (Strobel et al., 2007, Means et al., 2005), it is possible that some acinar cells regulate the *Ck19* gene and, thus, harbour a constant low activation of the locus or a high protein degradation.

As we know from the literature, adult acinar cells do not undergo any tumourigenic transformation up to one year after tumour induction, even in the context of p53 homozygous deletion with *KRas*^{G12V} oncogenic activation, without chronic caerulein treatment (Guerra et al., 2011). Moreover, my time course analysed allowed me to

observe time-dependent transformation in the ducts without acinar cell transformation before mPDAC onset. Therefore, it is improbable that the acinar cell targeting of the Ck19-CreER affects my observations. Nonetheless, the ductal targeting should be repeated, both for the Fbw7 and for p53 loss with a different CreER mouse line that is more specific to ductal cells. We have recently obtained the Hnf1β-CreER mouse, kindly provided by Dr Jorge Ferrer (Solar et al., 2009). Hnf1β is a transcription factor expressed in ductal cells during embryonic development and adulthood. While this protein is also present in other tissues, such as liver, intestine and kidney (Serfas and Tyner, 1993, Coffinier et al., 2002), it has been reported, by means of lineage tracing (Rosa26-LacZ) (Solar et al., 2009), and preliminary results from our group confirm, that in the pancreas, tamoxifen treatment of Hnf1β-CreER mice does not induce Cre-dependent recombination in acinar cells. Moreover, no mesenteric recombination was detected. Thus, the substitution of the Ck19-CreER for the Hnf1β-CreER model can provide solid data supporting the cell of origin effect in determining PDAC pre-neoplastic lesions.

3.2.3 Origin of low-grade mPanIN lesions

Low grade PanINs are described as the earliest, and most common, PDAC pre-neoplastic lesions (Hruban et al., 2007). In my efforts to understand PDAC progression from different cell types, I observed that the ductal-derived mPDAC from the F7KCk19-CreER model does not develop mPanIN1 before tumour onset. However, to my surprise, end-stage murine tumours revealed the presence of rare low-grade, AB/PAS-positive mPanINs embedded in the stroma, in close proximity to mPDAC. This finding was considered at the time to be a possible side effect of the acinar cell targeting with the Ck19-CreER line. This hypothesis was then challenged when I observed the presence of rare, non-lineage traced, low-grade mPanINs in the F7KYEla1-CreER.

These low-grade mucinous PanINs, present in the context of duct-derived tumour or as a non-labelled lesion in acinar cell specific tumour models following caerulein treatment, both appeared in pancreatic scenarios of extensive injury. Therefore, I hypothesized that low-grade PanINs, such as PanIN1, could be generated in hostile

environments, in a KRas wild type background. I observed that orthotopic transplantation of cultured YFP lineage-traced tumour cells from p53KYPdx1-Cre mice into immunodeficient *Nu/Nu* mice led to the development of YFP-negative PanIN1 lesions in close proximity with the tumour. These low grade PanINs presented a columnar epithelium and were positive for markers of early grade PanIN, such as AB/PAS and Muc5AC. While the true wild type nature of these lesions has to be assessed by possible laser capture microdissection of the bystander mPanINs followed by genotyping PCR, these results suggest that KRas wild type cells are able to give rise to PanIN1, which might have a great impact in both PDAC diagnosis and prognostic value of these structures following surgical pancreatectomy in PDAC patients (In depth discussion in Chapter 5, page 205).

Chapter 4. Results

4.1 CD9 marks a tumour-initiating population in multiple mouse models of PDAC

4.1.1 Introduction to the aim

It has been proposed, and demonstrated, for numerous neoplasias, such as for brain (Singh et al., 2004), breast (Al-Hajj et al., 2003), colon (Ricci-Vitiani et al., 2006) and small intestinal cancers (Barker et al., 2008), that the capacity to initiate tumour formation (tumourigenicity) relies on a subset of specialized cells, commonly referred to as cancer stem cells (CSCs) or tumour-initiating cells (TICs). These cells are particularly important for tumour biology given their unique ability to self-renew and give rise to differentiated progeny, initiating and maintaining tumour growth (Nguyen et al., 2012). Hence, great efforts have been employed towards the better understanding of tumour hierarchy.

The existence of PDAC TICs has been a controversial subject. Studies conducted so far have failed to provide an accurate identification of the PDAC cells with a higher tumourigenic capacity, mainly due to lack of distinction between tumour cells versus stroma (Li et al., 2007, Hermann et al., 2007, Oshima et al., 2007, Immervoll et al., 2011) (for in depth explanation see Chapter 5, page 216).

As mentioned above, Fbw7 deletion (*Fbw7*$^{F/F}$, where loxP sites flank exon 5), with concomitant KRas^{G12D} activation (*KRas*$^{LSL\text{-}G12D/wt}$), in adult ductal cells (F7KCk19-CreER), led to the development of murine PDAC following tamoxifen treatment (Chapter 3, Figure 20). This provided me with a model to study the tumour-initiating capacity of adult epithelial cells.

With the present study I aimed to identify and characterize a PDAC tumour-initiating population by studying early stages of adult duct-derived murine PDAC.

4.1.2 Duct cells have different susceptibilities to tumour formation

Most investigations on PDAC TICs use human xenografts as source of tumour material (Hermann et al., 2007, Li et al., 2007). However, the use of fully developed tumours as a starting point hampers the distinction between pre-existent susceptible cells or *de novo* acquisition of self-renewal potential of TICs from progenitors or more differentiated cells. Therefore, I focused on the use of mouse models where tumour initiation could be thoroughly analysed. As mentioned above, in our research group I had access to a mPDAC inducible tumour model where Fbw7 loss with simultaneous $KRas^{G12D}$ oncogenic activation in adult duct cells led to murine PDAC development. To follow tumour cells throughout tumour development, I crossed in the lineage tracer R26-LSL-YFP (explained in 3.1.9). The resulting mice from the mentioned cross will be referred hereinafter as F7KYCk19-CreER (*$Fbw7^{F/F}$; $KRas^{LSL\text{-}G12D/wt}$; R26-LSL-YFP; CK19-CreER*) (Figure 28a).

Given the structural and protein sequence similarity, as well as absorption and emission spectra resemblance, between the green fluorescence protein (GFP) and, its mutant derivative, yellow fluorescence protein (YFP), YFP can be detected using the GFP antibody and the same fluorescent lasers and detection filters used for GFP in flow cytometry analysis. Thus, in this chapter cells expressing the YFP will be referred to as GFP-expressing cells.

As demonstrated in Figure 28a, 8-week-old adult mice were intraperitoneally injected with tamoxifen at a dose of one injection per day, for two days (100mg/kg of body weight). Following 4 weeks after tamoxifen treatment, mice were euthanized due to weight loss (data not shown) and presence of a prominent swollen abdomen. Post mortem analyses revealed the presence of GFP-positive mPDAC (Figure 28b).

In order to understand if all ductal cells have the same potential for tumour initiation, I decided to analyse early time points after tamoxifen-induced recombination, in search of recombined cells (GFP-expressing cells) with different responses to the oncogenic hits. As a result of my previous characterization of duct-derived murine PDAC of F7KCk19-CreER mice (Figure 20c from Chapter 3), I focused on 2 weeks after tamoxifen treatment as the time point of choice, as it was the earliest stage transformed cells could be identified by histological analysis. By performing GFP immunohistological studies on pancreas of F7KYCk19-CreER mice, two weeks after

tamoxifen treatment, I observed that some GFP-expressing recombined cells had acquired a different morphology (Figure 28c1) while others remained unaltered (Figure 28c2). Based on my previous characterization of the F7KCk19-CreER derived PDAC (Figure 20 from Chapter 3), the morphological difference found in these cells resembled the initial stages of tumour formation from duct cells. Therefore, I considered these cells to be transformed.

Interestingly, this observation was not only restricted to early time points, but also 4 weeks after recombination. Pancreas of adult F7KYCk19-CreER mice, 4 weeks after tamoxifen treatment, exhibited 2 fundamentally different responses: focal PDAC lesions composed of GFP-expressing transformed cells (Figure 28c3), and ducts harbouring GFP-positive cells with no evident tumourigenic response (Figure 28c4), suggesting a ductal heterogeneity regarding tumour susceptibility.

To ensure that all cells that recombined the *Rosa26* locus (GFP-expressing) had also recombined, and excised, the *Fbw7* floxed exon 5 and the STOP (LSL) cassette before the $KRas^{G12D}$ mutant sequence, I sorted live (DAPI-negative) GFP-positive (recombined) and negative (non recombined) cells from F7KYCk19-CreER mice, 2 weeks after tamoxifen treatment (Figure 28d), extracted DNA from these two populations and performed a genotyping PCR (Figure 28e). A 3-primer set was used to test recombination of the *Fbw7* locus that recognizes the floxed (388 bp) and the recombined (744 bp) sequences in the same reaction. I observed that the GFP-expressing population had completely lost the floxed-specific band (388 bp) indicative of complete recombination. Similarly, a 3-primer set was used to assess the recombination in the *KRas* locus. The selected primers amplify the LSL cassette (500 bp), the wild type band (622 bp) and the recombined sequence (650 bp). Results demonstrated a complete recombination of the LSL cassette in the GFP-positive population based on the complete loss of the LSL-specific band (500 bp) and appearance of the recombined mutant G12D band (650 bp). As expected, the genotyping PCR on the GFP-negative cells demonstrated the presence of the floxed band for the *Fbw7* locus (388 bp) and LSL cassette (500 bp). A faint band for the *Fbw7* recombination (744 bp) was detected in the GFP-negative population, which demonstrates that the *Fbw7* locus recombines more efficiently than the *Rosa26* locus.

Nonetheless, this does not interfere with the observation of differential susceptibility of ductal cells.

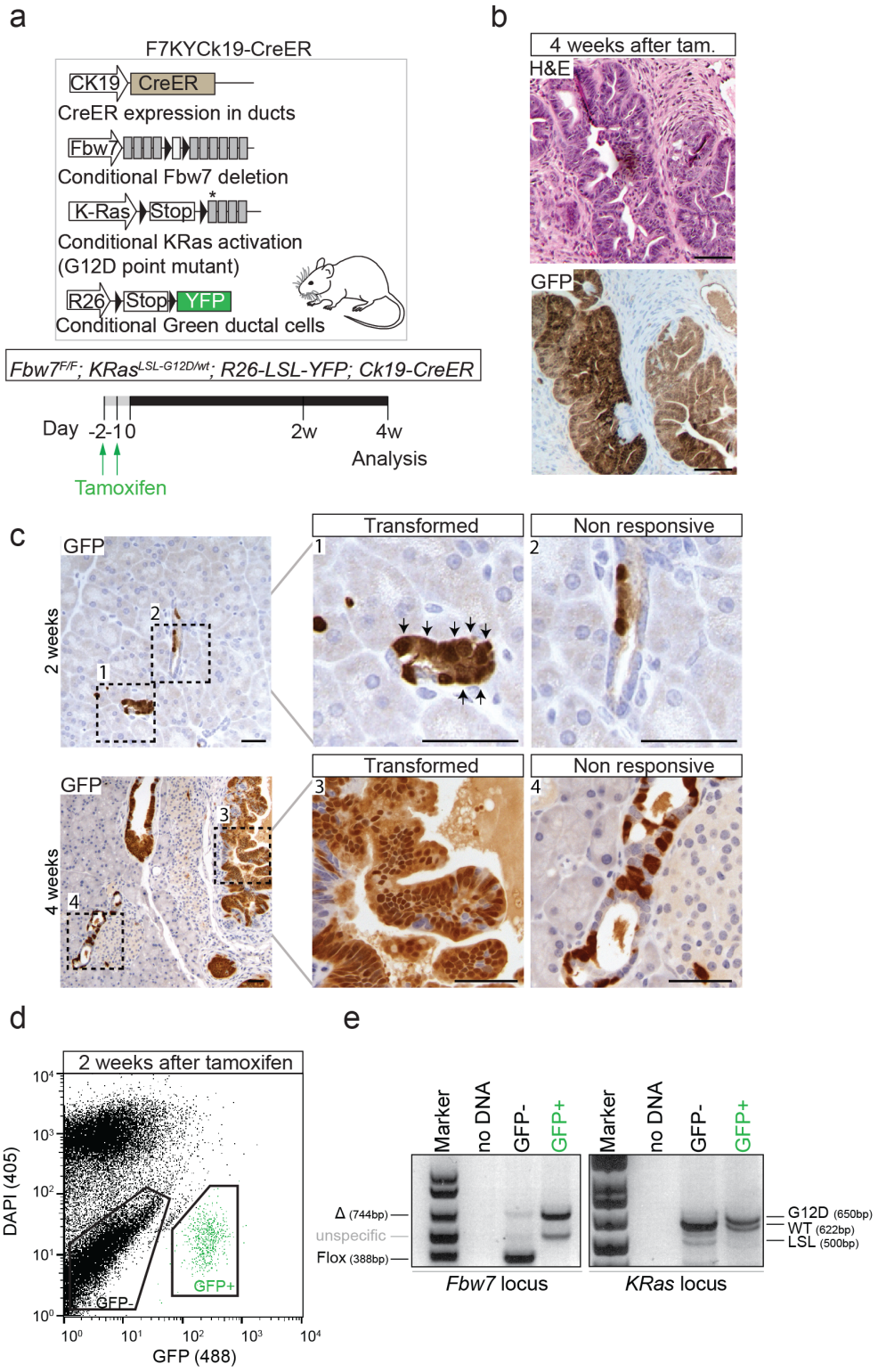

Figure 28 - Duct cells have different susceptibilities to tumour formation

a) Schematic representation of the F7KYCk19-CreER mouse (*Fbw7$^{F/F}$; KRas$^{LSL-G12D/wt}$; R26-LSL-YFP; Ck19-CreER*) and experimental approach. Black triangles indicate loxP

(Figure 28, legend continued)

sites and asterisk indicates the exon with the G12D mutation. 8-week-old mice were intraperitoneally injected with tamoxifen (100 mg/kg of body weight) once a day for two days. Pancreatic tissue was collected for analysis at day 14 (2 weeks) and 28 (4 weeks) after last tamoxifen dose. **b)** Histological analysis of F7KYCk19-CreER-derived mPDAC generated 4 weeks after last tamoxifen (tam.) dose. H&E (above) and GFP immunostain (below; to detect the YFP tracer in consecutive sections). **c)** GFP immunological stain of pancreatic sections of F7KYCk19-CreER mice 2 and 4 weeks after tamoxifen treatment. Transformed ducts (**c1** and **c3**) and non-responsive ducts (**c2** and **c4**) and 2 and 4 weeks after last tamoxifen dose, respectively, are magnified on the right. Black arrows point to examples of transformed cells. The difference in transformation was observed in all the mice analysed (n=6 mice for each time point) **d)** Flow cytometry plot of the sorting performed on the isolated pancreatic cells of F7KYCk19-CreER mice, 2 weeks after tamoxifen injection. DAPI was used to assess viability (DAPI-negative, live cells). Sorted populations are indicated in black (GFP-negative) and green (GFP-positive). **e)** DNA agarose gel for the assessment of Cre dependent recombination on GFP positive and negative populations by PCR. Expected bands and respective fragment sizes (in base pairs) are indicated.
Scale bars in **b** and **c** (low magnification) represent 100 μm while high magnifications in **c** represent 50 μm.

4.1.3 CD44 expression marks early stages of tumour development allowing distinction between transformed and non-transformed cells

It is believed that not all tumour cells are capable of tumour initiation. Instead, a subset of cells with stem cell-like properties is able to initiate and maintain tumour development (TICs). Different surface proteins have been described as identifiers of PDAC TICs, such as cluster of differentiation 133 (CD133), also known as prominin-1, and CD44 (Hermann et al., 2007, Li et al., 2007). However, the significance of their expression is still not clear (Immervoll et al., 2011).

In order to assess if these proteins could also identify TICs in our model, I performed immunological stains on F7KYCk19-CreER mouse pancreas, at early stages of tumour initiation (2 weeks after tamoxifen treatment). Confirming previous published data (Oshima et al., 2007, Immervoll et al., 2011), CD133 was present in the apical surface of every ductal cell, excluding it as a good marker for a subpopulation of tumour initiating cells (Figure 29a). On the other hand, there was a correlation between cell surface expression of CD44 and oncogenic transformation. As described above (see 3.1.5, page 129), ductal cell transformation is initially detected by change in cellular morphology (cell enlargement) with no obvious change in the nucleus:cytoplasm ratio. Following CD44 immunological stain, I observed that morphologically different cells (transformed) expressed CD44, while flat cuboidal cells in the same duct did not (Figure 29a), suggesting that CD44 is marking cells with tumour initiation capacity, supporting previous findings (Li et al., 2007).

I decided to further assess CD44 expression in pancreatic cancer. In order to validate CD44 as a TIC marker, I performed CD44 antibody stains in pancreatic sections of control mice (Ck19-CreER) and of different stages of PDAC development from F7KYCk19-CreER mice (Figure 29b). I observed that duct cells from Ck19-CreER mice did not express CD44, even after tamoxifen treatment. As mentioned above, in contrast, 2 weeks after tamoxifen treatment in F7KYCk19-CreER mice, duct cells changed their morphology, expanded towards the lumen of the duct and initiated CD44 expression, while morphologically unaltered cells remained negative for CD44. 4 weeks after tamoxifen treatment the entire tumour was composed of CD44-expressing cells (Figure 29b). Given the global expression of CD44 in the developed tumour, instead of its presence in a selected sub-population, the value of CD44 expression shifted from

TIC marker to general tumour cell marker, as it had also been demonstrated before for human and murine PDAC (Hill et al., 2010). These results highlighted a possibility for distinction of transformed and non-transformed cells at a molecular level by the use of CD44 levels.

The results in Figure 28e suggested that recombination in GFP-expression cells was complete. However, it was possible that some incomplete recombination in non-transformed, GFP-positive, cells could be masked by a larger population of transformed GFP-positive cells. To control for this possibility, I repeated the genotyping PCR with a more stringent approach. As CD44 expression could discriminate a transformed from a non-transformed population, I obtained, by fluorescent activated cell sorting (FACS), GFP-recombined cells, positive for CD44 (targeted and transformed) and GFP-recombined, CD44-negative cells (targeted and non-transformed) and repeated the genotyping PCR.

F7KYCk19-CreER mice were intraperitoneally injected with tamoxifen and the pancreas was collected at early stages of tumour development (2 weeks after tamoxifen). The pancreatic tissue was digested and stained for CD44. To control for CD44-specific staining, I included a control where only the secondary antibody for CD44 stain was used. As observed in Figure 29c, secondary antibody alone gave no significant signal. Consistent with the existence of a more susceptible population within the ducts, I observed that, soon after recombination, only 0.13% of live pancreatic cells (9.5% of live GFP recombined cells) underwent oncogenic transformation and exhibited CD44 protein on the cell surface. DNA was extracted from $GFP^{+}CD44^{+}$ (recombined and transformed) and $GFP^{+}CD44^{-}$ (recombined and non-transformed) cells, and a genotyping PCR was performed for the *Fbw7* and *KRas* loci (Figure 29d). Both $GFP^{+}CD44^{+}$ and $GFP^{+}CD44^{-}$ cell DNA lacked the flox specific sequence (388 bp) for the *Fbw7* locus and exhibited the recombined specific sequence (744 bp). Similarly, both populations lost the LSL cassette on the *KRas* locus, indicated by the absence of the LSL specific band (500 bp), and exhibited the G12D recombined sequence (650 bp). These results confirmed that absence of transformation of some recombined duct cells was not due to inefficient recombination of one of the genetic alterations induced, and that CD44 expression could be used at, early stages of tumour development, to distinguish cells with different susceptibilities to tumour formation.

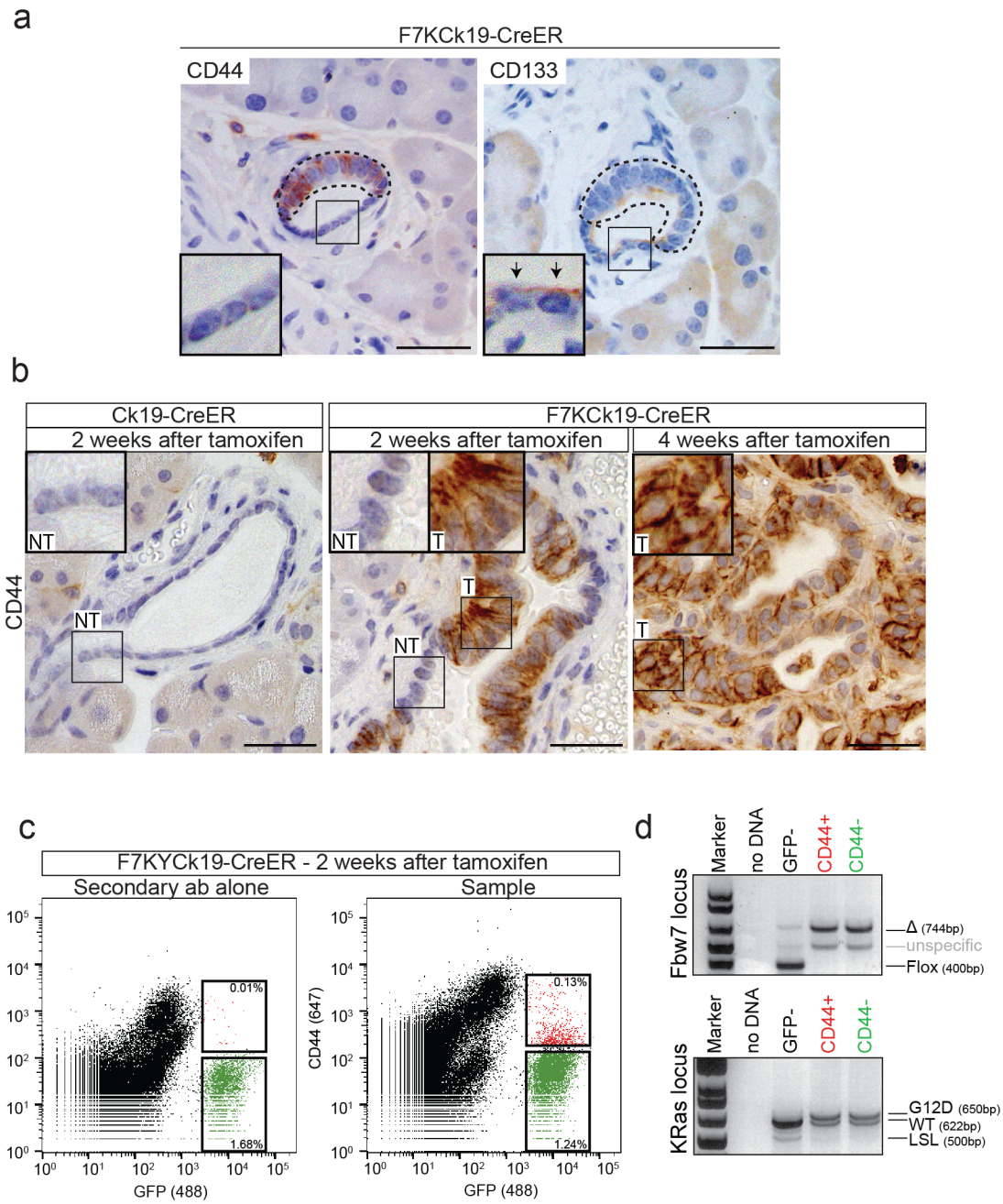

Figure 29 - CD44 expression marks early stages of tumour development allowing distinction between transformed and non-transformed cells

a) Immunological stain of CD44 and CD133 in semi consecutive section of pancreatic samples of 3 F7KCk19-CreER mice (n=3), 2 weeks after tamoxifen treatment. Non-transformed regions are digitally magnified. Black arrows show apical expression of CD133 in non-transformed cells. **b)** CD44 immunological stain in pancreas of 2 CK19-CreER control mice two weeks after tamoxifen treatment and 3 F7KCk19-CreER mice two and four weeks after tamoxifen treatment. Magnifications of regions of interest are marked. NT- non-transformed; T- transformed. **c)** Flow cytometry analysis of pancreas of F7KYCK19-CreER mice 2 weeks after tamoxifen injection. DAPI was used to assess viability; cells were gated for DAPI negativity. Plot shows entire live pancreatic

(Figure 29, legend continued)

population assessed for CD44 (647 nm excitation - Y axis) and GFP (488 nm excitation - X axis) fluorescent signal. Secondary fluorescent antibody alone was used to gate the CD44 positve and negative populations. Sorted populations are indicated in green (GFP^+CD44^-) and red (GFP^+CD44^+) **d)** DNA agarose gel for the assessment of Cre dependent recombination in GFP^+CD44^+ (red) and GFP^+CD44- (green) populations by PCR. Expected bands and respective fragment sizes (in base pairs) are indicated. The genotyping assessment was performed for 2 F7KYCK19-CreER mice.
All scale bars represent 50 μm.

4.1.4 Gene expression analysis and validation to identify novel PDAC TIC markers

The observation that not all duct cells harbouring the same oncogenic hits get transformed, together with the detection of CD44 expression in early transformed cells, provided a valuable strategy to distinguish between adult duct cells susceptible to transformation (TICs) and cells not capable of tumour initiation with the same genetic background, excluding any additional mutation that could lead to higher tumourigenicity. Therefore, to identify PDAC TIC markers, I performed a microarray to assess genome-wide differential gene expression between GFP^+CD44^+ (transformed - T) and GFP^+CD44^- (non transformed - NT) cells at early stages of tumour development (Figure 30a).

Ten F7KYCk19-CreER mice were treated with tamoxifen for 2 days (one IP injection per day of 100 mg/kg of body weight), pancreata were collected 2 weeks after last tamoxifen injection and pooled for further processing. Following enzymatic cellular dissociation and CD44 antibody stain, live cells (DAPI negative) were sorted according to their GFP and CD44 expression (GFP^+CD44^+ vs GFP^+CD44^-). Due to the harsh enzymatic treatment, and possibly the additional deleterious effect of acinar-derived enzymes, the viability after cellular dissociation was extremely compromised. Less than $25x10^3$ cells were obtained for each population providing less than 0.5µg of RNA. Given the low amount of RNA, an amplification step took place and GeneChip ® Mouse Gene 1.0 ST Array from affymetrix was performed. Results were analysed by Richard Mitter from the Bioinformatics and BioStatistics core facility at The Francis Crick Institute – Lincoln's Inn Fields Laboratories, who normalized the raw values and calculated the fold change in gene expression between both populations (relative to GFP^+CD44^-). Significance was not calculated due to the lack of replicates.

Differences in gene expression were extremely subtle, as expected for initial steps of tumour formation (Figure 30c). I observed that amongst the 30 most upregulated genes were several well established, and previously described, PDAC markers. Cathepsin E (CTSE) (Cruz-Monserrate et al., 2012); Matrix metalloproteinase-7 (Mmp7) (Park et al., 2012), Anterior Gradient 2 (Agr2) (Riener et al., 2009), Trefoil Factor 2 (TFF2) (Buchholz et al., 2005) and Mucin 1 (Muc1) (Rachagani et al., 2012) were 3.36, 3.44, 3.32, 3.20 and 2.25 fold, respectively, upregulated in the transformed population

(GFP^+CD44^+) (Figure 30b). Moreover, CD44 was 3.8-fold upregulated in GFP^+CD44^+ cells reinforcing the validity of the array (Figure 30c).

Specific criteria were followed for the selection of genes of interest: **(1)** overexpressed in the GFP^+CD44^+ cell fraction (downregulated genes were discarded from the analysis); **(2)** coding for proteins with an extracellular domain (to allow further and easy identification/isolation and possible therapeutic approaches); and **(3)** overexpressed at least 1.5 fold above the GFP^+CD44^- fraction (given the already low expression of global PDAC markers the cut off was established low to allow inclusion of very rare populations). A second selection step was employed to narrow down the number of genes of interest. For this next step, a bibliographic search on the relevance of the gene in cancer and tumour initiation biology was carried out. In parallel, the protein expression profile was virtually analysed using The Human Protein Atlas (Uhlen et al., 2015). Only proteins detected by antibody stain in scattered ductal cells in the normal pancreatic tissue and present either in all or in a subpopulation of PDAC cells were selected. A handful of genes was classified as potential TIC markers and, in this thesis, I describe my characterisation of the most promising candidate.

I focused on CD9, also known as Motility related protein 1 (MRP1), as a potential gene of interest as it met all criteria required. It was 1.5 fold upregulated in the GFP^+CD44^+ population (Figure 30c); it is a tetraspanin protein and consequently it consists of four transmembrane helices, one small intracellular loop and a large extracellular loop (extracellular domain); it has been shown to be involved in several types of cancer, such as gastric, lung and breast tumours (Hemler, 2014); it has been suggested as a stem cell marker in certain human malignancies, mainly haematopoietic (Nishida et al., 2009) and, according to The Human Protein Atlas, it is expressed in a subset of duct cells in normal human pancreatic tissue and, depending on the sample, in all or a subpopulation of human pancreatic cancer cells.

Microarray validation was performed by quantitative RT-PCR (Q-PCR) (Figure 30d). F7KYCk19-CreER mice were treated as described in Figure 28a and GFP^+CD44^+ (T) and GFP^+CD44^- (NT) cells were sorted 2 weeks after the last tamoxifen intraperitoneal injection. As expected, expression of *Fbw7* exon 5 (loxP flanked exon) was undetectable in both transformed (T) and non-transformed populations (NT) when compared to the remaining pancreatic tissue (WT) indicative of efficient deletion of the

gene. *Ck19* expression levels were not changed. *CD44* and epithelial cell adhesion molecule (*EpCAM*), both upregulated in the microarray by 3.8 and 2.25-fold, respectively, exhibited an approximately 4-fold upregulation by Q-PCR. Finally, *CD9* expression demonstrated a statistically significant increase in the transformed cellular fraction, being 2.5-fold upregulated.

Therefore, CD9 was followed for further characterization as a PDAC TIC marker.

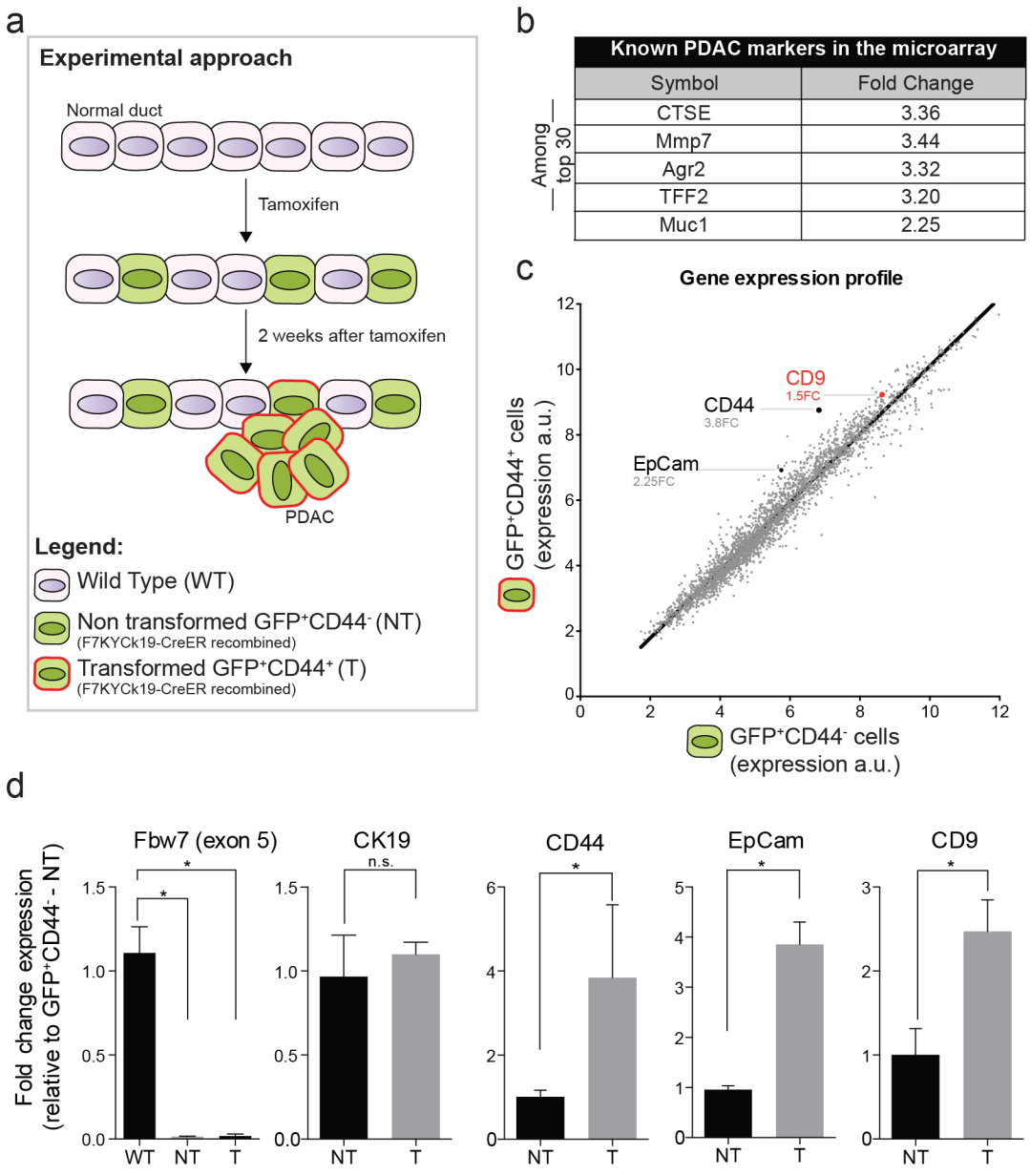

Figure 30 - Gene expression analysis and validation to identify novel PDAC TIC markers

a) Schematic representation of the experimental rationale and approach. Ten F7KYCk19-CreER mice were injected with tamoxifen for 2 days (one intraperitoneal injection per day 100 mg/kg of body weight). Recombined cells initiate GFP

expression. 2 week after tamoxifen injection some recombined cells (GFP^+) undergo oncogenic transformation and upregulate CD44 expression (GFP^+CD44^+ - transformed T) while other recombined cells do not respond to the oncogenic hit (GFP^+CD44^- - Non-transformed NT). T and NT were sorted and RNA used for gene expression array. **b)** List of known human PDAC markers that were also upregulated in the present microarray amongst the 30 top upregulated hits. Respective fold changes in gene expression of T compared to NT are represented. **c)** Gene expression profiles of T and NT cells. Normalized expression values (arbitrary units – a.u.) for each identified gene were plotted; each dot represents one gene. *CD9*, *CD44* and *EpCam* are indicated with respective fold change calculated. **d)** Validation of selected hits by quantitative PCR. *Fbw7* floxed exon 5, *CK19*, *CD44*, *EpCam* and *CD9* expression levels were measured in freshly sorted GFP^+CD44^+ (T) and GFP^+CD44^- (NT) cells. WT – non-recombined pancreatic cells (GFP^-). Q-PCRs were performed in biological triplicates (3 independent sorts). In each experiment, a pool of 2 mice was used. Gene expression values were normalized to a loading control (tubulin) and fold changes were calculated relative to NT or WT in the case of *Fbw7*. Bar chart shows the mean values plus SD. Significance was calculated with the Mann-Whitney test. * Shows p= or <0.05. n.s = not significant

4.1.5 CD9 expression marks a subpopulation of transformed cells in the F7KYCk19-CreER mouse model of PDAC

As indicated by the microarray and Q-PCR validation, the *CD9* gene was shown to be overexpressed in the transformed population at early stages of tumour development. Nonetheless, there was a possibility of global presence of this protein in all tumour cells. To investigate CD9 protein expression, I performed flow cytometry analysis on live PDAC tumour cells from F7KYCk19-CreER mice (Figure 31a). Mice were injected with tamoxifen as described in Figure 28a and the pancreas collected 4 weeks after the last tamoxifen injection. As demonstrated in Figure 31a, the analysis was performed on live (DAPI-negative) recombined (GFP-positive) cells. For this particular staining, I used a CD44 antibody conjugated to the fluorophore allophycocyanin (CD44-APC; emission peak at 660 nm) and an unconjugated antibody was used for CD9. Therefore, I included a control for the specificity of the secondary antibody used for the CD9 staining (antibody isotype controls were also performed – see Figure 33, discussed below). It was observed that 90% of the GFP^+ live cells were expressing CD44, consistent with the advanced stage of tumour development. Compatible with the definition of a TIC marker, CD9 protein was not observed in all tumour cells. CD9 was only detected in approximately 15% of the GFP^+ population and was restricted to CD44-expressing cells (Figure 31a). Replicates were performed to allow quantification of the percentage of GFP^+ cells expressing CD44 only, CD9 only and both CD44 and CD9 (Figure 31b). It was observed that the $CD44^+CD9^+$ population was consistently, and significantly, smaller than the $CD44^+$ (tumour cell) population, reinforcing the potential value as a TIC marker.

To confirm the results obtained by flow cytometry, I performed immunofluorescence stains for CD9 and E-Cadherin (an epithelial cell marker that distinguishes tumour cells from stroma) in tumours of F7KYCk19-CreER mice, 4 weeks after tamoxifen treatment (Figure 31c). I observed that, while the majority of the tumour cells were negative for CD9 (Figure 31c1), a small subset of E-cadherin-expressing tumour cells exhibited membrane CD9 stain and were organized in clusters (Figure 31c2). The dotted pattern of expression of CD9 was not surprising, as it has been described that the tetraspanin CD9 protein can cluster laterally in the cell membrane forming tetraspanin-enriched microdomains (TEMs) (Hemler, 2014).

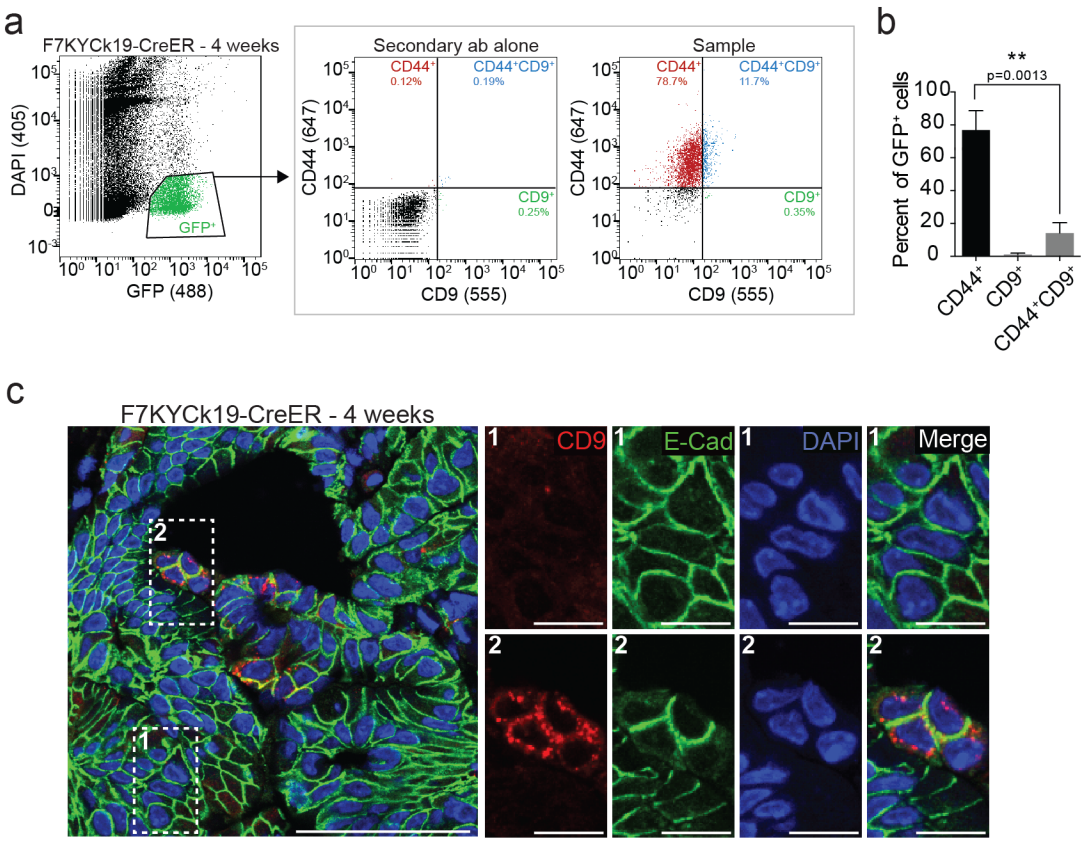

Figure 31 - CD9 expression marks a subpopulation of transformed cells in the F7KYCk19-CreER mouse model of PDAC

a) Flow cytometry analysis of pancreas of F7KYCk19-CreER mice 4 weeks after tamoxifen injection. DAPI was used to assess viability. Plot on the left shows cells gated for DAPI negativity and GFP positivity to only assess live, recombined cells. Analysis was only performed in this $DAPI^{-}GFP^{+}$ population. Plots on the right show CD44 (647 nm excitation - Y axis) and CD9 (555 nm excitation - X axis). CD9 secondary fluorescent antibody alone control (555nm emission) was used to set up gates. Sample - all antibodies used. Percentages (of $DAPI^{-}GFP^{+}$ population) are highlighted within the respective gates. **b)** Percentage of CD44 only, CD9 only and CD44, CD9 double positive cells within $DAPI^{-}GFP^{+}$ cells. Significance calculated using unpaired t test. Bar chart shows the mean values plus SD. Flow cytometry analysis was performed in triplicates (n=3 mice). **c)** Immunofluorescence analysis of CD9 and E-Cadherin on pancreatic tumours of F7KYCk19-CreER mice, 4 weeks after tamoxifen injection. DAPI used for DNA stain (nuclear). Regions of interest are highlighted: **1** - magnification of CD9-negative cells. **2** - magnification of CD9-expressing cells. Scale bars in low magnification image represent 50 µm and 10 µm in high magnification.

4.1.6 CD9 expression marks a subpopulation of transformed cells in the p53KYPdx1-Cre mouse model of PDAC

The value of tumour initiation cell markers, and their applicability in human disease, relies on their robustness to identify a subset of cells with tumour initiation capacity in a wide range of genetic backgrounds. Therefore, to rule out a dependency of the existence of the CD9 population on Fbw7 deletion, I also assessed the presence of CD9-positive tumour cells in the well-established p53KYPdx1-Cre (*$p53^{F/F}$; $KRas^{LSL\text{-}G12D/wt}$, R26-LSL-YFP, Pdx1-Cre*) mouse model of PDAC (Bardeesy et al., 2006a). In this model, the *Pdx1* transcription factor's promoter, active in pancreatic progenitors, drives Cre expression inducing p53 deletion and $KRas^{G12D}$ oncogenic activation, during pancreatic development. At 5 to 8 weeks of age, mice had to be euthanized (Figure 32a) due to the presence of a swollen abdomen and weight loss (data not shown).

Autopsies revealed a solid and enlarged cell mass in the abdominal cavity in the pancreatic region. Regarding histological presentation, haematoxylin and eosin analysis demonstrated the presence of a strong stromal expansion (desmoplasia) and expanded neoplastic ductal structures, both commonly found in PDAC (Figure 32b H&E). Tumour cells were shown to be GFP-positive by immunological analysis, indicating that transformed cells could be traced by R26-LSL-YFP (Figure 32b GFP). As described previously (Bardeesy et al., 2006a), some regions exhibited cells with a spindle-like morphology embedded in the stroma, thus this tumour was classified as poorly-differentiated PDAC (Figure 32b).

To assess the presence of CD9-expressing cells in the p53KYPdx1-Cre-derived tumours, I collected the pancreatic tumours of 5-week-old mice, stained for CD9 and performed flow cytometry (Figure 32c). A fluorescent secondary antibody control was included to validate the specificity of the CD9 stain in this new sample. Only live (DAPI-negative) GFP^+ cells were used for the analysis. I observed that, also in this model, there is a CD9-positive subpopulation of PDAC tumour cells, composing approximately 5% of the GFP^+ cells.

The results obtained confirmed heterogeneity within the tumour population (at least at the molecular level of CD9 expression).

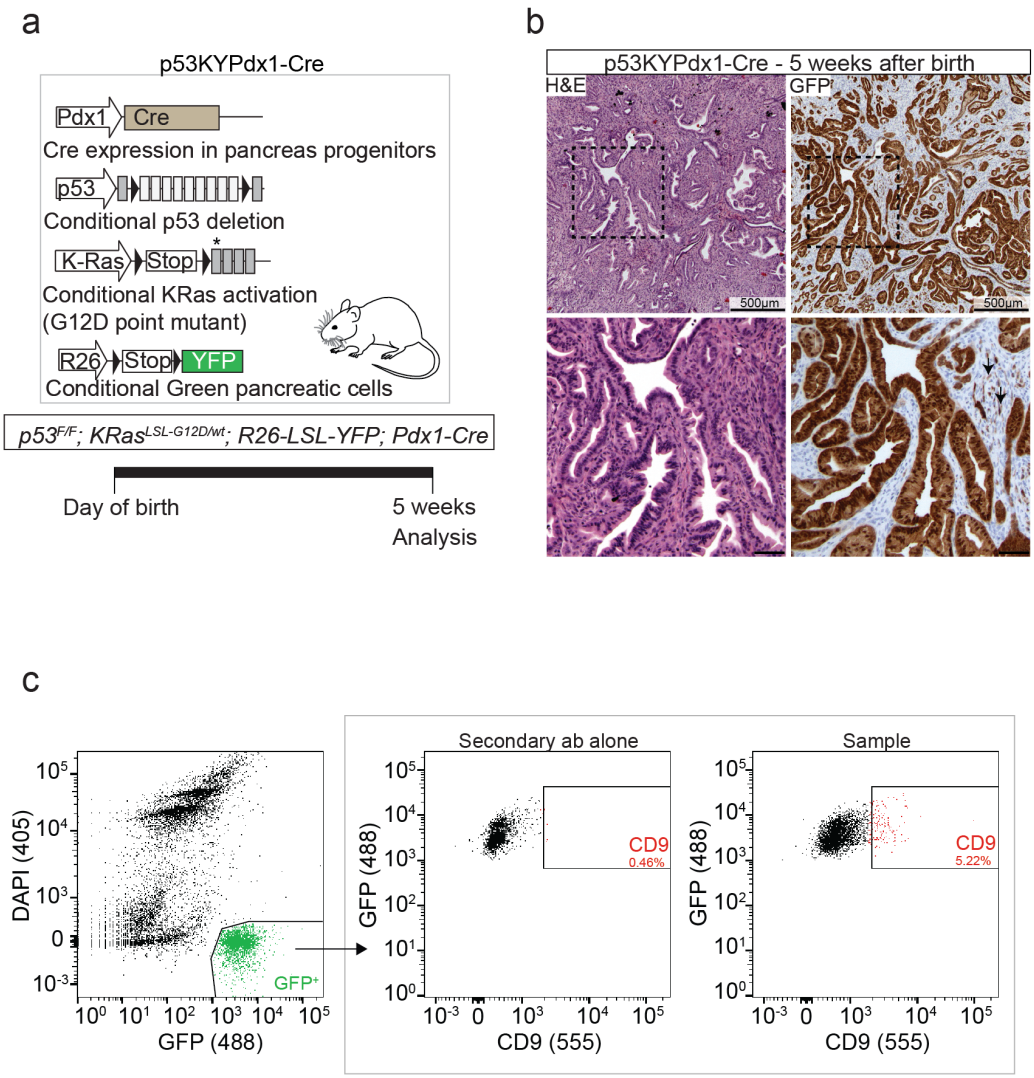

Figure 32 - CD9 expression marks a subpopulation of transformed cells in the p53KYPdx1-Cre mouse model of PDAC

a) Schematic representation of the p53KYPdx1-Cre mouse (*p53$^{F/F}$; KRas$^{LSL-G12D/wt}$; R26-LSL-YFP; Pdx1-Cre*) and experimental approach. Black triangles represent loxP sites and asterisk represents *KRas^{G12D}* mutation. Mice developed pancreatic tumours 5 weeks after birth. **b)** H&E and GFP immunological stain of PDAC tumours from 5-week-old p53KYPdx1-Cre mice. Regions of interest are highlighted and magnified. Black arrows show spindle-shaped tumour cells. Scale bars in low magnification represent 500 µm and in high magnification represent 100 µm. **c)** Flow cytometry analysis of pancreas of 5-week-old p53KYPdx1-Cre mice. DAPI was used to assess viability. Plot on the left shows cells gated for DAPI negativity and GFP positivity, to only assess live, recombined cells. Analysis was only performed in this DAPI$^-$GFP$^+$ population. Plots on the right show GFP (488 nm excitation - Y axis) and CD9 (555 nm excitation - X axis). CD9 secondary fluorescent antibody alone control (555 nm excitation) was used to set up gates. Sample - all antibodies used. Percentages (of DAPI$^-$ GFP$^+$ population) are highlighted within the respective gates.

It has been described that CD44 expression in tumour-initiating cells goes from low (non-TICs) to high (TICs) expression rather than absent to positive, i.e, there is not a distinctive observable population expressing CD44 (Li et al., 2007). The same has been demonstrated for other tumour initiating markers, such as CD133 and CD24, and not only for pancreatic samples (Hermann et al., 2007, Li et al., 2007, Al-Hajj et al., 2003). Since the flow cytometry results obtained with both the CD44 conjugated antibody and the CD9 unconjugated antibody were shifts of the fluorescence intensity, rather than the appearance of a distinct positive population, I decided to validate our antibodies by performing additional analysis with the respective isotype controls. Validation of the CD9 antibody was performed with cultured cells from the p53KYPdx1-Cre-derived tumours (Figure 33a). Cells were expanded as organoids (see Chapter 2, page 102), dissociated by trypsin and stained with the fluorescent secondary antibody alone, with the CD9 primary antibody plus secondary, or with rat IgG_{2a} isotype primary antibody plus secondary. While "unstained", "secondary antibody alone" and "rat IgG_{2a} isotype primary antibody plus secondary" samples showed no positive signal, the combination CD9 primary antibody plus secondary promoted a shift in the population to give a $CD9^{Low/Intermediate}$ and a $CD9^{High}$ populations (these populations will hereinafter be referred to as $CD9^{Low}$ and $CD9^{High}$).

A similar specificity was observed for the CD44 conjugated antibody. Fully developed tumours from F7KYCk19-CreER mice were dissociated and stained for CD44 (Figure 33b). Only live recombined cells ($DAPI^{-}GFP^{+}$) were included for the analysis. As seen for the CD9 antibody, the rat APC-isotype IgG_{2b} showed no staining while the APC-conjugated CD44 antibody marked most of the GFP tumour cells, as expected.

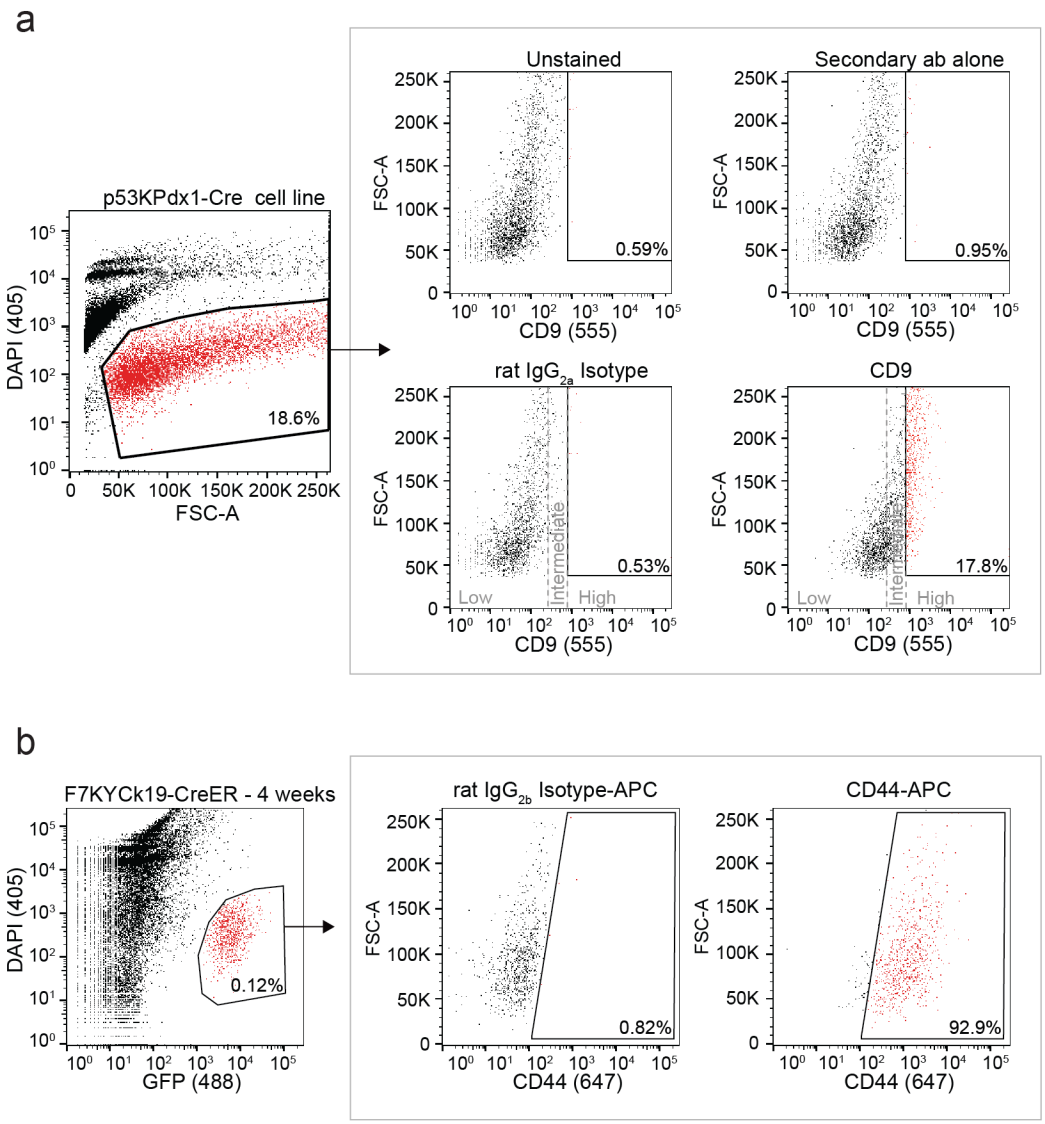

Figure 33 - Assessing CD44-APC and unconjugated CD9 antibody specificity

a) Flow cytometry analysis of CD9 unconjugated antibody specificity using cultured cells from p53KYPdx1-Cre-derived PDAC organoids. Only live cells were included in the analysis (DAPI negative –marked red in the plot on the left). Flow cytometry plots on the right show fluorescence intensity following 555 nm excitation, on the x axis, as a readout of CD9 signal for: unstained, secondary antibody alone, rat IgG_{2a} plus secondary antibody and rat CD9 plus secondary antibody. **b)** Flow cytometry analysis of CD44 APC-conjugated antibody specificity using primary tumour cells from 4 weeks F7KYCk19-CreER-derived PDAC. Only live recombined cells were included in the analysis ($DAPI^-GFP^+$ – marked red in plot on the left). Flow cytometry plots on the right show fluorescence intensity following 647 nm excitation, in the x axis, as a readout of CD44 signal for: rat $IgG2_{2b}$-APC and rat CD44-APC.
Percentages of positive cells from previous gate are indicated.

4.1.7 CD9 surface expression identifies a subpopulation with higher *in vitro* organoid-forming capacity in primary and cultured tumour cells of different mouse models of PDAC

TICs, initially referred to as "cancer stem cells", have been described as a population with stem cell-like properties, such as the ability to self-renew and to give rise to differentiated progeny (Clarke et al., 2006). These stem cell-like features have been extensively studied *in vitro*. Numerous research groups have demonstrated that TICs of different tumour types and tissues, unlike non-tumourigenic cells, can initiate and propagate cell cultures, in non-adherent conditions as spheres or as organoids in 3D matrices (Pastrana et al., 2011).

Sphere-forming assays have also been established for pancreatic cancer TICs, where tumour cells expressing TIC markers are isolated from the remaining population and their ability to propagate the culture in non-adherent conditions is compared to their marker-negative counterpart (Gaviraghi et al., 2010, Hermann et al., 2007, Lonardo et al., 2011). However, it is known that not all pancreatic tumour cell lines are able to form spheres, even though they are able to give rise to tumours upon transplantation into recipient mice (*in vivo* self-renewal property) (Gaviraghi et al., 2010). Therefore, I assessed the ability of freshly isolated tumour cells from F7KYCk19-CreER and p53KYPdx1-Cre-derived PDAC to grow as floating spheres in serum-deprived medium, as previously described (Gaviraghi et al., 2010, Hermann et al., 2007). Unfortunately, the F7KYCk19-CreER tumour cells failed to grow in these conditions (data not shown), which led me to use 3D matrices.

It has been recently shown that pancreatic tumour cells derived from murine PDAC can be maintained and expanded as organoids in a matrigel matrix (Boj et al., 2014). It has also been shown that these conditions favour the growth of cells with stem cell-like phenotypes that are able to give rise to differentiated pancreatic progeny, while the remaining cells fail to grow (Huch et al., 2013). Therefore, I decided to use this 3D culture system to assess differences in organoid-initiation potential (see Chapter 2, page 105) of $CD9^{High}$ versus $CD9^{Low}$ freshly isolated tumour cells from both F7KYCk19-CreER and p53KYPdx1-Cre-derived murine PDAC (Figure 34a).

F7KYCk19-CreER mice were intraperitoneally injected with tamoxifen for 2 days (one injection per day 100 mg/kg of body weight). Four weeks after injection, tumours were

removed, isolated $DAPI^{-}GFP^{+}$ cells were FAC sorted according to their CD9 expression and 1000 cells per well were plated in matrigel in 24-well plates. The experiment was repeated four times (four independent cell sortings, biological quadruplicates) and, at least technical duplicates were performed per experiment for significance assessment (n mice = 4). I observed that $CD9^{High}$ cells were significantly more capable of forming organoids ($p<0.001$) when compared with their negative counterparts, being able to generate an average of 0.0025 organoids per plated cell (0.25%) (Figure 34b,c).

To verify if the organoid-initiating capacity was conserved throughout different oncogenic genotypes, a similar assessment was performed for tumour cells from the p53KYPdx1-Cre-derived PDAC. Five weeks after birth, PDAC tumours from p53KYPdx1-Cre mice were collected, the cells dissociated and 1000 GFP^{+} cells, sorted according to their CD9 expression, were plated per well in matrigel in 24-well plates. The experiment was performed in biological duplicates for significance assessment (n mice = 2). A significant difference was observed ($p=0.05$) when comparing both populations. While approximately 10% of the $GFP^{+}CD9^{High}$ cells were capable of organoid formation, only 1% of $GFP^{+}CD9^{Low}$ cells formed organoids (Figure 34d,e). Moreover, it was visually evident that the $GFP^{+}CD9^{High}$-derived organoids were bigger in size (no measurement was performed) (Figure 34c,e).

Thus, the in vitro results provided the first functional evidence of a higher tumourigenic capacity of $CD9^{High}$ tumour cells.

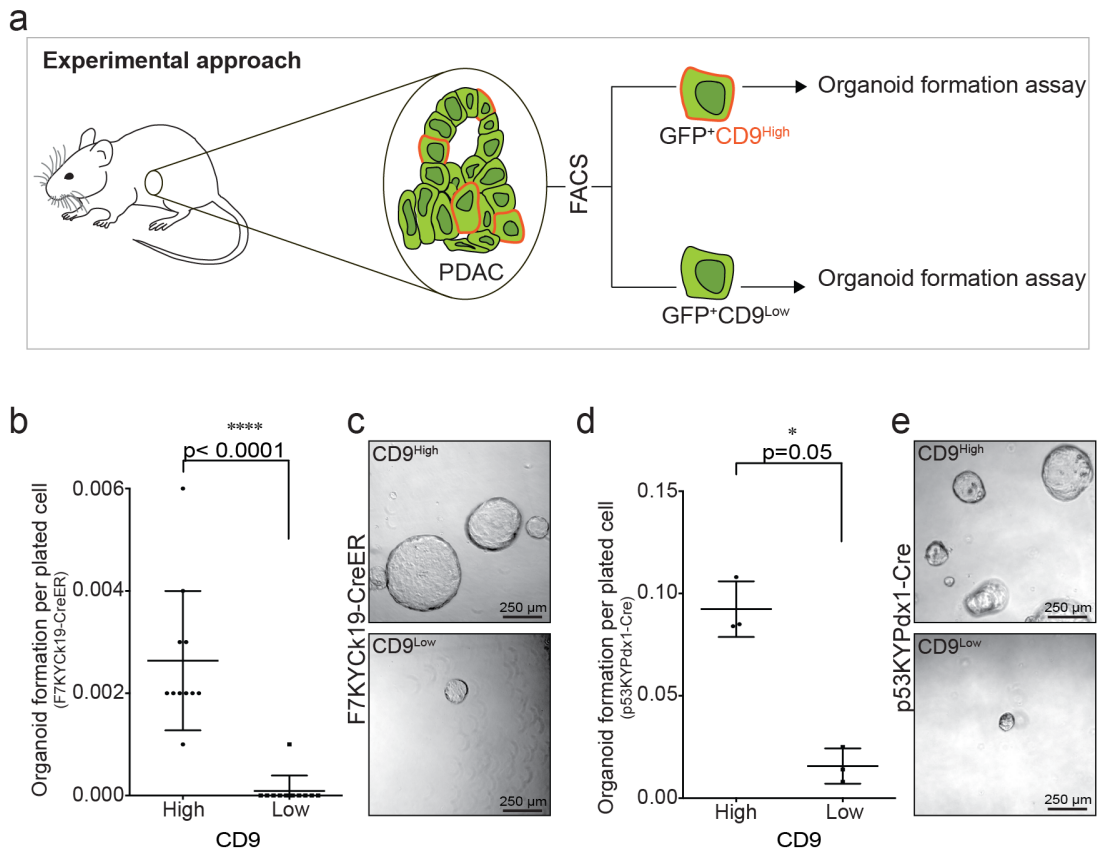

Figure 34 - CD9^{High} murine PDAC primary tumour cells have a higher organoid forming capacity

a) Schematic representation of the experimental approach. Murine PDAC from F7KYCk19-CreER or p53KYPdx1-Cre mice were isolated and tumour cells (GFP^{+}) were sorted according to their CD9 expression. GFP^{+}CD9^{High} and GFP^{+}CD9^{Low} cells were plated in matrigel and the organoid formation capacity was compared between the populations. **b)** Number of organoids per plated cell (1000 cells plated) formed by the sorted F7KYCk19-CreER tumour cells. (n=4 mice) **c)** Representative bright field images of generated organoids from the F7KYCk19-CreER GFP^{+}CD9^{High} (above) or GFP^{+}CD9^{Low} (below) sorted cells, 10 days after plating. **d)** Number of organoids per plated cell (1000 cells plated) formed by the sorted p53KYPdx1-Cre tumour cells. (n=2 mice) **e)** Representative bright field images of generated organoids from the p53KYPdx1-Cre GFP^{+}CD9^{High} (above) or GFP^{+}CD9^{Low} (below) sorted cells, 10 days after plating.
All scale bars show 250 µm.
Dot blots show mean +/- SD. Significance was calculated with the Mann Whitney test.

Given the low percentage of tumour cells which were $CD9^{High}$ in both PDAC mouse models (10% for F7KYCk19-CreER and 5% for p53KYPdx1-Cre – Figure 31a,b and Figure 32c) it became apparent that the number of cells extracted per murine tumour constituted a challenge for *in vivo* studies, i.e., the number of cells obtained was not enough for homograft tumour analysis. Consequently, PDAC tumour cells had to be expanded before any *in vivo* approach could take place.

For tumour cell *in vitro* expansion, I decided to use the 3D organoid system since cells from these cultures can recapitulate the human disease upon orthotopic transplantation (Boj et al., 2014). To ensure that culturing these freshly obtained tumour cells would not change the phenotypic difference between the $CD9^{High}$ and the $CD9^{Low}$ tumour cells, p53KYPdx1-Cre bulk tumour cells were expanded *in vitro* as organoids for several passages, sorted as single cells according to their CD9 expression and assessed for their ability to generate further organoids (Figure 35a).

I dissociated murine PDAC from p53KYPdx1-Cre mice and plated the unsorted population in matrigel with organoid media (see Chapter 2, page 102). Six passages later, the cultured cells were dissociated with trypsin, stained for CD9 and plated in organoid-forming conditions according to their CD9 expression, as above. While in the previous assessment cells were plated by hand, for this experiment, to avoid human error during cell counting and plating, I FAC sorted 100 $GFP^{+}CD9^{High}$ or 100 $GFP^{+}CD9^{Low}$ cells directly into pre-cooled, matrigel-coated wells of 96-well plates (100 cells per well). Experiments were performed in duplicate (two independent sorts, biological duplicates) with, at least, technical triplicates (n mice = 2). A secondary antibody control was used to assess the specificity of the stain in these new conditions, which was shown not to have a signal (Figure 35b).

As observed for the primary tumour cells, $GFP^{+}CD9^{High}$ organoid-derived tumour cells formed 10 times more organoids than $GFP^{+}CD9^{Low}$ cells with a significance of P=0.006. While the $CD9^{High}$ population showed 12% efficiency in organoid formation, only 2.5% of the $CD9^{Low}$ cells formed organoids (Figure 35c). The organoids formed by the $CD9^{High}$ sorted population were not only greater in number but also statistically significantly bigger in size ($p<0.0001$) (Figure 35d).

These results demonstrated that the organoid forming capacity of the CD9^{High} tumour cells was a robust phenotype over several passages and allowed me to proceed to *in vivo* analysis.

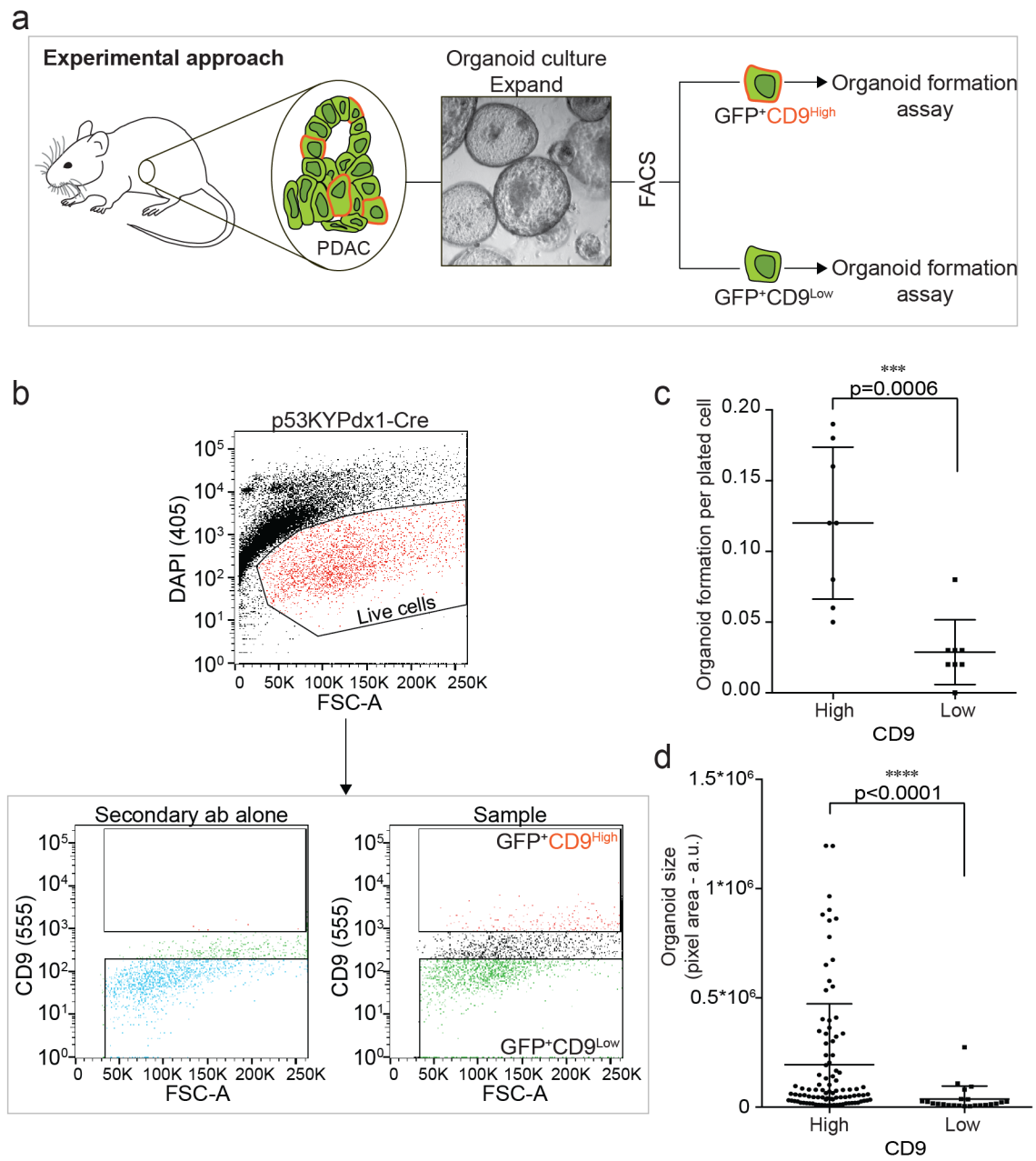

Figure 35 - CD9^{High} murine PDAC organoid-derived tumour cells retain a higher organoid forming capacity

a) Schematic representation of the experimental approach. Murine PDAC from p53KYPdx1-Cre mice were isolated and tumour cells grown for several passages as organoids. Organoids were dissociated and sorted according to their CD9 expression. GFP^{+}CD9^{High} and GFP^{+}CD9^{Low} cells were plated in matrigel and the organoid formation capacity was compared between the populations. **b)** Representative flow cytometry plot of a sort performed on the P53KYPdx1-Cre-derived tumour organoids.

(Figure 35, legend continued)

Only live cells (DAPI-negative) were analysed (upper plot). Lower plots show secondary antibody alone control (left) and the CD9 stain (right). Positive CD9 gate was established based on the unstained population; negative CD9 gate was designed to reduce the chance of including cells with intermediate CD9 expression. **c)** Number of organoids per plated cell (100 cells plated) formed by the sorted p53KYPdx1-Cre-derived PDAC tumour organoids. (n=2 mice, 4 experimental replicates). **d)** Organoid size. Pixel area (arbitrary units - a.u.) was measured using ImageJ to quantify organoid size. Every organoid formed in **c** was measured and their respective sizes were plotted in the dot plot ($nCD9^{High}$organoids = 96; $nCD9^{Low}$organoids = 23).
Dot plots show mean +/- SD. Significance was calculated with the Mann Whitney test.

4.1.8 CD9 surface expression identifies a murine PDAC tumour population with higher *in vivo* tumourigenic potential

While *in vitro* observations of higher organoid-forming potential from $CD9^{High}$ cells suggest a tumour-initiating property, by definition, tumour-initiating cells have to be capable of tumour formation and maintenance in xenograft or homograft models, reproducing the primary disease (Clarke et al., 2006).

Therefore, the classification of tumour-initiating cells is highly dependent on the greater ability of the putative TIC population to form tumours, when compared to the negative population in recipient mice. To assess, *in vivo*, the cancer stem cell-like potential, I generated and expanded p53KYPdx1-Cre PDAC tumour-derived organoids, sorted the expanded tumour cells according to their CD9 expression ($GFP^{+}CD9^{High}$ versus $GFP^{+}CD9^{Low}$) and subcutaneously injected the sorted population into the flanks of immunodeficient *NuNu* mice (the same mouse was subcutaneously injected with both populations, one in each opposite flank, for comparable analysis) (Figure 36a). Represented results are the combination of two independent experiments.

The tumorigenic capacity was measured by: (1) the ability of selected populations to form tumourigenic nodules (a nodule was considered a mass equal to $4mm^3$), at a particular time (time X), following serial dilution and (2) their capacity to maintain tumour development by comparing tumour sizes at endpoint. I injected $200x10^3$, $20x10^3$, $2x10^3$ or $0.2x10^3$ $GFP^{+}CD9^{High}$ and $GFP^{+}CD9^{Low}$ tumour cells in the flanks of *NuNu* mice. I had observed before that p53KYPdx1-Cre organoid-derived PDAC cells have a pronounced tumour formation capacity even as a bulk population, since orthotopic transplantation of $500x10^3$ cells generated palpable sized tumours two weeks after surgery (Figure 26b, Chapter 3, page 148). Therefore, measurements of initial nodules started one week after homograft transplantation and continued until all experimental animals developed tumours.

It was seen that, in all dilutions, the $CD9^{High}$ cell-containing flanks developed nodules in all mice before all flanks with $CD9^{Low}$-injected cells showed nodule formation (Figure 36b). As expected, the biggest difference in nodule onset was observed when $2x10^3$ and $0.2x10^3$ cells were injected. Upon injection of $2x10^3$ cells, 50% of the $CD9^{High}$ cell-containing flanks developed nodules at 2 weeks and all flanks were found with nodules at 4 weeks. However, when the same number of $CD9^{Low}$ cells was injected, at the third

week, only 50% of the mice were found with nodules, with the last nodule formation being registered 6 weeks after injection (Figure 36b,c). When $0.2x10^3$ cells were injected, 50% of the mice developed nodules in the flank injected with $CD9^{High}$ cells as soon as 2 weeks after injection while no nodule was detected at this time point for $CD9^{Low}$ cell-containing flanks (Figure 36b,d). It is important to mention that, in accordance with the inability of $CD9^{Low}$ cells to sustain tumour development, when 200 cells were injected, 1 out of the 4 mice demonstrated $CD9^{Low}$-derived tumour regression and, consequently, no tumour was detected when the experiment was terminated. Moreover, 1 out of the remaining 3 tumours was so small at the time of removal that embedding and sectioning was compromised. Thus, only two tumours from the flanks of $0.2x10^3$ $CD9^{Low}$ injected cells were left for histological analysis.

Tumour initiation is a feature that only self-renewing cells possess given their unique ability to continuously give rise to tumour cells. Nevertheless, the remaining "non-tumour-initiating cells" harbour some limited proliferative potential enabling nodule formation (Reya et al., 2001). Therefore, the functional assessment of TICs cannot be restricted to their ability to initiate nodules in recipient mice, but also to sustain the growth of the initiated tumour. For this reason, tumours were allowed to grow until one of the flanks reached 1 cm^3 of tumour content or appearance of animal distress due to tumour load or location. Mice harbouring one 1 cm^3 tumour were culled, tumours from both flanks were removed and their size measured. Tumour volume was calculated using the following formula: volume=(Height*Length*width)/2 (Tomayko and Reynolds, 1989).

It was observed that while $CD9^{High}$ tumour cells were able to form $1cm^3$ tumours, regardless of the number of cells injected, $CD9^{Low}$ tumour cells failed to maintain tumour growth with increase in dilution (Figure 36e). I calculated the fold difference in tumour size between $CD9^{High}$ and $CD9^{Low}$-developed tumours, for all dilutions performed, and observed that, despite the low difference in tumour onset, $CD9^{High}$ cells were 4, 3.5, 8 and 13-fold more capable of tumour growth than $CD9^{Low}$ cells when $200x10^3$, $20x10^3$, $2x10^3$ and $0.2x10^3$ cells were injected, respectively (Figure 36f).

To assess tumour maintenance, i.e., the ability to propagate and maintain tumour growth after tumour initiation, I calculated the final tumour volume relative to the volume of the initially detected nodule ($=Volume_{Final}/Volume_{Initial}$). The biggest difference was

observed when 200 cells were inoculated. While $CD9^{High}$ cells demonstrated over a 100-fold increase in tumour size compared to the initial nodule, the $CD9^{Low}$ cells were only capable of a 10-fold increase (Figure 36g). Importantly, and as mentioned above, 2 out of 4 nodules from 200 $CD9^{Low}$ injected mice exhibited tumour growth regression/inefficient growth following nodule onset, reinforcing their limited proliferation capacity.

These results corroborate the higher tumourigenic capacity suggested from my *in vitro* studies and demonstrate that $CD9^{High}$ PDAC tumour cells are capable of both tumour initiation and maintenance, while the $CD9^{Low}$ tumour cells fail to maintain tumour growth.

a

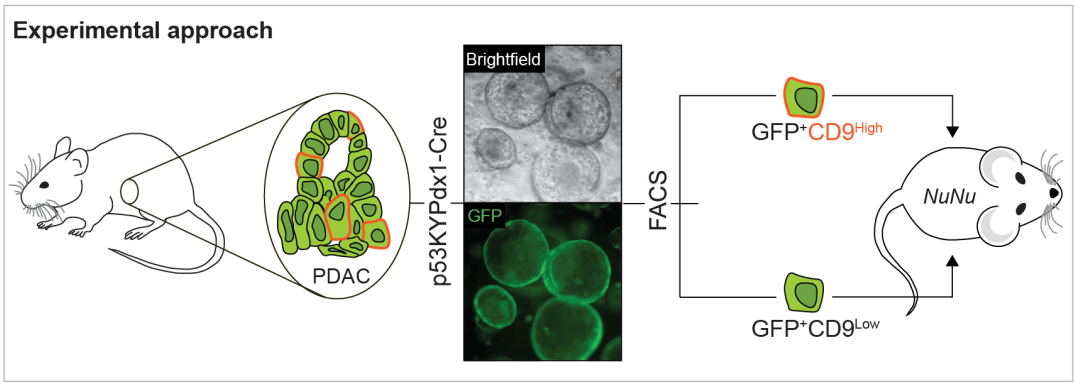

b

Tumourigenic capacity of CD9^{High} versus CD9^{Low} cells from p53KYPdx1-Cre organoids							
Population injected	No. of injected cells	No. mice with tumour formation/Total no. mice injected, at week x					
		1 week	2 weeks	3 weeks	4 weeks	5 weeks	6 weeks
CD9^{High}	200.000	3/3	-	-	-	-	-
	20.000	4/5	5/5	-	-	-	-
	2000	1/6	3/6	5/6	6/6	-	-
	200	0/4	2/4	3/4	4/4	-	-
CD9^{Low}	200.000	2/3	3/3	-	-	-	-
	20.000	0/5	2/5	4/5	5/5	-	-
	2000	0/6	1/6	4/6	4/6	5/6	6/6
	200	0/4	0/4	1/4	2/4	2/4	4/4

c

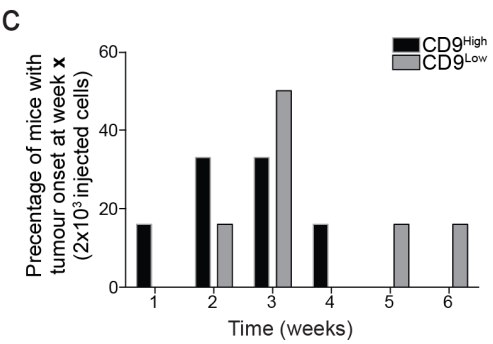

d

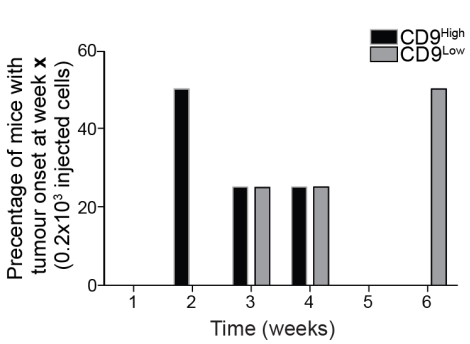

e

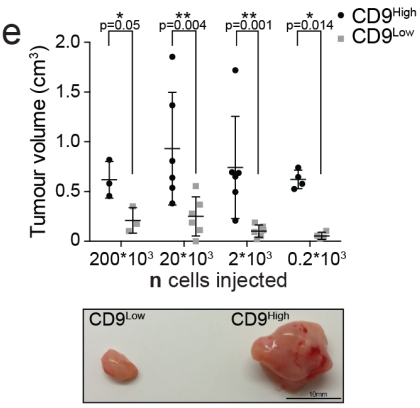

f

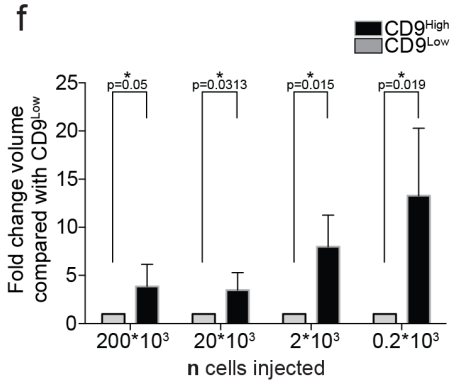

g

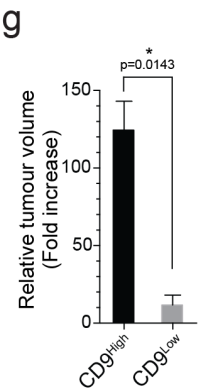

Figure 36 - CD9 surface expression identifies a murine PDAC tumour population with higher *in vivo* tumourigenic potential (TICs)

a) Schematic representation of the experimental approach. Murine PDAC from p53KYPdx1-Cre mice were isolated and tumour cells grown for several passages as

(Figure 36, legend continued)

organoids. Two independent cell lines were generated from 2 individual p53KYPdx1-Cre mice-derived PDAC. Organoids were dissociated and sorted according to their CD9 expression. $GFP^{+}CD9^{High}$ and $GFP^{+}CD9^{Low}$ cells were injected (serial dilutions) in the flanks of *NuNu* mice and tumour initiation and growth were analysed. **b)** Tumourigenic capacity of $CD9^{High}$ versus $CD9^{Low}$ tumour cells from p53KYPdx1-Cre PDAC-derived organoids. $200x10^3$, $20x10^3$, $2x10^3$ and $0.2x10^3$ sorted tumour cells were injected in the flanks of *NuNu* mice and the number of weeks necessary for nodule ($4mm^3$) detection was registered. **c)** Percentage of mice injected with $2x10^3$ sorted $CD9^{High}$ or ^{Low} tumour cells that developed tumours per week x. **d)** Percentage of mice injected with $0.2x10^3$ sorted $CD9^{High}$ or ^{Low} tumour cells that developed tumours per week x. **e)** Tumour sizes per flank, per dilution, in cm^3. Mice were culled when one of the flanks developed a tumour of $1cm^3$. Each dot indicates a tumour (one $CD9^{High}$ and one $CD9^{Low}$ tumour per mouse). Dot blot indicates mean +/- SD. Volume was calculated as: volume=(Height*Length*width)/2. Representative image of generated tumours. Scale bar represents 1cm. **f)** Fold change of the volume between the $CD9^{Low}$ and $CD9^{High}$-derived tumours at each dilution. Bar chart shows mean +/- SD. **g)** Relative tumour volume (RTV) of the $CD9^{High}$ and $CD9^{Low}$-derived tumours when $0.2x10^3$ cells were subcutaneously injected. $RTV = Volume_{Final}/Volume_{Initial}$. Bar chart shows mean plus SD.

Significance was calculated using the Mann Whitney test for **e** and **g**, and the Wilcoson test was used to calculate significance in **f** (values were normalized to the $CD9^{Low}$ control)

4.1.9 $CD9^{High}$ PDAC TICs re-establish the cellular heterogeneity observed in the primary tumour

Similar to tissue stem cells with their capacity to give rise to different cell types, tumour-initiating cells are known to be responsible for the cellular heterogeneity found in cancers, given their ability to generate differentiated progeny (Clarke et al., 2006). I performed histological studies in order to compare the tumours generated by the $CD9^{High}$ and $CD9^{Low}$ cells with their original primary tumour. For the purpose of simplicity, only the tumours derived from $2x10^3$ injected cells will be described. Tumours formed after injection of $200x10^3$ and $20x10^3$ cells followed a similar pattern as $2x10^3$-derived tumours. Regarding tumours formed following injection of $0.2x10^3$ $CD9^{Low}$ tumour cells, their histologic assessment is still ongoing.

Hematoxylin and eosin analysis of tumours generated following injection of $2x10^3$ cells demonstrated that, while both the primary and the $CD9^{High}$-derived tumours were compact masses of tissue, the $CD9^{Low}$-derived tumours possessed mainly cystic structures (Figure 37a,b,c). Ck19 and GFP immunohistochemical analysis allowed a better understanding of the tumour histology. Ck19 stain demonstrated that all three tumours presented regions of ductal differentiation by the detection of branching epithelial elements with ductal morphology and thus could be classified as PDAC (Figure 37d,e,f). However, when analysing the GFP signal (lineage tracer of injected tumour cells), I could detect that, while there was a good co-localization with the Ck19 stain in the $CD9^{Low}$-derived tumours, the primary and the $CD9^{High}$-generated tumours exhibited large regions that expressed GFP but had lost Ck19 protein (Figure 37g,h,i).

Since GFP is expressed in all tumour cells, the results suggest that some of the tumour cells had lost their ductal epithelial identity. Confirming the previous hypothesis, high magnification of GFP expression regions, that had lost Ck19 expression, demonstrated that most of the tumour cells in the primary and the $CD9^{High}$-derived tumours presented a mesenchymal differentiation with cells exhibiting a spindle shape. On the other hand, $CD9^{Low}$-derived tumours were entirely composed of cells expressing Ck19 and GFP with a ductal cuboidal/columnar epithelial morphology (Figure 37j,k,l,m,n,o).

Given the difference between the generated tumours, I requested a complete pathology report, which was provided by our on-site consultant histopathologist, Professor Gordon Stamp. It has been described before that the homozygous deletion of p53 in pancreatic

progenitors with concomitant $KRas^{G12D}$ activation leads to the development of pancreatic ductal adenocarcinoma embedded in dense fibrous stroma or in conjunction with sarcomatoid or anaplastic carcinomas, characterized by the presence of spindle-shaped cells and concomitant ductal differentiation (Bardeesy et al., 2006a). Similar to the primary tumour, $CD9^{High}$-derived tumours presented regions with semi-polarized cuboidal cells, resembling a pancreatic ductal phenotype, combined with GFP-expressing sarcomatous elements with single cell invasion. Both tumours were classified as carcinosarcomas. In contrast, $CD9^{Low}$-derived tumours were described to possess similar branching tubuloglandular ductal structures but no obvious sarcomatous transformation, with epithelial cells clearly distinct from the desmoplastic stroma. These tumours were not classified as carcinosarcomas.

The results suggest that $CD9^{High}$-sorted PDAC organoid-derived tumour cells were capable of giving rise to the cell types found in the primary tumour reproducing the p53KYPdx1-Cre-derived PDAC histological heterogeneity, and that $CD9^{Low}$ cells retain their epithelial differentiation, failing to generate more mesenchymal cells.

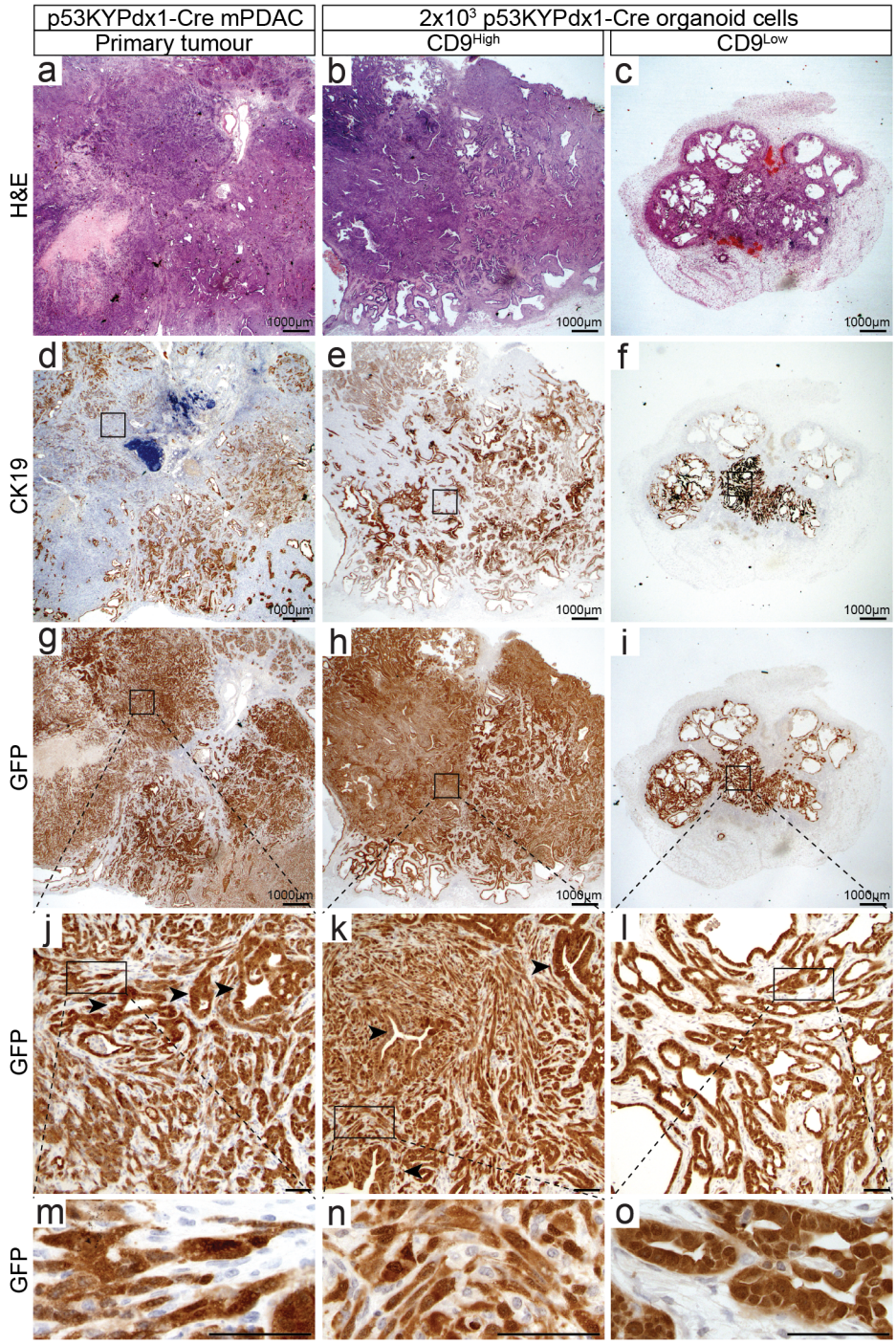

Figure 37 - CD9^{High} PDAC TICs re-establish the cellular histological heterogeneity observed in the primary tumour

Representative histological analysis of the p53KYPdx1-Cre primary tumour and the tumours generated following injection of 2x10^3 p53KYPdx1-Cre PDAC organoid-derived sorted CD9 high and low tumour cells. More than 3 p53KYPdx1-Cre primary tumours were analysed. Tumours from all injected mice were collected and used for histological analysis. **a,b,c)** H&E section of **(a)** primary, **(b)** CD9^{High} and **(c)** CD9^{Low} tumours. **d,e,f)** CK19 immunological staining of **(d)** primary, **(e)** CD9^{High} and **(f)** CD9^{Low} tumours. **g,h,i)** GFP immunological staining of **(g)** primary, **(h)** CD9^{High} and **(i)**

(Figure 37, legend continued)

$CD9^{Low}$ tumours. **j,k,l)** Magnified regions highlighted in **g**, **h** and **i**, respectively. Black arrows highlight ductal differentiation in primary and $CD9^{High}$-derived tumours. All regions in $CD9^{Low}$ tumours possess ductal differentiation. **m,n,o)** Magnified regions highlighted in **j**, **k** and **l**, respectively.
All scale bars represent 100μm, unless indicated otherwise in the figure.

4.1.10 Tumours derived from CD9^{High} cells are more proliferative than the CD9^{Low} generated tumours

The assumption that the CD9^{Low} tumour cells are non-tumour-initiating cells with limited proliferative potential requires the observation of reduced proliferation in CD9^{Low}-generated tumours when compared with tumours generated by CD9^{High} sorted cells. For this purpose, I stained the tumours generated by subcutaneous injection for phosphorylated histone 3 (pH3) (Figure 38a), a marker of on-going mitosis (Hans and Dimitrov, 2001). I could observe that CD9^{High} tumours were significantly more proliferative than CD9^{Low}-derived neoplasias (Figure 38b). As described above, tumours generated from CD9^{Low} injected cells exhibited a pronounced ductal differentiation compared to the ones generated by CD9^{High} injected cells. Nonetheless, I also observed increased proliferation in epithelial regions with ductal differentiation of CD9^{High} derived tumours, excluding the status of differentiation as a cause of the proliferative difference (Figure 38a).

These results corroborate a limited proliferative potential of CD9^{Low} cells and incapability to maintain tumour growth, hence, their classification as non-TICs.

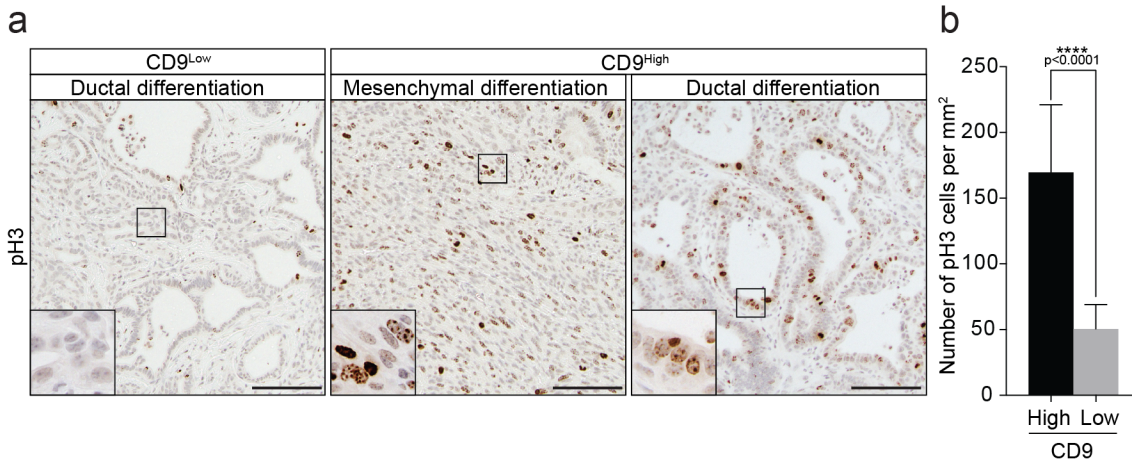

Figure 38 - Tumours derived from CD9^{High} cells are more proliferative than CD9^{Low}-generated tumours

a) Immunological staining of CD9^{High} and ^{Low}-derived tumours for pH3. Images show ductal epithelial regions of CD9^{Low}-derived tumours and both ductal and mesenchymal differentiated regions of CD9^{High}-derived tumours. Scale bars represent 100µm. **b)** Quantification of number of cells positive for pH3 per mm^2. Four tumours per population and 3 levels per tumour were used for quantification (n mice =4). Bar chart shows mean plus SD. Significance was calculated using the Mann Whitney test.

4.2 Discussion: Identification of a specialized tumour-initiating population in murine PDAC

4.2.1 Differential cancer susceptibility of ductal cells

The pancreatic ductal compartment is commonly described as a structure composed of a homogeneous cellular population (ductal cells) responsible for the conduction of acinar-derived digestive enzymes to the duodenum (Reichert and Rustgi, 2011). However, injuries to the organ and selective genetic manipulations have unravelled a cellular plasticity that might only be present in a subset of ductal cells (Sancho et al., 2014, Inada et al., 2008).

Adding to this cellular heterogeneity, I observed a differential susceptibility to tumourigenic transformation in adult ductal cells. When the initial stages of adult PDAC development of F7KYCk19-CreER mice were analysed, it was observed that only a fraction of the lineage traced cells (recombined, GFP^+) exhibited morphological features of transformation. Protein level analysis identified CD44, a surface protein previously identified in human PDAC TICs to be selectively expressed in transformed cells. Its presence was detected as early as 2 weeks after tamoxifen treatment, allowing distinction between early transformed and non-transformed cells, and persisted throughout tumour development proving to be a good tumour cell marker. Important to highlight is the fact that the GFP^+CD44^+ and GFP^+CD44^- populations harboured the same oncogenic hits, since genotyping PCR could not detect inefficient recombination for the *Fbw7* and *KRas* loci in any of the populations assessed.

Our research group has previously described that loss of Fbw7 protein, in adult ductal cells, promotes a cellular conversion of ductal cells into endocrine insulin-producing β-cells (Sancho et al., 2014). In that study, a simultaneous increase in proliferation was also observed with Fbw7 loss, which was independent from the conversion, as ductal cell-derived newly formed β-cells did not arise through a proliferation step. This suggested that, within the ductal network, some cells are more prone to proliferate than others (Sancho et al., 2014). Corroborating previous findings, my results support this proliferative heterogeneity by demonstrating that ductal cells respond differently to the same oncogenic hit. These results encouraged me in the search for markers of tumour initiating cells for PDAC development.

4.2.2 $CD9^{High}$ PDAC cells constitute a tumour-initiating population

The identification of tumour-initiating cells has increased the understanding of tumour biology and changed the way medicine approaches cancer treatments. While TIC identification was initially reported in haematological malignancies (Lapidot et al., 1994), solid tumours have also been the target of tumour-initiating cell identification. Pancreatic cells with higher tumourigenic capacity have been reported (Hermann et al., 2007, Lonardo et al., 2011, Li et al., 2007). However, inconsistent data has been obtained in different laboratories (see Chapter 5, 5.4) highlighting the need for better understanding of PDAC tumour-initiating biology.

I performed a gene expression array to assess differentially expressed genes in transformed versus non-transformed pancreatic cells ($GFP^{+}CD44^{+}$ vs $GFP^{+}CD44^{-}$) with the same oncogenic hits (Fbw7 deletion and $KRas^{G12D}$ oncogenic activation), and combined it with literature and database searches (Uhlen et al., 2015). I identified CD9 as a potential marker for a subpopulation of transformed cells. Due to technical difficulties, such as the number of cells of interest obtained in each pancreatic isolation, the execution of replicates was not possible. However, the observation that described pancreatic tumour markers such as CTSE, Mmp7, Agr2, TFF2 and Muc1 were included amongst the most upregulated genes in the transformed cell population illustrated a biological accuracy of the expression array. Nevertheless, validation was performed following repetition of the experimental outline and Q-PCR analysis of selected hits.

The cancer stem cell hypothesis postulates that tumour-initiating cells are equipped with stem cell features; such as self-renewal capacity and ability to give rise to differentiated progeny, culminating in the observed cellular heterogeneity. These features are routinely assessed by *in vitro* differential sphere/organoid-forming capacity and by the unique aptitude to generate tumours when transplanted into recipient mice (Nguyen et al., 2012, Clarke et al., 2006, Jordan et al., 2006, Pastrana et al., 2011). The *in vitro* organoid-forming capacity and the *in vivo* tumourigenic potential, following homograft transplantation, of the $CD9^{High}$ murine PDAC population was significantly increased when compared with their $CD9^{Low}$-expressing counterpart.

In particular cases, such as in haematopoietic malignancies, tumour-initiating cells depend on the oncogenic hit received. While some genetic alterations were shown to be

capable of inducing TIC properties in progenitor cells, other oncogenic hits failed to do so (Huntly et al., 2004). Thus, my assessment included two different genetic backgrounds: *Fbw7* or *p53* homozygous deletion, both harbouring the PDAC oncogenic driver mutation (*KRas*^{G12D} activation). I observed that, independently of the oncogenic hit, CD9^{High} cells, present in murine PDAC, exhibit a significantly increased *in vitro* organoid-forming potential compared to CD9^{Low} tumour cells.

Interestingly, despite the higher number of CD9^{High} cells present in the F7KYCk19-CreER-derived murine PDAC (approximately, 15% of the tumour cell population), the p53KYPdx1-Cre murine PDAC-derived CD9^{High} cells (containing approximately 5% CD9^{High} cells of the tumour cell population) exhibited higher *in vitro* organoid-forming potential. Unfortunately, the organoid formation from CD9^{High} cells of the two genotypes was not simultaneously assessed, introducing a great experimental variability, which impedes comparison. Nonetheless, replicates within each genotype were consistent, excluding inter-experiment variability as a causative element. The cellular origin of these murine PDAC should also be borne in mind. While the F7KYCk19-CreER-derived PDAC have their origin in adult duct cells, the murine PDAC derived from p53KYPdx1-Cre is formed from pancreatic progenitors. It is clear that both initial cell types (adult ducts and pancreatic progenitors) greatly differ in their transcriptional programs and expression profiles, which might affect the self-renewal potential of the tumour-initiating cells. To accurately compare both genetic alterations, the same Cre driver should be used. Thus, the *in vitro* organoid-formation assessment should be repeated comparing F7KYPdx1-Cre with p53KYPdx1-Cre PDAC-derived CD9^{High} cells (pancreatic progenitors) and the F7KYHnf1β-CreER with the p53KYHnf1β-CreER CD9^{High} PDAC-derived cells (adult duct cells). However, the fact that the CD9-positive TIC population was present in PDACs originated from 2 different genetic profiles and cells of origin suggests that CD9 might be a general marker for PDAC TICs.

I have also observed that the frequencies of organoid-initiating cells were extremely low for both murine PDAC models. Only 0.3% of the F7KYCk19-CreER PDAC-derived CD9^{High} cells and approximately 10% of the p53KYPdx1-Cre PDAC-derived CD9^{High} cells were capable of organoid initiation. This result can be partially explained by the cellular viability after FACS sorting. The tumour dissociation, the long term incubation of the cells in media deprived conditions before FACS (2% FBS in PBS cell

suspension), followed by the fluorescence activated cell sorting at high pressures, constitutes an extremely harsh process, which compromises cell survival. It is, thus, likely that not all sorted cells survive in culture and are capable of organoid formation. Nonetheless, the same methodology has been applied to other systems and, while 100% efficiency in organoid formation is never observed, a higher percentage of organoid-forming cells is expected if the selected population constitutes a pure tumour-initiating cell population. It is possible that the $CD9^{High}$ is still a heterogeneous population. Therefore, it would be interesting to know if this TIC population could be further narrowed down. This could be addressed by single cell gene expression. Single cell RNA sequencing has been used to identify subpopulation within tissues based on their gene expression profile, reconstructing lineage hierarchies (Treutlein et al., 2014). Hence, the single cell gene expression analysis of the $CD9^{High}$ population could unveil a possible heterogeneity and identify additional markers that would allow the enrichment of the PDAC TICs.

Homograft transplantation of $CD9^{High}$ and $CD9^{Low}$ PDAC tumour cells from p53KYPdx1-Cre-derived organoids confirmed the $CD9^{High}$ population as PDAC tumour-initiating cells. $CD9^{High}$ PDAC cells injected subcutaneously in a serial dilution approach were capable of generating tumour nodules faster than the $CD9^{Low}$ injected cells and were uniquely able to maintain tumour development demonstrating a 100-fold increased growth of the originating nodule when 200 cells were injected. On the other hand, $CD9^{Low}$ PDAC cells showed very limited tumour maintenance capacity with only a 10-fold increase in tumour growth when compared with the size of the initial nodule. Moreover, regression of two out of four nodules formed was observed (200 cells injected).

It is common to focus only on nodule formation to identify TICs. However, tumours exhibit a cellular hierarchy that can be correlated with their proliferative potential. While tumour-initiating cells, or cancer stem cells, are described to possess unlimited proliferative capacity, the remaining tumour mass is known to have a limited proliferative potential (Reya et al., 2001). This definition suggests that, when injected, these non-tumour-initiating cells can expand the population to a certain extent being able to form nodules that do not grow extensively. In accordance with the previous

statement, despite their ability to form nodules, at low cell numbers the $CD9^{Low}$ tumour cells were not capable of maintaining the growth of the tumour as efficiently as the $CD9^{High}$ cells and exhibited significantly reduced proliferation, as assessed by the presence of phosphorylated histone 3.
The complete absence of nodule formation by $CD9^{Low}$ cells might be observed if a less aggressive/highly proliferative genotype is used for homograft transplantation assays. It is known that the homozygous deletion of p53 in the embryonic pancreas with simultaneous $KRas^{G12D}$ oncogenic activation leads to anaplastic PDAC with visible EMT and undifferentiated cellular populations (Bardeesy et al., 2006a). Therefore, organoids from a less aggressive genetic background known to give rise to well-differentiated PDAC with later onset, such as the $p53^{F/WT}$; $KRas^{LSL\text{-}G12D/Wt}$; Pdx1-Cre (Rhim et al., 2012), should be generated and the experiment repeated.

As mentioned above, TICs are known to reproduce the originating disease. I observed that $CD9^{High}$-derived tumours reproduced the p53KYPdx1-Cre-derived carcinosarcoma with local ductal differentiation. Conversely, $CD9^{Low}$-derived tumours failed to reproduce the PDAC heterogeneity of the originating tumour giving rise to a well-differentiated PDAC with no sarcomatous elements. As opposed to the approach taken for *in vitro* studies, for *in vivo* assessment of tumour initiating potential, only cells derived from p53KYPdx1-Cre tumours were used. For this reason, it is still not clear if this *in vivo* tumourigenic potential is dependent on the oncogenic hit. Hence, a similar approach with a comparable Cre model and a different induced genetic alteration (such as F7KYPdx1-Cre) should be performed.

The results obtained so far strongly suggest that CD9 expression and surface localization marks a population within pancreatic tumours that is responsible for tumour initiation, maintenance and cellular heterogeneity. The implications and potential utility of such marker will be discussed further in Chapter 5.

Chapter 5. Discussion

5.1 Introduction to the aim

Pancreatic ductal adenocarcinoma (PDAC), comprising 85% of all pancreatic cancers, is a neoplastic disease of the pancreas with an extremely poor prognosis (less than 4% 5-year survival) (Hariharan et al., 2008, Hezel, 2006). Given the non-specific nature of symptoms, PDAC is usually detected at advanced stages, where tumour grade/stage and presence of metastases compromise the benefits of surgical resection. Current PDAC chemotherapy strategies rely on the unspecific targeting of proliferative cells by the use of nucleoside analogues, such as Gemcitabine (Burris et al., 1997). However, not all patients benefit from this approach. So, there is a urgent need for improvement in drug development and cell-specific therapeutic targeting (Bittoni et al., 2014). Therefore, extensive efforts have been made to fully understand the molecular and cellular biology of the disease.

At the molecular level, it is well known that PDAC tumour initiation is driven by *KRAS* mutations, mainly occurring in exon 1 (codon 12), leading to a glycine to aspartic acid or valine change (G12D or G12V) (Eser et al., 2014). While *KRAS* mutations are present in over 90% of human PDAC samples, other, less represented, genetic/epigenetic alterations, such as inactivation of *p53* (50-70%), *SMAD4* (30-80%) and *CDKN2A* (35-50%), have also been reported to have crucial roles in PDAC biology (Waddell et al., 2015, Eser et al., 2014, Rozenblum et al., 1997, Hong et al., 2011). Moreover, comprehensive genetic analysis and genome-wide studies on human PDAC samples confirmed its complex molecular profile and highlighted the possible contribution of other genes to PDAC development (Waddell et al., 2015, Jones et al., 2008), calling for more in depth studies on additional genetic players.

At the cellular level, based on human and mouse data, a histological progression from low to high-grade cellular dysplasia has been proposed. Four types of precursor lesions have been described to precede PDAC: intraductal papillary mucinous neoplasia (IPMN); pancreatic mucinous cystic neoplasm (MCN); intraductal tubular papillary neoplasm (ITPN); and, the most common pre-neoplastic lesion, pancreatic

intraepithelial neoplasia (PanIN) (Distler et al., 2014, Cooper et al., 2013). The identification of pre-neoplastic lesions has made it possible to develop strategies for PDAC early detection (Cruz-Monserrate et al., 2012, Stefan Eser, 2011, Tanaka et al., 2012). Furthermore, survival studies have reported that different pre-neoplastic lesions confer different prognosis for the developed PDAC (Cooper et al., 2013). Since mouse models of PDAC have demonstrated that PDAC arising from different pre-neoplastic lesions have no discernible features at endpoint (von Figura et al., 2014, Bardeesy et al., 2006b), a better understanding of PDAC origin and biology might allow patient stratification and development of personalized medicine.

During the course of my studies I focused on the role of the tumour suppressor gene *Fbw7* in PDAC development and investigated the cellular origins of this pancreatic neoplasia.

5.2 The role of FBW7 in PDAC tumourigenesis

FBW7 is an F-box protein that confers substrate specificity to an SCF-type E3 ubiquitin ligase, responsible for protein ubiquitination and consequent proteasomal degradation of its targets. Due to the nature of its substrates, FBW7 has been described as a tumour suppressor, targeting several proteins involved in cell fate decisions and proliferation for degradation, such as c-Myc, cyclin E, Notch, c-Jun and Mcl-1 (Welcker and Clurman, 2008). Numerous studies have addressed the role of FBW7 in cancer development and progression (Cheng and Li, 2011, Crusio et al., 2010). However, its relevance in PDAC tumourigenesis is still not well established.

In this thesis, I confirmed and followed up Rocio Sancho's findings that Fbw7 protein loss with concomitant $KRas^{G12D}$ oncogenic activation, in the developing pancreas, greatly accelerates murine PDAC (mPDAC) onset, when compared to $KRas^{G12D}$ activation alone. Histologically, $Fbw7^{F/F}$; $KRas^{LSL\text{-}G12D/wt}$; *Pdx1-Cre* pancreatic tumours (F7KPdx1-Cre mice) resembled the mPDAC derived from the established $KRas^{LSL\text{-}G12D/wt}$; *Pdx1-Cre* model (KPdx1-Cre mice) (Hingorani et al., 2003). Furthermore, tumours from both models exhibited increased pErk (downstream target of the Ras

pathway) and nuclear Hes1 (readout of Notch pathway activation) immunoreactivity, as described for human PDAC (Hezel, 2006).

The mPDAC obtained with the KPdx1-Cre model has been described to closely mimic human PDAC (Hingorani et al., 2003). Therefore, the similarity between mPDAC from the KPdx1-Cre and the F7KPdx1-cre mouse models indicates that Fbw7 deletion does not change the tumour type of a $KRas^{G12D}$-driven pancreatic tumour, but it accelerates PDAC onset and recapitulates the human disease, adding Fbw7 to the list of mPDAC tumour suppressors.

Interestingly, I also observed that Cre-dependent Fbw7 deletion in the embryonic pancreas, with or without $KRas^{G12D}$, mainly increased proliferation of the ducts, having no effect on acinar cell proliferation, and that ductal dysplasia occurred without any obvious alteration to remaining organ. This finding highlighted the importance of Fbw7 in ductal cell biology and shifted the focus of my research to explore this new finding. Thus, the mechanism by which Fbw7 deletion accelerates PDAC in the F7KPdx1-Cre model is still an open question.

FBW7 mutations have been identified in *KRAS* wild type human pancreatic cancer samples (Calhoun et al., 2003). However, while no mutations have been reported in *KRAS* mutant PDAC, downregulation of FBW7 has been observed by immunohistochemistry of some *KRAS* mutant patient samples and in mouse models of PDAC harbouring mutant *KRas* (Ji et al., 2015). In that study, the mechanism by which FBW7 is downregulated was attributed to ERK kinase-dependent FBW7 degradation. The authors demonstrated that overexpression of ERK1 in human PDAC cell lines led to phosphorylation of FBW7 at threonine 205 and protein ubiquitination, with detectable reduction in FBW7 levels. Expression of a phospho-deficient mutant version of *FBW7* led to stabilization of the protein and reduction in tumourigenic potential, following subcutaneous injection of PDAC transfected cell lines (Ji et al., 2015), corroborating the role of FBW7 in PDAC biology. While the regulation of the protein has begun to be addressed, the tumour suppressive mechanism of FBW7 in PDAC biology is still poorly understood.

The Notch pathway has been suggested to be involved in PDAC tumourigenesis, as members of the pathway, such as HES1 and NOTCH1, are upregulated in human

PDAC. Moreover, mouse model studies have identified this pathway as capable of increasing PDAC oncogenesis by promoting the development of pancreatic pre-neoplastic lesions (Miyamoto et al., 2003, De La O et al., 2008). Interestingly, in the F7KPdx1-Cre-derived PDAC, I observed an increase in Hes1, compared with wild type pancreatic. Additionally, this increase in protein levels seemed to be more pronounced when compared to KPdx1-Cre-derived PDAC. It is, thus, possible that Fbw7 deletion accentuates the activation of the Notch pathway, promoting PDAC tumourigenesis. Nonetheless, in order to validate the hypothesis, *Notch*, or its downstream targets, should be knocked out in an Fbw7 deleted background.

Additionally, it is possible that other FBW7 targets are involved in PDAC tumourigenesis. It has been observed that cyclin E is overexpressed in PDAC samples and that high levels of this protein is a good indicator of poor prognosis (Skalicky et al., 2006). It has been shown that oncogenic Ras can promote cyclin E protein stability, and its consequent cellular increase, at least partially, by inhibiting FBW7-dependent cyclin E degradation (Minella et al., 2005). Furthermore, c-Myc has also been implicated in PDAC development, as its expression under the acinar-specific Elastase1 promoter, during pancreatic development, is sufficient to induce ductal adenocarcinoma (Sandgren et al., 1991). While it is necessary to address which of Fbw7's targets are deregulated in the F7KPdx1-Cre-derived PDAC, given the suggested involvement of most of the targets in human PDAC oncogenesis, it is likely there is not one unique mechanism to PDAC development in the absence of FBW7, but a complex cooperation of various pathways.

5.3 Origins of PDAC: The importance of the pancreatic cellular compartment of origin.

5.3.1 Adult ductal cells give rise to PDAC without the formation of mucinous pre-neoplastic lesions

PDAC has been proposed to originate from different types of precursor lesions such as IPMN, MCN, ITPN and PanIN1 to 3 (Distler et al., 2014, Yonezawa et al., 2008, Feldmann et al., 2007). It is hypothesized that different pre-neoplastic lesions might be determined by the cell of origin, or, alternatively, by the genetic alteration induced (von Figura et al., 2014, Bardeesy et al., 2006b, Hingorani et al., 2003, Guerra et al., 2007, Izeradjene et al., 2007).

Histological analysis of human samples has demonstrated that, while MCNs have no direct connection to the ductal network, IPMNs, ITPN and PanINs do. This observation, coupled with the ductal morphology of the pre-neoplastic lesions, led to the assumption that most of the PDAC precursors, and by association PDAC, had their origin in the ductal network. However, mouse model studies have allowed a better understanding of the pancreatic compartment of origin for PDAC.

Initial GEM studies targeted the PDAC driver mutation ($KRas^{G12D}$) to the developing pancreas, showing that $KRas^{G12D}$ initiates mPDAC development and $KRas^{G12D}$-driven mPDAC evolves from mPanIN1-2 lesions (low-grade), which progress to mPanIN3 (high-grade, *carcinoma in situ*) and PDAC (Hingorani et al., 2003). Additional work suggested that the type of pre-neoplastic lesion formed is dependent on the oncogenic hit, as the concomitant loss of Smad4 protein with the $KRas^{G12D}$ mutation, in the embryonic pancreas, led to the development of murine IPMN instead of mPanINs (Bardeesy et al., 2006b). However, later studies have also induced the loss of Smad4 with $KRas^{G12D}$ expression in pancreatic progenitor and showed that it leads to the formation of MCN instead of PanIN and IPMNs (Izeradjene et al., 2007). Interestingly, different Cre mouse lines were used to target the genetic alteration to pancreatic progenitors. While Bardeesy and co-workers used Pdx1-Cre (expressed from E8.5), Izeradjene and co-workers used Ptf1a-Cre (Expressed from E9.5). Thus, while the molecular cell signalling at these two days might differ, it also raises the possibility of different cells being targeted by the Cre mouse line.

The development of inducible mouse models, able to target the genetic alteration to specific exocrine compartments in the adult pancreas (acinar vs duct), has greatly contributed to a better assessment of the compartment of origin of PDAC (Kopp et al., 2012, von Figura et al., 2014, Guerra et al., 2007, Ray et al., 2011, Friedlander et al., 2009). Using acinar-specific inducible models (Ela-tTA/tetO-Cre, Ptf1a-CreER and CPA1-CreER) it was demonstrated that, while acinar cells of young mice can initiate mPDAC development via mPanIN1-2-3 lesion formation, adult acinar cells (8-week-old mice) are very refractory to PDAC initiation. Nevertheless, the combination of oncogenic hit ($KRas^{G12D}$) and pancreatitis (caerulein-induced, acinar cell-specific damage) enabled all grades of mPanIN formation and mPDAC onset (Kopp et al., 2012, Guerra et al., 2007, Friedlander et al., 2009).

Conversely, the assessment of the ability of the ductal network to form PDAC had only been superficially performed at the start of this project. The Sox9-CreER and the Ck19-CreER mouse models (duct-specific) were used to target the PDAC driver $KRas^{G12D}$ mutation to the ductal network. In both studies, ductal cells were shown to be refractory to tumourigenesis, as no significant transformation was observed, besides the formation of some rare low-grade mPanIN lesions (Kopp et al., 2012, Ray et al., 2011). From the results obtained with the oncogenic targeting of both exocrine compartments, before the start of my thesis, it was accepted that acinar cells were the origin of PDAC and they would evolve via PanIN lesions.

However, a few caveats with the approaches taken at the time to assess ductal cell-derived tumourigenesis were detected. Firstly, while the Sox9-CreER and the Ck19-CreER mouse models mainly induce Cre-dependent recombination in ductal cells, results from our group, and from published reports, indicate that both models also induce some acinar cell recombination (Means et al., 2008, Kopp et al., 2012). Therefore, the possibility that the mPanIN lesions observed were due to acinar cell targeting remained. Secondly, while, acinar cell injury (by caerulein treatment) had to be performed to induce adult acinar cell-derived mPDAC, ductal cell injury was not tested. Lastly, the additional deletion of tumour suppressors in acinar cells such as p16 and p19 or p53, reinforced the ability of this pancreatic compartment to induce PDAC (Guerra et al., 2011). However, before the start of my studies, this had not been done for the ductal compartment.

In this thesis, I reported that the loss of Fbw7 protein with concomitant activation of mutant KRas^{G12D} expression in the adult ductal compartment (*Fbw7$^{F/F}$; KRas$^{LSL-G12D/wt}$; Ck19-CreER* – F7KCk19-CreER mice) led to mPDAC development, which was not preceded by low-grade mPanIN lesions. Other mucinous pre-neoplastic lesions, such as IPMN or MCN were also not detected. Additionally, loss of p53 protein with simultaneous *KRas^{G12D}* expression in adult ductal cells (*p53$^{F/F}$; KRas$^{LSL-G12D/wt}$; Ck19-CreER* – p53KCk19-CreER mice) was also able to induce mPDAC with no low-grade mPanIN lesion development. This is particularly important, as it has been shown that p53 deletion with concomitant KRas^{G12D} expression leads to the formation of mPanINs in the developing pancreas (Aguirre, 2003). While results obtained in this thesis with the F7KCk19-CreER and p53KCk19-CreER mouse models need confirmation from more specific models, as discussed in Chapter 3, page 155, the data so far suggests that ductal cells can generate PDAC in the absence of previously described mucinous lesions.

To confirm that the absence of mucinous precursor lesions in the F7KCk19-CreER model was dependent on the cell of origin, I induced acinar cell-specific loss of the Fbw7 protein with concomitant KRas^{G12D} activation in adult acinar cells (*Fbw7$^{F/F}$; KRas$^{LSL-G12D/wt}$; Ela1-CreER* – F7KEla1-CreER mice) before acinar cell injury. I observed the presence of AB/PAS-positive mucinous low-grade mPanIN lesions, indicating that the loss of Fbw7 does not prevent their formation. These results suggest that the cell of origin has a great impact in determining the presence of mucinous pre-neoplastic lesion. Hence, while acinar cells formed PanINs, ductal cells did not form mucinous precursor lesions with these genetic alterations. Nevertheless, it can be argued that ducts were able to give rise to PDAC in this study while acinar cells, with the genetic alteration, were not. Thus, it is not yet clear whether in our model the Fbw7 deletion with KRas^{G12D} activation in acinar cells would lead to PDAC preceded by PanIN lesions. Longer time points after tamoxifen-induced recombination are necessary to address the issue.

In summary, contrasting with previous findings, results in this thesis demonstrate that ductal cells should also be considered cells of origin of PDAC (Figure 39).

During the course of my studies, work performed by Matthias Hebrok's research group suggested that, while ductal cells are capable of PDAC formation, ductal cell oncogenic targeting leads to PDAC preceeded by IPMN lesions (IPMN-PDAC) (von Figura et al., 2014, Roy et al., 2015). In the work published in 2014, von Figura and co-workers studied the effect of Brg1 deletion (a component of the SWI-SNF chromatin remodelling complex) in the developing pancreas with concomitant $KRas^{G12D}$ activation. They observed that loss of Brg1 protein rapidly accelerated $KRas^{G12D}$-driven murine PDAC, which was preceded by AB/PAS-positive IPMN lesions (IPMN-PDAC). All the characterization of the murine IPMN lesions was performed in the pancreatic embryonic Cre driver model - Pdx1-Cre (*$Brg1^{F/F}$; $KRas^{LSL\text{-}G12D/wt}$; Pdx1-Cre*). Nine weeks after birth, mice developed cystic lesions expressing mucin (detected by AB/PAS), which resembled human pancreatobiliary IPMNs with pronounced tree-resembling papillae. The suggestion of a ductal origin was indicated by the direct connection of these structures to the ductal network. However, acinar cells also have a direct connection to the ductal network. Since the Pdx1-Cre model induces Cre-dependent recombination in pancreatic progenitors, work performed with this model did not provide sufficient evidence to establish a ductal origin. In order to assess if ductal cells give rise to IPMN-PDAC, the authors generated *$Brg1^{F/F}$; $KRas^{LSL\text{-}G12D/wt}$; Hnf1β-CreER* mice. Hnf1β is a transcription factor and, in the pancreas, is specifically expressed in ductal cells. Therefore, in this model, upon tamoxifen treatment, *Brg1* expression is lost specifically in ductal cells, together with oncogenic *KRas* activation. Firstly, *$Brg1^{F/F}$; $KRas^{LSL\text{-}G12D/wt}$; Hnf1β-CreER* mice failed to generate mPDAC, impeding the assessment of whether ductal cell-derived PDAC progresses via IPMN. Secondly, only one out of 5 mice developed enlarged ductal structures that the authors refer to as mucinous reminiscent of the IPMN lesion (von Figura et al., 2014). Interestingly, the mucinous nature of this lesion was not assessed by any mucin or AB/PAS staining. Moreover, according to the images in the published work, these structures did not present a papillary structure, nor the extended papillae characteristic of IPMN. Images show an enlargement of the ductal cells morphologically similar to the ones obtained in early stages of my time point assessment of duct-derived PDAC. Therefore, while the proposal of Brg1 as a tumour suppressor in embryonic pancreas is

convincing, the suggestion that its deletion in a *KRas*^{G12D} background induces duct-derived IPMN-PDAC is not supported by their data.

Nevertheless, Brg1 loss of expression has been shown to be common in IPMN lesions in human samples (Dal Molin et al., 2012). Therefore, while results presented in this thesis suggest that the cell of origin is the main determinant in the presence or absence of mucinous pre-neoplastic lesions, they do not exclude the possibility that genetic alterations can have a strong effect. It would be interesting to assess whether Brg1 loss in adult ductal cells with *KRas*^{G12D} expression would, in fact, lead to PDAC, to better understand if, in the context of Brg1 loss, KRas^{G12D}-driven duct cell-PDAC occurs via IPMN.

The majority of the knowledge obtained so far on the precursor lesions of PDAC (IPMN, MCN, PanIN and ITPN) has been acquired from the study of human samples. This static analysis of fixed tissue and mutational landscapes from biopsies and tumour samples, fails to incorporate time course analysis and detailed investigation of initiating events. It is obvious from the literature that there is no consensus on the origin of these lesions. The integration of data obtained from GEM models is essential for the thorough understanding of these lesions and their roles in PDAC development. While some studies have reported that the cell of origin determines the pre-neoplastic lesion (von Figura et al., 2014, Roy et al., 2015, Kopp et al., 2012), others described the oncogenic hit as the determinant for the PDAC precursor (Izeradjene et al., 2007, Bardeesy et al., 2006b). In this study I tested the same oncogenic hit in different pancreatic compartment components (acinar versus duct cells) and observed different morphological responses, suggesting that the cell receiving the hit has a great influence in the determination of the pre-neoplastic lesion. However, it is known that, while the different precursor lesions roughly harbour mutations in the main key genes (*KRAS*, *p53*, *CDKN2A*) some mutations are more common than others in particular lesions. As an example, it has been observed that while MCNs frequently present loss of SMAD4 (Iacobuzio-Donahue et al., 2000b), IPMNs only rarely show low SMAD4 expression (Iacobuzio-Donahue et al., 2000a). Additionally, IPMNs present frequent inactivation of the Serine/threonine kinase 11 (*STK11*) gene, also known as liver kinase B1 (*LKB1*) (Sato et al., 2001); however, no alterations have been reported for MCNs, ITPNs or

PanINs. Therefore, it is possible, that additional mutations might define the route of PDAC development. Hence, it is important to test additional genetic alterations in acinar and ductal cells-derived PDAC.

Moreover, the ductal network is a heterogeneous entity. While cells in large-calibre ducts have a columnar morphology, interlobular ducts exhibit a cuboidal epithelial morphology (Reichert and Rustgi, 2011). Thus, it is possible that different calibre ducts respond differently to oncogenic hits. Hence, the influence of the type of duct, in combination with additional genetic backgrounds, on the mode of PDAC induction and progression should be assessed. This could be performed *in vivo* by carefully analysing the oncogenic effect in ducts of different calibres or *ex vivo* by the use of slice cultures combined with *in vitro* recombination of ducts of different calibres (Marciniak et al., 2013). By combining slice cultures with live imaging, the morphologic changes induced by oncogenic hits can be followed for individual ducts; thus enabling the identification of potential differences in response from ducts of different calibre.

5.3.2 Clinical relevance of acinar and duct derived PDAC

In this thesis, murine PDAC developed from either the developing pancreas or from adult duct cells were morphologically indistinguishable. However, as mentioned above, ductal targeting of oncogenic hits led to murine PDAC without the development of mucinous precursors. It is known that human PDAC derived from different pre-neoplastic lesions is associated with different prognoses (Cooper et al., 2013). Moreover, it has been hypothesized that these tumours originating from different precursors might be biologically distinct (von Figura et al., 2014). Therefore, results obtained in this thesis raise important questions: (1) Are acinar and duct derived tumours different entities with regard to aggressiveness? (2) Are they characterized by different prognoses? (3) Are they equally represented in the human disease or is one type of origin more common than the other? (4) Can acinar and duct-derived tumours be distinguished?

It has been reported that some human PDAC patients (9% of samples) do not exhibit PanINs at the time of diagnosis (Hassid et al., 2014). The absence of PanIN lesions in

these patients was associated with poor survival independent of tumour size, stage of the disease, tumour location and lymphovascular invasion (Hassid et al., 2014). The absence of PanINs could be explained by the high aggressiveness of the tumours, and thus quick progression of the pre-neoplastic lesions. Alternatively, It could be explained by the fact that some human PDAC might arise in a PanIN-independent manner. Given that the absence of PanINs was correlated to a worse prognosis independent of stage of the tumour, it is more luckily that some PDAC arise independently of these lesions.
This has great implications based on the findings reported in this thesis. If in fact ductal cell-derived PDAC does not evolve via PanINs, PDAC arising from ductal cells might be rarer than acinar-derived PDAC but they might be biologically distinct, exhibiting a more aggressive phenotype. Another important point is that, I observed that low-grade PanIN lesions can be generated as a consequence of tumour formation (bystander PanINs) and not necessarily as a precursor lesion. Thus, some duct-derived tumours might not be identified as such due to detection of bystander PanINs at the time of diagnosis.

Evidence regarding the different aggressiveness of acinar and duct-derived pancreatic tumours remains inconclusive. Fbw7 protein loss, in an oncogenic $KRas^{G12D}$ background, led to mPDAC from ductal cells, but it failed to induce tumour formation in acinar cells at comparable time points with additional injury. Moreover, p53 deletion in ductal cells led to more rapid mPDAC development, compared to the onset described in the literature for acinar cells with the same genetic alteration (Guerra et al., 2011). While the present results suggest that ductal cells exhibit a more profound transformation before observation of acinar-cell-derived PDAC, it is not clear if duct-derived tumours are more aggressive than acinar cell-derived ones. Genetic alterations in different cells might have different phenotypes, which are cell-dependent. Thus, Fbw7 deletion might have no tumourigenic effect in acinar cells, impairing the cell dependence assessment. Additionally, the onset of PDAC development reported in this thesis for ductal cells cannot be compared with published data for acinar cells, as it is known that the strain background has a significant impact on tumour onset (J Puccini, 2013, Demant, 2003). Moreover, the genetic Cre line used for acinar cell targeting in other studies relied on doxycycline rather than tamoxifen (Guerra et al., 2011); thus, the

treatments used to induce recombination are significantly different. To better assess differences in tumourigenic capacity and aggressiveness from the different pancreatic compartments, comparable genetic models should be generated, such as p53KEla1-CreER (*$p53^{F/F}$; $KRas^{LSL\text{-}G12D/WT}$; Ela1-CreER*) and p53KHnf1β-CreER (*$p53^{F/F}$; $KRas^{LSL\text{-}G12D/WT}$; Hnf1β-CreER*) mice.

5.3.2.1 Acinar and duct-derived PDAC gene signatures

The answers to the above questions will have great implications for PDAC medicine, as the full understanding of PDAC origins might allow patient stratification and development of different therapies based on the origin of the tumours (Figure 39). Therefore, a distinction between acinar and duct-derived tumours, such as gene signature, is necessary. In fact, it has been proposed that human PDAC can be molecularly sub-classified into 3 different types: classical; exocrine-like and quasi-mesenchymal (Collisson et al., 2011). While gene signature analysis on PDAC samples mostly suggests a ductal origin, this study unveiled the existence of a tumour type (exocrine-like) that might reflect an acinar cell origin due to the high content of acinar-specific digestive enzyme genes expressed. Interestingly, these PDAC subtypes showed different responses to therapy and were associated with different survival rates (Collisson et al., 2011). This study raises the idea that ductal and acinar cell-derived tumours might be identified on the basis of their molecular profile and that this could bring new critical information for the clinic. To assess the possible gene signature associated with ductal versus acinar-derived tumours, the tumours generated from adult duct- and acinar-specific PDAC mouse models (with the same genetic alterations) should be collected and compared at the gene expression level. If a differential signature is found, this should be compared with human samples.

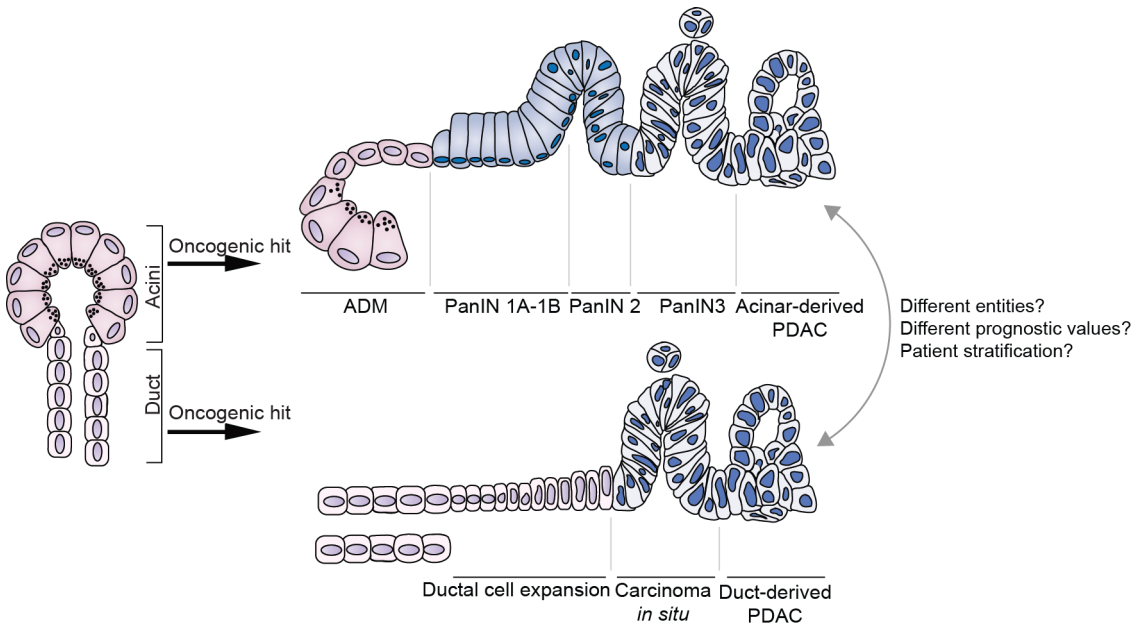

Figure 39 – Proposed model for acinar and duct-derived PDAC

Schematic representation of the proposed model for progression of PDAC tumours derived from the acinar and ductal pancreatic exocrine compartments.
Acinar cells in the presence of a PDAC-generating oncogenic hit undergo a transdifferentiation process known as acinar-to-ductal metaplasia (ADM) where cells acquire a ductal morphology. These lesions develop increasing cellular atypia and progress to pancreatic intraepithelial neoplasias (PanINs). The initial low-grade PanIN (PanIN1A-B) is characterized by expansion of the cytoplasm with supranuclear mucin production and the nuclei organize basally. In PanIN2 the structure becomes papillary with increased nuclear abnormalities. These structures lose polarity and start budding into the lumen of the lesions where they form PanIN3 (or *carcinoma in situ*). Carcinoma in situ is the first recognized tumourigenic lesion and progresses to PDAC with observed loss of the basement membrane.
When the oncogenic hit occurs in ducts, an increase in proliferation is observed, with increased cellularity of the ductal tree. Ductal cells increase in size, expanding towards the lumen of the duct. In this case, the nuclei do not organize basally, instead they increase in size with the cytoplasm. Without forming mucinous structures, the ducts become papillary, present pseudostratification, lose polarity, and shedding of cells towards the lumen is observed, resembling the *carcinoma in situ* neoplastic lesion. Loss of the basement membrane takes place and the lesions progress to PDAC.
While morphologically and architecturally indistinguishable, PDAC derived from acinar cells and ductal cells might be different entities and better understanding of their biology might allow patient stratification.

5.3.3 Low-grade PanIN lesions can be formed as a consequence of tumour formation (bystander).

In this thesis, I observed that low-grade PanIN lesions can be induced in wild type tissues in the presence of tumours. By injecting lineage-traced mPDAC tumour cells into the unlabelled pancreas of immunodeficient mice, I detected the formation of unlabelled mucinous low-grade mPanINs in close proximity to labelled mPDAC. Interestingly, while low-grade PanIN lesions, such as PanIN1, were described as pre-neoplastic lesions that evolve into PDAC, reports have indicated that they can be detected in the context of other pancreatic neoplasias such as acinar cell carcinomas, mucinous cystic neoplasms, pancreatic endocrine tumours, serous cystadenomas, solid pseudopapillary tumours and ampullary tumours (Recavarren et al., 2011, Stelow et al., 2006a). Additional evidence against the sole pre-neoplastic nature of these lesions is the fact that the majority of low-grade PanINs do not harbour mutations in the *KRAS* gene (Feldmann et al., 2007). Moreover, gene expression profiles performed in PanIN lesions of different grades have separated PanIN1 from the remaining PanINs. In that study it was suggested that PanIN1 lesions are not true pre-neoplastic lesions (Buchholz et al., 2005). While the neoplastic nature of PanIN1 lesions was not addressed in this thesis, my results reinforce the fact that the diagnostic value of PanIN1 lesions should include the appreciation that they can arise as a result of tumour formation, as a bystander, and not always as precursor lesions.

The mechanism behind this observation is still far from being understood. It is possible that the inflammatory environment signals to acinar cells, activating signalling pathways involved in ADM, such as Sox9 upregulation (shown to drive mucinous ductal structures when overexpressed in acinar cells) and cytokine-induced responses (Liou et al., 2013, Kopp et al., 2012).

The fact that the observation was obtained in immunodeficient *NuNu* mice could lead to the exclusion of an inflammatory driven mechanism. *NuNu* mice have a homozygous deletion of Forkhead box protein N1 (Foxn1) leading to the lack of Thymus and consequently, lack of immune T-cells. However, it has been shown that ADM depends on macrophage-secreted cytokines (Liou et al., 2013). Hence, the absence of T-cells would not impair macrophage-mediated phenotypes. If the inflammatory response is the

driver of bystander PanIN formation, it would be by a mechanism independent of T-cell and macrophage interaction. The role of macrophages in this bystander PanIN formation could be tested chemically by intravenous treatment with gadolinium chloride promoting transient macrophage depletion or using inducible mouse models for cell targeted depletion (Gheryani et al., 2013).

Additionally, it is possible that tumour cells directly promote the acinar to mucinous ductal metaplasia conversion by vesicle-mediated signal exchange. Cancer cells have been shown to release exosomes, small vesicles of endocytic origin. These exosome carry cargo such as protein, DNA or RNA, which, are release in the microenvironment or transferred to neighbouring cells by internalization of the vesicle (Kahlert and Kalluri, 2013, Zomer et al., 2015). Depending on their cargo, exosomes could mediate the cancer cell-dependent induction of bystander PanINs. To test the hypothesis, exosomes from murine PDAC could be isolated and injected into the pancreas of *NuNu* mice to generate bystander PanINs. Interestingly, all bystander PanINs observed during my studies were in close proximity to the tumour. This suggests that signals that induce bystander PanIN formation are mainly short-range. More in depth studies are necessary to further dissect the mechanism of PanIN bystander formation.

5.4 Origins of PDAC: CD9 as a marker for PDAC tumour-initiating cells

5.4.1 $CD9^{High}$ PDAC cells constitute a tumour-initiating population

It has become increasingly evident that tumours of most organs exhibit cellular heterogeneity regarding tumourigenic capacity, i.e., not all cells within a tumour are responsible for tumour propagation. An extensive search for and characterization of these tumour-propagating cells has been performed and it is now accepted that, a subpopulation of cells, named cancer stem cells or tumour-initiating cells (TICs), resides within certain tumours, that is able to propagate the tumour upon transplantation, to give rise to the cellular heterogeneity characteristic of the primary tumour and to recapitulate the primary tumour histology (Nguyen et al., 2012).

This definition implies that for complete therapeutic remission, this specific subpopulation of cells should be targeted and eradicated. Moreover, numerous studies have addressed the clinical relevance of TICs by demonstrating that they possess a unique ability to evade or resist drug treatments and to generate metastases (Li et al., 2007, Hirschmann-Jax et al., 2004, Zhou et al., 2001, Alvi et al., 2003). Therefore, it has been suggested that, in combination with tumour-bulk targeting strategies, more cell-specific therapeutic approaches are necessary for improvement of current survival figures (Jordan et al., 2006).

While initially described in haematopoietic malignancies, cancer stem cells/TICs have been reported in solid tumours of the brain (Singh et al., 2004), breast (Al-Hajj et al., 2003), colon (Ricci-Vitiani et al., 2006) and small intestine (Barker et al., 2008), providing important information on the tumour biology and its molecular dependencies. The importance of the identification of this tumour-initiating subpopulation has prompted the development of assays and tools that allow both their isolation and the investigation of their functional cancer stem cell-like features. Thus, efforts have been made to identify markers that might be differentially expressed in TICs versus non-TICs. Several proteins have been commonly described to be present at the surface of these tumour-initiating cells, such as CD133, CD24 and CD44, amongst others, with each type of tumour exhibiting a different marker or combination of markers. The identification of these surface proteins aided in the isolation of tumour-initiating cells

and their functional assessment versus the remaining tumour cells. As well as the identification of markers, cancer stem cell assays have been developed. Current *in vitro* investigation of tumour-initiating properties relies on the ability of cells to grow as spheres in non-adherent conditions or as organoids in soft matrices. However, as the name indicates, the gold standard in assessing tumour-initiating potential is their unique ability to initiate secondary tumours in recipient mice, when isolated from the bulk population, recapitulating the histology and cellular hierarchy of the primary source (Clarke et al., 2006).

The identification of tumour-initiating cells in human PDAC has also been reported. In 2007, two different groups approached the problem in different ways. Li and co-workers took advantage of the described CD44, CD24 and ESA (epithelial-specific antigen) surface proteins to isolate human PDAC cells that were positive for one or more of these markers and tested their ability to generate tumours following xenograft transplantation (Li et al., 2007). On the other hand, Hermann and co-workers used CD133 surface protein to isolate a putative tumour-initiating population from human PDAC samples (Hermann et al., 2007). Both studies demonstrated that, following serial dilution and transplantation into immunodeficient mice, cells which were either positive for $CD44^{+}CD24^{+}ESA^{+}$ or $CD133^{+}$ exhibited a unique capacity to generate secondary PDAC, when compared with $CD44^{-}CD24^{-}ESA^{-}$ and $CD133^{-}$ cells, respectively. However, they failed to address the origin of the population negative for the markers of choice. According to their protocol description, human primary PDAC samples were enzymatically dissociated into single cells, stained for the proteins of interest (CD44, CD24, ESA and CD133) and injected into mice at a serial dilution. No epithelial cell isolation or stromal exclusion was performed. This generates a great concern of the possibility of inclusion of stromal cells in their negative cellular fractions. It is known that PDAC exhibits a pronounced stromal expansion (desmoplasia). While the extent of expansion varies from patient to patient, it has been reported that it can account for up to 90% of the tumour volume (Xie and Xie, 2015). Knowing that stromal cells are CD133-negative, as the authors have nicely shown by immunofluorescence (Hermann et al., 2007), and that pancreatic stromal cells are also ESA-negative (Miranda-Lorenzo et al., 2014), there is a high probability that the majority of their $CD44^{-}CD24^{-}ESA^{-}$ and

$CD133^-$ cells were, in fact, stromal cells and thus it is not surprising that they are non-tumourigenic. Moreover, follow up work from the group of Christopher Heeschen has highlighted that the presence of CD133 protein can vary between samples. Thus, they focused on the autofluorescence as a marker of cells with higher tumourigenic potential (Miranda-Lorenzo et al., 2014). While their results are compelling, it is well accepted that autofluorescence is a cell property that can result from the handling of the sample. In sum, before the start of this project, there were significant gaps in knowledge regarding PDAC tumour-initiating cells.

During my studies, I used a mouse model where loss of Fbw7 protein, with concomitant $KRas^{G12D}$ expression, could be induced in adult ductal cells by tamoxifen treatment, leading to mPDAC development. To further characterize these duct-derived PDAC, I crossed in the R26-LSL-YFP tracer (F7KYCk19-CreER mice), which enabled the identification of recombined cells throughout different stages of tumour development. I observed that, soon after recombination, some lineage-traced cells exhibited morphological alteration, reminiscent of initial stages of tumour development, while others remained morphologically unaltered. This difference persisted even 4 weeks after tamoxifen treatment, excluding the possibility of asynchronous recombination at early time-points. Additional profiling for surface proteins by immunohistochemistry highlighted a correlation between CD44 and initial stages of tumour development. Furthermore, sorting of recombined cells (GFP^+) positive and negative for CD44 protein, and consequent genotyping PCR, demonstrated that the difference in the response to the tumourigenic hit was not due to incomplete recombination of any of the genetically altered alleles. Thus, I used this system to address the gene expression profile (by microarray) of cells with similar genetic backgrounds but different phenotypes (GFP^+CD44^+ [recombined and transformed] versus GFP^+CD44^- [recombined and non-transformed]) at early stages of tumour development. Analysis was performed searching for possible cell surface markers of tumour-initiating cells that would be upregulated by, at least, 1.5-fold in the GFP^+CD44^+ cellular fraction. The most promising candidate was the protein CD9.

CD9, also known as motility-related protein 1 (MRP1), is a member of the tetraspanin protein family of transmembrane proteins. It is composed of four transmembrane

domains, 2 extracellular loops and a small intracellular domain (one loop, one small N-terminus tail and one c-terminus region) and it is present at the cell membrane, in organelle membranes and in granules, such as exosomes. Little is known about tetraspanin proteins. However, evidence has been gathered demonstrating that members of this family can directly interact with intracellular and extracellular ligands, and associate laterally, forming tetraspanin-enriched microdomains (TEMs), which can modulate crucial cellular functions such as cell adhesion and migration, signalling and survival (Hemler, 2014).

CD9 has been shown to identify cells with *in vitro* and *in vivo* tumour-initiating ability in human B cell acute lymphoblastic leukemia (Nishida et al., 2009). Moreover, it was recently described as a marker for haematopoietic stem cells, allowing a pure isolation of the entire population (Karlsson et al., 2013). Its role in cancer is still under debate as it has been described to promote, or be associated with, contrasting tumour-related phenotypes. CD9 was primarily described as a tumour suppressor where its high expression correlated with better prognosis and lower lymph node status in esophageal squamous cell carcinoma and gastric cancer (S Uchida, 1999, Yoko Murayama, 2015). Moreover, CD9 re-expression in CD9-depleted small-cell lung cancer cells reduced their *in vitro* and *in vivo* motility/metastatic and proliferative potential (Zheng et al., 2005). Nevertheless, tumour-promoting features have also been associated with the CD9 protein. Overexpression was shown to increase *in vitro* cell invasion in human fibrosarcoma cells (Herr et al., 2013). Furthermore, the *in vivo* use of a CD9-blocking antibody reduced the establishment of bone metastasis following tail vein injection of highly metastatic breast cancer cells (Kishel et al., 2012). Interestingly, contradicting the abovementioned results, CD9 expression in gastric cancers has also been found to significantly correlate with lymphatic invasion, clinical stage and vessel invasion (Hori et al., 2004). It is difficult to speculate the reason for the conflicting data obtained so far. However, it is hypothesized that different functions might be due to association of CD9 with different molecular partners, which include integrins, surface receptors and other tetraspanin proteins (Hemler, 2014).

In PDAC, CD9 has not been thoroughly studied. As observed for other tumour types, data obtained by gene expression profiles and proteome arrays, comparing tumour and normal tissue, and survival analysis, has attributed conflicting roles to CD9 (Grønborg

et al., 2006, Sho et al., 1998, Gesierich, 2005). While initial studies have proposed low CD9 expression to correlate with PDAC poor prognosis (Sho et al., 1998), subsequent studies have described CD9 to be overexpressed in PDAC patient samples and pancreatic cancer cells lines compared with normal pancreatic tissue. CD9 expression was higher in high-grade PDAC and in PDAC-derived metastasis to the liver (Grønborg et al., 2006, Gesierich, 2005).

In this study, I used CD9 as a surface marker to isolate tumour cells and address its potential in identifying a tumour-initiating population within murine PDAC. In addition, since variable results have been obtained with TIC markers, I addressed the value of CD9 across different genetic backgrounds. $CD9^{High}$ primary tumour cells from F7KYCk19-CreER and p53KYPdx1-Cre-derived PDAC exhibited higher *in vitro* stem cell potential compared to $CD9^{Low}$ cells, assessed by their capacity to form organoids when plated in, previously described, organoid-forming conditions (Huch et al., 2013). Interestingly, *in vitro* expansion of dissociated murine PDAC cells did not change the outcome. Sorted $CD9^{High}$ tumour cells, which grew in matrigel for several passages, continued exhibiting higher organoid-forming capacity compared to their $CD9^{Low}$ counterparts. Lastly, $CD9^{High}$ and $CD9^{Low}$ cells were sorted from murine PDAC organoids, grown for several passages, and injected into the flanks of immunodeficient *NuNu* mice, following serial dilution. Measurements of initial nodule formation indicated that $CD9^{High}$ cells were faster in establishing nodules. Upon termination of the experiment, $CD9^{High}$-derived tumours recapitulated the cellular heterogeneity observed in the primary mPDAC, while the $CD9^{Low}$ tumour cells failed to do so. Moreover, contrasting with $CD9^{High}$-derived tumours, which exhibited over a 100-fold increase in tumour size, $CD9^{Low}$ tumour cells were not capable of tumour maintenance, as injection of 200 cells led to the regression of the nodule initially detected.

The results indicate that CD9 protein can identify a population within primary mPDAC, and cultured cells, with *in vitro* tumour-initiating properties and capable of *in vivo* tumour initiation, tumour maintenance and cellular heterogeneity (Figure 40).

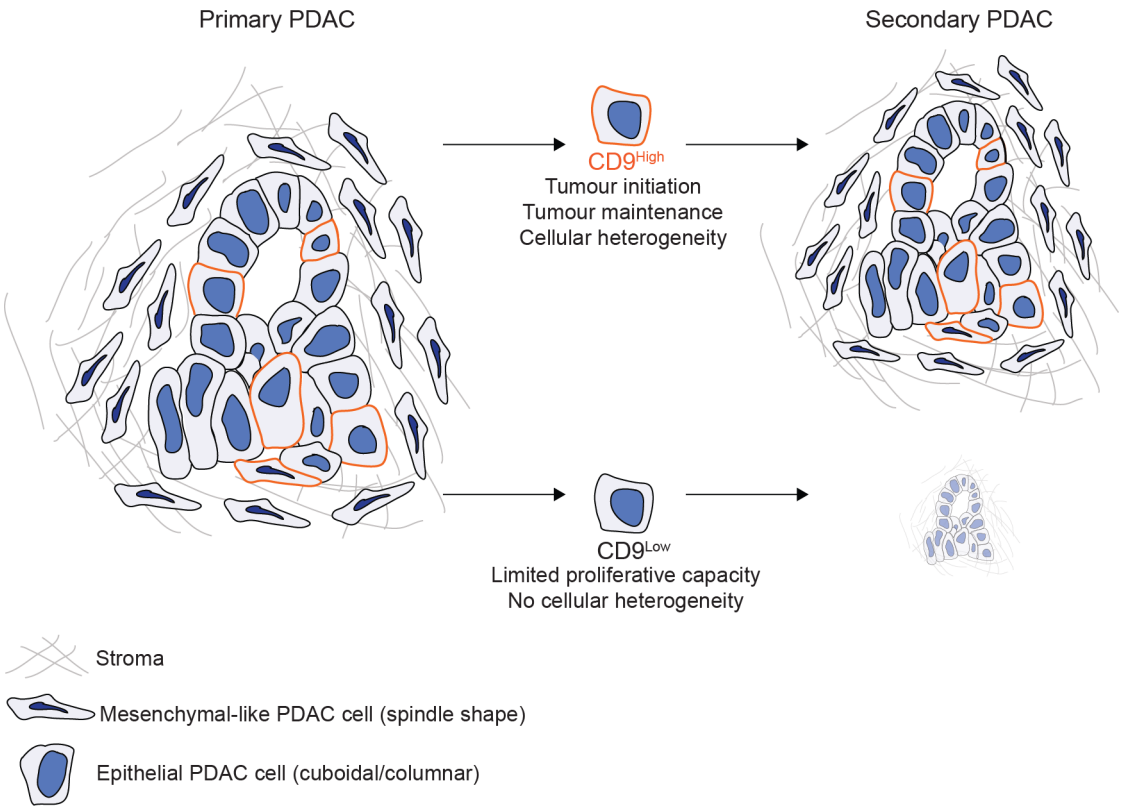

Figure 40 - CD9 marks a PDAC tumour-initiating cell population

Schematic representation of the cellular histological hierarchy in PDAC and main findings. Advanced PDAC tumours exhibit a cellular heterogeneity with presence of both epithelial (cuboidal or columnar shaped cells) and mesenchymal-like cells (spindle shaped). PDAC TICs can be identified by their levels of CD9 protein at the cell surface. $CD9^{High}$ cells are able to initiate tumour formation in recipient mice (at serial dilutions of up to 200 cells) and maintain tumour growth. $CD9^{High}$-derived tumours recapitulate the cellular heterogeneity of the primary source. The remaining population ($CD9^{Low}$) is not capable of initiating and sustaining the growth transplants when 200 cells are injected. Injecting a higher number of cells leads to small tumours, but which do not recapitulate the primary counterpart.

5.4.2 Potential therapeutic value of CD9

Contrasting with previously described PDAC TIC markers, the surface presence of CD9 was able to identify a more tumourigenic population within murine PDAC across different genotypes and isolation protocols. Given that one of the main clinical concerns in using surface markers for the identification of the TIC subpopulation is their unreliability, CD9 seems to offer a more reliable identification of mPDAC TICs for therapeutic approaches. However, it is important to bear in mind that the findings obtained for CD9 were based on mouse tissues with genetic labelling of tumour cells. Thus, it is important to address whether CD9 also identifies a more tumourigenic population within human PDAC. Since CD9 is expressed in some immune cells, this assessment might require the additional use of tumour or epithelial cell specific markers, such as EpCam, to discriminate tumour cells from remaining microenvironment components.

While I have demonstrated a higher tumourigenic capacity of $CD9^{High}$ tumour cells, in this study, I did not address whether eradication of the CD9-expressing population from an established PDAC would lead to tumour regression. Human PDAC is known for its strong drug resistance (Ryan et al., 2014) which is not only explained by the tumour molecular heterogeneity and strong desmoplasia, but also due to the presence of a drug resistant subpopulation of cells with tumour-initiating properties (Hermann et al., 2007). Therefore, the selective elimination of this population, and possible PDAC remission, could represent a promising therapeutic strategy with high probability of efficiency. In order to test the clinical value of CD9 two routes could be pursued. (1) The use of mice expressing conditional diphtheria toxin (DT) or diphtheria toxin receptor (DTR) under the control of a cell-specific promoter or knock-in in a specific locus, has allowed the selective eradication of specific cell populations (Saito et al., 2001). Mice with an inducible knock-in DTR in the CD9 locus could be crossed with the p53KYPdx1-Cre to address the effect of $CD9^{High}$ cell depletion specifically in murine PDAC at different stages of tumour development. (2) An alternative approach could be the use of cytotoxic drug-coupled antibodies (antibody-drug conjugates – ADC) against CD9. One would have to initially check whether these antibodies are internalized upon binding to CD9 at

the cell surface. If that would be the case, then the antibody would bind to CD9-expressing cells, would be internalized and selectively kill cells expressing CD9.
This particular approach might be more relevant for clinical purposes, as human cells could be used in xenograft models and then targeted using ADC. Also, the effect of whole body CD9-expressing cell ablation could be addressed. Importantly, ADCs conjugated to toxins have been used in the clinic for the treatment of acute myeloid leukaemia, Hodgkin's lymphoma and other haematopoietic malignancies (Scott et al., 2012). Therefore, the successful regression of PDAC xenografts from human patients could constitute the first step for PDAC targeted therapies.
Additionally, it would be interesting to compare the gene expression profiles of $CD9^{High}$ PDAC cells (human or murine) with $CD9^{Low}$ tumour cells in order to identify pathways that might be important for the survival and self-renewal of the $CD9^{High}$ cells, or to find druggable targets that could be explored in the clinic.

The $CD9^{High}$ mPDAC cells studied here were shown to constitute a TIC population in tumours derived from both adult ducts (F7KYCk19-CreER) and developing pancreas (p53KYPdx1-Cre). However, it would be important to address if CD9 also identifies a TIC population in adult acinar cell-derived mPDAC (p53KYEla1-CreER) and human PDAC. In the search for the PDAC compartment of origin, acinar cells were proposed as the main origin of PDAC. It was described that, in the presence of an oncogenic hit and acinar cell injury (caerulein), acinar cells undergo a metaplastic change where they transdifferentiate into ducts (ADM) (Guerra et al., 2007, Kopp et al., 2012). Besides the morphologic similarity and the mutual presence of a small number of ductal proteins (including CK19 and Hnf1β), it is not clear if ADM-derived ductal cells are the same as true pancreatic ductal cells. Supporting a possible difference is my observation that tumour progression from ducts and acinar cells seems to differ in the morphology of the initial steps. Nonetheless, it is possible that the cells driving tumourigenesis in both models are comparable. Therefore, the potential of CD9 to identify a general PDAC TIC population should also be tested on acinar-derived mPDAC in order to gain a complete understanding of the origins of the disease. As mentioned before, it should also be addressed if human PDAC samples contain a $CD9^{High}$ population and if

xenograft transplantations also demonstrate a higher tumourigenic capacity for these cells to increase relevance for the human disease.

5.4.3 Is CD9 a functional PDAC TIC marker?

Conflicting data has been published on the value and role of CD9 in various tumour models. Also, for PDAC, it is not clear from the studies conducted so far if *CD9* acts as a tumour suppressor or oncogene (Hemler, 2014). CD9 has a wide range of interacting partners, such as integrins (mainly α3β1) (Gesierich, 2005), growth factors (Shi et al., 2000), membrane proteases (Yáñez-Mó et al., 2011), and other signalling proteins (Zhang et al., 2001, Hemler, 2014). For this reason, CD9 modulation has been shown to affect migration, angiogenesis, proliferation, apoptosis and drug resistance, which could explain the discrepant results reported. In this thesis, I did not assess whether the tumour-initiating capacities detected in the $CD9^{High}$ population were due to CD9 expression itself or if CD9 surface detection was a consequence of additional molecular mechanisms. It would be interesting to either knockdown or knockout *CD9* in $CD9^{High}$ cells and assess whether they retain their tumour-initiating potential. As a different approach, $CD9^{Low}$ cells could be used for overexpression of the *CD9* gene. If CD9 has a functional role in this high-expressing population, the therapeutic value and applicability could be increased by the use of blocking antibodies. The use of monoclonal antibodies such as cetuximab (epidermal growth factor inhibitor), and trastuzumab (HER2/neu receptor inhibitor) has greatly improved clinical outcome for colorectal and breast cancer patients. By inhibiting the respective targeted receptor, the monoclonal antibodies have demonstrated to be extremely successful in abrogating tumour cell signalling, reviewed in Scott et al., 2012.

5.4.4 Do PDAC TICs originate from pancreatic adult progenitor cells?

Nowadays, the concept of tumour-initiating cells, or cancer stem cells, does not necessarily reflect a stem cell origin of the formed tumours in question. It rather implies, that some cells within the tumour possess the capacity to initiate a tumour and maintain its growth, regardless of whether this property is derived from a transformation step of differentiated or progenitor/stem cells. Nevertheless, it is known that, in some, mainly hematopoietic, malignancies, it is in fact a tissue stem cell or an immediate progenitor that, upon an oncogenic hit, undergoes transformation and initiates tumour development. The existence of progenitor cells in the pancreas is still a controversial subject. Studies investigating the ability of the pancreatic organ to regenerate have suggested that differentiated cells undergo a transdifferentiation process to convert into other cell types and then proliferate, rather than an existence of a pool of progenitor cells that continuously gives rise to more differentiated cell types (see 1.1.2, page 26). However, studies from our laboratory have implied the existence of subpopulation within the ducts that responds differentially to genetic alterations (Sancho et al., 2014).

I observed in the F7KYCk19-CreER model that, 4 weeks after tamoxifen treatment, not all recombined duct cells gave rise to tumours. Corroborating previous hypotheses, this suggests that the ductal network is a heterogeneous entity, since only a subset of cells was capable of being transformed by the genetic tools used. Given that CD9 was capable of distinguishing between TICs and non-TICs in murine PDAC, it would be interesting to assess whether the adult ductal network of wild type animals harbours a $CD9^{High}$ population and if so, whether these cells represent an adult pancreatic progenitor population more susceptible to tumour transformation. Preliminary data suggest that the ductal network does have a rare $CD9^{High}$ population. Thus, while genetic approaches could be developed to address the different tumourigenic potential of these cells, it would also be possible to sort $CD9^{High}$ and $CD9^{Low}$ cells from a $p53^{F/F}$; $KRas^{LSL\text{-}G12D/wt}$ mouse and, following *in vitro* recombination of floxed alleles, assess the ability of the two cell populations to initiate PDAC in the flanks of immunodeficient *NuNu* mice. The meaning of the existence of a $CD9^{High}$ population in adult wild-type ductal cells is not yet clear. Nonetheless, it would be interesting to study a possible

progenitor nature of this population in the adult organ in more detail. Preliminary data could be gathered by genetically tracing CD9-expressing cells in the wild type pancreas and follow the fate of the labelled cells over time in both normal conditions and after various injuries to specific pancreatic compartments.

5.5 Concluding remarks

This thesis addresses the origins of pancreatic ductal adenocarcinoma by: (1) evaluating how the different components of the pancreatic exocrine compartment (acinar and duct cells) contribute to PDAC development, and (2) by identifying the cell population responsible for initiation and maintenance of PDAC.

I was able to confirm that murine adult ductal cells can originate mPDAC when potent tumour suppressors (*Fbw7* and *p53*) are deleted with concomitant induction of the PDAC driver mutation ($KRas^{G12D}$). Adding to this observation, I described a different progression model for mPDAC development from that described for acinar cell-derived mPDAC (Figure 39), which could provide useful information for patient stratification in clinical strategies.

Furthermore, the investigation of mPDAC TICs led me to the identification of CD9 as a surface marker for pancreatic tumour cells with the capacity to initiate secondary mPDAC upon transplantation and to recapitulate the cellular heterogeneity observed in primary mPDAC tumours (Figure 40). These findings offer valuable information on PDAC biology and might aid in the development of PDAC targeted therapies.

Chapter 6. Appendix

- Figure 1 was adapted from Shih et al., 2013. No permission was required from the publisher Annuals Reviews for the purposes of thesis and dissertations (RightsLink).

- Figure 11 was adapted from Tanaka et al., 2012. Reprinted from Pancreatology, Vol 12/3, Masao Tanaka, Carlos Fernández-del Castillo, Volkan Adsay, Suresh Chari, Massimo Falconi, Jin-Young Jang, Wataru Kimura, Philippe Levy, Martha Bishop Pitman, C. Max Schmidt, Michio Shimizu, Christopher L. Wolfgang, Koji Yamaguchi, Kenji Yamao, "International consensus guidelines 2012 for the management of IPMN and MCN of the pancreas", page 191, with permission from Elsevier. License number 3702040187175. 04 September 2015

- Figure 12 was adapted from Distler et al., 2014. No permission was required from BioMed Research International. Copyright © 2014 M. Distler et al. This is an open access article distributed under the Creative Commons Attribution License, which permits unrestricted use, distribution, and reproduction in any medium, provided the original work is properly cited.

- Figure 13 was adapted from Distler et al., 2014. No permission was required from BioMed Research International. Copyright © 2014 M. Distler et al. This is an open access article distributed under the Creative Commons Attribution License, which permits unrestricted use, distribution, and reproduction in any medium, provided the original work is properly cited.

Reference List

AGUIRRE, A. J. 2003. Activated Kras and Ink4a/Arf deficiency cooperate to produce metastatic pancreatic ductal adenocarcinoma. *Genes & Development,* 17**,** 3112-3126.

AL-HAJJ, M., WICHA, M. S., BENITO-HERNANDEZ, A., MORRISON, S. J. & CLARKE, M. F. 2003. Prospective identification of tumorigenic breast cancer cells. *Proceedings of the National Academy of Sciences of the United States of America,* 100**,** 3983-3988.

ALEXANDROV, L. B., NIK-ZAINAL, S., WEDGE, D. C., APARICIO, S. A. J. R., BEHJATI, S., BIANKIN, A. V., BIGNELL, G. R., BOLLI, N., BORG, A., BØRRESEN-DALE, A.-L., BOYAULT, S., BURKHARDT, B., BUTLER, A. P., CALDAS, C., DAVIES, H. R., DESMEDT, C., EILS, R., EYFJÖRD, J. E., FOEKENS, J. A., GREAVES, M., HOSODA, F., HUTTER, B., ILICIC, T., IMBEAUD, S., IMIELINSK, M., JÄGER, N., JONES, D. T. W., JONES, D., KNAPPSKOG, S., KOOL, M., LAKHANI, S. R., LÓPEZ-OTÍN, C., MARTIN, S., MUNSHI, N. C., NAKAMURA, H., NORTHCOTT, P. A., PAJIC, M., PAPAEMMANUIL, E., PARADISO, A., PEARSON, J. V., PUENTE, X. S., RAINE, K., RAMAKRISHNA, M., RICHARDSON, A. L., RICHTER, J., ROSENSTIEL, P., SCHLESNER, M., SCHUMACHER, T. N., SPAN, P. N., TEAGUE, J. W., TOTOKI, Y., TUTT, A. N. J., VALDÉS-MAS, R., VAN BUUREN, M. M., VAN T VEER, L., VINCENT-SALOMON, A., WADDELL, N., YATES, L. R., ZUCMAN-ROSSI, J., ANDREW FUTREAL, P., MCDERMOTT, U., LICHTER, P., MEYERSON, M., GRIMMOND, S. M., SIEBERT, R., CAMPO, E., SHIBATA, T., PFISTER, S. M., CAMPBELL, P. J. & STRATTON, M. R. 2013. Signatures of mutational processes in human cancer. *Nature,* 500**,** 415-421.

ALVI, A. J., CLAYTON, H., JOSHI, C., ENVER, T., ASHWORTH, A., VIVANCO, M. D. M., DALE, T. C. & SMALLEY, M. J. 2003. Functional and molecular characterisation of mammary side population cells. *Breast cancer research : BCR,* 5**,** R1-8.

ANDERSSON, E. R., SANDBERG, R. & LENDAHL, U. 2011. Notch signaling: simplicity in design, versatility in function. *Development,* 138**,** 3593-3612.

ASANO, T., YAO, Y., ZHU, J., LI, D., ABBRUZZESE, J. L. & REDDY, S. A. G. 2004. The PI 3-kinase/Akt signaling pathway is activated due to aberrant Pten expression and targets transcription factors NF-κB and c-Myc in pancreatic cancer cells. *Oncogene,* 23**,** 8571-8580.

BAEYENS, L., LEMPER, M., LEUCKX, G., DE GROEF, S., BONFANTI, P., STANGÉ, G., SHEMER, R., NORD, C., SCHEEL, D. W., PAN, F. C., AHLGREN, U., GU, G., STOFFERS, D. A., DOR, Y., FERRER, J., GRADWOHL, G., WRIGHT, C. V. E., VAN DE CASTEELE, M., GERMAN, M. S., BOUWENS, L. & HEIMBERG, H. 2013. Transient cytokine treatment induces acinar cell reprogramming and regenerates functional beta cell mass in diabetic mice. *Nature Biotechnology,* 32**,** 76-83.

BARDEESY, N., AGUIRRE, A. J., CHU, G. C., CHENG, K.-H., LOPEZ, L. V., HEZEL, A. F., FENG, B., BRENNAN, C., WEISSLEDER, R., MAHMOOD, U., HANAHAN, D., REDSTON, M. S., CHIN, L. & DEPINHO, R. A. 2006a.

Both p16(Ink4a) and the p19(Arf)-p53 pathway constrain progression of pancreatic adenocarcinoma in the mouse. *Proceedings of the National Academy of Sciences of the United States of America,* 103**,** 5947-5952.

BARDEESY, N., CHENG, K.-H., BERGER, J. H., CHU, G. C., PAHLER, J., OLSON, P., HEZEL, A. F., HORNER, J., LAUWERS, G. Y., HANAHAN, D. & DEPINHO, R. A. 2006b. Smad4 is dispensable for normal pancreas development yet critical in progression and tumor biology of pancreas cancer. *Genes & Development,* 20**,** 3130-3146.

BARDEESY, N., SHARPLESS, N. E., DEPINHO, R. A. & MERLINO, G. 2001. The genetics of pancreatic adenocarcinoma: a roadmap for a mouse model. *Seminars in Cancer Biology,* 11**,** 201-218.

BARKER, N. 2014. Adult intestinal stem cells: critical drivers of epithelial homeostasis and regeneration. *Nature reviews. Molecular cell biology,* 15**,** 19-33.

BARKER, N., RIDGWAY, R. A., VAN ES, J. H., VAN DE WETERING, M., BEGTHEL, H., VAN DEN BORN, M., DANENBERG, E., CLARKE, A. R., SANSOM, O. J. & CLEVERS, H. 2008. Crypt stem cells as the cells-of-origin of intestinal cancer. *Nature,* 457**,** 608-611.

BENITEZ, C. M., GOODYER, W. R. & KIM, S. K. 2012. Deconstructing pancreas developmental biology. *Cold Spring Harbor perspectives in biology,* 4.

BITTONI, A., SANTONI, M., LANESE, A., PELLEI, C., ANDRIKOU, K. & STEFANO, C. 2014. Neoadjuvant Therapy in Pancreatic Cancer: An Emerging Strategy. *Gastroenterology Research and Practice,* 2014**,** 1-9.

BOJ, S. F., HWANG, C.-I., BAKER, L. A., CHIO, I. I. C., ENGLE, D. D., CORBO, V., JAGER, M., PONZ-SARVISE, M., TIRIAC, H., SPECTOR, M. S., GRACANIN, A., ONI, T., YU, K. H., VAN BOXTEL, R., HUCH, M., RIVERA, K. D., WILSON, J. P., FEIGIN, M. E., ÖHLUND, D., HANDLY-SANTANA, A., ARDITO-ABRAHAM, C. M., LUDWIG, M., ELYADA, E., ALAGESAN, B., BIFFI, G., YORDANOV, G. N., DELCUZE, B., CREIGHTON, B., WRIGHT, K., PARK, Y., MORSINK, F. H. M., MOLENAAR, I. Q., BOREL RINKES, I. H., CUPPEN, E., HAO, Y., JIN, Y., NIJMAN, I. J., IACOBUZIO-DONAHUE, C., LEACH, S. D., PAPPIN, D. J., HAMMELL, M., KLIMSTRA, D. S., BASTURK, O., HRUBAN, R. H., OFFERHAUS, G. J., VRIES, R. G. J., CLEVERS, H. & TUVESON, D. A. 2014. Organoid Models of Human and Mouse Ductal Pancreatic Cancer. *Cell*.

BONNER-WEIR, S., BAXTER, L. A., SCHUPPIN, G. T. & SMITH, F. E. 1993. A second pathway for regeneration of adult exocrine and endocrine pancreas. A possible recapitulation of embryonic development. *Diabetes,* 42**,** 1715-1720.

BONNER-WEIR, S., TANEJA, M., WEIR, G. C., TATARKIEWICZ, K., SONG, K. H., SHARMA, A. & O&APOS;NEIL, J. J. 2000. In vitro cultivation of human islets from expanded ductal tissue. *Proceedings of the National Academy of Sciences of the United States of America,* 97**,** 7999-8004.

BONNER-WEIR, S., TOSCHI, E., INADA, A., REITZ, P., FONSECA, S. Y., AYE, T. & SHARMA, A. 2004. The pancreatic ductal epithelium serves as a potential pool of progenitor cells. *Pediatric diabetes,* 5 Suppl 2**,** 16-22.

BORGGREFE, T. & OSWALD, F. 2009. The Notch signaling pathway: transcriptional regulation at Notch target genes. *Cellular and molecular life sciences : CMLS,* 66**,** 1631-1646.

BREMBECK, F. H., SCHREIBER, F. S., DERAMAUDT, T. B., CRAIG, L., RHOADES, B., SWAIN, G., GRIPPO, P., STOFFERS, D. A., SILBERG, D. G. & RUSTGI, A. K. 2003. The Mutant K-ras Oncogene Causes Pancreatic Periductal Lymphocytic Infiltration and Gastric Mucous Neck Cell Hyperplasia in Transgenic Mice. *Cancer Research,* 63**,** 2005-2009.

BUCHHOLZ, M., BRAUN, M., HEIDENBLUT, A., KESTLER, H. A., KLÖPPEL, G., SCHMIEGEL, W., HAHN, S. A., LÜTTGES, J. & GRESS, T. M. 2005. Transcriptome analysis of microdissected pancreatic intraepithelial neoplastic lesions. *Oncogene,* 24**,** 6626-6636.

BURRIS, H. A., MOORE, M. J., ANDERSEN, J., GREEN, M. R., ROTHENBERG, M. L., MODIANO, M. R., CRIPPS, M. C., PORTENOY, R. K., STORNIOLO, A. M., TARASSOFF, P., NELSON, R., DORR, F. A., STEPHENS, C. D. & VON HOFF, D. D. 1997. Improvements in survival and clinical benefit with gemcitabine as first-line therapy for patients with advanced pancreas cancer: a randomized trial. *Journal of Clinical Oncology,* 15**,** 2403-2413.

CALDAS, C., HAHN, S. A., HRUBAN, R. H., REDSTON, M. S., YEO, C. J. & KERN, S. E. 1994. Detection of K-ras mutations in the stool of patients with pancreatic adenocarcinoma and pancreatic ductal hyperplasia. *Cancer Research,* 54**,** 3568-3573.

CALHOUN, E. S., JONES, J. B., ASHFAQ, R., ADSAY, V., BAKER, S. J., VALENTINE, V., HEMPEN, P. M., HILGERS, W., YEO, C. J., HRUBAN, R. H. & KERN, S. E. 2003. BRAF and FBXW7 (CDC4, FBW7, AGO, SEL10) mutations in distinct subsets of pancreatic cancer: potential therapeutic targets. *The American journal of pathology,* 163**,** 1255-1260.

CARDOZO, T. & PAGANO, M. 2004. The SCF ubiquitin ligase: insights into a molecular machine. *Nature reviews. Molecular cell biology,* 5**,** 739-751.

CARPENTIER, R., SUÑER, R. E., VAN HUL, N., KOPP, J. L., BEAUDRY, J.-B., CORDI, S., ANTONIOU, A., RAYNAUD, P., LEPREUX, S., JACQUEMIN, P., LECLERCQ, I. A., SANDER, M. & LEMAIGRE, F. P. 2011. Embryonic ductal plate cells give rise to cholangiocytes, periportal hepatocytes, and adult liver progenitor cells. *Gastroenterology,* 141**,** 1432-8- 1438.e1-4.

CARRIÈRE, C., YOUNG, A. L., GUNN, J. R., LONGNECKER, D. S. & KORC, M. 2009. Acute pancreatitis markedly accelerates pancreatic cancer progression in mice expressing oncogenic Kras. *Biochemical and Biophysical Research Communications,* 382**,** 561-565.

CARRIÈRE, C., YOUNG, A. L., GUNN, J. R., LONGNECKER, D. S. & KORC, M. 2011. Acute Pancreatitis Accelerates Initiation and Progression to Pancreatic Cancer in Mice Expressing Oncogenic Kras in the Nestin Cell Lineage. *PLoS ONE,* 6**,** e27725.

CASTELLANO, E. & DOWNWARD, J. 2011. RAS Interaction with PI3K: More Than Just Another Effector Pathway. *Genes & Cancer,* 2**,** 261-274.

CHAN, A., PRASSAS, I., DIMITROMANOLAKIS, A., BRAND, R. E., SERRA, S., DIAMANDIS, E. P. & BLASUTIG, I. M. 2014. Validation of Biomarkers That Complement CA19.9 in Detecting Early Pancreatic Cancer. *Clinical Cancer Research,* 20**,** 5787-5795.

CHENG, Y. & LI, G. 2011. Role of the ubiquitin ligase Fbw7 in cancer progression. *Cancer and Metastasis Reviews,* 31**,** 75-87.

CHERA, S., BARONNIER, D., GHILA, L., CIGLIOLA, V., JENSEN, J. N., GU, G., FURUYAMA, K., THOREL, F., GRIBBLE, F. M., REIMANN, F. & HERRERA, P. L. 2014. Diabetes recovery by age-dependent conversion of pancreatic δ-cells into insulin producers. *Nature,* 514**,** 503-507.

CHRISTOPHE, J. 1994. Pancreatic tumoral cell line AR42J: an amphicrine model. *The American journal of physiology,* 266**,** G963-71.

CHUNG, C.-H., HAO, E., PIRAN, R., KEINAN, E. & LEVINE, F. 2010. Pancreatic β-Cell Neogenesis by Direct Conversion from Mature α-Cells. *STEM CELLS,* 28**,** 1630-1638.

CLARKE, M. F., DICK, J. E., DIRKS, P. B., EAVES, C. J., JAMIESON, C. H. M., JONES, D. L., VISVADER, J., WEISSMAN, I. L. & WAHL, G. M. 2006. Cancer stem cells--perspectives on current status and future directions: AACR Workshop on cancer stem cells. *Cancer research.*

COFFINIER, C., GRESH, L., FIETTE, L., TRONCHE, F., SCHÜTZ, G., BABINET, C., PONTOGLIO, M., YANIV, M. & BARRA, J. 2002. Bile system morphogenesis defects and liver dysfunction upon targeted deletion of HNF1beta. *Development,* 129**,** 1829-1838.

COLLINS, M. A., BEDNAR, F., ZHANG, Y., BRISSET, J.-C., GALBÁN, S., GALBÁN, C. J., RAKSHIT, S., FLANNAGAN, K. S., ADSAY, N. V. & PASCA DI MAGLIANO, M. 2012a. Oncogenic Kras is required for both the initiation and maintenance of pancreatic cancer in mice. *Journal of Clinical Investigation,* 122**,** 639-653.

COLLINS, M. A., BEDNAR, F., ZHANG, Y., BRISSET, J.-C., GALBÁN, S., GALBÁN, C. J., RAKSHIT, S., FLANNAGAN, K. S., ADSAY, N. V. & PASCA DI MAGLIANO, M. 2012b. Oncogenic Kras is required for both the initiation and maintenance of pancreatic cancer in mice. *Journal of Clinical Investigation,* 122**,** 639-653.

COLLISSON, E. A., SADANANDAM, A., OLSON, P., GIBB, W. J., TRUITT, M., GU, S., COOC, J., WEINKLE, J., KIM, G. E., JAKKULA, L., FEILER, H. S., KO, A. H., OLSHEN, A. B., DANENBERG, K. L., TEMPERO, M. A., SPELLMAN, P. T., HANAHAN, D. & GRAY, J. W. 2011. Subtypes of pancreatic ductal adenocarcinoma and their differing responses to therapy. *Nature Medicine***,** 1-5.

COLLISSON, E. A., TREJO, C. L., SILVA, J. M., GU, S., KORKOLA, J. E., HEISER, L. M., CHARLES, R.-P., RABINOVICH, B. A., HANN, B., DANKORT, D., SPELLMAN, P. T., PHILLIPS, W. A., GRAY, J. W. & MCMAHON, M. 2012. RAF/MEK Dependence of KRAS-Mutant Pancreatic Ductal Adenocarcinomas. *Cancer discovery,* 2**,** 666-669.

COOPER, C. L., O&APOS;TOOLE, S. A. & KENCH, J. G. 2013. Classification, morphology and molecular pathology of premalignant lesions of the pancreas. *Pathology,* 45**,** 286-304.

CRUSIO, K. M., KING, B., REAVIE, L. B. & AIFANTIS, I. 2010. The ubiquitous nature of cancer: the role of the SCFFbw7 complex in development and transformation. *Oncogene,* 29**,** 4865-4873.

CRUZ-MONSERRATE, Z., ABD-ELGALIEL, W. R., GROTE, T., DENG, D., JI, B., ARUMUGAM, T., WANG, H., TUNG, C. H. & LOGSDON, C. D. 2012.

Detection of pancreatic cancer tumours and precursor lesions by cathepsin E activity in mouse models. *Gut,* 61**,** 1315-1322.

CUBILLA, A. L. & FITZGERALD, P. J. 1976. Morphological lesions associated with human primary invasive nonendocrine pancreas cancer. *Cancer Research,* 36**,** 2690-2698.

CUI, M., AUGERT, A., RONGIONE, M., CONKRITE, K., PARAZZOLI, S., NIKITIN, A. Y., INGOLIA, N. & MACPHERSON, D. 2014. PTEN Is a Potent Suppressor of Small Cell Lung Cancer. *Molecular Cancer Research,* 12**,** 654-659.

DAL MOLIN, M., HONG, S.-M., HEBBAR, S., SHARMA, R., SCRIMIERI, F., DE WILDE, R. F., MAYO, S. C., GOGGINS, M., WOLFGANG, C. L., SCHULICK, R. D., LIN, M.-T., ESHLEMAN, J. R., HRUBAN, R. H., MAITRA, A. & MATTHAEI, H. 2012. Loss of expression of the SWI/SNF chromatin remodeling subunit BRG1/SMARCA4 is frequently observed in intraductal papillary mucinous neoplasms of the pancreas. 43**,** 585-591.

DAY, J. D., DIGIUSEPPE, J. A., YEO, C., LAI-GOLDMAN, M., ANDERSON, S. M., GOODMAN, S. N., KERN, S. E. & HRUBAN, R. H. 1996. Immunohistochemical evaluation of HER-2/neu expression in pancreatic adenocarcinoma and pancreatic intraepithelial neoplasms. 27**,** 119-124.

DE GONZALEZ, A. B., SWEETLAND, S. & SPENCER, E. 2003. A meta-analysis of obesity and the risk of pancreatic cancer. *British Journal of Cancer,* 89**,** 519-523.

DE LA O, J. P., EMERSON, L. L., GOODMAN, J. L., FROEBE, S. C., ILLUM, B. E., CURTIS, A. B. & MURTAUGH, L. C. 2008. Notch and Kras reprogram pancreatic acinar cells to ductal intraepithelial neoplasia. *Proceedings of the National Academy of Sciences,* 105**,** 18907-18912.

DELPU, Y., HANOUN, N., LULKA, H., SICARD, F., SELVES, J., BUSCAIL, L., TORRISANI, J. & CORDELIER, P. 2011. Genetic and epigenetic alterations in pancreatic carcinogenesis. *Current genomics,* 12**,** 15-24.

DEMANT, P. 2003. Cancer susceptibility in the mouse: genetics, biology and implications for human cancer. *Nature reviews. Genetics,* 4**,** 721-734.

DESAI, B. M., OLIVER-KRASINSKI, J., DE LEON, D. D., FARZAD, C., HONG, N., LEACH, S. D. & STOFFERS, D. A. 2007. Preexisting pancreatic acinar cells contribute to acinar cell, but not islet β cell, regeneration. *Journal of Clinical Investigation,* 117**,** 971-977.

DESGRAZ, R. & HERRERA, P. L. 2009. Pancreatic neurogenin 3-expressing cells are unipotent islet precursors. *Development,* 136**,** 3567-3574.

DEXTER, D. L. & LEITH, J. T. 1986. Tumor heterogeneity and drug resistance. *Journal of clinical oncology : official journal of the American Society of Clinical Oncology,* 4**,** 244-257.

DISTLER, M., AUST, D., WEITZ, J., PILARSKY, C. & GRÜTZMANN, R. 2014. Precursor Lesions for Sporadic Pancreatic Cancer: PanIN, IPMN, and MCN. *BioMed Research International,* 2014**,** 1-11.

DONEHOWER, L. A., HARVEY, M., SLAGLE, B. L., MCARTHUR, M. J., MONTGOMERY, C. A., BUTEL, J. S. & BRADLEY, A. 1992. Mice deficient for p53 are developmentally normal but susceptible to spontaneous tumours. *Nature,* 356**,** 215-221.

E H CHANG, M. A. G. R. W. E. E. M. S. D. R. L. 1982. Human genome contains four genes homologous to transforming genes of Harvey and Kirsten murine sarcoma viruses. *Proceedings of the National Academy of Sciences of the United States of America,* 79**,** 4848.

EDLUND, H., APELQVIST, Å., LI, H., SOMMER, L., BEATUS, P., ANDERSON, D. J., HONJO, T., DE ANGELIS, M. H. & LENDAHL, U. 1999. Notch signalling controls pancreatic cell differentiation. *Nature,* 400**,** 877-881.

ERKAN, M., HAUSMANN, S., MICHALSKI, C. W., FINGERLE, A. A., DOBRITZ, M., KLEEFF, J. & FRIESS, H. 2012. *The role of stroma in pancreatic cancer: diagnostic and therapeutic implications : Article : Nature Reviews Gastroenterology and Hepatology* [Online]. 9].

ESER, S., REIFF, N., MESSER, M., SEIDLER, B., GOTTSCHALK, K., DOBLER, M., HIEBER, M., ARBEITER, A., KLEIN, S., KONG, B., MICHALSKI, C. W., SCHLITTER, A. M., ESPOSITO, I., KIND, A. J., RAD, L., SCHNIEKE, A. E., BACCARINI, M., ALESSI, D. R., RAD, R., SCHMID, R. M., SCHNEIDER, G. & SAUR, D. 2013. Selective requirement of PI3K/PDK1 signaling for Kras oncogene-driven pancreatic cell plasticity and cancer. *Cancer Cell,* 23**,** 406-420.

ESER, S., SCHNIEKE, A., SCHNEIDER, G. & SAUR, D. 2014. Oncogenic KRAS signalling in pancreatic cancer. *British Journal of Cancer,* 111**,** 817-822.

EVERHART, J. 1995. Diabetes Mellitus as a Risk Factor for Pancreatic Cancer. *JAMA,* 273**,** 1605-1609.

FEIL, R., BROCARD, J., MASCREZ, B., LEMEUR, M., METZGER, D. & CHAMBON, P. 1996. Ligand-activated site-specific recombination in mice. *Proceedings of the National Academy of Sciences of the United States of America,* 93**,** 10887-10890.

FELDMANN, G., BEATY, R., HRUBAN, R. H. & MAITRA, A. 2007. Molecular genetics of pancreatic intraepithelial neoplasia. *Journal of hepato-biliary-pancreatic surgery,* 14**,** 224-232.

FERRER, J., MARTÍN, M. & SERVITJA, J. M. 2007. Putting pancreatic cell plasticity to the test. *Journal of Clinical Investigation,* 117**,** 859-862.

FERRONE, C. R., MARCHEGIANI, G., HONG, T. S., RYAN, D. P., DESHPANDE, V., MCDONNELL, E. I., SABBATINO, F., SANTOS, D. D., ALLEN, J. N., BLASZKOWSKY, L. S., CLARK, J. W., FARIS, J. E., GOYAL, L., KWAK, E. L., MURPHY, J. E., TING, D. T., WO, J. Y., ZHU, A. X., WARSHAW, A. L., LILLEMOE, K. D. & FERNÁNDEZ-DEL CASTILLO, C. 2015. Radiological and surgical implications of neoadjuvant treatment with FOLFIRINOX for locally advanced and borderline resectable pancreatic cancer. *Annals of surgery,* 261**,** 12-17.

FIÚZA, U.-M. & ARIAS, A. M. 2007. Cell and molecular biology of Notch. *The Journal of endocrinology,* 194**,** 459-474.

FLANAGAN, S. P. 1966. 'Nude', a new hairless gene with pleiotropic effects in the mouse. *Genetical research,* 8**,** 295-309.

FORSMARK, C. E., LAMBIASE, L. & VOGEL, S. B. 1994. Diagnosis of pancreatic cancer and prediction of unresectability using the tumor-associated antigen CA19-9. *Pancreas,* 9**,** 731-734.

FREED-PASTOR, W. A. & PRIVES, C. 2012. Mutant p53: one name, many proteins. *Genes & Development,* 26**,** 1268-1286.

FRIEDLANDER, S. Y. G., CHU, G. C., SNYDER, E. L., GIRNIUS, N., DIBELIUS, G., CROWLEY, D., VASILE, E., DEPINHO, R. A. & JACKS, T. 2009. Context-Dependent Transformation of Adult Pancreatic Cells by Oncogenic K-Ras. *Cancer Cell,* 16**,** 379-389.

FUCHS, C. S. 1996. A Prospective Study of Cigarette Smoking and the Risk of Pancreatic Cancer. *Archives of Internal Medicine,* 156**,** 2255.

FURUKAWA, T., CHIBA, R., KOBARI, M., MATSUNO, S., NAGURA, H. & TAKAHASHI, T. 1994. Varying grades of epithelial atypia in the pancreatic ducts of humans. Classification based on morphometry and multivariate analysis and correlated with positive reactions of carcinoembryonic antigen. *Archives of pathology & laboratory medicine,* 118**,** 227-234.

FURUYAMA, K., KAWAGUCHI, Y., AKIYAMA, H., HORIGUCHI, M., KODAMA, S., KUHARA, T., HOSOKAWA, S., ELBAHRAWY, A., SOEDA, T., KOIZUMI, M., MASUI, T., KAWAGUCHI, M., TAKAORI, K., DOI, R., NISHI, E., KAKINOKI, R., DENG, J. M., BEHRINGER, R. R., NAKAMURA, T. & UEMOTO, S. 2011. Continuous cell supply from a Sox9-expressing progenitor zone in adult liver, exocrine pancreas and intestine. *Nature Genetics,* 43**,** 34-41.

GANGOPADHYAY, S., NANDY, A., HOR, P. & MUKHOPADHYAY, A. 2013. Breast cancer stem cells: a novel therapeutic target. *Clinical breast cancer,* 13**,** 7-15.

GAVIRAGHI, M., TUNICI, P., VALENSIN, S., ROSSI, M., GIORDANO, C., MAGNONI, L., DANDREA, M., MONTAGNA, L., RITELLI, R., SCARPA, A. & BAKKER, A. 2010. Pancreatic cancer spheres are more than just aggregates of stem marker-positive cells. *Bioscience Reports,* 31**,** 45-55.

GESIERICH, S. 2005. Colocalization of the Tetraspanins, CO-029 and CD151, with Integrins in Human Pancreatic Adenocarcinoma: Impact on Cell Motility. *Clinical Cancer Research,* 11**,** 2840-2852.

GHERYANI, N., COFFELT, S. B., GARTLAND, A., RUMNEY, R. M. H., KISS-TOTH, E., LEWIS, C. E., TOZER, G. M., GREAVES, D. R., DEAR, T. N. & MILLER, G. 2013. Generation of a novel mouse model for the inducible depletion of macrophages in vivo. *Genesis (New York, N.Y. : 2000),* 51**,** 41-49.

GITHENS, S. 1988. The pancreatic duct cell: proliferative capabilities, specific characteristics, metaplasia, isolation, and culture. *Journal of pediatric gastroenterology and nutrition,* 7**,** 486-506.

GITHENS, S., SCHEXNAYDER, J. A., MOSES, R. L., DENNING, G. M., SMITH, J. J. & FRAZIER, M. L. 1994. Mouse pancreatic acinar/ductular tissue gives rise to epithelial cultures that are morphologically, biochemically, and functionally indistinguishable from interlobular duct cell cultures. *In vitro cellular & developmental biology. Animal,* 30A**,** 622-635.

GOLOSOW, N. & GROBSTEIN, C. 1962. Epitheliomesenchymal interaction in pancreatic morphogenesis. *Developmental biology,* 4**,** 242-255.

GRAF, T. 2011. Historical origins of transdifferentiation and reprogramming. *Cell Stem Cell,* 9**,** 504-516.

GRIPPO, P. J., NOWLIN, P. S., DEMEURE, M. J., LONGNECKER, D. S. & SANDGREN, E. P. 2003. Preinvasive pancreatic neoplasia of ductal phenotype

induced by acinar cell targeting of mutant Kras in transgenic mice. *Cancer Research,* 63**,** 2016-2019.

GRIPPO, P. J. & SANDGREN, E. P. 2012. Acinar-to-ductal metaplasia accompanies c-myc-induced exocrine pancreatic cancer progression in transgenic rodents. *International journal of cancer. Journal international du cancer,* 131**,** 1243-1248.

GRØNBORG, M., KRISTIANSEN, T. Z., IWAHORI, A., CHANG, R., REDDY, R., SATO, N., MOLINA, H., JENSEN, O. N., HRUBAN, R. H., GOGGINS, M. G., MAITRA, A. & PANDEY, A. 2006. Biomarker Discovery from Pancreatic Cancer Secretome Using a Differential Proteomic Approach. *Molecular & Cellular Proteomics,* 5**,** 157-171.

GUERRA, C., COLLADO, M., NAVAS, C., SCHUHMACHER, A. J., HERNÁNDEZ-PORRAS, I., CAÑAMERO, M., RODRIGUEZ-JUSTO, M., SERRANO, M. & BARBACID, M. 2011. Pancreatitis-induced inflammation contributes to pancreatic cancer by inhibiting oncogene-induced senescence. *Cancer Cell,* 19**,** 728-739.

GUERRA, C., SCHUHMACHER, A. J., CAÑAMERO, M., GRIPPO, P. J., VERDAGUER, L., PÉREZ-GALLEGO, L., DUBUS, P., SANDGREN, E. P. & BARBACID, M. 2007. Chronic Pancreatitis Is Essential for Induction of Pancreatic Ductal Adenocarcinoma by K-Ras Oncogenes in Adult Mice. *Cancer Cell,* 11**,** 291-302.

HABBE, N., SHI, G., MEGUID, R. A., FENDRICH, V., ESNI, F., CHEN, H., FELDMANN, G., STOFFERS, D. A., KONIECZNY, S. F., LEACH, S. D. & MAITRA, A. 2008. Spontaneous induction of murine pancreatic intraepithelial neoplasia (mPanIN) by acinar cell targeting of oncogenic Kras in adult mice. *Proceedings of the National Academy of Sciences,* 105**,** 18913-18918.

HAHN, S. A., SCHUTTE, M., SHAMSUL HOQUE, A. T. M., MOSKALUK, C. A., DA COSTA, L. T., ROZENBLUM, E., WEINSTEIN, C. L., FISCHER, A., YEO, C. J., HRUBAN, R. H. & KERN, S. E. 1996. DPC4, A Candidate Tumor Suppressor Gene at Human Chromosome 18q21.1. *Science,* 271**,** 350-353.

HAMILTON, S. R. & AALTONEN, L. A. 2000. *World Health Organization Classification of Tumours. Pathology and Genetics of Tumours of the Digestive System.*, IARC Press: Lyon 2000.

HANLON, L., AVILA, J. L., DEMAREST, R. M., TROUTMAN, S., ALLEN, M., RATTI, F., RUSTGI, A. K., STANGER, B. Z., RADTKE, F., ADSAY, V., LONG, F., CAPOBIANCO, A. J. & KISSIL, J. L. 2010. Notch1 Functions as a Tumor Suppressor in a Model of K-ras–Induced Pancreatic Ductal Adenocarcinoma. *Cancer Research,* 70**,** 4280-4286.

HANS, F. & DIMITROV, S. 2001. Histone H3 phosphorylation and cell division. *Oncogene,* 20**,** 3021-3027.

HAO, Z. & RAJEWSKY, K. 2001. Homeostasis of peripheral B cells in the absence of B cell influx from the bone marrow. *The Journal of experimental medicine,* 194**,** 1151-1164.

HARIHARAN, D., SAIED, A. & KOCHER, H. M. 2008. Analysis of mortality rates for pancreatic cancer across the world. *HPB,* 10**,** 58-62.

HASSID, B. G., LUCAS, A. L., SALOMAO, M., WENG, C., LIU, F., KHANNA, L. G., KUMAR, S., HWANG, C., CHABOT, J. A. & FRUCHT, H. 2014. Absence

of pancreatic intraepithelial neoplasia predicts poor survival after resection of pancreatic cancer. *Pancreas,* 43**,** 1073-1077.

HEBROK, M., KIM, S. K. & MELTON, D. A. 1998. Notochord repression of endodermal Sonic hedgehog permits pancreas development. *Genes & Development,* 12**,** 1705-1713.

HEMLER, M. E. 2014. Tetraspanin proteins promote multiple cancer stages. *Nature Reviews Cancer,* 14**,** 49-60.

HERMANN, P. C., HUBER, S. L., HERRLER, T., AICHER, A., ELLWART, J. W., GUBA, M., BRUNS, C. J. & HEESCHEN, C. 2007. Distinct Populations of Cancer Stem Cells Determine Tumor Growth and Metastatic Activity in Human Pancreatic Cancer. *Cell Stem Cell,* 1**,** 313-323.

HERR, M. J., KOTHA, J., HAGEDORN, N., SMITH, B. & JENNINGS, L. K. 2013. Tetraspanin CD9 Promotes the Invasive Phenotype of Human Fibrosarcoma Cells via Upregulation of Matrix Metalloproteinase-9. *PLoS ONE,* 8**,** e67766.

HEZEL, A. F. 2006. Genetics and biology of pancreatic ductal adenocarcinoma. *Genes & Development,* 20**,** 1218-1249.

HIDALGO, M. 2010. Pancreatic Cancer. *New England Journal of Medicine,* 362**,** 1605-1617.

HILL, R., CALVOPINA, J. H., KIM, C., WANG, Y., DAWSON, D. W., DONAHUE, T. R., DRY, S. & WU, H. 2010. PTEN Loss Accelerates KrasG12D-Induced Pancreatic Cancer Development. *Cancer Research,* 70**,** 7114-7124.

HINGORANI, S. R., PETRICOIN, E. F., MAITRA, A., RAJAPAKSE, V., KING, C., JACOBETZ, M. A., ROSS, S., CONRADS, T. P., VEENSTRA, T. D., HITT, B. A., KAWAGUCHI, Y., JOHANN, D., LIOTTA, L. A., CRAWFORD, H. C., PUTT, M. E., JACKS, T., WRIGHT, C. V. E., HRUBAN, R. H., LOWY, A. M. & TUVESON, D. A. 2003. Preinvasive and invasive ductal pancreatic cancer and its early detection in the mouse. *Cancer Cell,* 4**,** 437-450.

HINGORANI, S. R., WANG, L., MULTANI, A. S., COMBS, C., DERAMAUDT, T. B., HRUBAN, R. H., RUSTGI, A. K., CHANG, S. & TUVESON, D. A. 2005. Trp53R172H and KrasG12D cooperate to promote chromosomal instability and widely metastatic pancreatic ductal adenocarcinoma in mice. *Cancer Cell,* 7**,** 469-483.

HIRSCHMANN-JAX, C., FOSTER, A. E., WULF, G. G., NUCHTERN, J. G., JAX, T. W., GOBEL, U., GOODELL, M. A. & BRENNER, M. K. 2004. A distinct 'side population' of cells with high drug efflux capacity in human tumor cells. *Proceedings of the National Academy of Sciences of the United States of America,* 101**,** 14228-14233.

HOECK, J. D., JANDKE, A., BLAKE, S. M., NYE, E., SPENCER-DENE, B., BRANDNER, S. & BEHRENS, A. 2010. Fbw7 controls neural stem cell differentiation and progenitor apoptosis via Notch and c-Jun. *Nature Neuroscience,* 13**,** 1365-1372.

HONG, S.-M., PARK, J. Y., HRUBAN, R. H. & GOGGINS, M. 2011. Molecular Signatures of Pancreatic cancer. *Archives of Pathology & Laboratory Medicine,* 135**,** 716-727.

HORI, H., YANO, S., KOUFUJI, K., TAKEDA, J. & SHIROUZU, K. 2004. CD9 expression in gastric cancer and its significance. *The Journal of surgical research,* 117**,** 208-215.

HRUBAN, R. H. 2006. Pathology of Genetically Engineered Mouse Models of Pancreatic Exocrine Cancer: Consensus Report and Recommendations. *Cancer Research,* 66**,** 95-106.

HRUBAN, R. H., ADSAY, N. V., ALBORES-SAAVEDRA, J., COMPTON, C., GARRETT, E. S., GOODMAN, S. N., KERN, S. E., KLIMSTRA, D. S., KLÖPPEL, G., LONGNECKER, D. S., LÜTTGES, J. & OFFERHAUS, G. J. 2001. Pancreatic intraepithelial neoplasia: a new nomenclature and classification system for pancreatic duct lesions. *The American journal of surgical pathology,* 25**,** 579-586.

HRUBAN, R. H., GOGGINS, M., PARSONS, J. & KERN, S. E. 2000a. Progression Model for Pancreatic Cancer. *Clinical Cancer Research,* 6**,** 2969.

HRUBAN, R. H., MAITRA, A., KERN, S. E. & GOGGINS, M. 2007. Precursors to pancreatic cancer. *Gastroenterology clinics of North America,* 36**,** 831-49- vi.

HRUBAN, R. H., WILENTZ, R. E. & KERN, S. E. 2000b. Genetic progression in the pancreatic ducts. *The American journal of pathology,* 156**,** 1821-1825.

HUCH, M., BONFANTI, P., BOJ, S. F., SATO, T., LOOMANS, C. J. M., VAN DE WETERING, M., SOJOODI, M., LI, V. S. W., SCHUIJERS, J., GRACANIN, A., RINGNALDA, F., BEGTHEL, H., HAMER, K., MULDER, J., VAN ES, J. H., DE KONING, E., VRIES, R. G. J., HEIMBERG, H. & CLEVERS, H. 2013. Unlimited in vitro expansion of adult bi‐potent pancreas progenitors through the Lgr5/R‐spondin axis. *The EMBO Journal,* 32**,** 2708-2721.

HUNTLY, B. J. P., SHIGEMATSU, H., DEGUCHI, K., LEE, B. H., MIZUNO, S., DUCLOS, N., ROWAN, R., AMARAL, S., CURLEY, D., WILLIAMS, I. R., AKASHI, K. & GILLILAND, D. G. 2004. MOZ-TIF2, but not BCR-ABL, confers properties of leukemic stem cells to committed murine hematopoietic progenitors. *Cancer Cell,* 6**,** 587-596.

IACOBUZIO-DONAHUE, C. A., KLIMSTRA, D. S., ADSAY, N. V., WILENTZ, R. E., ARGANI, P., SOHN, T. A., YEO, C. J., CAMERON, J. L., KERN, S. E. & HRUBAN, R. H. 2000a. Dpc-4 Protein Is Expressed in Virtually All Human Intraductal Papillary Mucinous Neoplasms of the Pancreas: Comparison with Conventional Ductal Adenocarcinomas. *The American journal of pathology,* 157**,** 755-761.

IACOBUZIO-DONAHUE, C. A., WILENTZ, R. E., ARGANI, P., YEO, C. J., CAMERON, J. L., KERN, S. E. & HRUBAN, R. H. 2000b. Dpc4 protein in mucinous cystic neoplasms of the pancreas: frequent loss of expression in invasive carcinomas suggests a role in genetic progression. *The American journal of surgical pathology,* 24**,** 1544-1548.

IJICHI, H., CHYTIL, A., GORSKA, A. E., AAKRE, M. E., FUJITANI, Y., FUJITANI, S., WRIGHT, C. V. E. & MOSES, H. L. 2006. Aggressive pancreatic ductal adenocarcinoma in mice caused by pancreas-specific blockade of transforming growth factor-beta signaling in cooperation with active Kras expression. *Genes & Development,* 20**,** 3147-3160.

IMMERVOLL, H., HOEM, D., STEFFENSEN, O. J., MILETIC, H. & MOLVEN, A. 2011. Visualization of CD44 and CD133 in normal pancreas and pancreatic ductal adenocarcinomas: non-overlapping membrane expression in cell populations positive for both markers. *The journal of histochemistry and cytochemistry : official journal of the Histochemistry Society,* 59**,** 441-455.

INADA, A., NIENABER, C., KATSUTA, H., FUJITANI, Y., LEVINE, J., MORITA, R., SHARMA, A. & BONNER-WEIR, S. 2008. Carbonic anhydrase II-positive pancreatic cells are progenitors for both endocrine and exocrine pancreas after birth. *Proceedings of the National Academy of Sciences of the United States of America,* 105**,** 19915-19919.

IWANAGA, K., YANG, Y., RASO, M. G., MA, L., HANNA, A. E., THILAGANATHAN, N., MOGHADDAM, S., EVANS, C. M., LI, H., CAI, W.-W., SATO, M., MINNA, J. D., WU, H., CREIGHTON, C. J., DEMAYO, F. J., WISTUBA, I. I. & KURIE, J. M. 2008. Pten Inactivation Accelerates Oncogenic K-ras–Initiated Tumorigenesis in a Mouse Model of Lung Cancer. *Cancer Research,* 68**,** 1119-1127.

IZERADJENE, K., COMBS, C., BEST, M., GOPINATHAN, A., WAGNER, A., GRADY, W. M., DENG, C.-X., HRUBAN, R. H., ADSAY, N. V., TUVESON, D. A. & HINGORANI, S. R. 2007. Kras(G12D) and Smad4/Dpc4 haploinsufficiency cooperate to induce mucinous cystic neoplasms and invasive adenocarcinoma of the pancreas. *Cancer Cell,* 11**,** 229-243.

J PUCCINI, L. D. S. K. 2013. Genetic background and tumour susceptibility in mouse models. *Cell Death and Differentiation,* 20**,** 964-964.

JACKSON, E. L. 2001. Analysis of lung tumor initiation and progression using conditional expression of oncogenic K-ras. *Genes & Development,* 15**,** 3243-3248.

JAFFEE, E. M., HRUBAN, R. H., CANTO, M. & KERN, S. E. 2002. Focus on pancreas cancer. *Cancer Cell,* 2**,** 25-28.

JANDKE, A., DA COSTA, C., SANCHO, R., NYE, E., SPENCER-DENE, B. & BEHRENS, A. 2011. The F-box protein Fbw7 is required for cerebellar development. *Developmental biology,* 358**,** 201-212.

JEMAL, A., SIEGEL, R., WARD, E., HAO, Y., XU, J., MURRAY, T. & THUN, M. J. 2008. Cancer statistics, 2008. *CA: a cancer journal for clinicians,* 58**,** 71-96.

JENSEN, J. N., CAMERON, E., GARAY, M. V. R., STARKEY, T. W., GIANANI, R. & JENSEN, J. 2005. Recapitulation of elements of embryonic development in adult mouse pancreatic regeneration. *YGAST,* 128**,** 728-741.

JI, S., QIN, Y., SHI, S., LIU, X., HU, H., ZHOU, H., GAO, J., ZHANG, B., XU, W., LIU, J., LIANG, D., LIU, L., LIU, C., LONG, J., ZHOU, H., CHIAO, P. J., XU, J., NI, Q., GAO, D. & YU, X. 2015. ERK kinase phosphorylates and destabilizes the tumor suppressor FBW7 in pancreatic cancer. *Cell Research,* 25**,** 561-573.

JONES, S., ZHANG, X., PARSONS, D. W., LIN, J. C. H., LEARY, R. J., ANGENENDT, P., MANKOO, P., CARTER, H., KAMIYAMA, H., JIMENO, A., HONG, S. M., FU, B., LIN, M. T., CALHOUN, E. S., KAMIYAMA, M., WALTER, K., NIKOLSKAYA, T., NIKOLSKY, Y., HARTIGAN, J., SMITH, D. R., HIDALGO, M., LEACH, S. D., KLEIN, A. P., JAFFEE, E. M., GOGGINS, M., MAITRA, A., IACOBUZIO-DONAHUE, C., ESHLEMAN, J. R., KERN, S. E., HRUBAN, R. H., KARCHIN, R., PAPADOPOULOS, N., PARMIGIANI, G., VOGELSTEIN, B., VELCULESCU, V. E. & KINZLER, K. W. 2008. Core Signaling Pathways in Human Pancreatic Cancers Revealed by Global Genomic Analyses. *Science,* 321**,** 1801-1806.

JONSSON, J., AHLGREN, U., EDLUND, T. & EDLUND, H. 1995. IPF1, a homeodomain protein with a dual function in pancreas development. *The International journal of developmental biology,* 39**,** 789-798.

JORDAN, C. T. 2007. The leukemic stem cell. *Best Practice & Research Clinical Haematology,* 20**,** 13-18.

JORDAN, C. T., GUZMAN, M. L. & NOBLE, M. 2006. Cancer stem cells. *New England Journal of Medicine,* 355**,** 1253-1261.

KAHLERT, C. & KALLURI, R. 2013. Exosomes in tumor microenvironment influence cancer progression and metastasis. *Journal of molecular medicine (Berlin, Germany),* 91**,** 431-437.

KANDA, M., MATTHAEI, H., WU, J., HONG, S.-M., YU, J., BORGES, M., HRUBAN, R. H., MAITRA, A., KINZLER, K., VOGELSTEIN, B. & GOGGINS, M. 2012. Presence of somatic mutations in most early-stage pancreatic intraepithelial neoplasia. *Gastroenterology,* 142**,** 730-733.e9.

KARLSSON, G., RÖRBY, E., PINA, C., SONEJI, S., RECKZEH, K., MIHARADA, K., KARLSSON, C., GUO, Y., FUGAZZA, C., GUPTA, R., MARTENS, J. H. A., STUNNENBERG, H. G., KARLSSON, S. & ENVER, T. 2013. The tetraspanin CD9 affords high-purity capture of all murine hematopoietic stem cells. *CellReports,* 4**,** 642-648.

KERN, S., HRUBAN, R., HOLLINGSWORTH, M. A., BRAND, R., ADRIAN, T. E., JAFFEE, E. & TEMPERO, M. A. 2001. A white paper: the product of a pancreas cancer think tank. *Cancer research.*

KIM, W. Y. & SHARPLESS, N. E. 2006. The Regulation of INK4/ARF in Cancer and Aging. *Cell,* 127**,** 265-275.

KISHEL, P., BELLAHCENE, A., DEUX, B., LAMOUR, V., DOBSON, R., DE PAUW, E., CLEZARDIN, P. & CASTRONOVO, V. 2012. Overexpression of CD9 in Human Breast Cancer Cells Promotes the Development of Bone Metastases. *Anticancer research,* 32**,** 5211-5220.

KONSTANTINIDIS, I. T., VINUELA, E. F., TANG, L. H., KLIMSTRA, D. S., D'ANGELICA, M. I., DEMATTEO, R. P., KINGHAM, T. P., FONG, Y., JARNAGIN, W. R. & ALLEN, P. J. 2013. Incidentally Discovered Pancreatic Intraepithelial Neoplasia: What Is Its Clinical Significance? *Annals of Surgical Oncology,* 20**,** 3643-3647.

KOPP, J. L., DUBOIS, C. L., SCHAFFER, A. E., HAO, E., SHIH, H. P., SEYMOUR, P. A., MA, J. & SANDER, M. 2011. Sox9+ ductal cells are multipotent progenitors throughout development but do not produce new endocrine cells in the normal or injured adult pancreas. *Development,* 138**,** 653-665.

KOPP, J. L., VON FIGURA, G., MAYES, E., LIU, F.-F., DUBOIS, C. L., MORRIS, I., JOHN P, PAN, F. C., AKIYAMA, H., WRIGHT, C. V. E., JENSEN, K., HEBROK, M. & SANDER, M. 2012. Identification of Sox9-Dependent Acinar-to-Ductal Reprogramming as the Principal Mechanism for Initiation of Pancreatic Ductal Adenocarcinoma. *Cancer Cell,* 22**,** 737-750.

LAND, H., PARADA, L. F. & WEINBERG, R. A. 1983. Cellular oncogenes and multistep carcinogenesis. *Science,* 222**,** 771-778.

LAPIDOT, T., SIRARD, C., VORMOOR, J., MURDOCH, B., HOANG, T., CACERES-CORTES, J., MINDEN, M., PATERSON, B., CALIGIURI, M. A.

& DICK, J. E. 1994. A cell initiating human acute myeloid leukaemia after transplantation into SCID mice. *Nature,* 367**,** 645-648.

LEE, C. J., DOSCH, J. & SIMEONE, D. M. 2008. Pancreatic Cancer Stem Cells. *Journal of Clinical Oncology,* 26**,** 2806-2812.

LESCHE, R., GROSZER, M., GAO, J., WANG, Y., MESSING, A., SUN, H., LIU, X. & WU, H. 2002. Cre/loxP-mediated inactivation of the murine Pten tumor suppressor gene. *Genesis (New York, N.Y. : 2000),* 32**,** 148-149.

LI, C., HEIDT, D. G., DALERBA, P., BURANT, C. F., ZHANG, L., ADSAY, V., WICHA, M., CLARKE, M. F. & SIMEONE, D. M. 2007. Identification of Pancreatic Cancer Stem Cells. *Cancer Research,* 67**,** 1030-1037.

LIM, S. & KALDIS, P. 2013. Cdks, cyclins and CKIs: roles beyond cell cycle regulation. *Development,* 140**,** 3079-3093.

LIOU, G.-Y., DÖPPLER, H., NECELA, B., KRISHNA, M., CRAWFORD, H. C., RAIMONDO, M. & STORZ, P. 2013. Macrophage-secreted cytokines drive pancreatic acinar-to-ductal metaplasia through NF-κB and MMPs. *The Journal of Cell Biolgy,* 202**,** 563-577.

LÖHR, M., KLÖPPEL, G., MAISONNEUVE, P., LOWENFELS, A. B. & LÜTTGES, J. 2005. Frequency of K-ras mutations in pancreatic intraductal neoplasias associated with pancreatic ductal adenocarcinoma and chronic pancreatitis: a meta-analysis. *Neoplasia (New York, N.Y.),* 7**,** 17-23.

LONARDO, E., HERMANN, P. C., MUELLER, M.-T., HUBER, S., BALIC, A., MIRANDA-LORENZO, I., ZAGORAC, S., ALCALA, S., RODRIGUEZ-ARABAOLAZA, I., RAMIREZ, J. C., TORRES-RUÍZ, R., GARCIA, E., HIDALGO, M., CEBRIÁN, D. Á., HEUCHEL, R., LÖHR, M., BERGER, F., BARTENSTEIN, P., AICHER, A. & HEESCHEN, C. 2011. Nodal/Activin Signaling Drives Self-Renewal and Tumorigenicity of Pancreatic Cancer Stem Cells and Provides a Target for Combined Drug Therapy. *Stem Cell,* 9**,** 433-446.

LOWENFELS, A. B., MAISONNEUVE, P., DIMAGNO, E. P., ELITSUR, Y., GATES, L. K., PERRAULT, J., WHITCOMB, D. C. & GROUP, I. H. P. S. 1997. Hereditary Pancreatitis and the Risk of Pancreatic Cancer. *JNCI Journal of the National Cancer Institute,* 89**,** 442-446.

LÜTTGES, J., SCHLEHE, B., MENKE, M. A., VOGEL, I., HENNE-BRUNS, D. & KLÖPPEL, G. 1999. The K-ras mutation pattern in pancreatic ductal adenocarcinoma usually is identical to that in associated normal, hyperplastic, and metaplastic ductal epithelium. *Cancer,* 85**,** 1703-1710.

MADSEN, O. D., JENSEN, J., PEDERSEN, E. E., GALANTE, P., HALD, J., HELLER, R. S., ISHIBASHI, M., KAGEYAMA, R., GUILLEMOT, F. & SERUP, P. 2000. Control of endodermal endocrine development by Hes-1. *Nature Genetics,* 24**,** 36-44.

MAGENHEIM, J., KLEIN, A. M., STANGER, B. Z., ASHERY-PADAN, R., SOSA-PINEDA, B., GU, G. & DOR, Y. 2011. Ngn3+ endocrine progenitor cells control the fate and morphogenesis of pancreatic ductal epithelium. *Developmental biology,* 359**,** 26-36.

MARCINIAK, A., SELCK, C., FRIEDRICH, B. & SPEIER, S. 2013. Mouse Pancreas Tissue Slice Culture Facilitates Long-Term Studies of Exocrine and Endocrine Cell Physiology in situ *PLoS ONE,* 8**,** e78706.

MARIELLE WG RUIJS, A. B. F. H. M. M. G. A. A. W. R. O. H. M.-H. L. J. V. A. T. V. S. V. 2009. The contribution of CHEK2 to the TP53-negative Li-Fraumeni phenotype. *Hereditary Cancer in Clinical Practice,* 7**,** 4.

MARINO, S., VOOIJS, M., VAN DER GULDEN, H., JONKERS, J. & BERNS, A. 2000. Induction of medulloblastomas in p53-null mutant mice by somatic inactivation of Rb in the external granular layer cells of the cerebellum. *Genes & Development,* 14**,** 994-1004.

MASHIMA, H., OHNISHI, H., WAKABAYASHI, K., MINE, T., MIYAGAWA, J., HANAFUSA, T., SENO, M., YAMADA, H. & KOJIMA, I. 1996. Betacellulin and activin A coordinately convert amylase-secreting pancreatic AR42J cells into insulin-secreting cells. *Journal of Clinical Investigation,* 97**,** 1647-1654.

MASON, M. N. & MAHONEY, M. J. 2010. Inhibition of gamma-secretase activity promotes differentiation of embryonic pancreatic precursor cells into functional islet-like clusters in poly(ethylene glycol) hydrogel culture. *Tissue engineering. Part A,* 16**,** 2593-2603.

MASSAGUÉ, J. 1998. TGF-β SIGNAL TRANSDUCTION. *Annu. Rev. Biochem.,* 67**,** 753-791.

MATSUDA, Y., KURE, S. & ISHIWATA, T. 2012. Nestin and other putative cancer stem cell markers in pancreatic cancer. *Medical Molecular Morphology,* 45**,** 59-65.

MEANS, A. L., MESZOELY, I. M., SUZUKI, K., MIYAMOTO, Y., RUSTGI, A. K., COFFEY, R. J., WRIGHT, C. V. E., STOFFERS, D. A. & LEACH, S. D. 2005. Pancreatic epithelial plasticity mediated by acinar cell transdifferentiation and generation of nestin-positive intermediates. *Development,* 132**,** 3767-3776.

MEANS, A. L., XU, Y., ZHAO, A., RAY, K. C. & GU, G. 2008. A CK19(CreERT) knockin mouse line allows for conditional DNA recombination in epithelial cells in multiple endodermal organs. *Genesis (New York, N.Y. : 2000),* 46**,** 318-323.

MILLER, D. G. 1980. On the nature of susceptibility to cancer. The presidential address. *Cancer,* 46**,** 1307-1318.

MINELLA, A. C., WELCKER, M. & CLURMAN, B. E. 2005. Ras activity regulates cyclin E degradation by the Fbw7 pathway. *Proceedings of the National Academy of Sciences of the United States of America,* 102**,** 9649-9654.

MING, M. & HE, Y.-Y. 2009. PTEN: New Insights into Its Regulation and Function in Skin Cancer. *Journal of Investigative Dermatology,* 129**,** 2109-2112.

MINGYI CHEN, M. V. N. Y. G. J. G. 2012. Molecular pathology of pancreatic neuroendocrine tumors. *Journal of Gastrointestinal Oncology,* 3**,** 182.

MIRANDA-LORENZO, I., DORADO, J., LONARDO, E., ALCALA, S., SERRANO, A. G., CLAUSELL-TORMOS, J., CIOFFI, M., MEGIAS, D., ZAGORAC, S., BALIC, A., HIDALGO, M., ERKAN, M., KLEEFF, J., SCARPA, A., SAINZ, B. & HEESCHEN, C. 2014. Intracellular autofluorescence: a biomarker for epithelial cancer stem cells. *Nature Methods,* 11**,** 1161-1169.

MIYAMOTO, Y., MAITRA, A., GHOSH, B., ZECHNER, U., ARGANI, P., IACOBUZIO-DONAHUE, C. A., SRIURANPONG, V., ISO, T., MESZOELY, I. M., WOLFE, M. S., HRUBAN, R. H., BALL, D. W., SCHMID, R. M. & LEACH, S. D. 2003. Notch mediates TGF alpha-induced changes in epithelial differentiation during pancreatic tumorigenesis. *Cancer Cell,* 3**,** 565-576.

MOLL, U. M. & PETRENKO, O. 2003. The MDM2-p53 interaction. *Molecular cancer research : MCR,* 1**,** 1001-1008.

MOORE, M. J., GOLDSTEIN, D., HAMM, J., FIGER, A., HECHT, J. R., GALLINGER, S., AU, H. J., MURAWA, P., WALDE, D., WOLFF, R. A., CAMPOS, D., LIM, R., DING, K., CLARK, G., VOSKOGLOU-NOMIKOS, T., PTASYNSKI, M. & PARULEKAR, W. 2007. Erlotinib Plus Gemcitabine Compared With Gemcitabine Alone in Patients With Advanced Pancreatic Cancer: A Phase III Trial of the National Cancer Institute of Canada Clinical Trials Group. *Journal of Clinical Oncology,* 25**,** 1960-1966.

MORRIS, I., JOHN P, CANO, D. A., SEKINE, S., WANG, S. C. & HEBROK, M. 2010. β-catenin blocks Kras-dependent reprogramming of acini into pancreatic cancer precursor lesions in mice. *Journal of Clinical Investigation,* 120**,** 508-520.

NGUYEN, L. V., VANNER, R., DIRKS, P. & EAVES, C. J. 2012. Cancer stem cells: an evolving concept. *Nature Reviews Cancer,* 12**,** 133-143.

NISHIDA, H., YAMAZAKI, H., YAMADA, T., IWATA, S., DANG, N. H., INUKAI, T., SUGITA, K., IKEDA, Y. & MORIMOTO, C. 2009. CD9 correlates with cancer stem cell potentials in human B-acute lymphoblastic leukemia cells. *Biochemical and Biophysical Research Communications,* 382**,** 57-62.

OLINER, J. D., PIETENPOL, J. A., THIAGALINGAM, S., GYURIS, J., KINZLER, K. W. & VOGELSTEIN, B. 1993. Oncoprotein MDM2 conceals the activation domain of tumour suppressor p53. *Nature,* 362**,** 857-860.

OLIVE, K. P., JACOBETZ, M. A., DAVIDSON, C. J., GOPINATHAN, A., MCINTYRE, D., HONESS, D., MADHU, B., GOLDGRABEN, M. A., CALDWELL, M. E., ALLARD, D., FRESE, K. K., DENICOLA, G., FEIG, C., COMBS, C., WINTER, S. P., IRELAND-ZECCHINI, H., REICHELT, S., HOWAT, W. J., CHANG, A., DHARA, M., WANG, L., RUCKERT, F., GRUTZMANN, R., PILARSKY, C., IZERADJENE, K., HINGORANI, S. R., HUANG, P., DAVIES, S. E., PLUNKETT, W., EGORIN, M., HRUBAN, R. H., WHITEBREAD, N., MCGOVERN, K., ADAMS, J., IACOBUZIO-DONAHUE, C., GRIFFITHS, J. & TUVESON, D. A. 2009. Inhibition of Hedgehog Signaling Enhances Delivery of Chemotherapy in a Mouse Model of Pancreatic Cancer. *Science,* 324**,** 1457-1461.

OSHIMA, Y., SUZUKI, A., KAWASHIMO, K., ISHIKAWA, M., OHKOHCHI, N. & TANIGUCHI, H. 2007. Isolation of Mouse Pancreatic Ductal Progenitor Cells Expressing CD133 and c-Met by Flow Cytometric Cell Sorting. *Gastroenterology,* 132**,** 720-732.

PALMER, D. H., STOCKEN, D. D., HEWITT, H., MARKHAM, C. E., HASSAN, A. B., JOHNSON, P. J., BUCKELS, J. A. C. & BRAMHALL, S. R. 2007. A Randomized Phase 2 Trial of Neoadjuvant Chemotherapy in Resectable Pancreatic Cancer: Gemcitabine Alone Versus Gemcitabine Combined with Cisplatin. *Annals of Surgical Oncology,* 14**,** 2088-2096.

PAN, F. C., BANKAITIS, E. D., BOYER, D., XU, X., VAN DE CASTEELE, M., MAGNUSON, M. A., HEIMBERG, H. & WRIGHT, C. V. E. 2013. Spatiotemporal patterns of multipotentiality in Ptf1a-expressing cells during pancreas organogenesis and injury-induced facultative restoration. *Development,* 140**,** 751-764.

PARK, H.-D., KANG, E.-S., KIM, J.-W., LEE, K.-T., LEE, K. H., PARK, Y. S., PARK, J.-O., LEE, J., HEO, J. S., CHOI, S. H., CHOI, D. W., KIM, S., LEE, J. K. & LEE, S.-Y. 2012. Serum CA19-9, cathepsin D, and matrix metalloproteinase-7 as a diagnostic panel for pancreatic ductal adenocarcinoma. *Proteomics,* 12**,** 3590-3597.

PASTRANA, E., SILVA-VARGAS, V. & DOETSCH, F. 2011. Eyes wide open: a critical review of sphere-formation as an assay for stem cells. *Cell Stem Cell,* 8**,** 486-498.

PÉREZ-MANCERA, P. A., RUST, A. G., VAN DER WEYDEN, L., KRISTIANSEN, G., LI, A., SARVER, A. L., SILVERSTEIN, K. A. T., GRÜTZMANN, R., AUST, D., RÜMMELE, P., KNÖSEL, T., HERD, C., STEMPLE, D. L., KETTLEBOROUGH, R., BROSNAN, J. A., LI, A., MORGAN, R., KNIGHT, S., YU, J., STEGEMAN, S., COLLIER, L. S., TEN HOEVE, J. J., DE RIDDER, J., KLEIN, A. P., GOGGINS, M., HRUBAN, R. H., CHANG, D. K., BIANKIN, A. V., GRIMMOND, S. M., BIANKIN, A. V., JOHNS, A. L., MAWSON, A., CHANG, D. K., BRANCATO, M.-A. L., ROWE, S. J., SIMPSON, S. L., MARTYN-SMITH, M., CHANTRILL, L. A., CHIN, V. T., CHOU, A., COWLEY, M. J., HUMPHRIS, J. L., JONES, M. D., SCOTT MEAD, R., NAGRIAL, A. M., PAJIC, M., PETTIT, J., PINESE, M., ROOMAN, I., WU, J., DALY, R. J., MUSGROVE, E. A., SUTHERLAND, R. L., GRIMMOND, S. M., WADDELL, N., KASSAHN, K. S., MILLER, D. K., WILSON, P. J., PATCH, A.-M., SONG, S., HARLIWONG, I., IDRISOGLU, S., NOURSE, C., NOURBAKHSH, E., MANNING, S., WANI, S., GONGORA, M., ANDERSON, M., HOLMES, O., LEONARD, C., TAYLOR, D., WOOD, S., XU, C., NONES, K., LYNN FINK, J., CHRIST, A., BRUXNER, T., CLOONAN, N., NEWELL, F., PEARSON, J. V., SAMRA, J. S., GILL, A. J., PAVLAKIS, N., GUMINSKI, A., TOON, C., BLANKIN, A. V., ASGHARI, R., MERRETT, N. D., CHANG, D. K., PAVEY, D. A., DAS, A., COSMAN, P. H., ISMAIL, K., O'CONNOR, C., LAM, V. W., MCLEOD, D., PLEASS, H. C., JAMES, V., KENCH, J. G., COOPER, C. L., et al. 2012. The deubiquitinase USP9X suppresses pancreatic ductal adenocarcinoma. *Nature,* 486**,** 266-270.

PICTET, R. L., CLARK, W. R., WILLIAMS, R. H. & RUTTER, W. J. 1972. 130 Search Results - ALL(An ultrastructural analysis of the developing embryonic pancreas) - ScienceDirect. *Developmental biology,* 29**,** 436-467.

PLENTZ, R., PARK, J. S., RHIM, A. D., ABRAVANEL, D., HEZEL, A. F., SHARMA, S. V., GURUMURTHY, S., DESHPANDE, V., KENIFIC, C., SETTLEMAN, J., MAJUMDER, P. K., STANGER, B. Z. & BARDEESY, N. 2009. Inhibition of γ-Secretase Activity Inhibits Tumor Progression in a Mouse Model of Pancreatic Ductal Adenocarcinoma. *Gastroenterology,* 136**,** 1741-1749.e6.

POLYAK, K. & HAHN, W. C. 2006. Roots and stems: stem cells in cancer. *Nature Medicine,* 12**,** 296-300.

PURI, S. & HEBROK, M. 2010. Cellular Plasticity within the Pancreas- Lessons Learned from Development. *Developmental Cell,* 18**,** 342-356.

RACHAGANI, S., TORRES, M. P., KUMAR, S., HARIDAS, D., BAINE, M., MACHA, M. A., KAUR, S., PONNUSAMY, M. P., DEY, P., SESHACHARYULU, P., JOHANSSON, S. L., JAIN, M., WAGNER, K.-U. &

BATRA, S. K. 2012. Mucin (Muc) expression during pancreatic cancer progression in spontaneous mouse model: potential implications for diagnosis and therapy. *Journal of Hematology & Oncology,* 5**,** 68.

RAJALINGAM, K., SCHRECK, R., RAPP, U. R. & ALBERT, Š. 2007. Ras oncogenes and their downstream targets. *Biochimica et Biophysica Acta (BBA) - Molecular Cell Research,* 1773**,** 1177-1195.

RAVID, T. & HOCHSTRASSER, M. 2008. Diversity of degradation signals in the ubiquitin-proteasome system. *Nature reviews. Molecular cell biology,* 9**,** 679-690.

RAY, K. C., BELL, K. M., YAN, J., GU, G., CHUNG, C. H., WASHINGTON, M. K. & MEANS, A. L. 2011. Epithelial Tissues Have Varying Degrees of Susceptibility to KrasG12D-Initiated Tumorigenesis in a Mouse Model. *PLoS ONE,* 6**,** e16786.

RECAVARREN, C., LABOW, D. M., LIANG, J., ZHANG, L., WONG, M., ZHU, H., WANG, J., FRANCIS, F. & XU, R. 2011. Histologic characteristics of pancreatic intraepithelial neoplasia associated with different pancreatic lesions. 42**,** 18-24.

REICHERT, M. & RUSTGI, A. K. 2011. Pancreatic ductal cells in development, regeneration, and neoplasia. *Journal of Clinical Investigation,* 121**,** 4572-4578.

REICHERT, M., TAKANO, S., HEEG, S., BAKIR, B., BOTTA, G. P. & RUSTGI, A. K. 2013. Isolation, culture and genetic manipulation of mouse pancreatic ductal cells. *Nature Protocols,* 8**,** 1354-1365.

REYA, T., MORRISON, S. J., CLARKE, M. F. & WEISSMAN, I. L. 2001. Stem cells, cancer, and cancer stem cells : Article : Nature. *Nature,* 414**,** 105-111.

RHIM, A. D., MIREK, E. T., AIELLO, N. M., MAITRA, A., BAILEY, J. M., MCALLISTER, F., REICHERT, M., BEATTY, G. L., RUSTGI, A. K., VONDERHEIDE, R. H., LEACH, S. D. & STANGER, B. Z. 2012. EMT and dissemination precede pancreatic tumor formation. *Cell,* 148**,** 349-361.

RICCI-VITIANI, L., LOMBARDI, D. G., PILOZZI, E., BIFFONI, M., TODARO, M., PESCHLE, C. & DE MARIA, R. 2006. Identification and expansion of human colon-cancer-initiating cells. *Nature,* 445**,** 111-115.

RICH, J. N. & BAO, S. 2007. Chemotherapy and Cancer Stem Cells. *Cell Stem Cell,* 1**,** 353-355.

RIECK, S. & KAESTNER, K. H. 2010. Expansion of beta-cell mass in response to pregnancy. *Trends in endocrinology and metabolism: TEM,* 21**,** 151-158.

RIENER, M.-O., PILARSKY, C., GERHARDT, J., GRÜTZMANN, R., FRITZSCHE, F. R., BAHRA, M., WEICHERT, W. & KRISTIANSEN, G. 2009. Prognostic significance of AGR2 in pancreatic ductal adenocarcinoma. *Histology and histopathology,* 24**,** 1121-1128.

ROSTY, C., GERADTS, J., SATO, N., WILENTZ, R. E., ROBERTS, H., SOHN, T., CAMERON, J. L., YEO, C. J., HRUBAN, R. H. & GOGGINS, M. 2003. p16 Inactivation in pancreatic intraepithelial neoplasias (PanINs) arising in patients with chronic pancreatitis. *The American journal of surgical pathology,* 27**,** 1495-1501.

ROY, N., MALIK, S., VILLANUEVA, K. E., URANO, A., LU, X., VON FIGURA, G., SEELEY, E. S., DAWSON, D. W., COLLISSON, E. A. & HEBROK, M. 2015.

Brg1 promotes both tumor-suppressive and oncogenic activities at distinct stages of pancreatic cancer formation. *Genes & Development,* 29**,** 658-671.

ROZENBLUM, E., SCHUTTE, M., GOGGINS, M., HAHN, S. A., PANZER, S., ZAHURAK, M., GOODMAN, S. N., SOHN, T. A., HRUBAN, R. H., YEO, C. J. & KERN, S. E. 1997. Tumor-suppressive Pathways in Pancreatic Carcinoma. *Cancer Research,* 57**,** 1731-1734.

RYAN, D. P., HONG, T. S. & BARDEESY, N. 2014. Pancreatic adenocarcinoma. *New England Journal of Medicine,* 371**,** 1039-1049.

S UCHIDA, Y. S. G. W. Z. G. L. T. H. M. M. M. I. 1999. Motility-related protein (MRP-1/CD9) and KAI1/CD82 expression inversely correlate with lymph node metastasis in oesophageal squamous cell carcinoma. *British Journal of Cancer,* 79**,** 1168.

SAITO, M., IWAWAKI, T., TAYA, C., YONEKAWA, H., NODA, M., INUI, Y., MEKADA, E., KIMATA, Y., TSURU, A. & KOHNO, K. 2001. Diphtheria toxin receptor-mediated conditional and targeted cell ablation in transgenic mice. 19**,** 746-750.

SAMPIERI, K. & FODDE, R. 2012. Cancer stem cells and metastasis. *Seminars in Cancer Biology,* 22**,** 187-193.

SAMUEL, N. & HUDSON, T. J. 2011. The molecular and cellular heterogeneity of pancreatic ductal adenocarcinoma. *Nature Reviews Gastroenterology & Hepatology,* 9**,** 77-87.

SANCHO, R., GRUBER, R., GU, G. & BEHRENS, A. 2014. Loss of Fbw7 reprograms adult pancreatic ductal cells into α, δ, and β cells. *Cell Stem Cell,* 15**,** 139-153.

SANCHO, R., JANDKE, A., DAVIS, H., DIEFENBACHER, M. E., TOMLINSON, I. & BEHRENS, A. 2010. F-box and WD Repeat Domain-Containing 7 Regulates Intestinal Cell Lineage Commitment and Is a Haploinsufficient Tumor Suppressor - Gastroenterology. *YGAST,* 139**,** 929-941.

SANDGREN, E. P., QUAIFE, C. J., PAULOVICH, A. G., PALMITER, R. D. & BRINSTER, R. L. 1991. Pancreatic tumor pathogenesis reflects the causative genetic lesion. *Proceedings of the National Academy of Sciences of the United States of America,* 88**,** 93.

SATO, N., ROSTY, C., JANSEN, M., FUKUSHIMA, N., UEKI, T., YEO, C. J., CAMERON, J. L., IACOBUZIO-DONAHUE, C. A., HRUBAN, R. H. & GOGGINS, M. 2001. STK11/LKB1 Peutz-Jeghers gene inactivation in intraductal papillary-mucinous neoplasms of the pancreas. *The American journal of pathology,* 159**,** 2017-2022.

SAUER, B. 1998. Inducible gene targeting in mice using the Cre/lox system. *Methods (San Diego, Calif.),* 14**,** 381-392.

SCHENK, M., SCHWARTZ, A. G., O&APOS;NEAL, E., KINNARD, M., GREENSON, J. K., FRYZEK, J. P., YING, G. S. & GARABRANT, D. H. 2001. Familial Risk of Pancreatic Cancer. *JNCI Journal of the National Cancer Institute,* 93**,** 640-644.

SCHNEIDER, G., HAMACHER, R., ESER, S., FRIESS, H., SCHMID, R. M. & SAUR, D. 2008. Molecular biology of pancreatic cancer--new aspects and targets. *Anticancer research,* 28**,** 1541-1550.

SCOTT, A. M., WOLCHOK, J. D. & OLD, L. J. 2012. Antibody therapy of cancer. *Nature Reviews Cancer,* 12**,** 278-287.

SEGER, R. & KREBS, E. G. 1995. The MAPK signaling cascade. *The FASEB Journal,* 9**,** 726-735.

SERFAS, M. S. & TYNER, A. L. 1993. HNF-1 alpha and HNF-1 beta expression in mouse intestinal crypts. *American Journal of Physiology - Gastrointestinal and Liver Physiology,* 265**,** G506-G513.

SHI, G., DIRENZO, D., QU, C., BARNEY, D., MILEY, D. & KONIECZNY, S. F. 2012. Maintenance of acinar cell organization is critical to preventing Kras-induced acinar-ductal metaplasia. *Oncogene,* 32**,** 1950-1958.

SHI, W., MEDEMA, J. P., FAN, H., SHUM, L. & DERYNCK, R. 2000. The Tetraspanin Cd9 Associates with Transmembrane TGF-α and Regulates TGF-α–Induced Egf Receptor Activation and Cell Proliferation. *The Journal of cell biology,* 148**,** 591-602.

SHIH, H. P., WANG, A. & SANDER, M. 2013. Pancreas organogenesis: from lineage determination to morphogenesis. *Annual Review of Cell and Developmental Biology,* 29**,** 81-105.

SHO, M., ADACHI, M., TAKI, T., HASHIDA, H., KONISHI, T., HUANG, C. L., IKEDA, N., NAKAJIMA, Y., KANEHIRO, H., HISANAGA, M., NAKANO, H. & MIYAKE, M. 1998. Transmembrane 4 superfamily as a prognostic factor in pancreatic cancer. *International journal of cancer. Journal international du cancer,* 79**,** 509-516.

SINGH, S. K., HAWKINS, C., CLARKE, I. D., SQUIRE, J. A., BAYANI, J., HIDE, T., HENKELMAN, R. M., CUSIMANO, M. D. & DIRKS, P. B. 2004. Identification of human brain tumour initiating cells. *Nature cell biology,* 432**,** 396-401.

SKALICKY, D. A., KENCH, J. G., SEGARA, D., COLEMAN, M. J., SUTHERLAND, R. L., HENSHALL, S. M., MUSGROVE, E. A. & BIANKIN, A. V. 2006. Cyclin E Expression and Outcome in Pancreatic Ductal Adenocarcinoma. *Cancer epidemiology, biomarkers & prevention,* 15**,** 1941-1947.

SLACK, J. M. 1995. Developmental biology of the pancreas. *Development,* 121**,** 1569-1580.

SOLAR, M., CARDALDA, C., HOUBRACKEN, I., MARTÍN, M., MAESTRO, M. A., DE MEDTS, N., XU, X., GRAU, V., HEIMBERG, H., BOUWENS, L. & FERRER, J. 2009. Pancreatic exocrine duct cells give rise to insulin-producing beta cells during embryogenesis but not after birth. *Developmental Cell,* 17**,** 849-860.

SOLOMON AFELIK, Y. C. T. P. 2006. Combined ectopic expression of Pdx1 and Ptf1a/p48 results in the stable conversion of posterior endoderm into endocrine and exocrine pancreatic tissue. *Genes & Development,* 20**,** 1441-1446.

SPAGNOLI, F. M. 2007. From endoderm to pancreas: a multistep journey. *Cellular and molecular life sciences : CMLS,* 64**,** 2378-2390.

SRINIVAS, S., WATANABE, T., LIN, C.-S., WILLIAM, C. M., TANABE, Y., JESSELL, T. M. & COSTANTINI, F. 2001. Cre reporter strains produced by targeted insertion of EYFP and ECFP into the ROSA26 locus. *BMC Developmental Biology,* 1**,** 4.

SRIVASTAVA, S., ZOU, Z., PIROLLO, K., BLATTNER, W. & CHANG, E. H. 1990. Germ-line transmission of a mutated p53 gene in a cancer-prone family with Li–Fraumeni syndrome. *Nature,* 348**,** 747-749.

STANGER, B. Z., STILES, B., LAUWERS, G. Y., BARDEESY, N., MENDOZA, M., WANG, Y., GREENWOOD, A., CHENG, K.-H., MCLAUGHLIN, M., BROWN, D., DEPINHO, R. A., WU, H., MELTON, D. A. & DOR, Y. 2005. Pten constrains centroacinar cell expansion and malignant transformation in the pancreas. *Cancer Cell,* 8**,** 185-195.

STEFAN ESER, M. M. P. E. A. V. W. B. S. M. B. R. V. A. M. J. V. B. H. A. P. P. A. E. S. I. E. R. M. 2011. In vivo diagnosis of murine pancreatic intraepithelial neoplasia and early-stage pancreatic cancer by molecular imaging. *Proceedings of the National Academy of Sciences,* 108**,** 9945-9950.

STELOW, E. B., ADAMS, R. B. & MOSKALUK, C. A. 2006a. The prevalence of pancreatic intraepithelial neoplasia in pancreata with uncommon types of primary neoplasms. *The American journal of surgical pathology,* 30**,** 36-41.

STELOW, E. B., BARDALES, R. H., SHAMI, V. M., WOON, C., PRESLEY, A., MALLERY, S., LAI, R. & STANLEY, M. W. 2006b. Cytology of pancreatic acinar cell carcinoma. *Diagnostic cytopathology,* 34**,** 367-372.

STROBEL, O., DOR, Y., ALSINA, J., STIRMAN, A., LAUWERS, G., TRAINOR, A., CASTILLO, C. F.-D., WARSHAW, A. L. & THAYER, S. P. 2007. In vivo lineage tracing defines the role of acinar-to-ductal transdifferentiation in inflammatory ductal metaplasia. *Gastroenterology,* 133**,** 1999-2009.

TANAKA, M., FERNÁNDEZ-DEL CASTILLO, C., ADSAY, V., CHARI, S., FALCONI, M., JANG, J.-Y., KIMURA, W., LEVY, P., PITMAN, M. B., SCHMIDT, C. M., SHIMIZU, M., WOLFGANG, C. L., YAMAGUCHI, K., YAMAO, K. & PANCREATOLOGY, I. A. O. 2012. International consensus guidelines 2012 for the management of IPMN and MCN of the pancreas. *Pancreatology : official journal of the International Association of Pancreatology (IAP) ... [et al.]*.

TERADA, T. 2011. Immunohistochemical profile of normal mesothelium and histiocytic/methothelial hyperplasia: a case report. *International Journal of Clinical and Experimental Pathology,* 4**,** 631.

TETA, M., RANKIN, M. M., LONG, S. Y., STEIN, G. M. & KUSHNER, J. A. 2007. Growth and Regeneration of Adult β Cells Does Not Involve Specialized Progenitors. *Developmental Cell,* 12**,** 817-826.

THOREL, F., NÉPOTE, V., AVRIL, I., KOHNO, K., DESGRAZ, R., CHERA, S. & HERRERA, P. L. 2010. Conversion of adult pancreatic α-cells to β-cells after extreme β-cell loss. *Nature,* 464**,** 1149-1154.

TOMAYKO, M. M. & REYNOLDS, C. P. 1989. Determination of subcutaneous tumor size in athymic (nude) mice. *Cancer chemotherapy and pharmacology,* 24**,** 148-154.

TREUTLEIN, B., BROWNFIELD, D. G., WU, A. R., NEFF, N. F., MANTALAS, G. L., ESPINOZA, F. H., DESAI, T. J., KRASNOW, M. A. & QUAKE, S. R. 2014. Reconstructing lineage hierarchies of the distal lung epithelium using single-cell RNA-seq. *Nature,* 509**,** 371-375.

TUVESON, D. A., ZHU, L., GOPINATHAN, A., WILLIS, N. A., KACHATRIAN, L., GROCHOW, R., PIN, C. L., MITIN, N. Y., TAPAROWSKY, E. J., GIMOTTY, P. A., HRUBAN, R. H., JACKS, T. & KONIECZNY, S. F. 2006. Mist1-KrasG12D Knock-In Mice Develop Mixed Differentiation Metastatic Exocrine

Pancreatic Carcinoma and Hepatocellular Carcinoma. *Cancer Research,* 66**,** 242-247.

UHLEN, M., FAGERBERG, L., HALLSTROM, B. M., LINDSKOG, C., OKSVOLD, P., MARDINOGLU, A., SIVERTSSON, A., KAMPF, C., SJOSTEDT, E., ASPLUND, A., OLSSON, I., EDLUND, K., LUNDBERG, E., NAVANI, S., SZIGYARTO, C. A. K., ODEBERG, J., DJUREINOVIC, D., TAKANEN, J. O., HOBER, S., ALM, T., EDQVIST, P. H., BERLING, H., TEGEL, H., MULDER, J., ROCKBERG, J., NILSSON, P., SCHWENK, J. M., HAMSTEN, M., VON FEILITZEN, K., FORSBERG, M., PERSSON, L., JOHANSSON, F., ZWAHLEN, M., VON HEIJNE, G., NIELSEN, J. & PONTEN, F. 2015. Tissue-based map of the human proteome. *Science,* 347**,** 1260419-1260419.

VIDAL, S. J., RODRIGUEZ-BRAVO, V., GALSKY, M., CORDON-CARDO, C. & DOMINGO-DOMENECH, J. 2013. Targeting cancer stem cells to suppress acquired chemotherapy resistance. *Oncogene,* 33**,** 4451-4463.

VILLASENOR, A., CHONG, D. C., HENKEMEYER, M. & CLEAVER, O. 2010. Epithelial dynamics of pancreatic branching morphogenesis. *Development,* 137**,** 4295-4305.

VOGELSTEIN, B. & KINZLER, K. W. 1993. The multistep nature of cancer. *Trends in genetics : TIG,* 9**,** 138-141.

VOGELSTEIN, B., LANE, D. & LEVINE, A. J. 2000. Surfing the p53 network. *Nature*, Nov 16, p.6810.

VON FIGURA, G., FUKUDA, A., ROY, N., LIKU, M. E., MORRIS, I., JOHN P, KIM, G. E., RUSS, H. A., FIRPO, M. A., MULVIHILL, S. J., DAWSON, D. W., FERRER, J., MUELLER, W. F., BUSCH, A., HERTEL, K. J. & HEBROK, M. 2014. The chromatin regulator Brg1 suppresses formation of intraductal papillary mucinous neoplasm and pancreatic ductal adenocarcinoma. *Nature cell biology,* 16**,** 255-267.

WADDELL, N., PAJIC, M., PATCH, A.-M., CHANG, D. K., KASSAHN, K. S., BAILEY, P., JOHNS, A. L., MILLER, D., NONES, K., QUEK, K., QUINN, M. C. J., ROBERTSON, A. J., FADLULLAH, M. Z. H., BRUXNER, T. J. C., CHRIST, A. N., HARLIWONG, I., IDRISOGLU, S., MANNING, S., NOURSE, C., NOURBAKHSH, E., WANI, S., WILSON, P. J., MARKHAM, E., CLOONAN, N., ANDERSON, M. J., FINK, J. L., HOLMES, O., KAZAKOFF, S. H., LEONARD, C., NEWELL, F., POUDEL, B., SONG, S., TAYLOR, D., WADDELL, N., WOOD, S., XU, Q., WU, J., PINESE, M., COWLEY, M. J., LEE, H. C., JONES, M. D., NAGRIAL, A. M., HUMPHRIS, J., CHANTRILL, L. A., CHIN, V., STEINMANN, A. M., MAWSON, A., HUMPHREY, E. S., COLVIN, E. K., CHOU, A., SCARLETT, C. J., PINHO, A. V., GIRY-LATERRIERE, M., ROOMAN, I., SAMRA, J. S., KENCH, J. G., PETTITT, J. A., MERRETT, N. D., TOON, C., EPARI, K., NGUYEN, N. Q., BARBOUR, A., ZEPS, N., JAMIESON, N. B., GRAHAM, J. S., NICLOU, S. P., BJERKVIG, R., GRÜTZMANN, R., AUST, D., HRUBAN, R. H., MAITRA, A., IACOBUZIO-DONAHUE, C. A., WOLFGANG, C. L., MORGAN, R. A., LAWLOR, R. T., CORBO, V., BASSI, C., FALCONI, M., ZAMBONI, G., TORTORA, G., TEMPERO, M. A., INITIATIVE, A. P. C. G., GILL, A. J., ESHLEMAN, J. R., PILARSKY, C., SCARPA, A., MUSGROVE, E. A., PEARSON, J. V., BIANKIN, A. V. & GRIMMOND, S. M. 2015. Whole

genomes redefine the mutational landscape of pancreatic cancer. *Nature,* 518**,** 495-501.

WAGNER, M., LÜHRS, H., KLÖPPEL, G., ADLER, G. & SCHMID, R. M. 1998. Malignant transformation of duct-like cells originating from acini in transforming growth factor transgenic mice. *YGAST,* 115**,** 1254-1262.

WANG, J. C. Y. & DICK, J. E. 2005. Cancer stem cells: lessons from leukemia. *Trends in Cell Biology,* 15**,** 494-501.

WANG, Z., LI, J., CHEN, X., DUAN, W., MA, Q. & LI, X. 2014. Disrupting the balance between tumor epithelia and stroma is a possible therapeutic approach for pancreatic cancer. *Medical science monitor : international medical journal of experimental and clinical research,* 20**,** 2002-2006.

WATANABE, S., ABE, K., ANBO, Y. & KATOH, H. 1995. Changes in the mouse exocrine pancreas after pancreatic duct ligation: a qualitative and quantitative histological study. *Archives of histology and cytology,* 58**,** 365-374.

WEISS, A. & ATTISANO, L. 2013. The TGFbeta superfamily signaling pathway. *Wiley interdisciplinary reviews. Developmental biology,* 2**,** 47-63.

WELCKER, M. & CLURMAN, B. E. 2008. FBW7 ubiquitin ligase: a tumour suppressor at the crossroads of cell division, growth and differentiation. *Nature Reviews Cancer,* 8**,** 83-93.

WHELAN, A. J., BARTSCH, D. & GOODFELLOW, P. J. 1995. A Familial Syndrome of Pancreatic Cancer and Melanoma with a Mutation in the CDKN2Tumor-Suppressor Gene. *New England Journal of Medicine,* 333**,** 975-977.

WHITCOMB, D. C., GORRY, M. C., PRESTON, R. A., FUREY, W., SOSSENHEIMER, M. J., ULRICH, C. D., MARTIN, S. P., GATES, L. K., AMANN, S. T., TOSKES, P. P., LIDDLE, R., MCGRATH, K., UOMO, G., POST, J. C. & EHRLICH, G. D. 1996. Hereditary pancreatitis is caused by a mutation in the cationic trypsinogen gene. *Nature Genetics,* 14**,** 141-145.

WILENTZ, R. E., IACOBUZIO-DONAHUE, C. A., ARGANI, P., MCCARTHY, D. M., PARSONS, J. L., YEO, C. J., KERN, S. E. & HRUBAN, R. H. 2000. Loss of Expression of Dpc4 in Pancreatic Intraepithelial Neoplasia: Evidence That DPC4 Inactivation Occurs Late in Neoplastic Progression. *Cancer Research,* 60**,** 2002-2006.

XIE, D. & XIE, K. 2015. Pancreatic cancer stromal biology and therapy. *Genes & Diseases,* 2**,** 133-143.

XU, X., D&APOS;HOKER, J., STANGÉ, G., BONNÉ, S., DE LEU, N., XIAO, X., VAN DE CASTEELE, M., MELLITZER, G., LING, Z., PIPELEERS, D., BOUWENS, L., SCHARFMANN, R., GRADWOHL, G. & HEIMBERG, H. 2008. β Cells Can Be Generated from Endogenous Progenitors in Injured Adult Mouse Pancreas. *Cell,* 132**,** 197-207.

YANAGISAWA, A., OHTAKE, K., OHASHI, K., HORI, M., KITAGAWA, T., SUGANO, H. & KATO, Y. 1993. Frequent c-Ki-ras oncogene activation in mucous cell hyperplasias of pancreas suffering from chronic inflammation. *Cancer Research,* 53**,** 953-956.

YÁÑEZ-MÓ, M., GUTIÉRREZ-LÓPEZ, M. D. & CABAÑAS, C. 2011. Functional interplay between tetraspanins and proteases. *Cellular and molecular life sciences : CMLS,* 68**,** 3323-3335.

YOKO MURAYAMA, K. O. S. T. 2015. Novel CD9-targeted therapies in gastric cancer. *World Journal of Gastroenterology : WJG,* 21**,** 3206.

YONEZAWA, S., HIGASHI, M., YAMADA, N. & GOTO, M. 2008. Precursor Lesions of Pancreatic Cancer. *Gut and Liver,* 2**,** 137-154.

ZHANG, X. A., BONTRAGER, A. L. & HEMLER, M. E. 2001. Transmembrane-4 Superfamily Proteins Associate with Activated Protein Kinase C (PKC) and Link PKC to Specific β1 Integrins. *Journal of Biological Chemistry,* 276**,** 25005-25013.

ZHANG, Y. E. 2009. Non-Smad pathways in TGF-β signaling. *Cell Research,* 19**,** 128-139.

ZHENG, R., YANO, S., ZHANG, H., NAKATAKI, E., TACHIBANA, I., KAWASE, I., HAYASHI, S. & SONE, S. 2005. CD9 Overexpression Suppressed the Liver Metastasis and Malignant Ascites via Inhibition of Proliferation and Motility of Small-Cell Lung Cancer Cells in NK Cell-Depleted SCID Mice. *Oncology Research,* 15**,** 365-372.

ZHOU, Q., BROWN, J., KANAREK, A., RAJAGOPAL, J. & MELTON, D. A. 2008. In vivo reprogramming of adult pancreatic exocrine cells to β-cells. *Nature,* 455**,** 627-632.

ZHOU, Q., LAW, A. C., RAJAGOPAL, J., ANDERSON, W. J., GRAY, P. A. & MELTON, D. A. 2007. A Multipotent Progenitor Domain Guides Pancreatic Organogenesis. *Developmental Cell,* 13**,** 103-114.

ZHOU, Q., SCHAFFER, A. E., LAW, A. C., FREUDE, K. K., RAJAGOPAL, J., NELSON, S. B., ANDERSON, W. J., SANDER, M., GRAY, P. A. & MELTON, D. A. 2010. Nkx6 Transcription Factors and Ptf1a Function as Antagonistic Lineage Determinants in Multipotent Pancreatic Progenitors. *Developmental Cell,* 18**,** 1022-1029.

ZHOU, S., SCHUETZ, J. D., BUNTING, K. D., COLAPIETRO, A. M., SAMPATH, J., MORRIS, J. J., LAGUTINA, I., GROSVELD, G. C., OSAWA, M., NAKAUCHI, H. & SORRENTINO, B. P. 2001. The ABC transporter Bcrp1/ABCG2 is expressed in a wide variety of stem cells and is a molecular determinant of the side-population phenotype. *Nature Medicine,* 7**,** 1028-1034.

ZHU, L., SHI, G., SCHMIDT, C. M., HRUBAN, R. H. & KONIECZNY, S. F. 2007. Acinar Cells Contribute to the Molecular Heterogeneity of Pancreatic Intraepithelial Neoplasia. *The American journal of pathology,* 171**,** 263-273.

ZOMER, A., MAYNARD, C., VERWEIJ, F. J., KAMERMANS, A., SCHÄFER, R., BEERLING, E., SCHIFFELERS, R. M., DE WIT, E., BERENGUER, J., ELLENBROEK, S. I. J., WURDINGER, T., PEGTEL, D. M. & VAN RHEENEN, J. 2015. In Vivo imaging reveals extracellular vesicle-mediated phenocopying of metastatic behavior. *Cell,* 161**,** 1046-1057.